

Thesis 157

AQUEOUS SOLUTION CHEMISTRY OF
MOLYBDENUM TUNGSTEN
AND RUTHENIUM

Thesis submitted for completion of the
Doctor of Philosophy degree

Ayyub Patel GRSC

Chemistry Department
University of Stirling

December 1988

1/89.

Abstract

ABSTRACT

Dynamic multinuclear ($^{17}\text{O}/^{183}\text{W}$) NMR studies on the orange trimeric W(IV) aqua ion $[\text{W}_3\text{O}_4(\text{OH}_2)_6]^{4+}$ has led to additional proof for its solution structure as being analogous to the well established red $[\text{Mo}_3\text{O}_4(\text{OH}_2)_6]^{4+}$ aqua ion. However studies with regard to the published synthetic route employing acid aquation of $\text{K}_3[\text{WCle}_3]$ have given clear evidence that the major product is not the $[\text{W}_3\text{O}_4(\text{OH}_2)_6]^{4+}$ aqua ion but probably the monochloro species $([\text{W}_3\text{O}_4(\text{OH}_2)_6\text{Cl}]^{2+})$. New routes for the preparation of $[\text{Mo}_3\text{O}_4(\text{OH}_2)_6]^{4+}$ using MoCl_4 and $\text{MoCl}_4(\text{CH}_3\text{CN})_2$ are described. Interaction of MoCl_4 and $\text{K}_3[\text{WCle}_3]$ in HCl has led to the successful isolation of a purple mixed Mo/W aqua ion $[\text{Mo}_2\text{WO}_4-(\text{OH}_2)_6]^{4+}$, the electronic spectrum of which shows a peak at 530 nm (ϵ 188 M $^{-1}$ cm $^{-1}$) and a shoulder at 410 nm (ϵ 210) consistent with the presence of the new mixed aqua ion. Zinc amalgam reduction of this new aqua ion produces an orange-brown solution oxidation state 3.00 ± 0.04 corresponding to the fully reduced aqua ion $\text{M}(\text{III})_6$. Definitive evidence for the existence of a mixed-valence ion $\text{M}(\text{III},\text{III},\text{IV})$ is reported following re-oxidation of the orange-brown solution. A comparison is made with the known mixed valence $\text{Mo}(\text{III},\text{III},\text{IV})$ and $\text{W}(\text{III},\text{III},\text{IV})$ aqua ions. Kinetic studies of NCS $^-$ anation on $[\text{Mo}_2\text{WO}_4-(\text{OH}_2)_6]^{4+}$ are also reported and the study provides further proof for the existence of this new aqua ion. The anation proceeds solely by the conjugate-base form $([\text{Mo}_2\text{WO}_4-(\text{OH}_2)_6(\text{OH})]^{2+})$. The second-order rate constant for the anation

Abstract

reaction is $1.82 \pm 0.07 \text{ M}^{-1} \text{ s}^{-1}$ (298K, I = 2.0M NaCF₃SO₃) and the aqua ion shows an exceptionally high acid dissociation constant K_{ax} (298K) of $1.00 \pm 0.07 \text{ M}$. Activation parameters for the overall reaction are $\Delta H^\ddagger = 81.95 \pm 3.32 \text{ kJ mol}^{-1}$ and $\Delta S^\ddagger = +25.70 \pm 11.0 \text{ J K}^{-1} \text{ mol}^{-1}$. An *I_e* mechanism analogous to the NC₃⁻ anation of both the [Mo₂O₆(OH₂)₈]⁴⁺ and [W₂O₆(OH₂)₈]⁴⁺ aqua ions is proposed. Substitution is believed to be at the more labile d-H₂O positions (two on each Mo) trans to the μ-oxo groups (statistical factor of 2 operative), and is influenced by *cis*-conjugate-base formation at a coordinated H₂O. Aquation steps also proceed via conjugate-base pathways.

Studies with regard to the characterization of the Ru(IV) aqua ion are reported using ¹⁷O NMR, and positive ion FAB MS measurements on derivative complexes of the aqua ion prepared using the hydridotris(i-pyrazolyl)borate ligand. These have confirmed the existence of a tetranuclear structure as proposed by previous workers. On the basis of these results two possible structures ([Ru₄O₆(OH₂)₁₂]⁴⁺ and [Ru₄O₆(OH₂)₁₂]⁵⁺) are proposed which may be interconvertible above pH 1. Water exchange on the Ru₄O₆ core has been studied at pH 1 by variable-temperature ¹⁷O line broadening, with K_{ax} (298K) = $29.8 \pm 24.8 \text{ s}^{-1}$ and activation parameters for K_{ax} ($\Delta H^\ddagger = +85 \pm 16 \text{ kJ mol}^{-1}$, $\Delta S^\ddagger = +69 \pm 47 \text{ J K}^{-1} \text{ mol}^{-1}$). Labilization due to the presence of the μ-oxo groups and/or possible conjugate base pathways are thought responsible for the fast exchange when compared with that on Ru²⁺ and Ru³⁺ aqua ions.

Abstract

Oxalate anation on $[\text{Ru}(\text{OH}_2)_6]^{2+}$, and $[\text{Ru}(\text{OH}_2)_6]^{3+}$ is reported. Anation on $[\text{Ru}(\text{OH}_2)_6]^{2+}$ proceeds exclusively through $\text{HC}_{\text{uO}_4^-}$ with a rate constant $2.6 \times 10^{-2} \text{ M}^{-1} \text{ s}^{-1}$ (298K, and I=1.0M NaCF_3SO_3). The activation parameters are $\Delta H = 101.07 \pm 6.37 \text{ kJ mol}^{-1}$ and $\Delta S = +65.1 \pm 20.9 \text{ J K}^{-1} \text{ mol}^{-1}$. A dissociative interchange (I_a) mechanism is proposed.

Oxalate anation of $[\text{Ru}(\text{OH}_2)_6]^{2+}$ has been studied as a function of temperature and $[\text{H}^+]$ at I=1.0M NaCF_3SO_3 . The observed rate law for the reaction :

$$\begin{aligned}\frac{-d[\text{Ru}^{2+}]}{dt} &= \frac{k_s k_a' [\text{Ox}]_T [\text{Ru}^{2+}]}{([\text{H}^+] + k_a')} + \frac{k_s k_{\text{Ru}} [\text{H}^+] [\text{Ox}]_T [\text{Ru}^{2+}]}{([\text{H}^+] + k_a') ([\text{H}^+] + k_{\text{Ru}})} \\ &= \frac{k_s k_{\text{Ru}} k_a' [\text{Ox}]_T [\text{Ru}^{2+}]}{([\text{H}^+] + k_a') ([\text{H}^+] + k_{\text{Ru}})}\end{aligned}$$

is valid in the range $[\text{Ox}]_T = 4 \times 10^{-3} - 1.3 \times 10^{-2} \text{ M}$, $[\text{H}^+] = 0.03 - 0.15 \text{ M}$. The rate constants k_a , k_s and k_{Ru} were not separable however by consideration of extreme cases arguments are put forward in favour of a dominant involvement of the conjugate base $[\text{Ru}(\text{OH}_2)_6(\text{OH})]^{2+}$ reacting with both $\text{H}_2\text{C}_{\text{uO}_4}$ and $\text{HC}_{\text{uO}_4^-}$.

ACKNOWLEDGEMENTS

I wish to thank Dr D T Richens for his invaluable supervision, encouragement and guidance throughout the course of this work.

I also wish to record my gratitude to Professor A E Merbach for the use of the NMR facilities at the Institut de Chimie Minérale et Analytique, Lausanne (Switzerland); to Dr L Helm, Dr F G Riddell and Dr S Arumugam for their help with the NMR work and to Dr K Muir for X-ray crystallographic work at the University of Glasgow. The assistance of Dr M P Pujari and Dr R Ferguson with some of the computer programs is also acknowledged. Many thanks to all members of the technical staff of the Department especially to Mr G Castle and Mr G Reed for much needed reagents and glassware and to Mrs G Berry for the elemental analyses. I also wish to thank the SERC for financial support throughout this work and Johnson Matthey Ltd for generous loans of ruthenium trichloride.

Finally I would like to thank my parents, my wife Rashida and children Zubair and Kulsum for their patience, help and encouragement during the course of this work.

CONTENTS

	Page
List of Abbreviations	vi
Introduction	1
CHAPTER 1	
<u>Chapter 1: Aqueous solution chemistry of Mo and W</u>	3
1.1 Molybdates and tungstates	3
1.2 Halides and halo complexes	6
1.3 Aqua ions of Mo and W	9
1.3.1 Binuclear Mo(II) aqua ion	11
1.3.2 Mononuclear Mo(III) aqua ion	13
1.3.3 Binuclear Mo(III) aqua ion	14
1.3.4 Trinuclear Mo(IV) and W(IV) aqua ions	15
1.3.5 Oxo/Sulphido bridged trinuclear Mo(IV) aqua ions	22
1.3.6 Binuclear Mo(V) and W(V) aqua ions	25
1.3.7 Binuclear Mo(VI) aqua ions	27
1.4 Multinuclear NMR spectroscopy as a probe for structural analysis in solution	27
1.5 Mixed Mo-W complexes and scope for mixed trinuclear Mo-W aqua ions	32
<u>Chapter 1 : Experimental procedures and results</u>	37
1.6 Methods for preparation of $[Mo_2O_6]^{4+}$	38
1.6.1 Preparation of $[Mo_2O_6]^{4+}$ from Mo(III) and Mo(VI)	38
1.6.2 Preparation of $[Mo_2O_6]^{4+}$ from $MoCl_4(MeCN)_2$...	40
1.6.3 Preparation of $[Mo_2O_6]^{4+}$ from $MoCl_4$	42
1.7 The developments of improved methods for the synthesis of the $[W_2O_6]^{4+}$ aqua ion	44
1.7.1 Preparation of the $[W_2O_6]^{4+}$ aqua ion using $Na_2WO_3(C_2O_4)_2 \cdot 3H_2O$	44

Contents ii

1.7.2 Attempted Preparation of the $[W_5O_6]^{4+}$ aqua ion from $WCl_4(RCN)_2$ ($R = Me, Et, n-Pr$)	47
1.7.3 Attempted preparation of $[W_5O_6]^{4+}$ aqua ion from $WCl_4 \cdot (py)_2$	48
1.7.4 Preparation of $[W_5O_6]^{4+}$ aqua ion from $K_4W_5OCl_{10}/K_2W_5Cl_6$	48
1.7.5 Preparation of the $[W_5O_6]^{4+}$ aqua ion from $K_2[WCl_6]$	50
1.7.6 Determination of the tungsten content in the $[W_5O_6]^{4+}$ aqua ion by AAS	51
1.7.7 Estimation of the tungsten content of the $[W_5O_6]^{4+}$ aqua ion by Ce(IV) titration	52
1.7.8 Modifications to obtain higher yields and avoid the presence of excess Cl^- ions	53
1.7.9 Studies on the redox chemistry of the $[W_5O_6]^{4+}$ aqua ion	54
1.7.10 Determination of the formal oxidation state for W in the emerald green solution	56
1.7.11 Cyclic voltammetry of the $[W_5O_6]^{4+}$ and $[Mo_5O_6]^{4+}$ aqua ions	57
1.7.12 ^{17}O NMR studies on the $[W_5O_6]^{4+}$ aqua ion	60
1.7.13 Attempts to detect the presence of coordinated Cl^- in the $[W_5O_6Cl]^{3+}$ aqua ion	68
1.7.14 ^{17}O NMR studies on the reduction of $[W_5O_6]^{4+}$ to the W(III,III,IV) ion	68
1.8 Attempted preparation of mixed Mo-W aqua ions ...	69
1.8.1 Attempted preparation of the $[Mo_2W_3O_6]^{4+}$ aqua ion	70
1.8.2 Preparation of $[Mo_2W_3O_6]^{4+}$ from $MoCl_4$ and $K_2[WCl_6]$	70
1.8.3 Determination of Mo and W concentration in the $[Mo_2W_3O_6]^{4+}$ aqua ion by AAS	72
1.8.4 Determination of the formal oxidation state per metal in the $[Mo_2W_3O_6]^{4+}$ aqua ion	74
1.8.5 Studies on the redox chemistry of the $[Mo_2W_3O_6]^{4+}$ aqua ion	75
1.8.6 Preparation of derivative complexes of the $[Mo_2W_3O_6]^{4+}$, $[Mo_5O_6]^{4+}$ and $[W_5O_6]^{4+}$ aqua ions .	79
1.8.7 Attempts to prepare the $[W_5MoO_6]^{4+}$ aqua ion ..	82
1.8.8 ^{17}O NMR studies on the $[Mo_2W_3O_6]^{4+}$ aqua ion ..	84

Contents iii

1.9 Anation kinetics of thiocyanate on $[Mo_2WO_4]^{4-}$:	
Experimental section	88
<u>Chapter 1: Discussion</u>	91
1.10 Anation kinetics of thiocyanate on $[Mo_2WO_4]^{4-}$:	
Results and discussion	101
<u>Chapter 1: References</u>	118
CHAPTER 2	
<u>Chapter 2: Aqueous solution chemistry of ruthenium</u>	125
2.1 Oxide and oxo compounds of Ru	125
2.2 Halide and halo- complexes of Ru	128
2.3 Ru complexes with N donor ligands	133
2.4 Mononuclear Ru(II) and Ru(III) aqua ions	134
2.5 Studies on the nature of Ru(IV) aqua ion	136
2.6 The effect of Cl^- , Br^- and NCS^- on $Ru(IV)_{aq}$	139
2.7 Scope and objective of present work	141
<u>Chapter 2: Experimental procedures and results</u>	144
2.8 Preparation of Ru(IV) aqua ion from RuO_4	144
2.9 Preparation of Ru(IV) aqua ion from $RuBr_6^{2-}$	146
2.10 Determination of the charge per Ru in the Ru(IV) aqua ion by a cation exchange technique ..	147
2.11 Effect of perchloric acid on Ru(IV) aqua ion ...	148
2.12 Effect of Cl^- and NCS^- on Ru(IV) aqua ion	150
2.13 Cyclic voltammetric studies on the $Ru(IV)_{aq}$ ion .	154
2.14 Preparation of the Ru(IV) aqua ion from electrochemical oxidation of $[Ru(OH_2)_6]^{2+}$	156
2.15 ^{17}O NMR studies on the Ru(IV) aqua ion	157
2.15.1 ^{17}O NMR spectrum of the Ru(IV) aqua ion	157
2.15.2 Attempted study for the determination of the rate constant of water exchange on $Ru(IV)_{aq}$.	161

Contents iv

2.15.3 Effect of temperature on the ^{17}O NMR spectrum of the Ru(IV) aqua ion	164
2.15.4 Effect of Cl^- and NCS^- on the ^{17}O NMR spectrum of the Ru(IV) aqua ion	167
2.15.5 ^{17}O NMR studies following electrochemical reduction of the Ru(IV) aqua ion	168
2.16 Experiments aimed at obtaining crystalline derivatives of the Ru(IV) aqua ion core with various complexing ligands	168
2.16.1 Attempted preparation of an EDTA derivative ..	169
2.16.2 Preparation of a MIDA derivative	170
2.16.3 Preparation of a hydridotris(pyrazolyl)borate derivative	171
2.16.4 Analysis of derivative compounds by +ve ion FAB MS	175
<u>Chapter 2: Discussion</u>	178
<u>Chapter 2: References</u>	185

CHAPTER 3

<u>Chapter 3: Substitution reactions of octahedral complexes</u>	190
3.1 Classification of ligand substitution mechanisms ..	190
3.2 Diagnosis of mechanism of substitution	194
3.3 Water exchange rates	199
3.4 Formation of complexes from aqua ions	205
<u>Chapter 3: Experimental procedures</u>	212
3.5 Preparation of the $[\text{Ru}(\text{OH}_2)_6]^{2+}$ and $[\text{Ru}(\text{OH}_2)_6]^{3+}$ aqua ions	215
3.6 Oxalate anation on the $[\text{Ru}(\text{OH}_2)_6]^{2+}$ aqua ion	215
3.7 Oxalate anation on the $[\text{Ru}(\text{OH}_2)_6]^{3+}$ aqua ion	216
3.8 Attempted study of the NCS^- anation on the $[\text{Ru}(\text{OH}_2)_6]^{2+}$ aqua ion	217
3.9 Attempted study of the thiourea anation on the $[\text{Ru}(\text{OH}_2)_6]^{2+}$ aqua ion	217

Contents v

<u>Chapter 3: Results and discussion</u>	219
3.10 Oxalate anation on the $[\text{Ru}(\text{OH}_2)_6]^{2+}$ aqua ion ...	219
3.11 Oxalate anation on the $[\text{Ru}(\text{OH}_2)_6]^{2+}$ aqua ion ...	229
3.12 Analysis of final product of anation	242
3.13 Possible mechanisms for oxalate anation on the $[\text{Ru}(\text{OH}_2)_6]^{2+}$ and $[\text{Ru}(\text{OH}_2)_6]^{3+}$ aqua ions .	244
3.13.1 The mechanism of anation by HC_2O_4^- on $[\text{Ru}(\text{OH}_2)_6]^{2+}$	244
3.13.2 The mechanism of anation by oxalate on $[\text{Ru}(\text{OH}_2)_6]^{3+}$	246
3.14 Characterization of $[\text{Ru}(\text{SC}(\text{NH}_2)_2)_6](\text{CF}_3\text{SO}_3)_2$	250
<u>Chapter 3: References</u>	253
Appendix 1	257
Appendix 2	260
Appendix 3	268

LIST OF ABBREVIATIONS

A	Angstrom unit, 10^{-10} m
B.M.	Bohr magneton
DMF	N-N' dimethylformamide, HCONMe ₂
DMSO	dimethyl sulphoxide, Me ₂ SO
H ₄ EDTA	ethylenediaminetetraacetic acid
Hpts	p-toluenesulphonic acid
Htfms	trifluoromethanesulphonic acid
H ₂ MIDA	methyliminodiacetic acid
HOMO	Highest occupied molecular orbital
Hz	Hertz, sec ⁻¹
LUMO	Lowest unoccupied molecular orbital
py	pyridine
pz	pyrazolyl
THF	Tetrahydrofuran

INTRODUCTION

Although elements of the second and third row transition metals do form simple monomeric aqua ions (e.g. $[M(OH_2)_6]^{n+}$ where M = Mo, Ru, Rh, Ir), a more common feature of their aqueous chemistry is the formation of oligomeric species with metal-metal bonding and oxo, hydroxo and/or halo bridges. These are often called aqua ions but by strict definition they are oxo species. The availability of such aqua ions plays an important role in the chemistry of the corresponding element as they are viewed as being the simplest of complexes and can be frequently more labile than other complexes (e.g. halogeno-complexes) thus opening synthetic routes to compounds including organometallic ones not available otherwise.

There are several difficulties in preparing aqua ions of the 4d and 5d elements: they cannot be obtained by dissolution of the metal in noncomplexing acids because of their higher redox potentials compared to those of the 3d elements, they hydrolyse easily to oxides of higher oxidation states, and commercially available starting materials are often inert towards ligand exchange. Another problem encountered is in the structural analysis as most of the aqua ions are notoriously difficult to crystallize. Preparative routes often include redox reactions, comproportionation and disproportionation reactions. The structural analysis often requires preparation of derivatives by replacement of the H_2O ligands with other complexing ligands.

Introduction 2

such as EDTA and MIDA. More recently techniques such as multi-nuclear NMR have also been used in probing the structures.

Successful synthesis and characterization of an aqua ion opens the door to kinetic studies which will provide mechanistic information about its reactivity. In this area kinetics of water exchange using ^{17}O , and anation using ligands such as oxalate and thiocyanate have been studied.

The present work includes all the aspects discussed above with respect to the aqua ions of Mo, W, and Ru. The thesis is divided into three chapters the first of which discusses the preparation and characterization of the W(IV) aqua ion and a related mixed Mo-W aqua ion. The kinetics of NCS^- anation on the mixed Mo-W aqua ion was also studied and provided further evidence of the proposed structure. The second chapter is devoted to the characterization of the oligomeric Ru(IV) aqua ion. The final chapter describes kinetic studies of oxalate anation on hexaaquaruthenium(II), $[\text{Ru}(\text{OH}_2)_6]^{2+}$ and hexaaquaruthenium(III), $[\text{Ru}(\text{OH}_2)_6]^{3+}$. Interest stems from a comparison with regard to recent studies on mechanisms of water exchange. Each chapter carries a detailed literature survey dealing with the appropriate subject matter.

CHAPTER ONE

1. Aqueous solution chemistry of molybdenum and tungsten.

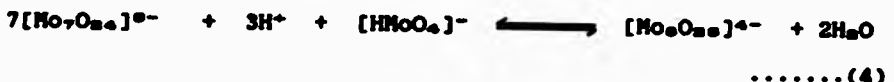
The aqueous solution chemistry of Mo and W has many basic similarities, although there are notable differences between them in various types of compounds. For example, both elements not only form simple molybdates and tungstates (MO_4^{2-}), but also polymolybdates and polytungstates in oxidation state (VI), halides and halo complexes that are isomorphous. A true aqua ion (ie. those containing M and OH_n only) is only found for Mo(II) and Mo(III), but both Mo and W form a range of oligomeric oxo species that can also be referred to as aqua ions, or as derivatives of. In the following pages, some of the recent literature describing the essential chemical features of the principal representative species in aqueous solution of Mo and W in their various oxidation states will be reviewed.

1.1 Molybdates and tungstates.

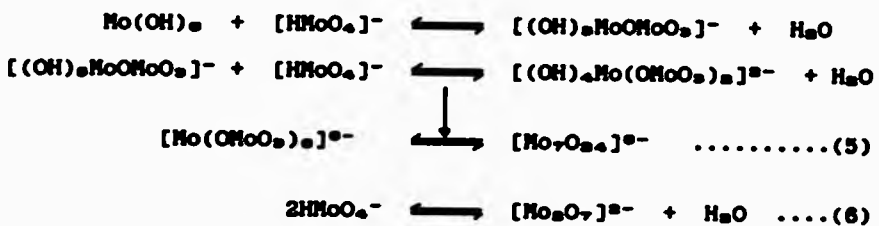
Simple molybdates(VI) and tungstates(VI) can be obtained from solutions of MO₃ in aqueous alkali.¹ Both show some oxidising capabilities, but lack the powerful oxidising property of their lighter group partner CrO₄²⁻. Upon acidification, in contrast to Cr, polynuclear anions are formed and for Mo the following protonation equilibria are established.² :



Ch. 1: Aqueous solution chemistry of Mo and W 4



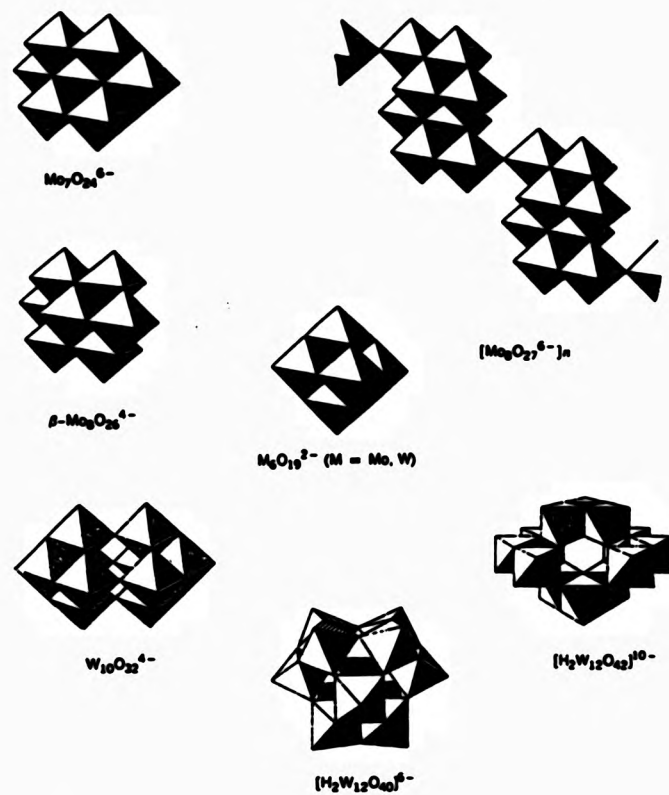
The absence of $[\text{Mo}_2\text{O}_7]^{2-}$ (very important for Cr(VI)) can be understood by considering the large K_a value. The amount of Mo(OH)_6 is only slightly less than $[\text{HMoO}_4]^-$ and this allows reaction (5) to compete effectively with (6).



Internal rearrangement of $[\text{Mo}(\text{OMoO}_5)_2]^{2-}$ gives the final $[\text{Mo}_7\text{O}_{24}]^{4-}$ structure, which consists entirely of octahedra. For tungsten⁶⁺, in the pH range 5 to 7.6, the equilibria involve $[\text{WO}_4]^{2-}$, $[\text{W}_2\text{O}_{10}(\text{OH})_2]^{2-}$, $[\text{W}_7\text{O}_{24}]^{4-}$, $[\text{HW}_7\text{O}_{24}]^{2-}$ and $[\text{HsW}_16\text{O}_{48}]^{4-}$. Figure 1.1 shows some of the known structures for the Mo and W isopoly anions. The work of Klemperer^a using ¹⁷O NMR has provided direct information on structures in solution and is discussed later. In addition to the species consisting only of Mo, W, and O, there are heteropoly anions which contain other atoms such as P, V, As etc. These are

Ch. 1: Aqueous solution chemistry of Mo and W 5

Figure 1.1 Some of the known isopoly anions of Mo and W.



Ch. 3: Aqueous solution chemistry of Mo and W is prepared by acidification of solutions containing the requisite simple anions, or by introduction of the heteroelement after first acidifying the molybdate or tungstate. The following are two such species :



1.2 Halides and Halo complexes.

Halide, halo and oxo-halo complexes play a major role in the aqueous chemistry of Mo and W and table 1.1 illustrates the diversity of compounds formed by both metals. Strong metal-metal interactions are observed for the lower valent complexes. These play an important role in stabilising the complexes.

Table 1.1 Halide, Halo and oxo-halo complexes of Mo and W.

Complex	Oxidation State				
	II	III	IV	V	VI
Halides	MoX_{12}	MX_6 MoI_6 MF_6	MX_4 MF_4	$[\text{Mo}_2]_n$ $[\text{WF}_6]_n$ $[\text{WCl}_6]_n$	MF_6 WCl_6
Halo-complexes	$[\text{MoX}_6]^{2-}$ $[\text{MoX}_{12}]^{2-}$	$[\text{MoCl}_{12}]^{2-}$ $[\text{MoX}_6]^{3-}$ $[\text{MoX}_6]^{4-}$ $[\text{MoF}_6]^{5-}$	$[\text{MCl}_6]^{2-}$ $\text{MCl}_6(\text{RN})_n$ MCl_6Py_n $\text{MCl}_6(\text{bipy})$	$[\text{PF}_6]^-$ $[\text{WCl}_6]^-$ $[\text{WF}_6]^-$	
Oxo-halo-complexes			$[\text{MoOCl}_{12}]^{2-}$ $[\text{MoO}_4\text{F}_6]^{2-}$	$[\text{MOCl}_6]^{2-}$ MO_6 MO_6I $[\text{MOCl}_6]^-$	MO_6 MO_6Cl_2 MO_6F_2 MO_6X_2 MO_6S_2
	$\text{M} = \text{Mo or W}$			$\text{X} = \text{Cl or Br}$	

Reduction of M(VI) (M = Mo or W) in concentrated HCl solution generates the $[MoOCl_5]^{2-}$ (emerald green) and $[WOCl_5]^{2-}$ (blue) species. The absorption spectrum of $[WOCl_5]^{2-}$ shows a single band at 653 nm ($\epsilon = 7 \text{ M}^{-1} \text{ cm}^{-1}$) which is consistent with a 5d² configuration of W(V) in an octahedral field of ligands. The $[MoOCl_5]^{2-}$ complex exhibits the same spectral transition at 712 nm. The shift to lower energy reflects the lower ligand field stabilization energy of the 2nd row transition element. In the case of W, relativistic effects² causes a contraction of the s and p orbitals and a consequence of this contraction is that the s and p orbitals more effectively screen the 4d orbitals from nuclear attraction. The increased shielding thus results in a radial expansion and destabilization of the d and f orbitals. The expansion in turn increases the interaction of the d orbitals with the valence orbitals on the ligand and thereby increase the ligand field stabilization.

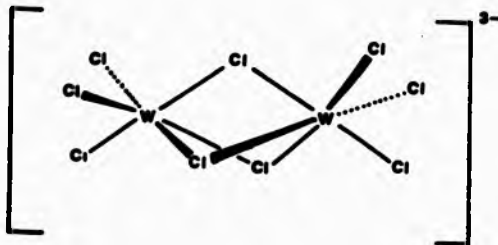
Reduction of WCl_6 in concentrated HCl solution beyond the pentavalent state produces an intensely violet coloured solution from which a red compound has been obtained by Ollson (as well as some other workers) who assigned it to be " $K_2[W^{IV}(OH)Cl_6]^{2-}$ ". Upon dissolution in aqueous as well as concentrated HCl solution marked colour changes were observed (violet \rightarrow wine-red \rightarrow yellow-green) as the compound decomposed. The electronic spectrum of " $K_2[W^{IV}(OH)Cl_6]^{2-}$ " shows 3 bands ($\lambda_{max.} \text{ } \epsilon \text{ M}^{-1} \text{ cm}^{-1}$) 781 (<100), 524 (535 from reflectance spectrum) (10.000), and 437 (<400). Such low energy bands

Ch. 1: Aqueous solution chemistry of Mo and W 8
showing high molar absorbtivities are frequently indicative of mixed-valence species. The feeling that the violet $[\text{W}(\text{OH})\text{Cl}_6]^{4-}$ species (formally W(IV)) might instead be a binuclear W(V) and W(III) compound of formula $[\text{Cl}_6\text{W}_2\text{OCl}_6]^{4-}$ has prompted further investigation into the exact nature of this compound.*

Recently, studies on a related green complex $[\text{W}_2\text{OCl}_{10}]^{4-}$ and similar decahalo complexes of other transition metals ($[\text{M}_2\text{OCl}_{10}]^{4-}$ M = Ru, Os) have been carried out by Di Salvo et al.* By using solid-state Raman spectroscopy together with magnetic susceptibilities, he confirmed that the two W centres were W(IV) (d^2) and not W(V) and W(III) as previously suggested.* These dinuclear compounds seem to be unique to W chemistry.

For the M(III) state, only Mo forms mononuclear $[\text{MoX}_6]^{3-}$ (X=F, Cl, Br). W tends to form dinuclear $[\text{W}_2\text{X}_6]^{3-}$ species (X=Cl, Br), which has a structure that consists of two octahedra sharing a common trigonal face. (Figure 1.2)

Figure 1.2 Structure of $\text{K}_3[\text{W}_2\text{Cl}_{10}]^{4-}$



Diamagnetic $[W_2Cl_6]^{2-}$ may be prepared by reducing WCl_6 in conc. HCl^{12} and can be oxidised to $[[W_2Cl_6]]^{2-}$ which has 1 unpaired electron. The same $[MnX_6]^{2-}$ compounds are also found for Mo and Cr, but are now paramagnetic ($\mu_{eff} = 0.47$, 0.7 and 3.94 B.M. for W, Mo and Cr compounds respectively) and it is clear that the strength of the interaction between the two d⁵ ions increases markedly (Cr<Mo<W).¹³ Thus for W, the interaction is strong enough (W-W 2.41 Å) to cause distortion of the structure and result in the absence of unpaired electrons.¹³ The stabilization of W(III) appears to require the presence of strong W—W bonds.

1.3 Aqua and oxo-aqua ions.

Intense interest in the aqueous solution chemistry of Mo has been stimulated by the knowledge that the element plays an important role in a number of redox metalloenzymes.¹⁴ As a consequence, intensive research by several workers¹⁵⁻¹⁸ over the past two decades has led to the characterization of Mo aqua ions in five oxidation states (table 1.2), a situation unprecedented for any other d-block element. Mo is the only d-block transition element of the 2nd and 3rd row known to have a definite biological redox role. $[Mo(OH_2)_6]^{2+}$ is the only mono-nuclear aqua ion. The remainder are bi- or trinuclear oxo-bridged species. All ions of lower valencies are oxidized by air to give eventually Mo(VI). Their preparation requires use of anaerobic techniques (N₂ or Ar gas, syringes, teflon tubing, stainless steel needles, and rubber seals).

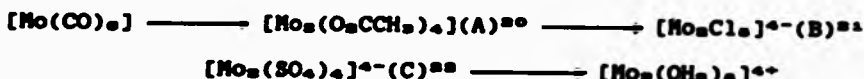
Ch. 1: Aqueous solution chemistry of Mo and W 10

Noncomplexing, redox inactive acids (e.g. Hpts., Htfms., HBF₄) have to be used as supporting media since ions such as ClO₄⁻ oxidize the lower valent ions especially Mo(II) and Mo(III) species, eventually to Mo(VI).

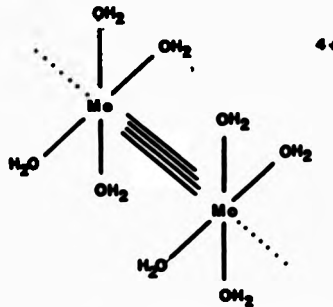
The following three reagents: Na₂MoO₄.2H₂O, Mo(CO)₆⁺ and K₂[MoCl₆] have been used as starting materials. The first two are commercially available whereas the latter is prepared by the electrochemical reduction of [MoO₄]²⁻ in conc. HCl followed by the addition of KCl.¹⁰

Table 1.2 The aqua ions of Molybdenum.¹⁰

Oxidation State	Formula	Description	Colour
+2	[Mo ₂ (OH) ₆] ²⁺	Mo ₂ H binuclear	bright red
+3	[Mo(OH) ₆] ³⁺	mononuclear	pale yellow
	[Mo ₂ (OH) ₆ (CH ₃ COO) ₂] ²⁺	binuclear	blue green
probably	[Mo ₃ (OH) ₆ (CH ₃ COO) ₃] ²⁺	trinuclear	green
+4	[Mo ₂ O ₄ (OH) ₆] ⁴⁻	trinuclear	red
+5	[Mo ₂ O ₅ (OH) ₆] ⁵⁻	binuclear	yellow-orange
+6 pH > 7	[MoO ₆] ⁶⁻	mononuclear	colourless
pH < 7	[Mo ₂ O ₆] ⁵⁻ /[Mo ₂ O ₆] ⁴⁻	polynuclear	colourless
pH < 1	[HMnO ₆] ²⁺ /[H ₂ MnO ₆] ³⁺	mono-/binuclear	colourless

1.3.1 Binuclear Mo(II) aqua ion $[\text{Mo}_2(\text{OH}_2)_8]^{4+}$.

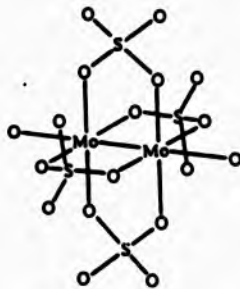
The aqua ion is generated in the final step by sulphate abstraction using Ba^{2+} in Htfms acid solution.²² The aqua ion is characterized by an electronic absorption maximum at 510 nm (ϵ 370 M⁻¹ cm⁻¹ per aqua ion). The oxidation state was verified by oxidising the Mo to Mo(VI) with Fe(III) and titrating the Fe(II) generated with Ce(IV). The electronic spectrum is similar to that of (B) (λ_{max} 515 nm) and (C) (λ_{max} 516 nm) suggesting an assignment to the $6 \rightarrow 6''$ transition and that a similar structure with two quadruply-bonded Mo(II) atoms and surrounded by eight water molecules in an eclipsed configuration is present. Crystal structures of (B) and (C) have been reported where Mo-Mo distances are ~2.1 Å.²⁴ Two additional weakly bonded axial water molecules are likely. (Figure 1.3)

Figure 1.3

Ch. 1: Aqueous solution chemistry of Mo and W 12

The Mo(II) aqua ion can be oxidized electrochemically in 1M HCl to generate the unstable triply-bonded $[Mo_3Cl_6]^{2+}$ ion (λ_{max} 430 nm).²⁸ A triply-bonded Mo(III)₂ complex can also be obtained by allowing a solution of (B) in aqueous orthophosphoric acid to stand in air for 24 hours. The $Cs_2[Mo_2(HPO_4)_4(OH_2)_2]$ compound has been reported²⁹, the crystal structure of which shows the axial MoO_6 's. When pink $K_4[Mo_2(SO_4)_4]$ is recrystallised from 1M H_2SO_4 in the presence of trace amounts of O_2 , red-blue crystals of a mixed-valence Mo(II,III) complex $K_2[Mo_2(SO_4)_4] \cdot 2\frac{1}{2}H_2O$ is obtained.²⁷ This complex is paramagnetic ($\mu_{eff}=1.65$ B.M.) and has been characterized by EPR. The structure (Figure 1.4) is very similar to that of $[Mo_2(SO_4)_4]^{4-}$ with M-M distances of 2.11 and 2.16 Å respectively (the axial O is from an adjacent sulphate).²⁸

Figure 1.4



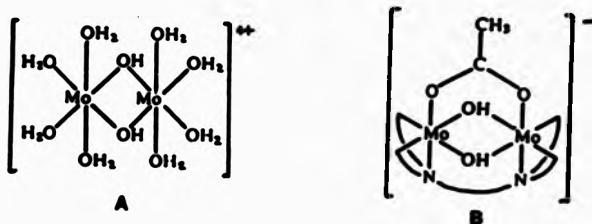
The preparation of both $W_2(O_2CC_2H_5)_4$ and $[W_2Cl_6]^{2-}$ have been reported^{28,29} but only in the absence of protons which spontaneously oxidise the W(II) complex. It is therefore unlikely that a W(II) aqua ion will exist.

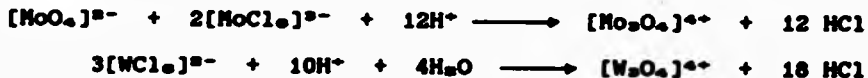
1.3.2 Mononuclear Mo(III) aqua ion $[\text{Mo}(\text{OH}_2)_6]^{2+}$.

Aquation of $[\text{MoCl}_6]^{4-}$ ^{20,21} under air-free conditions, followed by cation-exchange separation yields the mononuclear Mo(III) hexaqua ion. Traces of O_2 can result in contamination with the yellow Mo(V) ion (see later), which can obscure the d-d bands in the electronic spectrum.²¹ A comparison of the spectrum with that of MoCl_6^{4-} (established as mononuclear and octahedral) suggest that the aqua ion is also mononuclear. The aqua ion is more labile than $[\text{Cr}(\text{OH}_2)_6]^{2+}$ by a factor of ~10⁶ in the 1:1 NCS⁻ substitution reaction.²² This is explained by the increased associative character of the $[\text{Mo}(\text{OH}_2)_6]^{2+}$ reaction. A recent variable pressure kinetic study of the 1:1 NCS⁻ complexation reaction has given rise to a highly negative activation volume in further support for the dominant associative path.²³ The large size and low d-electron population are both factors probably contributing towards this behaviour. Unfortunately it has not so far been possible to obtain the rate constant for the water exchange process on $[\text{Mo}(\text{OH}_2)_6]^{2+}$ although an upper limit of ~ 1 s⁻¹ (10⁶ times faster than Cr²⁺) has been set as a result of ¹⁷O NMR measurements. Pathways involving the conjugate base $[\text{Mo}(\text{OH}_2)_6(\text{OH})]^{2+}$ appear to make no contribution.

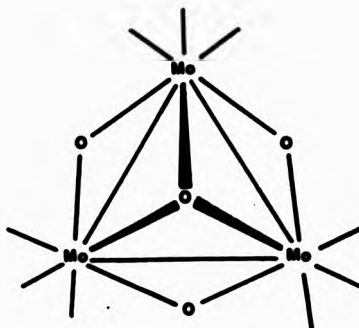
1.3.3 Binuclear Mo(III) aqua ion $[\text{Mo}_2(\text{OH})_8(\text{OH}_2)_4]^{4+}$.

The binuclear $[\text{Mo}_2(\text{OH})_8(\text{OH}_2)_4]^{4+}$ aqua ion is prepared via the reduction of Mo(VI) or Mo(V) as $[\text{Mo}_2\text{O}_4]^{4+}$ in acid solution (H^+) 0.5 - 2.0 M.²⁴ Traditional Zn/Hg Jones reductor columns or electrochemical methods are used to achieve the reduction. The elution behaviour of the ion on a cation-exchange column indicated a charge per species of 4+. The electronic spectrum in 2M Hpts shows peaks at 360 nm (ϵ 910 M⁻¹ cm⁻¹ per species), 572 nm (ϵ 96), and 624 nm (ϵ 110).²⁵ Possible structures are the di- μ -(OH) ion of formula $[\text{Mo}_2(\text{OH})_8(\text{OH}_2)_4]^{4+}$ (A) similar to that present in the $[\text{Mo}_2(\mu-\text{OH})_8\mu(\text{O}_2\text{CCH}_3)(\text{EDTA})]^-$ (B) complex²⁶ (figure 1.5) or the corresponding $\mu_2\text{-O}$ ion of formula $[\text{Mo}_2\text{O}(\text{OH}_2)_8]^{4+}$. The di- μ -hydroxo structure has been favoured on the basis of similarities in the electronic spectrum of the aqua ion with that of $[\text{Mo}_2(\mu-\text{OH})_8(\mu-\text{O}_2\text{CCH}_3)(\text{EDTA})]^-$ ²⁶ and confirmed by recent ¹⁷O NMR studies.²⁷ There are no aqua ions characterized for W(III) either mononuclear or binuclear.

Figure 1.5

1.3.4 Trinuclear Mo(IV) and W(IV) aqua ions $[M_3O_6(OH_2)_6]^{4+}$ (M = Mo or W).

First isolated by Souchay et al in 1966,²⁰ the red $[Mo_3O_6]^{4+}$ aqua ion is prepared via a comproportionation reaction between Mo(VI) or Mo(V) and Mo(III).²⁰ Early derivative complexes using oxalate²¹, thiocyanate²¹⁻²³, EDTA²², and NIDA²⁴ all demonstrated the presence of the incomplete cuboidal structure (Figure 1.6).

Figure 1.6

Despite these findings, it wasn't until 1980 that 180 labelling studies²⁵ and more recently 170 NMR²⁶ confirmed that the same incomplete cuboidal structure was present in solutions of the Mo(IV) aqua ion and that the structure $[Mo_3O_6(OH_2)_6]^{4+}$ is relevant. M.O. calculations by Cotton and co-workers²⁷ have interpreted the electronic structure of the ion as containing single M-M bonds forming a triangular Mo₃ cluster unit.

Ch. 1: Aqueous solution chemistry of Mo and W 18

Finally, after much sustained effort, a crystal structure of $[Mo_5O_4(OH_2)_8][pts]_4 \cdot 13H_2O$ determined at low temperature (240 K) was recently obtained⁴⁷ in final support of the structure (Figure 1.7). The average Mo-Mo distance in the Mo₅ cluster unit was $2.48 \pm 0.02 \text{ \AA}$ well inside the range for a single Mo-Mo bond. The W(IV) aqua ion $[W_2O_4(OH_2)_8]^{4+}$ apparently identical in structure to that of $[Mo_5O_4(OH_2)_8]^{4+}$ has been reported by Sasaki et al.⁴⁸ and McMahon⁴⁹ and has allowed the first comparative investigation of the solution chemistry of an aqua ion formed by both elements. The reported⁴⁸ synthesis of $[W_2O_4(OH_2)_8]^{4+}$ required the use of the labile W(IV) salt $K_2[WCl_6]$. A comproportionation reaction between W(VI) or W(V) and W(III) does not work here in contrast to Mo.⁴⁸ The reason for this is believed to be a combination of the mis-match of redox chemistry between the various oxidation states of W in the aqueous acidic Cl⁻ solutions employed and the inertness of W(III) complexes due to the difficulty of breaking the strong M-M bonding. Despite the expected thermodynamic and kinetic stability of the $[W_2O_4]^{4+}$ unit, the activation barriers involved in such a comproportionation reaction for W appear too great and side reactions leading to precipitation of highly insoluble deep blue polynuclear mixed W(VI)/W(V) oxides compete successfully.

Previously mono- and binuclear structures were assigned to the $[Mo_5O_4(OH_2)_8]^{4+}$ ion on the basis of EXAFS⁵⁰, cryoscopic⁵¹, electrochemical⁵², and kinetic studies.⁵³ Since the aqua ion

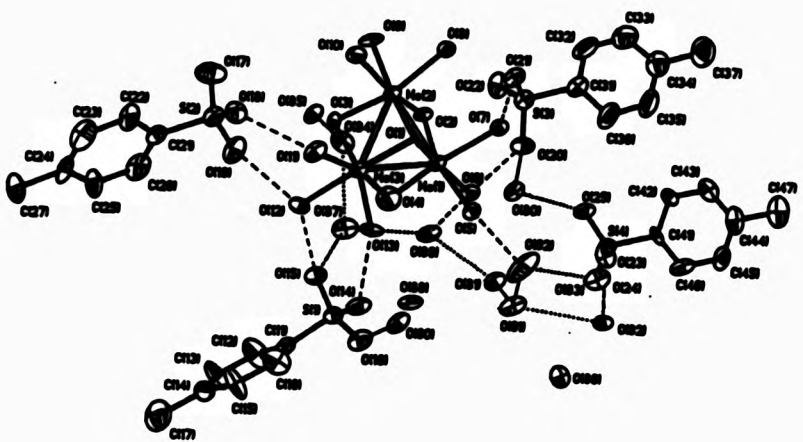


Figure 1.7 Crystal structure of $[Mo_6O_4(OH_2)_8][pts] \cdot 13H_2O$.⁴⁷

Ch. 1: Aqueous solution chemistry of Mo and W 18
has a 3-fold symmetrical structure, the reactive sites at each
Mo centre are statistically equivalent. Recent anation kinetic
studies by Sykes et al^{24,25} on both $[Mo_2O_6(OH_2)_6]^{4+}$ and
 $[W_2O_6(OH_2)_6]^{4+}$ using oxalate and NCS⁻ as the substituting
ligands have clearly shown the presence of the statistical
factor (=3). They found that the rate constants obtained with
[NCS⁻] in excess were three times those with $[Mo_2O_6(OH_2)_6]^{4+}$ in
excess, and to allow for this difference [NCS⁻] values were
divided by 3.

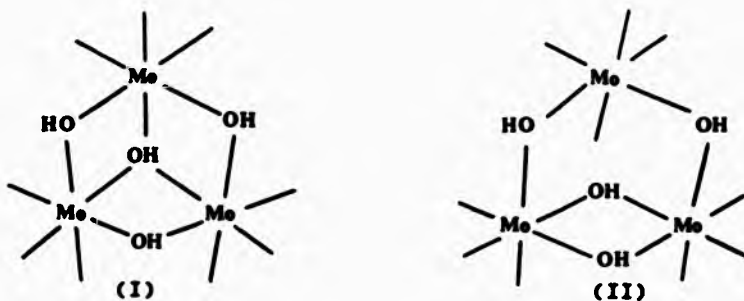
For both Mo and W 1:1 substitution was found to involve only
the conjugate base form of the ion; $[Mo_2O_6(OH_2)_6(OH)]^{3+}$, and in
the case of Mo, similar rate constants (25°C) were observed for
substitution of HCO₃⁻ ($3.3 \text{ M}^{-1} \text{ s}^{-1}$) and NCS⁻ ($4.8 \text{ M}^{-1} \text{ s}^{-1}$)²⁶
as incoming ligands leading to the proposal of a dissociative
interchange i.e. mechanism. Recent studies²⁷ of the water
exchange on $[Mo_2O_6(OH_2)_6]^{4+}$ by ¹⁷O NMR have demonstrated the
considerable inertness of the core μ_2 and μ_3 -oxo groups and the
two kinetically distinct water ligands those trans to the μ_2 -
oxo groups (d) exchanging 10⁶ x faster than those trans to the
single μ_3 -oxo group (c). Deprotonation occurs at a d-H₂O
presumably on the same Mo atom undergoing water exchange
leading to activation via a cis conjugate base effect. The
reason for the high acidity at the d-H₂O ligands ($K_a = 0.24 \text{ M}$)
is not clear on electronic grounds but may be related to the
formation of preferentially stronger hydrogen-bonds with the
secondary solvation shell.

Sykes also found that the 1:1 substitution of HCS^- for H_2O on the conjugate base $[\text{W}_2\text{O}_8(\text{OH}_2)_2(\text{OH})]^{2+}$ ($1.2\text{M}^{-1} \text{s}^{-1}$) was some ten-times smaller than the corresponding value for $[\text{Mo}_2\text{O}_8(\text{OH}_2)_2(\text{OH})]^{2+}$ ($13.5\text{M}^{-1} \text{s}^{-1}$ in perchlorate). Hence it would seem that W(IV) is more substitution inert. In view of the virtually identical ionic radii for W(IV) (80 pm) and Mo(IV) (79 pm) ions a simple explanation is not immediately apparent. Such effects are most likely related to the increased 5d participation due in the W case to the relativistic expansion effect*, which results in stronger W-OH₂ bonds. It should be noted that rate constants for exchange of H₂O (using ¹⁸O water) on the d⁶ ions $[\text{WO}_4]^{2-}$ (0.44 s^{-1}) and $[\text{MoO}_4]^{2-}$ (0.33 s^{-1}) are very similar. This now seems to be consistent with the proposal of an associative activation mode for these two reactions.**

Reduction of both $[\text{Mo}_2\text{O}_8]^{4+}$ and $[\text{W}_2\text{O}_8]^{4+}$ occurs readily with Zn/Hg and mixed valence (III/IV) species as well as, in the case of Mo, a $[\text{Mo}(\text{III})_3]$ aqua ion have been identified.^{44,57} Air oxidation together with electrochemical reversibility strongly suggest that the basic trinuclear unit is retained in solution.

For Mo, the intermediate mixed-valence ion titrates for oxidation state 3.33, thus formally consisting of one Mo(IV) and two Mo(III) atoms. The broad band maximum at 1.050 nm ($\epsilon = 100 \text{ M}^{-1} \text{ cm}^{-1}$ per Mo atom) has been assigned from an analysis of

its band shape and energy to an inter-valence charge transfer transition implying discrete Mo(III) and Mo(IV) centres in the mixed-valence ion. Cyclic voltammetric studies of the reduction of $[Mo_3O_4]^{4+}$ in the $[H^+]$ range 0.5 - 4.0 M suggest a structure $[Mo_3(OH)_6]^{n+}$ for the mixed-valence ion. Interestingly, there is evidence of only trace formation of the other intermediate mixed-valence ion; $Mo(III)(IV)_2(aq)$. Cotton had earlier predicted a stability in the d^0 $Mo(III)_2(IV)$ unit owing to the complete filling of the LUMO energy level in $Mo(IV)_2$ thus implying an instability in the d^1 half filled LUMO ($Mo(III)(IV)_2$) with respect to disproportionation to give the d^0 ($Mo(IV)$) and d^0 ($Mo(III)_2(IV)$) species. This argument would require the trinuclear cluster unit to remain intact but appears to explain the experimental observation of the $2e^-$ reduction. There is electrochemical and ^{17}O NMR evidence²⁰ for two forms of the $Mo(III)_2$ aqua ion probably containing the "open" and the "closed" structures shown below. (I) and (II)



Cyclic voltammetric studies²² show that formation of the "open" structure (II) is favoured by high acidity probably aiding breakage of one of the Mo- μ ₂(OH) bonds. In addition, a more recent close analysis of the earlier electrochemical results imply that the stable form of Mo(III)_n(IV) existing in solution also has the related open structure, its structure also appearing to be aided by protonation. Such a structural change for the d⁶ cluster may further lower the energy of the newly formed HOMO thus favouring its stability vs the d⁷ Mo(III)(IV)_n species which presumably still has the closed structure. It is conceivable that the structure of the Mo(III)_n(IV) aqua ion could consist essentially of a di- μ -hydroxo Mo(III) dimer bridged by a single Mo(IV) unit analogous to the μ -acetato bridged complexes. While such a proposed structure would appear to give a possible explanation for the discrete Mo(III) and Mo(IV) centres and the overall diamagnetism, it must be stressed that it remains unproven. Attempts to prepare a crystalline derivative of the Mo(III)_n(IV) aqua ion have so far failed. Sasaki et al.²³ reported the formation of the analogous W(III)_n(IV) aqua ion following Zn/Hg reduction of [W₃O₈]⁴⁺ but no evidence of W(III)(IV)_n or W(III)_n aqua ions. As part of our investigations into the solution chemistry of [W₃O₈]⁴⁺, we have conducted further experiments with regard to its reduction products including ¹⁷O NMR results (see next section) in the hope of further characterizing the solution species involved. These will be discussed in section 1.7)

1.3.5 Oxo/Sulphido bridged trimuclear Mo(IV) aqua ions.

Extensive work is currently being carried out by Sykes et al and Cotton et al in preparing sulphido bridged trimuclear aqua ions analogous to $[Mo_3O_6]^{4+}$. Sykes et al⁵⁵⁻⁵⁸ have reported electrochemical routes using pairs of Mo(V)_n complexes $[Mo_3O_6(cys)_n]^{2-}$, $[Mo_3O_6S(cys)_n]^{2-}$ and $[Mo_3O_6Se(cys)_n]^{2-}$ in equimolar amounts, followed by cation-exchange purification to make a series of 8 different aqua ions. Figure 1.8 illustrates the basic structures of these ions and table 1.3 gives their electronic spectral characteristics.

The triangular and cubic ions $[Mo_3S_4]^{4+}$ and $[Mo_3S_4]^{2+}$ have also been reported along with derivative crystal structures using thiocyanate and oxalate ligands.⁵¹⁻⁵³ The study of these sulphido bridged clusters is of interest as some of them are analogous to the biologically important ferredoxins.⁵⁴ They would also be expected to possess a rich redox chemistry.

Analogous electrochemical studies using the di- μ -O Mo(V) complex ($[Mo_3O_6(cys)_n]^{2+}$) have yielded the well established $[Mo_3O_6]^{4+}$ aqua ion and some evidence for the complete cubane $[Mo_3O_6]^{2+}$ aqua ion.⁵⁵

Similar success is not yet in evidence for the potential W analogues of these Mo compounds. It may also be noted that the synthetic routes used by Sykes will in any case not be possible because the corresponding W starting materials are not available. Hence Cotton et al have reported alternative routes for

Figure 1.6 Basic structures of the various oxo/sulphido bridged aqua ions and scheme showing possible mechanism of assembly.

(H₂O ligands have been omitted)

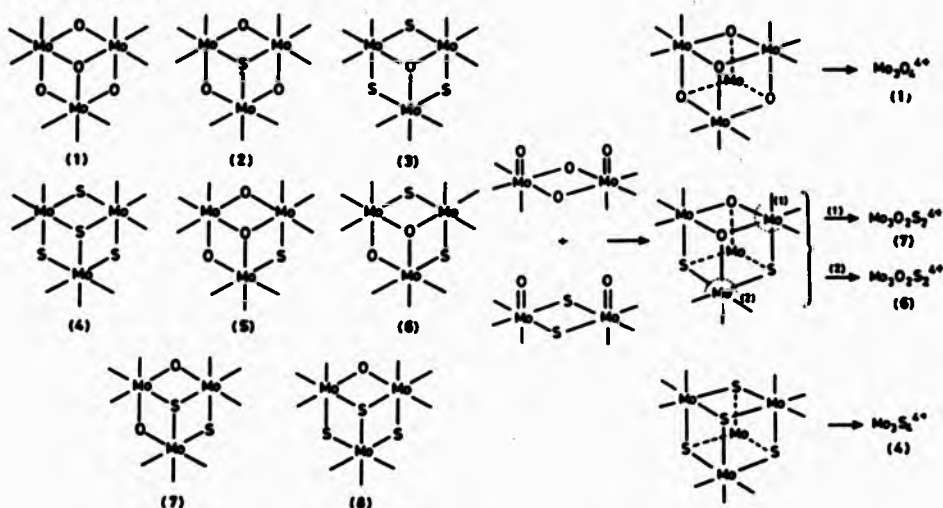


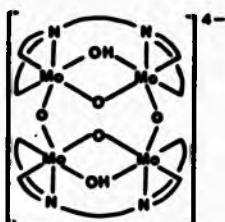
Table 1.3 Electronic spectra of triangular oxo/sulphido aqua ions.

		$\lambda_{\text{max.}}$ nm	ϵ^* $\text{M}^{-1} \text{cm}^{-1}$	$\lambda_{\text{max.}}$ nm	ϵ^* $\text{M}^{-1} \text{cm}^{-1}$
$[\text{Mo}_2\text{O}_4(\text{OH}_2)_6]^{4+}$	(1)	505	189	300(sh)	1560
$[\text{Mo}_2\text{O}_3\text{S}(\text{OH}_2)_6]^{4+}$	(5)	511	—	332	—
$[\text{Mo}_2\text{O}_3\text{S}(\text{OH}_2)_6]^{4+}$	(2)	512	153	333	930
$[\text{Mo}_2\text{O}_3\text{S}_2(\text{OH}_2)_6]^{4+}$	(6)	545	188	327	2490
$[\text{Mo}_2\text{O}_3\text{S}_2(\text{OH}_2)_6]^{4+}$	(7)	568	207	335	2330
$[\text{Mo}_2\text{O}_3\text{S}_2(\text{OH}_2)_6]^{4+}$	(3)	580	206	332	2500
$[\text{Mo}_2\text{O}_3\text{S}_2(\text{OH}_2)_6]^{4+}$	(8)	588'	263	332	2980
$[\text{Mo}_2\text{S}_3(\text{OH}_2)_6]^{4+}$	(4)	602	351		

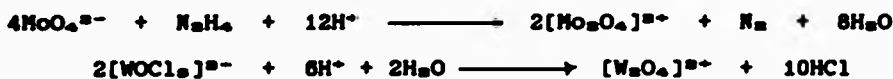
* ϵ quoted per aqua ion. ' shoulders at 410 and 370 nm

the preparation of Mo_3S_4 and Mo_4S_4 species.^{65-68,71} These have the advantage in that they may be readily applied to the W analogues. The preparation involves refluxing $\text{Mo}(\text{CO})_6$ with Na_2S and acetic anhydride followed by filtration, dilution and ion-exchange purification. Reaction using $\text{W}(\text{CO})_6$ yielded a complicated array of products one of which has been shown to be the $[\text{W}_3\text{S}_4]^{4+}$ aqua ion.⁷² Dori has reported a trinuclear tungsten thiocyanato complex which contains oxo/sulphido bridges.⁷³ Further interest in these oxo/sulphido clusters will stem from their behaviour with regard to redox and complexation reactions. In particular, the specific reactivity of Mo and W centres surrounded by mixture of oxo and sulphido groups with respect to the rates of terminal water ligand replacement. Recent studies imply that the metal centres co-ordinated preferentially to μ -S groups have larger rates of water ligand replacement indicating a pattern of increasing lability of H_2O ligands as more sulphido groups are substituted into the core.⁷⁴

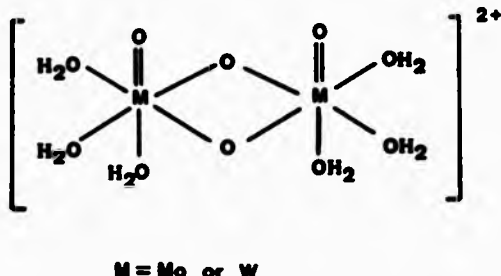
There is little evidence of a tetrานuclear Mo(IV) aqua ion although the red $[\text{Mo}_4\text{O}_4(\text{OH})_6(\text{EDTA})_2]^{4-}$ (figure 1.9) is known which has the Mo in (III.III.IV.IV) oxidation state.⁷⁵ The EDTA ligands may be the reason for the retention of the tetrานuclear structure in this case.

Figure 1.9

1.3.6 Binuclear Mo(V) and W(V) aqua ions $[M_2O_4]^{2+}$ ($M=Mo$ or W).



The $[\text{Mo}_2\text{O}_4]^{2+}$ aqua ion has been prepared via a variety of methods.^{71-78,80} The most commonly used one involves the reduction of an acidic molybdate solution by hydrazine. The $[\text{Mo}_2\text{O}_4]^{2+}$ is then purified by ion-exchange chromatography. Similar attempts to prepare the W analogue have failed to produce pure samples of the $[\text{W}_2\text{O}_4]^{2+}$ aqua ion. Methods involving the removal of an organic ligand (EDTA, oxalate etc.) from a complex containing the $[\text{W}_2\text{O}_4]^{2+}$ core have demonstrated the existence of the aqua ion in solution but do not allow its ready purification by ion-exchange. Instead, Sykes et al.⁷⁹ have reported its successful preparation via aquation of $[\text{WOCl}_6]^{2-}$. A structure with di- μ -oxo and terminal oxo groups is proposed for both aqua ions from the structure of the EDTA complex (Figure 1.10)

Figure 1.10

The electronic spectrum of the $[\text{Mo}_2\text{O}_4]^{2+}$ aqua ion shows absorption maxima at 295 nm (ϵ 3500 $\text{M}^{-1} \text{cm}^{-1}$), 384 (ϵ 103) and 490 (ϵ 43), whereas the $[\text{W}_2\text{O}_4]^{2+}$ show maxima at 340 (ϵ 278) and 430 (ϵ 193). The tungsten ion again shows a similar set of bands to the Mo analogue but the bands occur at higher energy and with slightly higher intensity.

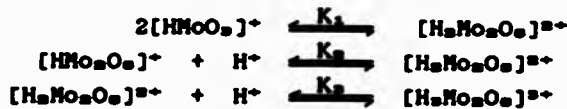
Sykes et al.⁷² have carried out 1:1 substitution reactions using NCS^- and have again showed that substitution on $[\text{W}_2\text{O}_4]^{2+}$ ($k_{\text{on}}(25^\circ\text{C}) = 2.52 \times 10^3 \text{ M}^{-1} \text{s}^{-1}$) is 10 x slower than on $[\text{Mo}_2\text{O}_4]^{2+}$ ($k_{\text{on}}(25^\circ\text{C}) = 2.90 \times 10^4 \text{ M}^{-1} \text{s}^{-1}$). A similar mechanism probably dissociative in character is suggested for each involving initial rapid complexation in the position trans to the terminal oxo groups.

With regard to all of the complexation studies on the W aqua ions, there was a worrying feeling that the ions themselves were not entirely free of the coordinated ligands e.g. Cl^- that had been presumed removed during synthesis via acid aquation.⁷⁴

On lowering the background acidity in order to achieve ion-exchange purification, some recomplexation might be occurring that was able to survive the ion-exchange treatment. As will be described, the present results with regard to $[W_2O_8]^{4+}$ have given cause to further concern over the ability of the published methods to generate pure solutions of W aqua ions.

1.3.7 Binuclear Mo(VI) aqua ions.

At pH > 7 both Mo(VI) and W(VI) exist as monomeric $[MO_4]^{2-}$. On decreasing the pH protonation occurs and this induces a change in the coordination number (4 - 6) and polymerization of octahedral M_2 , M_3 species occur. For Mo(VI), in the acid range 0.3M - 3 M, mono- and binuclear aqua ions have been reported.⁷⁸ They have been formulated as $[HMoO_6]^{2+}$, $[Mo_2O(OH)_6(OH_2)]^{2+}$, $[Mo_2O(OH)_6(OH_2)_2]^{2+}$, and $[Mo_2O(OH)_7(OH_2)_2]^{2+}$. All are colourless and their electronic spectra show various peaks in the 240 - 250 nm region that have been assigned to the various species. The relevant equilibria can be expressed as follows:



At 25°C, $K_1 = 97 \text{ M}^{-1}$, $K_2 = 4.7 \text{ M}^{-1}$ and $K_3 = 0.24 \text{ M}^{-1}$.⁷⁸

1.4 Multinuclear NMR spectroscopy as a probe for structural analysis in solution.

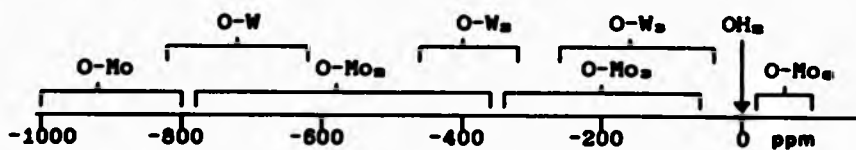
As mentioned earlier, characterization of aqua ions by X-ray crystallography is difficult. Many are highly soluble and do

not readily form sparingly soluble crystalline hydrates. The recently reported⁴⁷ structure of $[\text{Mo}_2\text{O}_6(\text{OH}_2)_6][\text{ptz}]_4 \cdot 13\text{H}_2\text{O}$ for example was a case where the correct conditions for crystallization; appropriate metal ion and background acid concentration, low temperature (240 K) and sufficient time (6 months) were achieved somewhat fortuitously. More serious however is the possibility that the structure in the crystal may not pertain to that in solution particularly if labile species are being investigated. One desires a direct probe of structure in solution and to this end, studies using ^{17}O , ^{95}Mo , and ^{183}W NMR have proved particularly useful. In studying the oxygen centres of the aqua ions, ^{17}O NMR potentially can give the most definitive structural information. As an alternative to the expensive use of ^{17}O , Murmann and Gamsjäger have pioneered the use of ^{18}O labelling techniques to study the kinetics of oxygen exchange with water and have given a comprehensive account⁴⁸ of the development of this area in a recent review. Studies on the kinetics of water exchange with the $[\text{Mo}_2\text{O}_6]^{4+}$ and $[\text{Mo}_3\text{O}_8]^{4+}$ aqua ions have been carried out by Murmann and co-workers using ^{18}O labelling coupled with mass spectral analysis. In 1980 Murmann and Shelton⁴⁹ obtained the first definitive proof of the trinuclear $[\text{Mo}_3\text{O}_8]^{4+}$ structure for the Mo(IV) aqua ion by this method from the lack of detectable exchange (>95% retention) shown by the core μ_2 and μ_3 -OXO groups. This technique suffers from the fact that it requires mass spectral analysis on a rapidly formed and structurally characterized solid

Ch. 1: Aqueous solution chemistry of Mo and W 29

derivative in which the water ligands are replaced, thus making studies on the water exchange itself virtually impossible. This technique clearly has limitations when many different exchanging oxygens are present; the nature of the analysis necessitating only an overall picture and making selective analysis difficult. The developments in ^{17}O NMR studies have led to a degree of controversy in the literature with regard to certain solution species. For example, recent ^{17}O NMR studies⁷⁷ on the decavanadate ion: $[\text{V}_{10}\text{O}_{24}]^{8-}$ are not consistent with the earlier ^{18}O labelling evidence of a fluxional mechanism in which all oxygens exchange with exactly the same rate. In being able to probe individually the nature and dynamic properties of oxygen sites, the ^{17}O NMR method is uniquely powerful as a solution probe. The extensive pioneering work of Klemperer⁷⁸⁻⁸⁰ has shown ^{17}O NMR spectroscopy to be a powerful tool for probing both structural and dynamic aspects of polyoxoanions (polyoxomolybdates) in solution.⁷⁸ Furthermore he was able to ultimately assign a chemical shift scale for the different oxygen atom environments in a given system e.g. for Mo in figure 1.11.⁷⁸

Figure 1.11 Oxygen-17 shifts scale for polyoxometallates.



Ch. 1: Aqueous solution chemistry of Mo and W 30

This has been extended by Burtseva⁵¹ to include the polyoxotungstates with the finding that the resonances of oxygen bound to W are shifted to the high field, as compared with resonances of the corresponding oxygen atoms bound to Mo. He also found that the difference in the chemical shifts of the oxygen atoms in the heptapolymetallates ($[Mo_7O_{24}]^{4-}$ and $[W_7O_{24}]^{4-}$) became less pronounced as the coordination number of the oxygen atom increased, and correspondingly, the paramagnetic contribution to the screening decreased. ^{183}W NMR was also used by Burtseva⁵¹ to provide additional confirmation of the 170 O studies by showing three ^{183}W resonances with the ratio of intensities 1:4:2 corresponding to the three different structural types of W atoms in the $[W_7O_{24}]^{4-}$ ion (4W-O-W, 2(W₂-O, W₄-O), and 1W=O). A chemical shift scale for polyoxotungstates similar to that of Klemperer has been reported by Fedotov et al.⁵² and is also illustrated in figure 1.11. Very recently, Pope et al.⁵³ applied ^{183}W NMR spectroscopy to investigate the nature of the reduction species of a number of heteropolytungstates (referred to as heteropoly blues and browns). The studies confirmed earlier suggestions of Launay⁵⁴ that the brown complexes contain W(IV) atoms in a trigonal metal-metal bonded W_2O_12 groups. Furthermore, they were able to confirm the assignment of W(IV) by studying the trinuclear $[W_3O_10(OH_2)_6]^{4+}$ aqua ion which showed the expected one resonance peak for equivalent W(IV) atoms.

Aside from studies on polyoxometallates, the NMR technique has been used by Gheller et al⁴⁴ who carried out ⁹⁵Mo ($I = 5/2$; $Q = 1.1 \times 10^{-28} \text{ cm}^2$) NMR studies on a number of complexes containing the $[\text{Mo}_5\text{O}_4]^{4+}$ and $[\text{Mo}_6\text{O}_4]^{5+}$ units. In non-complexing acid media the EDTA and MIDA complexes of both ions showed single resonances which occurred at much lower fields compared to mononuclear species. This information, coupled with the crystallographic data, was useful in establishing the structures of these species in solution.

The ¹⁷O NMR technique was first successfully applied to polyoxoanions in 1965 by two groups involved in independent investigations of the aqueous $[\text{Cr}_5\text{O}_7]^{3-}$ anions.⁴⁵ Due to sensitivity problems, however, little progress was possible until the advent of Fourier transform NMR spectroscopy. Since 1975, this technique has enabled ¹⁷O NMR spectra of polyvanadates, -niobates, -tantalates, -molybdates, and -tungstates to be obtained.^{46-70,80,81,88-90} The technique suffers from two major drawbacks. Firstly the low natural abundance of ¹⁷O (0.037%) necessitates the use of ¹⁷O-enriched samples. Hence the technique is limited to the study of those compounds which may be efficiently enriched. Secondly the ¹⁷O nucleus is a spin 5/2 nucleus with an appreciable quadrupole moment ($Q = -2.6 \times 10^{-28} \text{ cm}^2$) which in general leads to rapid nuclear quadrupole relaxation. This rapid relaxation is advantageous in that it allows rapid RF pulsing using the FT NMR technique. At the same time, however, it leads to broad resonances and

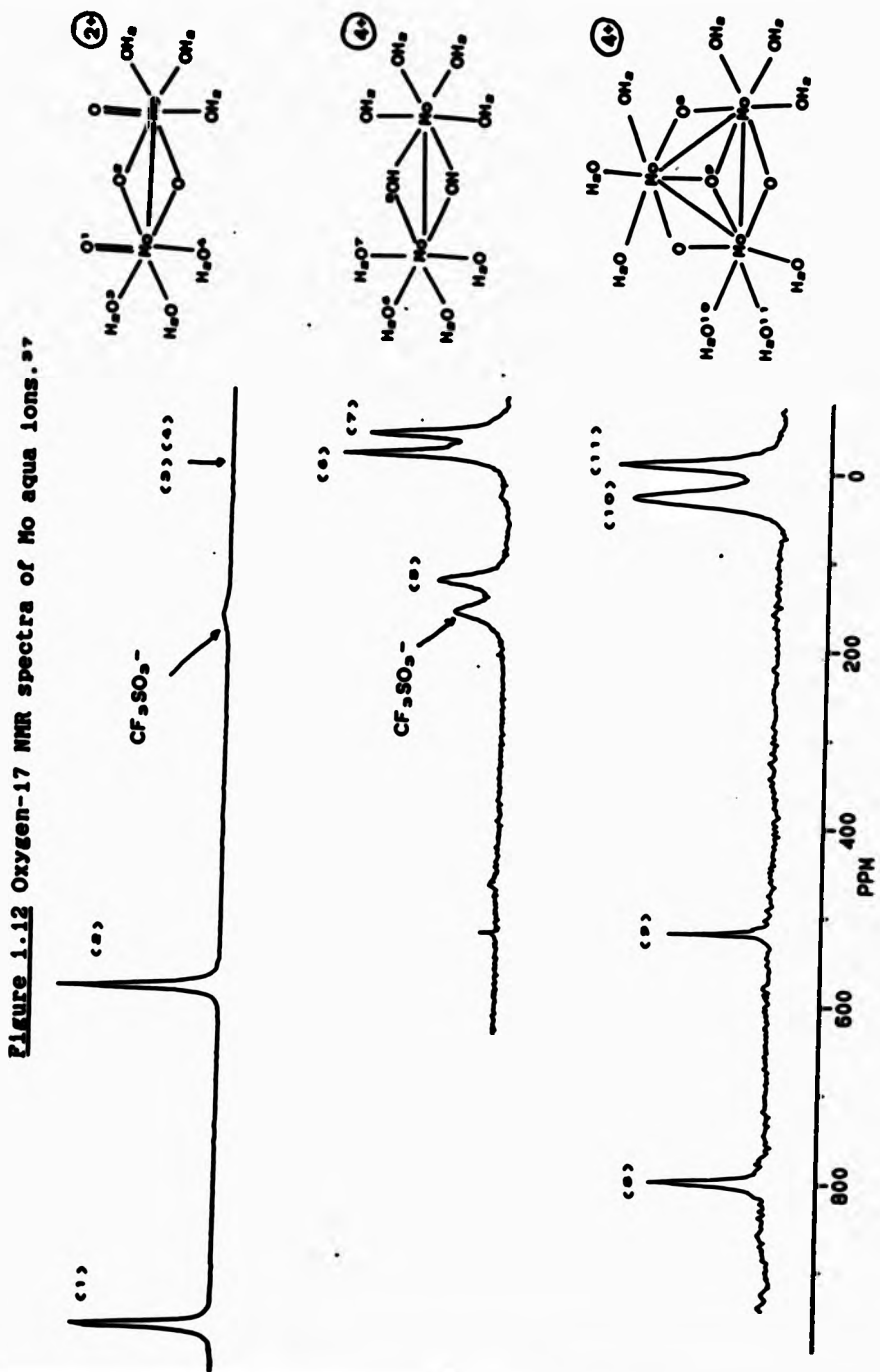
hence poor spectral resolution and poor signal to noise ratios. Furthermore, this rapid spin-spin relaxation necessitates the used of short delay times between the end of each RF pulse and the beginning of data collection, often resulting in incomplete spectrometer recovery and consequently baseline distortion in the transformed spectra.

The availability of powerful NMR instruments has partly cured the first problem and within the last few years the ^{17}O NMR technique has been applied successfully to the study of oligomeric aqua ions of molybdenum.⁴⁷ The study was carried out on three aqua ions of Mo, $[\text{Mo}_2\text{O}_6(\text{OH}_2)_6]^{2+}$, $[\text{Mo}_3(\text{OH})_5(\text{OH}_2)_6]^{4+}$, and $[\text{Mo}_5\text{O}_6(\text{OH}_2)_6]^{6+}$) and it allowed effective characterization and water exchange kinetics to be followed.⁴⁷ (Figure 1.12 shows the spectra and structures of the aqua ions)

One of the objectives of the present work was to study the $[\text{W}_3\text{O}_6(\text{OH}_2)_6]^{4+}$ aqua ion using ^{17}O NMR in an attempt to confirm both its structure and purity in solution, in the light of the uncertainty in the literature.

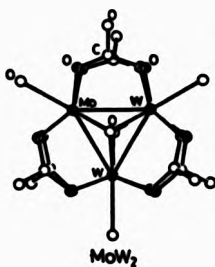
1.5 Mixed Mo-W complexes and scope for mixed trinuclear Mo-W aqua ions.

The successful preparation of the homo trinuclear aqua ions $[\text{Mo}_3\text{O}_6(\text{OH}_2)_6]^{4+}$ and $[\text{W}_3\text{O}_6(\text{OH}_2)_6]^{4+}$ had led to the feeling that it should be possible to make hetero mixed Mo-W analogues if synthetic method could be developed. In this context, a number of mixed trinuclear Mo-W cluster compounds have been charac-



Ch. 1: Aqueous solution chemistry of Mo and W 34
 terized.⁹¹⁻⁹⁶ These are at present limited to a number of complexes containing carbonyl ligands and bicapping μ_2 -oxo groups and bridging μ_2 -(CH₃COO)₂ and μ_2 -(Pr²O) groups.⁹⁷⁻⁹⁹ Interestingly, the complete series (i.e. Mo₂, Mo₂W, MoW₂, and W₂) has been reported¹⁰⁰ in the case of the complex [Mo₂(μ_2 -O)₂(μ_2 -CH₃COO)₆(OH₂)₂]⁴⁺ (figure 1.13)

Figure 1.13



Surprisingly, despite much interest in the chemistry of the trinuclear Mo(IV) and W(IV) ions and their sulphido analogues, there have been no reports of attempts to prepare the hetero aqua ions([Mo₂WO₄(OH₂)₂]⁴⁺(X), and MoW₂O₄(OH₂)₂]⁴⁺(Y)). Such ions, if identified, should possess intriguing properties. Their reactive properties may be similar to the homo aqua ions (i.e. (X) being similar to [Mo₂O₄(OH₂)₂]⁴⁺ and (Y) to [W₂O₄(OH₂)₂]⁴⁺) or they may display characteristics of both the homo aqua ions. Since both the two metals have similar size the assembly of the cuboidal structure is not likely to be disturbed. X-ray crystallography has shown that both [Mo₂O₄]⁴⁻ and [W₂O₄]⁴⁻ have almost the same size.⁴⁷⁻¹⁰⁰ The hetero aqua

Ch. 1: Aqueous solution chemistry of Mo and W 35
ions would be characterized by the same techniques (i.e. electronic spectra, Zn/Hg reduction studies, Mo and W analysis by AAS, and ^{17}O NMR spectroscopy) as those used for the homo aqua ions. Their 1:1 substitution kinetics with thiocyanate and oxalate ligands would give additional information to confirm their characterization. In particular, the statistical factor mentioned earlier, would help to confirm the structures of these aqua ions. In the absence of crystallographic data, ^{17}O NMR may be attempted on the new aqua ions to probe their structures. If the electron density around the cluster is delocalized, one would expect a similar spectrum as that for Mo. On the other hand, if the cluster is not delocalized, as is more likely the different oxygens might show further resonances.

The following section thus describes the experimental work carried out in order to establish unequivocally whether these hetero Mo-W aqua ions exists and if so to carry out structural as well as kinetic investigations of their chemical properties. ^{17}O NMR spectroscopy will be used, firstly to ascertain the structure in solution and purity of $[\text{W}_2\text{O}_4]^{4-}$ aqua ion and later to elucidate the structures of the mixed aqua ions following indirect proof of their existence from electronic spectroscopy, AAS, Zn/Hg reduction and electrochemical measurements.

Ch. I: Aqueous solution chemistry of Mo and W 36

The strategy for the experimental work was as follows :

1. Prepare the $[Mo_2O_4]^{4+}$ aqua ion from known methods in order to become familiar with the air-free techniques required.
2. Investigate the possibilities of new methods for the synthesis of the $[Mo_2O_4]^{4+}$ starting from monomeric Mo(IV) complexes. Since the reported preparation of the $[W_2O_4]^{4+}$ involves the aquation of $[WCl_6]^{2-}$, similar aquation routes for the Mo analogue might lead eventually to the synthesis of the mixed Mo-W aqua ions.
3. Prepare the $[W_2O_4]^{4+}$ aqua ion from known routes and investigate other methods in the hope of achieving higher yields of the aqua ion. Since Sasaki et al and McMahon do not report same extinction coefficients and the same cyclic voltammetric behaviour, the reported results will have to be verified before any attempts at the syntheses of the mixed Mo-W aqua ions.
4. Attempt ^{17}O and ^{183}W NMR studies on the $[W_2O_4]^{4+}$ aqua ion to confirm its structure in solution.
5. Attempt preparation of the mixed aqua ions.
6. Characterise the new species by AAS, Zn/Hg reduction, Cyclic voltammetry, derivative preparations using NCS^- and other ligands leading hopefully to an X-ray study.
7. Attempt ^{17}O NMR study on the mixed aqua ions.

EXPERIMENTAL PROCEDURES AND RESULTS

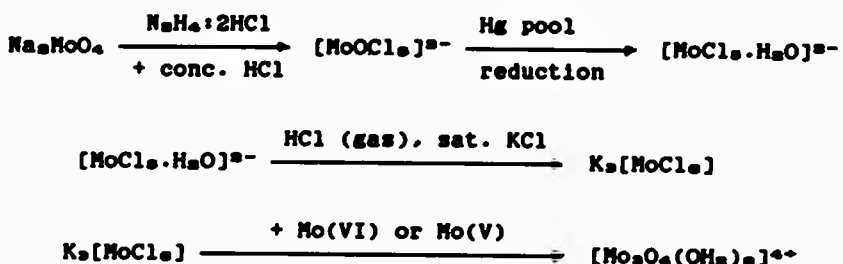
General details :

Standard AnalR or laboratory grade reagents were used without further purification unless otherwise stated. All electronic spectra were recorded on a Perkin-Elmer Lambda 5 UV-visible spectrophotometer at 25°C in 0.1 cm and 1.0 cm quartz cells. The tungsten and molybdenum contents of solution, where necessary were determined by using flame atomic absorption spectrophotometry on a Pye-Unicam SP9 spectrophotometer, using a fuel-enriched nitrous oxide/acetylene flame.

Samples of H_2O^{17} (10.5 atom %) were obtained from YEDA Isotope company, Rehovot, Israel and ^{17}O NMR spectra were recorded on Brüker AM-400 (Lausanne) and AM-300 (St. Andrews) spectrometers working at 54.24 and 40.68 MHz respectively. Electrochemical measurements were carried out with a Princeton Applied Research model 170 system using a standard three electrode cell design containing a mercury cup (or Platinum disc) working electrode, platinum counter electrode, and a saturated calomel reference electrode (see Appendix 1 for diagram of cell and electrodes). Elemental analyses (C, H and N) were carried out with a Carlo Erba Strumentazione elemental analyzer Model 1106. Air-free conditions had to be maintained throughout by means of N_2 or Ar, with manipulations performed using nylon syringes, Teflon tubing, stainless steel needles, and rubber serum caps.

1.6 Methods for the preparation of the $[Mo_3O_6]^{4+}$ aqua ion.1.6.1 Preparation of the $[Mo_3O_6]^{4+}$ aqua ion from Mo(III) and Mo(VI).¹⁰

The following scheme was adopted for the preparation of $[Mo_3O_6]^{4+}$ aqua ion:



Samples of $K_2[MoCl_6]$ were prepared following the method of Lohmann and Young.¹⁰ Sodium molybdate (B.D.H., 41 g) was dissolved in concentrated HCl (500 cm³) in a 600 cm³ beaker. Hydrazine hydrochloride (B.D.H., 33 g) was added and the mixture was kept at 80°C for 3 hours. The resulting emerald green solution was then filtered ($[MoOCl_6]^{4-}$). This solution was transferred to the mercury pool reduction vessel (using oxygen free conditions) and Mo(V) was reduced to Mo(III) ($[MoCl_6(OH_2)_6]^{4-}$, red-brown) using a current of 0.4 A. The reduction took approximately 2 hours. Gaseous HCl was passed through the brown solution leading to the precipitation of small quantities of the Na salt of $MoCl_6^{4-}$ which was removed.

* $[Mo_3O_6(OH_2)_6]^{4+}$ abbreviated to $[Mo_3O_6]^{4+}$ (M = Mo or W).

Ch. 1: Experimental procedures & Results 39

Subsequent addition of saturated KCl led to precipitation of brick red $K_2[MoCl_6]$. After filtration, and air-drying the purity of $K_2[MoCl_6]$ was checked by dissolving a known amount of solid in concentrated HCl and determining the Mo(III) concentration from its electronic spectrum ($\epsilon_{400} = 48 M^{-1} cm^{-1}$ and $\epsilon_{500} = 26 M^{-1} cm^{-1}$).¹² This showed that the salt was 60% pure with the principal impurity being probably KCl. Thus during experiments which required stoichiometric amounts of $K_2[MoCl_6]$, weights were used which accounted for the amount of KCl impurity present.

A solution of $Na_2[MoO_4] \cdot 2H_2O$ in 2M HCl (0.3M, 25 cm³) was added to a solution of $K_2[MoCl_6]$ in 2M HCl (0.3M, 50 cm³). Deoxygenation was achieved by bubbling N₂ through both solutions for 30 minutes prior to mixing. The reaction mixture was then kept for one hour at 80-90°C under N₂, and the resulting solution stored at 0-4°C in a refrigerator. A 10-20 cm³ sample of this stock was diluted 50 times with 0.5M Hpts and allowed to stand for at least one day to allow aquation of the coordinated chloride. To isolate the Mo(IV) aqua ion, the solution was passed through a Dowex 50W-X2 cation-exchange column (16x1 cm, H⁺ form). A dark-red band was formed with a diffused yellowish-brown band of the Mo(V) aqua ion $^{+}[Mo_2O_4]^{2+}$ forming below this. Elution of the Mo(V) aqua ion was achieved with 0.5M Hpts (200 cm³). The characteristic electronic spectrum

* $[Mo_2O_4(OH_2)_8]^{2+}$ abbreviated to $[Mo_2O_4]^{2+}$

showing peak maxima at 295 nm (ϵ 3500 M⁻¹ cm⁻¹), 384 nm (ϵ 103) and 490 nm (ϵ 43). The red Mo(IV) band moved down the column under these conditions and in some cases separated into two, the first of which was eluted with 1M Hpts (100 cm³) and contained chloride ions. The second band, which contained the [Mo₅O₆]⁴⁺ aqua ion was eluted with 2M Hpts. An electronic spectrum of the aqua ion is shown in figure 1.14. It has an absorption maximum at 505 nm (ϵ 63 M⁻¹ cm⁻¹) and a minimum at 437 nm (ϵ 54 M⁻¹ cm⁻¹). ϵ per Mo atom.¹⁰

1.6.2 Preparation of [Mo₅O₆]⁴⁺ aqua ion from MoCl₄(MeCN)₂.

The complex MoCl₄(MeCN)₂ was the first mononuclear Mo(IV) complex investigated with view to a possible preparation of the [Mo₅O₆]⁴⁺ aqua ion by direct aquation and was prepared following the method of Powles et al.^{10a} Molybdenum pentachloride (MoCl₅, Aldrich, 2 g) was added to acetonitrile (30 cm³) in a Schlenk vessel and the mixture was stirred for several hours. The addition of MoCl₅ was performed in a glove box as it is highly air and moisture sensitive. The acetonitrile was dried by using CaH₂ and purified by distillation. It was also deoxygenated prior to use by bubbling N₂ gas through it for half an hour. After 3 hours, brown MoCl₄(MeCN)₂ had precipitated out. This was filtered using a pressure of N₂ and dried by keeping a stream of N₂ over it for several hours. The CHN content was analyzed (found: C(15.24%), H(2.08%), N(8.64%); calculated for MoCl₄(MeCN)₂ : C(15.00%), H(1.88%), N(8.75%).



Figure 1.14 Electronic spectrum of $[\text{Mo}_3\text{O}_4(\text{OH}_2)_8]^{4+}$ (—), $[\text{W}_3\text{O}_4(\text{OH}_2)_8]^{4+}$ (— —) and $[\text{Mo}_2\text{WO}_4(\text{OH}_2)_8]^{4+}$ (— · —) in 2M Hpts.

Ch. 1: Experimental procedures & Results 42

A sample of $\text{MoCl}_4(\text{MeCN})_2$ (2 g) was added to deoxygenated 2M HCl (40 cm³) and the mixture was kept at 80°C for 2 hours. A 10 cm³ sample was removed and diluted 50 times with 0.5 M Hpts. The $[\text{Mo}_2\text{O}_4]^{4+}$ aqua ion was then separated and isolated as described in section 1.6.1. The yield of aqua ion obtained was 70% based on $\epsilon = 63 \text{ M}^{-1} \text{ cm}^{-1}$ (per Mo atom) at 505 nm absorption maximum.

1.6.3 Preparation of $[\text{Mo}_2\text{O}_4]^{4+}$ aqua ion from MoCl_4 .

Molybdenum tetrachloride (MoCl_4) was prepared following the method of Larson and Moore.¹⁰² For this preparation, MoCl_5 (20 g) had to be further purified by re-sublimation at 180°C in a 3 compartment carius tube which was sealed under vacuum (a diagram of the tube is given in figure 1.15). The sublimation took a total of 10 hours to complete. The tube was then transferred to the glove box and broken at each of the constrictions. The shiny black MoCl_5 , which collected in the middle compartment, was immediately isolated and added to deoxygenated benzene (150 cm³) in a two necked round bottom flask. The benzene had been dried over CaH_2 and distilled under N_2 prior to use. After removing the flask from the glove box, the mixture was refluxed under an atmosphere of N_2 for 10 hours. This operation was carried out in a fume cupboard. The excess benzene was then pumped off by means of a vacuum line leaving a black residue of MoCl_4 which was then stored under vacuum or in the glove box using a Schlenk vessel. This compound was found to be extremely air sensitive and samples

which were exposed to air for the briefest of periods turned greenish-brown and developed an Mo=O vibration at 980 cm^{-1} (probably from a mixture of MoOCl_3 and MoOCls).

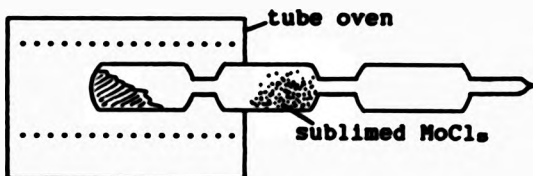


Figure 1.15 Diagram showing sublimation apparatus for MoCl_5

To a pre-weighed Schlenk vessel, a sample of freshly prepared MoCl_4 was added and its weight determined by difference. Deoxygenated 2M HCl (20 cm^3) was then added to it. The immediate yellow brown colour changed to reddish brown within 5 minutes. The mixture was kept at 80°C for half an hour and filtered. The red/brown solution was then diluted 10 times with 0.5 M HCl and left to equilibrate for several hours. It was then passed through a column of Dowex 50W-X2 cation-exchange resin (H^+ form). A red band was observed on the column but the eluent was yellow and indicated that a substantial amount of the $[\text{Mo}_2\text{O}_6]^{2+}$ aqua ion had been produced. The electronic spectrum of the eluent confirmed this showing peak maxima at 295 nm ($\epsilon 3500\text{ M}^{-1}\text{ cm}^{-1}$), 384 ($\epsilon 103$) and 490 ($\epsilon 43$). Samples of 0.5 M HCl (200 cm^3) were continually passed through the column to elute any remaining Mo(V) aqua ion and chloro

Mo(IV) species. The red band on the column was then eluted with 2M HCl. The electronic spectrum confirmed the presence of the $[W_3O_6]^{4+}$ aqua ion giving yield of 30% (based on λ_{max} 505 nm, ϵ 63 M $^{-1}$ cm $^{-1}$ per Mo atom).

1.7 The developments of improved methods for the synthesis of the W(IV) aqua ion $[W_3O_6]^{4+}$.

In order to pursue multinuclear NMR studies on the trinuclear W(IV) aqua ion, further investigation to the reported methods were required. The NMR technique, although diagnostic, suffers from the disadvantage that, where nuclei with low natural abundance are studied, high concentrations of the species are required.

1.7.1 A reinvestigation of the reported synthesis^a of the $[W_3O_6]^{4+}$ aqua ion using $Na_2WO_6(C_2O_4)_n \cdot 3H_2O$.

The procedure described earlier by Collenberg¹⁰³ has recently been used by Novak and Podlaha¹⁰⁴ to obtain $K_2[WO_6(C_2O_4)_n] \cdot 3H_2O$ and $[NH_4]_2[WO_6(C_2O_4)_n] \cdot 2H_2O$. A similar procedure was used in this study to obtain the Na^+ salt. Oxalic acid (20 g) and sodium tungstate (B.D.H., 15 g) were dissolved in H_2O (300 cm 3). Sodium tungstate (B.D.H., 15 g) was then added and the solution brought to the boil. At this point granulated tin (15 g) was slowly added with stirring. Oxygen-free conditions were maintained throughout the preparation, use being made of rubber

* $[W_3O_6(OH_2)_n]^{4+}$ abbreviated to $[W_3O_6]^{4+}$

Ch. I: Experimental procedures & Results 45

seals and teflon tubing for keeping a N_2 atmosphere over the reaction vessel. The mixture was then heated on a steam bath for 3-4 hours during which time, the colour changed to red-brown. After reduction of the volume to 100-120 cm³ and subsequent cooling to 0°C, oxalic acid and sodium oxalate were removed by filtration. Tin sulphide was then precipitated by passing Na_2S through the solution for 10 minutes at 0°C. After filtration air-free methanol (40 cm³) was added to precipitate any remaining oxalate. A further 300 cm³ of ethanol were added, and the orange powder filtered off, washed with ethanol and ether. The powder was dried by keeping a stream of N_2 over it for several hours. A yield of 13 g of $\text{Na}_2\text{WO}_6(\text{C}_2\text{O}_4)_n \cdot 3\text{H}_2\text{O}$ were obtained and the elemental analysis gave C = 10.07% and H = 1.12% which is in good agreement with the calculated (C = 9.30% and H = 1.15%).

A sample of $\text{Na}_2\text{WO}_6(\text{C}_2\text{O}_4)_n \cdot 3\text{H}_2\text{O}$ (2 g) was dissolved in deoxygenated conc. HCl (100 cm³) and the W(V) was reduced over a stirred slurry of amalgamated zinc (50 g)* until the initial deep blue colour had changed to greenish-brown. Deoxygenated water (200 cm³) was syphoned into the reaction vessel by using a pressure of N_2 to dilute the HCl to 4M. The solution was then kept at 80°C for 2 hours. The orange-brown solution was then syphoned into deoxygenated water (2 l) in a 3 1 flask and left for 4 hours to allow aquation of any remaining coordinated

*Amalgamated zinc prepared by stirring granulated zinc in a solution of 2 M HCl containing 0.1 M MgCl_2 .

Ch. 1: Experimental procedures & Results 48

oxalate. After passing the solution through a column of Dowex 50W-X8 cation-exchange resin (H^+ form) and eluting any low charged species with 1M HCl (2 l), the $[W_6O_4]^{4+}$ aqua ion was eluted with 2M HCl. At this stage it was dilute (0.02 M, based on $\epsilon = 89 M^{-1} cm^{-1}$ (per W) at 466 nm). Although the yield was 40%, the dilute solution would not be suitable for ^{17}O NMR study. In order to get a more concentrated sample, the aqua ion was rediluted ($[H^+] = 0.5$ M) and the solution was passed through a column of Dowex 50W-X2 cation-exchange resin. Elution with 3M HCl gave a concentrated sample ($=0.1$ M per W) but the yield had dropped to 10-13%. The electronic spectrum of the aqua ion is illustrated in figure 1.14.

Unlike the column behaviour of the $[Mo_6O_4]^{4+}$ aqua ion, the $[W_6O_4]^{4+}$ ion, at these concentrations swamps the whole column (50W-X2) and its elution with 3M acid does not clear the column. This indicated that other polymeric species are also produced which bind to the column very strongly. These species were not characterised further in the time available but clearly contributed to the low yields of the aqua ion obtained.

As a modification to this method, the initial reduction of $NasWO_6(C_2O_4)_n \cdot 3H_2O$ was carried out in 4M Hpts. The usual method of isolating the $[W_6O_4]^{4+}$ failed to give any improvement on the yield.

1.7.2 Attempted Preparation of the $[W_6O_4]^{4+}$ aqua ion from $WCl_6(RCN)_6$ (R = Me, Et, n-Pr).

Preparation of $WCl_6(RCN)_6$ was attempted via an analogous reaction to that for $MoCl_6(MeCN)_6$.¹⁰⁸ Tungsten hexachloride, WCl_6 (Aldrich, 2 g) was added to an excess of RCN (30 cm³) in a Schlenk vessel. On leaving the solution continuously stirring for up to 10 days no solid was observed to separate out. The following three procedures were attempted for obtaining the product.

- a) The excess RCN was removed using the vacuum line. This left a crude oily mixture which was brown in colour (probably $WCl_6(RCN)_6$ with trapped solvent).
- b) Various solvents (dichloromethane, hexane, benzene, toluene, diethyl ether) were added in the hope of precipitating the product. None of these proved successful. All solvents used were freshly distilled over CaH_2 and thoroughly deoxygenated prior to use and the reactions were carried out in the fume cupboard.
- c) Without further attempts, therefore to isolate the $WCl_6(RCN)_6$ complex, 4M HCl (30 cm³) was syphoned into the reaction vessel under N_2 and the mixture was kept at 80°C for 1 hour. Upon heating the colour immediately changed to blue and ultimately deposited a blue solid from a yellow solution. Cation-exchange chromatography on Dowex X6 and X2 resin however failed to detect the presence of $[W_6O_4]^{4+}$ from this solution.

1.7.3 Attempted preparation of $[W_5O_6]^{4+}$ aqua ion from

$WCl_6 \cdot (py)_n$

A sample of WCl_6 (2 g) was added to deoxygenated pyridine (60 cm³) in a Schlenk vessel and the dark brown solution left to stir. After several hours a light brown solid separated out which was filtered, washed with diethyl ether and dried by keeping a stream of N_2 over it for several hours. Filtration was done using a pressure of N_2 . The CHN analysis was in good agreement with the calculated values for $WCl_6(py)_n$ (found: C=32.2%, H=2.6%, N=7.2%; calculated: C=33.5%, H=2.6%, N=7.6%). A solid reflectance spectrum (Nujol mull) and an ir spectrum (KBr disc) were also taken. These were similar to those reported in the literature.^{7a}

A sample of $WCl_6 \cdot (py)_n$ (2 g) was then added to deoxygenated 4M HCl (30 cm³) in a Schlenk vessel and the mixture was kept at 80°C. The mixture again slowly turned blue and eventually deposited a blue solid from a yellow solution which appeared to be identical to that obtained with $WCl_6(MeCN)_n$. No $[W_5O_6]^{4+}$ ion was isolated following cation-exchange chromatography.

1.7.4 Preparation of $[W_5O_6]^{4+}$ aqua ion from $K_4W_5OCl_{10}/K_2W_5Cl_n$

A sample of WCl_6 (4 g) was added to 4M HCl (30 cm³) and the W(VI) was reduced to W(III) with granulated tin over a period of 2 hours (25°C). As the reduction proceeded the yellow colour changed to red-brown then violet and finally to green. The green solution was then saturated with HCl gas and

saturated KCl was added to precipitate the grey-green salt $K_2W_2Cl_{10}$. Partial reduction of the original solution as far as the violet colour gave a violet solid upon saturation with HCl gas and addition of saturated KCl. This is reported^a to contain the salt $K_2W_2OCl_{10}$. Both salts showed spectral properties similar to those reported in the literature^{a-c} but both were highly impure and contained ~ 40% excess KCl (table 1.4).

Table 1.4 Electronic spectral characteristics of $[W_2Cl_{10}]^{2-}$ and $[W_2OCl_{10}]^{4-}$

Species	λ_{max} (nm)	$\epsilon M^{-1} cm^{-1}$	ref.
$[W_2Cl_{10}]^{2-}$	757 614	ca. 25(10) ca. 400(160)	5b
$[W_2OCl_{10}]^{4-}$	535 sh 300 sh 288 sh 244 230 sh	$\geq 3\ 800^*$ 4 500(2250) 10 600 17 200(7000) 16 000	8

ϵ values obtained from present work given in parentheses.

Using both of these salts it was possible to make the $[W_2O_4]^{4-}$ aqua ion by adding the salts to 4M HCl and keeping the mixture at 80°C for 2 hours. The yield of the aqua ion obtained was only between 1-4% and thus of little practical use.

While this work was in progress, Sasaki et al^c reported a successful preparation of the $[W_2O_4]^{4-}$ ion via aquation of

* The intensity of this band is reported to decrease rapidly with time. The extrapolated ϵ value at t=0 is 19000.

Ch. I: Experimental procedures & Results 50

potassium hexachlorotungstate(IV). It was decided therefore to attempt a preparation of $[W_6O_4]^{4-}$ by this method in order to check the authenticity of the reported electronic spectral parameters as a result of differences in comparison with the method reported using $K_2[WO_3(C_2O_4)_2].3H_2O$.⁴⁸

1.7.5 Preparation of the $[W_6O_4]^{4-}$ aqua ion from $K_2[WCle]$.

Potassium hexachlorotungstate(IV), $K_2[WCle]$ was prepared following the method of Kennedy and Peacock.⁷⁰ A sample of $WCle$ (40 g) was heated to 180°C in a carius tube with an excess of KI (50 g) for 3 days. The tube was constantly pumped on the vacuum line ($\sim 10^{-2}$ mmHg). After 3 days the temperature was raised to 280°C and the excess I₂ was sublimed out by using the vacuum line. The red-brown $K_2[WCle]$ was removed and kept in a Schlenk tube.

A sample of $K_2[WCle]$ (2 g) was added to 2M HCl (25 cm³, deoxygenated) in a Schlenk vessel and kept at 90°C for 2 hours. Within 5 minutes the colour of the mixture became orange-brown. After 2 hours, the mixture was filtered using a pressure of N₂ and diluted 40 times by addition of deoxygenated Hpts (0.5M, 1 l). After leaving the solution for 4 hours (to aquate any coordinated chloride ions), the solution was passed through a Dowex 50W-X2 cation-exchange resin (H⁺ form, deoxygenated). The whole column (16 x 2 cm) became masked by an intense dark brown band with a brown solution found to pass straight through. A solution of Hpts (0.5M, 1 l) was passed through the

column followed by further washing with Hpts (1M, 500 cm³). The 1M Hpts washings were found to be orange-brown and an analysis of its electronic spectrum confirmed the presence of the [W₂O₆]⁴⁺ aqua ion. The colour was very faint and most probably contained mono- and/or dichloro complexes of the aqua ion having 3+ and 2+ charges respectively. The column was still intensely coloured and a sample of the aqua ion was obtained by eluting slowly with 2M Hpts. The spectrum shows a maximum at 455 nm and a shoulder at 320 nm. The spectrum is shown in figure 1.14.

1.7.6 Determination of the tungsten content of the orange [W₂O₆]⁴⁺ aqua ion by atomic absorption spectroscopy.

Tungsten samples were made up by dissolving sodium tungstate(VI) in distilled water and diluted into the range 0.5-10.0 mM for comparison with the samples of [W₂O₆]⁴⁺. Absorbance measurements (average of 10 readings) were taken following syphoning of each solution into a fuel enriched nitrous oxide/acetylene flame operating with the following settings:

Wavelength used = 255.1 nm

Fuel flow rates = N₂O 6.5 l min⁻¹, C₂H₂ 4.8 l min⁻¹

Under these conditions, the standard tungstate samples gave a linear calibration curve with an absorbance of 0.34 for 0.5 mM W. However, samples of the aqua ion solutions estimated to be in the same concentration range showed large fluctuations in

the absorbance readings and a value for the W content that was not in agreement with the ϵ_{455} value $125 \text{ M}^{-1} \text{ cm}^{-1}$ per W reported by Sasaki et al.⁴⁰ Since it has been established that this ion contains W(IV) it was decided to analyse the W content using titration to W(VI) with solution of Ce(IV).

1.7.7 Estimation of the tungsten content of the $[\text{W}_2\text{O}_7]^{4-}$ aqua ion by Ce(IV) titration, assuming W(IV).

A dilute Ce(IV) stock solution in 1 M H_2SO_4 (= 0.01 M) was standardized by titrating a known volume with a standard solution of ammonium ferrous sulphate. The exact [Ce(IV)] was found to be 0.0080 M. A sample of the aqua ion (2 cm^3 , accurately measured using a Hamilton syringe) was added to a 100 fold excess of Fe(III). (3 cm^3 of 1 M $\text{Fe}_2(\text{SO}_4)_3$ in 1 M H_2SO_4). The solution was stirred and kept under an inert atmosphere for 15 minutes. After this the mixture was opened to the atmosphere and 1M H_2SO_4 (10 cm^3) was added to it before titrating with Ce(IV) using ferroin ($[\text{Fe}(\text{phen})_3]^{2+}$) as indicator. Assuming that the oxidation state per W was 4+ the following set of equations illustrate the redox processes involved and allow the calculation of the total W(IV) content in the aqua ion and hence the extinction coefficient at the 455 nm peak maximum.

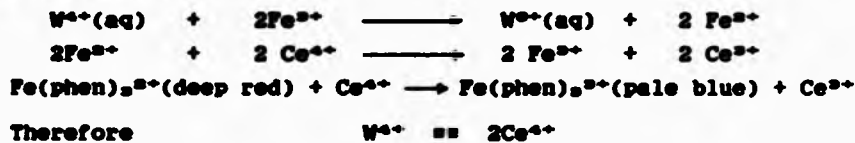


Table 1.5 gives the results for a solution of the aqua ion prepared in 2M Hpts. This solution of the aqua ion gave an absorbance at 455nm of 1.26 using a 1 cm quartz cell.

Table 1.5 Determination of ϵ at 455 nm peak maximum by Ce(IV) titrations.

Volume of Ce(IV) required	No of moles Ce(IV) required	No of moles W(IV) present	Extinction* coefficient at 455 nm
5.24 cm ³	4.18 x 10 ⁻³	2.08 x 10 ⁻³	122.4
5.12 ..	4.08 ...	2.04 ...	125.3
5.18 ..	4.13 ...	2.07 ...	123.8
5.04 ..	4.02 ...	2.01 ...	127.3
5.08 ..	4.05 ...	2.03 ...	125.3
5.12 ..	4.08 ...	2.04 ...	125.3
<i>Average $\epsilon = 125.0 \text{ M}^{-1} \text{ cm}^{-1}$</i>			

* per W atom ($\text{M}^{-1} \text{ cm}^{-1}$)

The value $125 \text{ M}^{-1} \text{ cm}^{-1}$ per W atom obtained from this study is exactly in agreement with that of Sasaki et al¹⁰ obtained using AAS though details of their method were not fully discussed.

1.7.8 Modifications to obtain higher yields and avoid the presence of excess chloride.

Subsequent studies using ^{17}O NMR on $[\text{W}_5\text{O}_4]^{4+}$ have indicated the possible presence of coordinated chloride ions surviving column treatment (see later). In order to remove the high levels of background chloride inherent in the reported preparation, a

number of improvements/modifications were investigated. The principal one involved heating $K_2[WCls]$ in 2 M Hpts at 90°C over varying time periods ranging from 10 minutes to 2 hours followed by dilution with 0.5 M Hpts and aquation for 1 day at 25°C. Following loading of the resulting solution onto a Dowex 50W-X2 column, it was washed with 0.5 M and 1.0 M Hpts prior to elution with 4 M Hpts. Similar yields of 25% (based on $\epsilon_{\text{abs}} = 125 \text{ M}^{-1} \text{ cm}^{-1}$ per W) were obtained following two hours heating. Much shorter 10 minute heating times gave rise to higher yields (50%) but evidence of coordinated chloride ions (see ^{17}O NMR section).

1.7.9 Studies on the redox chemistry of the $[W_2O_8]^{4-}$ aqua ion prepared via $K_2[WCls]$.

A solution of the $[W_2O_8]^{4-}$ aqua ion (3 mM) in 3M HCl was stirred under a continuous stream of N_2 with a slurry of freshly prepared zinc amalgam (10 g). Within 3 hours an emerald green solution had formed. The electronic spectrum of a solution of the aqua ion was taken by syphoning some of the solution through a serum cap into a de-oxygenated 1 cm quartz cell. The spectrum showed 2 peaks at 678 nm ($\epsilon 202 \text{ M}^{-1} \text{ cm}^{-1}$) and 313 nm ($\epsilon 342$) and a shoulder at ca. 420 nm (ϵ ca. 154) (figure 1.16).

When a sample of this emerald green species was studied spectrophotometrically after brief exposure to air over a 2 hour period it was seen to rapidly revert to its original

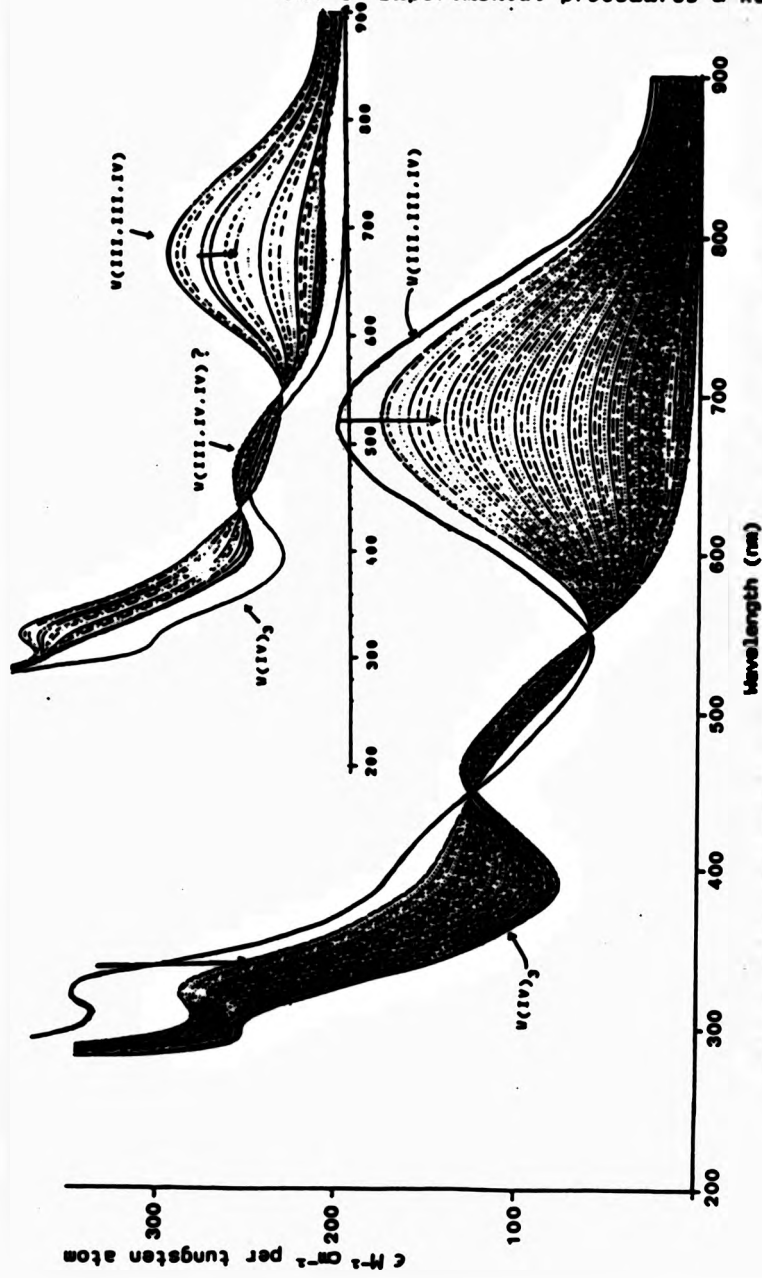


Figure 1.16 Electronic spectrum of the mixed-valence $\text{W}(\text{III},\text{III},\text{IV})$ aqua ion in 3M HCl monitored over 60 min. in air (Inset: Spectrum reported by McMahon⁴⁹)

Ch. 1: Experimental procedures & Results 56

orange colour (λ_{max} 480 nm), with isosbestic points being observed at 448 nm and 548 nm. Towards the end these isosbestic points were lost as the spectrum of $[\text{W}_5\text{O}_4]^{4+}$ aqua ion was regenerated. A similar study by McMahon⁴⁹ reported that a further intermediate species was present with λ_{max} at 750 nm. From this preparation however there was no clear evidence for this species.

1.7.10 Determination of the formal oxidation state for W in the emerald green solution.

A sample (15 cm³) of the $[\text{W}_5\text{O}_4]^{4+}$ aqua ion was fully reduced using Zn/Hg. The oxidation state of the emerald green solution was determined by redox titration with Ce(IV) as described previously. The results obtained are given in table 1.6 and are calculated based on $\epsilon = 125 \text{ M}^{-1} \text{ cm}^{-1}$ (at 455 nm).

Table 1.6 Formal oxidation state of W in the emerald green solution.

Volume of Ce(IV) required	No of moles Ce(IV) required	No of moles W(IV) added	Formal ox state of aqua ion
5.36 cm ³	4.30×10^{-3}	1.62×10^{-3}	3.35
5.32 ..	4.26 ...	1.62 ...	3.37
5.34 ..	4.27 ...	1.62 ...	3.36
Av. ox st = 3.36			

Ch. I: Experimental procedures & Results 57

On the basis of this value it can be concluded that emerald green species is the mixed oxidation state species: W(III,III,-IV) with formal oxidation state 3.33. This finding was in exact agreement with the similar detection of a W(III,III,IV) reduction product by Sasaki et al.⁴⁸

1.7.11 Cyclic voltammetry of the orange $[W_5O_4]^{4+}$ aqua ion and the red $[Mo_5O_4]^{4+}$ aqua ion in 3 M HCl.

The redox chemistry of both the aqua ions of $[Mo_5O_4]^{4+}$ and $[W_5O_4]^{4+}$ have been studied by the technique of cyclic voltammetry. The working electrode used was of the mercury cup design. A diagram of the basic cell design and some basic theory of the technique is given in appendix 1. The $[Mo_5O_4]^{4+}$ aqua ion shows two reduction waves in 3.0 M HCl at -0.1 V and -0.18 V (vs N.H.E.) at 25°C (figure 1.17) due to successive formation of the mixed-valence Mo(III,III,IV) and Mo(III)₂ aqua ions.

For $[W_5O_4]^{4+}$, Sasaki et al⁴⁸ reported an irreversible reduction wave at -0.25 V (vs N.H.E.) from polarographic measurements performed on $[W_5O_4]^{4+}$ in 2 M Hpts at 25°C. Studies in both 3 M HCl and 3M Hpts in this laboratory have failed to detect the presence of such a wave as far as the hydrogen overpotential on mercury at these acidities (= -0.6 V). However, in one isolated experiment on $[W_5O_4]^{4+}$ the use of freshly prepared double distilled mercury and pure analar acid reagents allowed the hydrogen overpotential to be extended to beyond - 0.9 V (vs

N.H.E.) allowing resolution of a reversible $2e^-$ reduction wave centred at -0.79 V (vs N.H.E., figure 1.17) believed to be due to formation of the emerald-green mixed-valence W(III,III,-IV) ion.

Consistent with the electronic spectroscopic observations the cyclic voltammetry results provided no evidence that a W(III)_{aqua} ion could be formed following reduction of $[W_6O_4]^{4+}$. The W(III,III,IV) mixed-valence aqua ion is believed to be the analogue of the corresponding Mo(III,III,IV) ion with possible structure $[W_6(OH)_4]^{4+}$. However, owing to the difficulties apparent in observing the reduction wave for $[W_6O_4]^{4+}$, further detailed studies on this process, for example, as a function of $[H^+]$ have not been possible so far. Furthermore, consistent with the highly negative reduction potential of -0.79 V (vs N.H.E.), solutions of the W(III,III,IV) aqua ion are extremely air sensitive and, from experiments in sealed tubes in the absence of air are also slowly oxidized by protons to give back $[W_6O_4]^{4+}$. Further redox studies have shown that solutions of Eu²⁺ ($E^\circ = -0.41$ V vs N.H.E.) rapidly reduced $[W_6O_4]^{4+}$ completely to the Mo(III)_{aqua} ion as expected but are unreactive towards $[W_6O_4]^{4+}$. It is thus concluded that the potential for reduction of $[W_6O_4]^{4+}$ is more negative than -0.41 V and clearly not consistent with the value of -0.25 V reported by Sasaki et al.⁴⁸ but rather more consistent with the value of -0.79 V obtained here from the one successful cyclic voltammetric experiment.

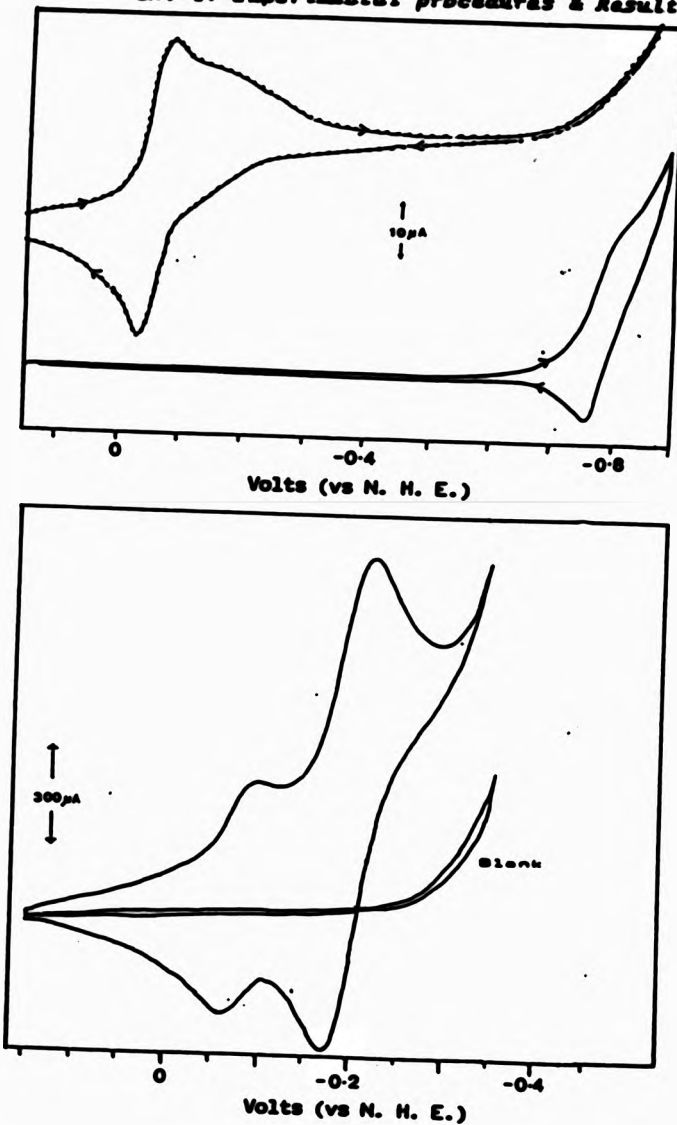


Figure 1.17 Cyclic voltammogram of $[\text{Mo}_5\text{O}_4(\text{OH}_2)_6]^{4+}$ (top left), $[\text{W}_5\text{O}_4(\text{OH}_2)_6]^{4+}$ (top right) and $[\text{Mo}_5\text{WO}_4(\text{OH}_2)_6]^{4+}$ (bottom) in 3M HCl using mercury cup electrode.

1.7.12 ^{17}O NMR studies on the $[\text{W}_5\text{O}_4]^{4-}$ aqua ion.

For the recording of a ^{17}O NMR spectrum of the $[\text{W}_5\text{O}_4]^{4-}$ ion, a sample totally enriched in ^{17}O had to be synthesized. This was achieved as follows:

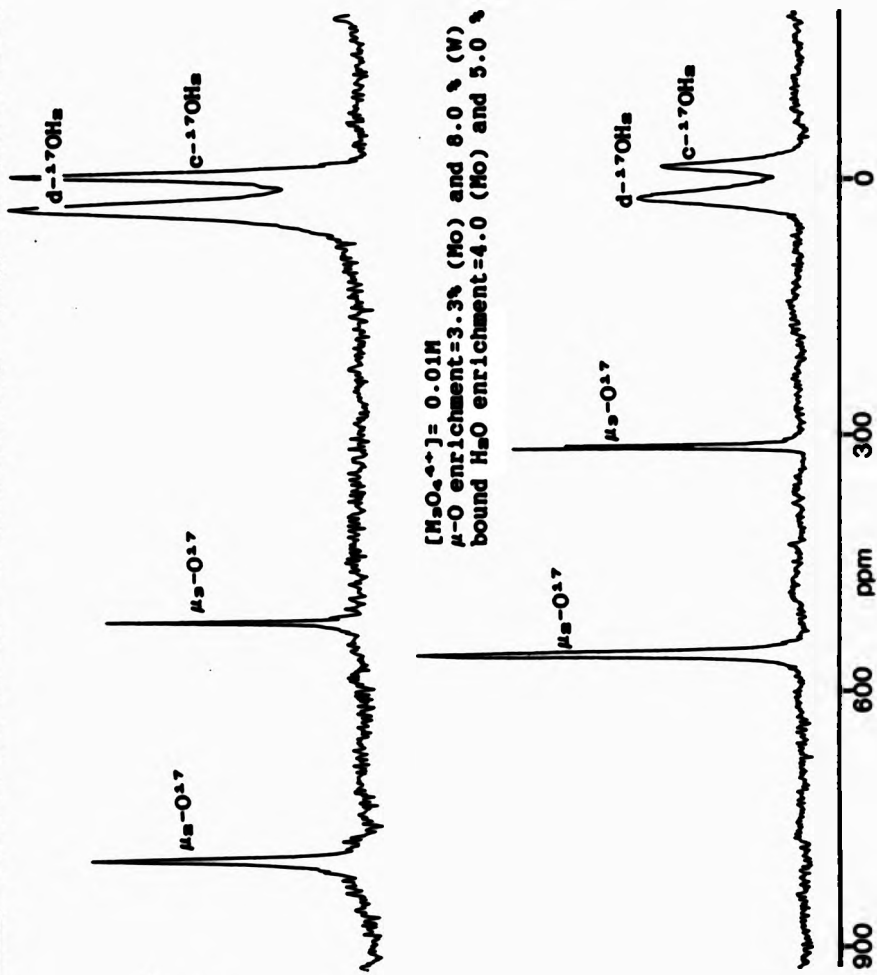
A sample of 4M HCl (2 cm³) was diluted with ^{17}O enriched water (2 cm³ of 8% H_2^{17}O) and deoxygenated with a stream of N_2 . A sample of $\text{K}_2[\text{WCl}_6]$ (3 g) was added to the HCl solution and kept at 80°C for 1 hour. Following dilution with 0.5 M Hpts and Dowex 50W-X2 cation-exchange chromatography as described previously enriched $[\text{W}_5\text{O}_4]^{4-}$ was eluted via displacement using a solution of 0.25M La(ptz)₃ in 1M Hpts. A narrow column (5 mm dia.) was used and elution was done at a very slow rate (1 drop every 30-60 sec). This enabled a concentrated sample of the $[\text{W}_5\text{O}_4]^{4-}$ aqua ion to be obtained (2 cm³, 0.25M per W). A 1 cm³ sample of this solution was diluted with a further 1 cm³ of H_2O^{17} (8%) containing 0.2 M $[\text{Mn}(\text{OH}_2)_6](\text{CF}_3\text{SO}_3)_2$. The addition of Mn^{2+} salts causes relaxation of the large ^{17}O enriched bulk water peak by paramagnetic exchange broadening (see Appendix 2) thus allowing resolution of the bound water resonances in the region ± 50 ppm from bulk water. The resonance line of CF_3SO_3^- , added via the Mn^{2+} salt, was used as reference (+159 ppm from bulk water) with the chemical shifts reported relative to this with bulk water = 0 ppm. The ^{17}O NMR spectrum was recorded at 54.24 MHz on a Brüker AM-400 instrument with the help of Dr L. Helm at the University of Lausanne (Switzerland). Between 1-4 K data points were used for the FID's using a pulse

Ch. 1: Experimental procedures & Results 81

width of 14 μ s. Typically 30-100 K scans were accumulated over the full sweep range of -400 to + 1200 ppm. Spline functions were applied to the transformed FID's in order to suppress the rolling base line. The resulting spectrum shown in figure 1.18 gave rise to the expected four principal resonance lines, two from the μ_2 and μ_3 -oxo groups in the expected 3:1 ratio and two from the bound water region. The spectrum was qualitatively similar to that obtained from a ^{17}O enriched solution of the $[\text{Mo}_3\text{O}_6]^{4+}$ aqua ion. The notable difference that can be immediately seen in figure 1.18 was that the resonances of the μ_2 and μ_3 -oxo groups in the W ion were shifted to higher field when compared to the Mo ion. The bound water region in contrast is little affected. This parallels the observations of Burtseva²¹ from comparisons of the ^{17}O chemical shifts of analogous polyoxomolybdates and polyoxotungstates and the chemical shifts scale shown in figure 1.11. For the $[\text{W}_3\text{O}_6]^{4+}$, close analysis of the integrations from the ^{17}O resonance lines, normalized with respect to their ^{17}O enrichment (~ 4%), allowed as with the $[\text{Mo}_3\text{O}_6]^{4+}$ ion a direct assignment of the $[\text{W}_3\text{O}_6(\text{OH}_2)_6]^{4+}$ triangular structure; the $\mu_2\text{-O}:\mu_3\text{-O}:\text{bound water}$ ratio being respectively 3:1:6:3 (~ 10%). As found with $[\text{Mo}_3\text{O}_6]^{4+}$, the bound water peak resonating at the higher field strength is due to the three water ligands lying trans to the capping μ_3 -oxo group in the structure.

The unique power of ^{17}O NMR in being able to directly assign under favorable conditions the correct oligomeric solution

Figure 1.18 Oxygen-17 NMR spectrum of $[\text{Mo}_2\text{O}_4(\text{OH}_2)_8]^{4+}$ (top) and $[\text{W}_2\text{O}_4(\text{OH}_2)_8]^{4+}$ (bottom).



Ch. 1: Experimental procedures & Results 63

structure for this aqua ion is once again apparent from this study (the alternative linear formulation for $[W_5O_6(OH_2)_6]^{4+}$ being neither consistent with the number of resonance peaks nor their respective integrations).

Close analysis of the resonances for $[W_5O_6]^{4+}$ due to the core μ_3 and μ_5 -oxo groups however showed that the line widths particularly for the capping μ_5 -oxo group (~50 Hz) were appreciably smaller than the corresponding lines for the $[Mo_5O_6]^{4+}$ (~ 200 Hz). Furthermore, it became clear that for the $[W_5O_6]^{4+}$ at least two overlapping bands for both core oxo groups were present. The initial conclusion was that this was due to the presence of both the conjugate base ion $[W_5O_6(OH_2)_6(OH)]^{3+}$ and $[W_5O_6]^{4+}$. This seemed reasonable on the basis of the known K_a (0.22 M)²⁴ for this aqua ion. However this possibility was ruled out by studies performed at higher acidity which led to no change in the features observed. The second conclusion was that the features were due to a change in the local electronic environment of the μ_5 -oxo group by coordination of 1 or more chloride ions to the $[W_5O_6]^{4+}$ core. Because of the small line widths observed in the case of the W ion, such small changes may be sufficient to allow resolution in this case. Further evidence for this came from a ^{183}W NMR study of this same solution determined at 16.67 MHz on the AM-400 instrument in Lausanne. Following 62,000 scans accumulated over a period of 12 hours, the spectrum in figure 1.19 was obtained referenced to $\delta^{183}W$ for 1M Na_2WO_4 = 0 ppm.

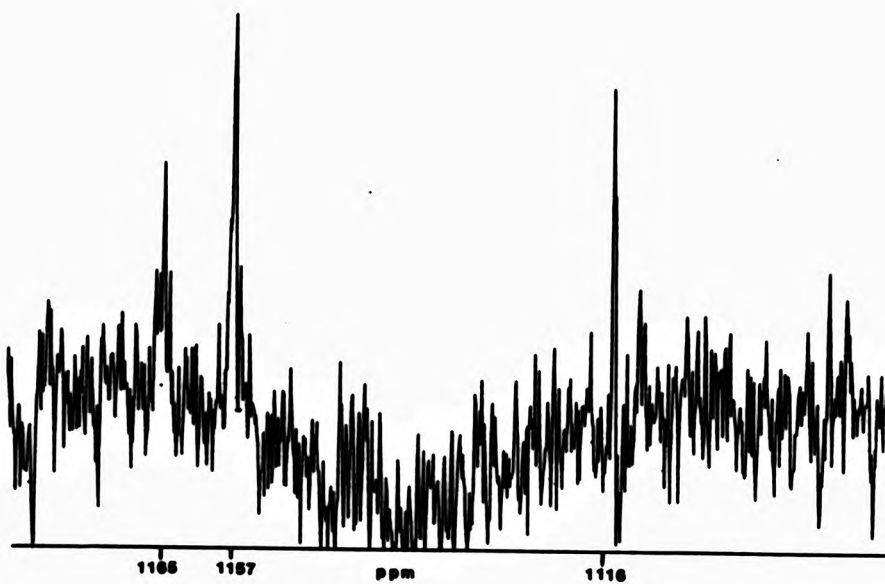
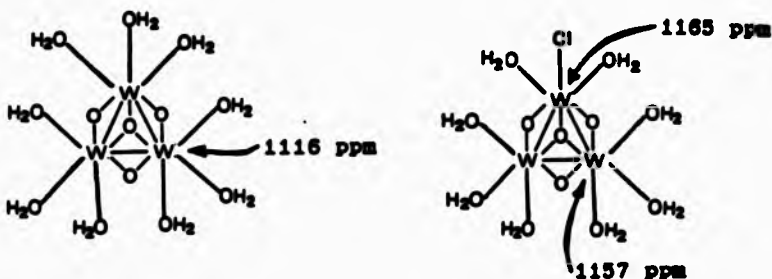


Figure 1.19 Tungsten-183 NMR spectrum of $[W_5O_4(OH_2)_2]^{4-}$.
 $[W_5O_4^{4-}] = 0.25$ M per W atom. (^{183}W referenced to 1M Na₂WO₄)

Pope et al.²² had recently reported a value for the ^{183}W chemical shift for the $[\text{W}_3\text{O}_6]^{4-}$ aqua ion of 1138 ppm (aqua ion prepared in saturated Hpts) but no experimental details were given. Three resonances in the range 1100-1200 ppm are observed for the $[\text{W}_3\text{O}_6]^{4-}$ in the present work. The single band at 1116 ppm is assigned to $[\text{W}_3\text{O}_6]^{4-}$. The other two bands are observed downfield at 1165 and 1157 ppm, are seen to be in approximately a 1:2 ratio and are therefore assigned to the two different W atoms present in a monochloro complex of $[\text{W}_3\text{O}_6]^{4-}$ shown in figure 1.20, the presence of the electron withdrawing chloride ion leading to the more downfield shifted W atom (1165 ppm) as expected.

Figure 1.20 ^{183}W chemical shifts for $[\text{W}_3\text{O}_6]^{4-}$ species.



Pope did not comment on the presence of several resonances from his sample of $[\text{W}_3\text{O}_6]^{4-}$ but it may be noted that his value of 1138 ppm is very close to the "average" value of the three chemical shifts obtained here.

Ch. 1: Experimental procedures & Results 88

Further experiments were conducted in the hope of further confirming the presence of a lower charged $[W_5O_4Cl]^{n+}$ species in addition to $[W_5O_4]^{n+}$ having survived the initial column treatment. It was thus decided to record ^{17}O NMR spectra of successive fractions of W(IV) eluted from a Dowex 50W-X2 column, which must, on the basis of charge, contain variable amounts of these W(IV) species and thus allow their detection. Surprisingly, the first fraction, most likely to contain both species, showed evidence of only one band for the μ_2 -oxo group whereas the later fractions showed increasing evidence of two bands (figure 1.21). The second of the two μ_2 -oxo bands observed at 317 ppm in the later fractions was thus assigned to $[W_5O_4]^{n+}$ with the band observed in all fractions, having the more downfield shift (320 ppm) assigned to $[W_5O_4Cl]^{n+}$.

Finally, confirmation that the appearance of the overlapping μ -oxo bands were due to Cl^- ions coordinated to the peripheral sites on the $[W_5O_4]^{n+}$ core was obtained by deliberately adding a 100 fold excess of Cl^- which caused further overlapping bands to appear in not only the μ_2 -oxo but also the μ_3 -oxo region (figure 1.22). Under these conditions, it was concluded that the major species being eluted from the Dowex column was the monochloro complex $[W_5O_4(OH_2)_nCl]^{n+}$ and not the aqua ion $[W_5O_4(OH_2)_n]^{n+}$.

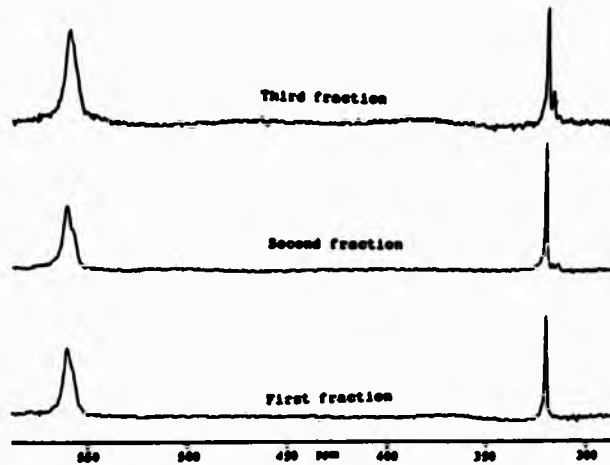


Figure 1.21 Oxygen-17 NMR spectra of successive fractions of $[W_3O_4]^{4+}$ eluted off the cation-exchange column. Resonance peak due to bound H_2O not shown.

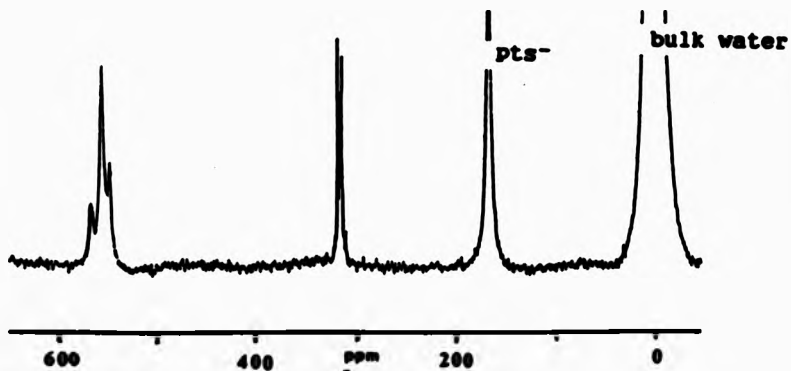


Figure 1.22 Oxygen-17 NMR spectrum of $[W_3O_4]^{4+}$ after deliberate addition of Cl^- . (Mn^{2+} not added)

1.7.13 Attempts to detect the presence of coordinated chloride in $[W_5O_9Cl]^{4+}$ aqua ion.

A sample of the $[W_5O_9]^{4+}$ aqua ion was prepared in Hpts/HCl medium as described previously. During the cation-exchange purification stages, 2 litres of 0.75M Hpts were passed through the column to ensure complete removal of any free Cl^- ions. The $[W_5O_9]^{4+}$ aqua ion was eluted with 2M Hpts and its electronic spectrum was recorded as a check of its presence. A sample (3 cm³) was added to concentrated HNO_3 (10 cm³) resulting in oxidation to a yellow precipitate of hydrated tungstic oxide. This was filtered and the supernatant was tested with $AgNO_3$ to check for free Cl^- . The solution immediately went turbid indicating the possible presence of Cl^- . However, when the test was repeated using a sample of Na_2WO_4 treated with nitric acid and filtered, this also showed turbidity. It was concluded that the turbidity also possibly results from the precipitation of sparingly soluble silver tungstates from amounts of W(VI) still present in solution. The results were therefore unfortunately inconclusive as a positive test for Cl^- under these conditions.

1.7.14 Oxygen-17 NMR studies on the reduction of $[W_5O_9]^{4+}$ to the mixed-valence W(III.III.IV) ion.

The core enriched sample of the $[W_5O_9]^{4+}$ aqua ion used in ¹⁷O NMR studies earlier was reduced to the emerald green mixed-valence W(III.III.IV) ion using amalgated zinc. Under

rigorous air-free conditions. the green solution was transferred to the NMR tube and sealed. An ^{17}O NMR spectrum was obtained following the same procedure as outlined for $[\text{W}_5\text{O}_6]^{4+}$ (figure 1.23). The spectrum showed the same features as those found for the $[\text{W}_5\text{O}_6]^{4+}$ aqua ion with the addition of a single resonance peak at 265 ppm. This was assigned to be a $\mu_2(\text{OH})$ peak thus supporting the "open" structure (discussed earlier in section 1.3.4 page 21) for the W(III,III,IV) mixed-valence species.

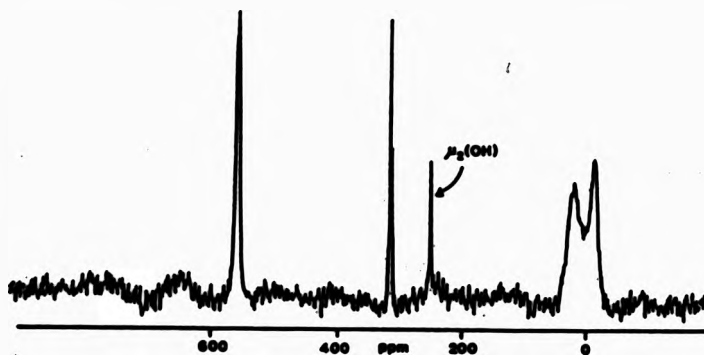


Figure 1.23 ^{17}O NMR spectrum of the emerald green mixed-valence W(III,III,IV) ion.

1.8 Attempted preparation of mixed Mo/W aqua ions.

Several methods were followed in order to prepare the $[\text{Mo}_2\text{WO}_4(\text{OH}_2)_8]^{4+}$ and $[\text{MoW}_2\text{O}_4(\text{OH}_2)_8]^{4+}$ mixed aqua ions. The ratio Mo:W was varied by taking the required amount of $\text{K}_2[\text{WCl}_6]$ and Na_2MoO_4 and $\text{K}_2[\text{MoCl}_6]$.

1.8.1 Attempted preparation of the $[Mo_2WO_6]^{4+}$ aqua ion.

Samples of $K_2[WClo_4]$ (2.35 g), and $K_2[MoCl_6]$ (7.7 g), representing a W:Mo ratio of 1:2, were added to 2M HCl (40 cm³) in a Schlenk vessel and the mixture was kept at 80°C for 2 hours. Filtration and subsequent cation-exchange purification as described previously for $[W_2O_6]^{4+}$ led to elution of a deep red-brown solution which contained a shoulder in the electronic spectrum at 500 nm. Cyclic voltammetry in 3M HCl using a Hg cup electrode showed two reversible waves at -0.08, and -0.25 V (vs N.H.E. at 25°C, figure 1.17). Neither of these waves were consistent with the presence of $[Mo_2O_6]^{4+}$ or $[W_2O_6]^{4+}$. Subsequent Zn/Hg reduction of this solution under N_2 led to an orange-brown colour after several hours. The electronic absorption spectrum of this solution was similar to the W(III,III,IV) ion generated from $[W_2O_6]^{4+}$ with a peak maximum at 680 nm. However, on exposure of this solution to air, a new peak at 850 nm, not consistent with either W(III,III,IV) or Mo(III,III,IV) was seen. This suggested that this solution in addition to the $[W_2O_6]^{4+}$ aqua ion contained a new species possibly a mixed Mo-W aqua ion. Further experiments were attempted in the hope of improving the yield of the mixed aqua ion.

1.8.2 Preparation of $[Mo_2WO_6]^{4+}$ from $MoCl_6$ and $K_2[WClo_4]$.

Freshly prepared $MoCl_6$ (1 g) and $K_2[WClo_4]$ (1 g) representing a Mo:W ratio of 2:1, were added to 2M HCl (20 cm³) in a Schlenk

vessel and the mixture was kept at 80°C for 30 minutes. The immediate yellow brown colour changed to red-brown within 5 minutes of heating. (When impure MoCl₆ was used the colour did not change to red brown and subsequent ion-exchange treatment led to recovery of [Mo₂O₆]²⁺ aqua ion as the only Mo containing species.) The red-brown mixture was filtered and the solution was diluted 5 times with 0.5M HCl (100 cm³). After leaving the solution to equilibrate for 4 hours, it was passed through a column of Dowex 50W-X2 cation-exchange resin (16 x 1 cm). Washing the column with 0.5M HCl (200 cm³) removed amounts of the yellow [Mo₂O₆]²⁺ aqua ion. A dark reddish-purple band remaining on the column was observed to move down during this stage. The column was further washed with 1M HCl (200 cm³). This brought down the purple species the electronic absorption spectrum of which showed a peak at 525 nm and a shoulder at 400 nm. Elution with 2M HCl eluted the purple band completely from the column. Its absorption spectrum showed a peak and a shoulder (λ_{max} 530. λ_{min} 470 nm. shoulder 400 nm) (figure 1.14). To prove that this was a genuine species it was rediluted to 0.5 M [H⁺] and reloaded on a fresh Dowex 50W-X2 column. A tight purple band was again formed on the column which could be eluted again with 2M HCl. In further experiments it was also possible to elute with 2M Hpts. When Hpts was used the band moved down much more slowly and its colour was more reddish. (λ_{max} 515 nm). Cyclic voltammetry on the resulting solution in 3 M HCl using a Hg cup electrode showed

the same two reversible waves (figure 1.17) as observed in the previous preparation (section 1.6.1).

The above procedure was repeated using Hpts instead of HCl. This was shown to yield an identical product. In this procedure initial purification was performed using a column of Dowex 50W-X8 cation-exchange resin followed by a second column of 50W-X2 cation-exchange resin.

1.8.3 Determination of Mo and W concentration in the mixed Mo-W aqua ion $[Mo_2WO_6]^{4+}$ by AAS.

Owing to the difficulties found previously with W(VI) standards when analyzing for W(IV), it was decided to use solutions of the well characterized homo aqua ions ($[W_2O_6]^{4+}$ and $[Mo_2O_6]^{4+}$) as AAS standards. Both were made by methods already described (1.6.1 and 1.7.5) and were eluted with 3M HCl. Standard solutions were made having concentrations: 0.44, 2.2, and 4.4 mM for W and 0.05, 0.25, and 0.5 mM for Mo (in 3M HCl). The mixed Mo₂W aqua ion was made as described in 1.8.2 and eluted with 3M HCl. Three diluted samples (in 3M HCl) were analyzed by AAS using a rich nitrous oxide flame. The results are given in table 1.7 and the calibration curves (Abs vs [Mo] and [W]) are illustrated in figure 1.24. The SP9 Pye-Unicam AAS uses a computer fitted method that firstly requires 3 standard solutions* in the ratio 1:5:10. When a sample is run it fits

*There are various programs that allow between 1-5 standard solutions to be used.

the absorbance directly to a concentration reading. The computer assumes the standards are in 1:5:10 ratio hence the actual concentration has to be calculated if the this ratio is different.

Molybdenum: Wavelength used = 313.3 nm

Fuel flow rates = NaO 5.5 l min^{-1} , C_2H_2 4.8 l min^{-1}

Tungsten : Wavelength used = 255.1 nm

Fuel flow rates = NaO 6.5 l min^{-1} , C_2H_2 4.8 l min^{-1}

Figure 1.24 Calibration curve for Mo(IV) and W(IV)

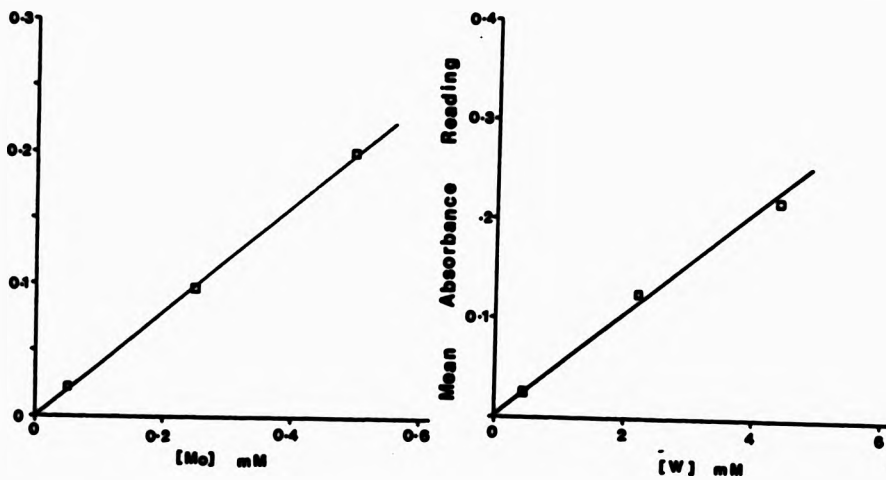


Table 1.7 Flame AAS analysis on samples of $[\text{Mo}_2\text{WO}_4]^{4+}$ in 3MHCl

Sample	Apparent concentration reading from spectrometer		Actual conc. of metal in sample mM		Conc. of Total metal mM
	for Mo	for W	Mo	W	
1	3.62 ± 0.2	0.26 ± 0.04	0.18	0.11	0.29
2	7.67 ± 0.2	0.54 ± 0.03	0.38	0.24	0.62
3	40.40 ± 1.0	2.47 ± 0.09	2.02	1.09	3.11

The electronic spectrum of sample 3 gave an absorbance of 0.175 at the 530 nm peak maximum using a 1cm cell. Therefore the extinction coefficient at 530 nm is $56.3 \text{ M}^{-1} \text{ cm}^{-1}$ per metal. From this experiment it can be successively concluded that both Mo and W are present in solutions of this purple species with a Mo:W ratio of 2:1 suggesting a Mo₂W mixed aqua ion of probable formula $[\text{Mo}_2\text{WO}_4(\text{OH}_2)_6]^{4+}$.

1.8.4 Determination of the formal oxidation state per metal in the $[\text{Mo}_2\text{WO}_4]^{4+}$ aqua ion.

The formal oxidation state of the $[\text{Mo}_2\text{WO}_4]^{4+}$ aqua ion was determined as before by redox titration with Ce(IV) using ferroin as indicator. Samples of $[\text{Mo}_2\text{WO}_4]^{4+}$ (1 cm³, 0.027 M based on ϵ 56 at 530 nm) in 3 M HCl were used. The results are given in table 1.8.

*Actual concentration = apparent conc. × conc. of lowest std. (fig. 1.24).

Table 1.8 Formal oxidation state of the $[Mo_5WO_4]^{4+}$ aqua ion in 3M HCl

Volume of Ce(IV) required cm ³	No. of moles Ce(IV)	No of moles H ⁺ added	Formal Ox State
5.48	5.51 x10 ⁻³	2.7 x10 ⁻³	3.98
5.45	5.49	3.97
5.45	5.49	3.97
5.40	5.45	3.98
Average ox. st =			3.97

It was thus concluded that the formal oxidation state was 4+ ($+3.97 \pm 0.01$) in this ion and that a formula $[Mo_5WO_4]^{4+}$ is indeed relevant.

1.8.5 Studies on the redox chemistry of the $[Mo_5WO_4]^{4+}$ aqua ion

A sample of the purple $[Mo_5WO_4]^{4+}$ aqua ion (3 cm³) prepared in 3M HCl was reduced under N₂ with a slurry of freshly prepared zinc amalgam (10 g). After 4 hours the solution was orange-brown in colour and had an absorption maximum at 840 nm (ϵ 85 M⁻¹ cm⁻¹ per metal) and shoulders at 630 (ϵ = 55) and 440 (ϵ = 95) (figure 1.25.1). A small sample (0.25 cm³) was removed from this solution and quickly added to a 100 fold excess of Fe(III) in 1 M H₂SO₄ solution under N₂. The resulting Fe(II) liberated was titrated with Ce(IV) as before using ferroin as indicator. A further sample (0.3 cm³) was removed and likewise titrated.

Ch. 1: Experimental procedures & Results 76

Values for the formal oxidation state of the metal were 3.00 and 3.04 respectively assuming oxidation to M(VI). From this it can be concluded that the fully reduced species is M(III) ($+3.02 \pm 0.02$).

Samples of this fully reduced orange-brown solution were extremely air sensitive and had to be handled under N_2 with extreme care. The air reoxidation was subsequently followed spectrophotometrically as performed previously with both $[Mo_2O_6]^{4+}$ and $[W_2O_6]^{4+}$. The initial change was characterized by a set of isosbestic points at 365, 540, and 715 nm leading to another orange-brown species showing peak maxima at 650 nm ($\epsilon = 96 M^{-1} cm^{-1}$ per metal) and 370 nm ($\epsilon = 190$) and a shoulder at 430 nm ($\epsilon = 120$) (figure 1.25.1). When the peak at 650 nm had reached a maximum absorbance, a sample ($0.5 cm^3$) was rapidly added to Fe(III) as before and titrated with Ce(IV). A formal oxidation state of +3.36 was found, indicating formation of a mixed-valence M(III,III,IV) ion similar to that obtained with $[Mo_2O_6]^{4+}$ and $[W_2O_6]^{4+}$. The band at 650 nm can thus be assigned to the intervalence charge transfer band associated with the M(III,III,IV) mixed-valence state.

On further air oxidation of this solution, a further set of isosbestic points at 660, and 530 nm were initially observed (figure 1.25.2) but then subsequently lost during the formation of a purple solution which had features similar to that of

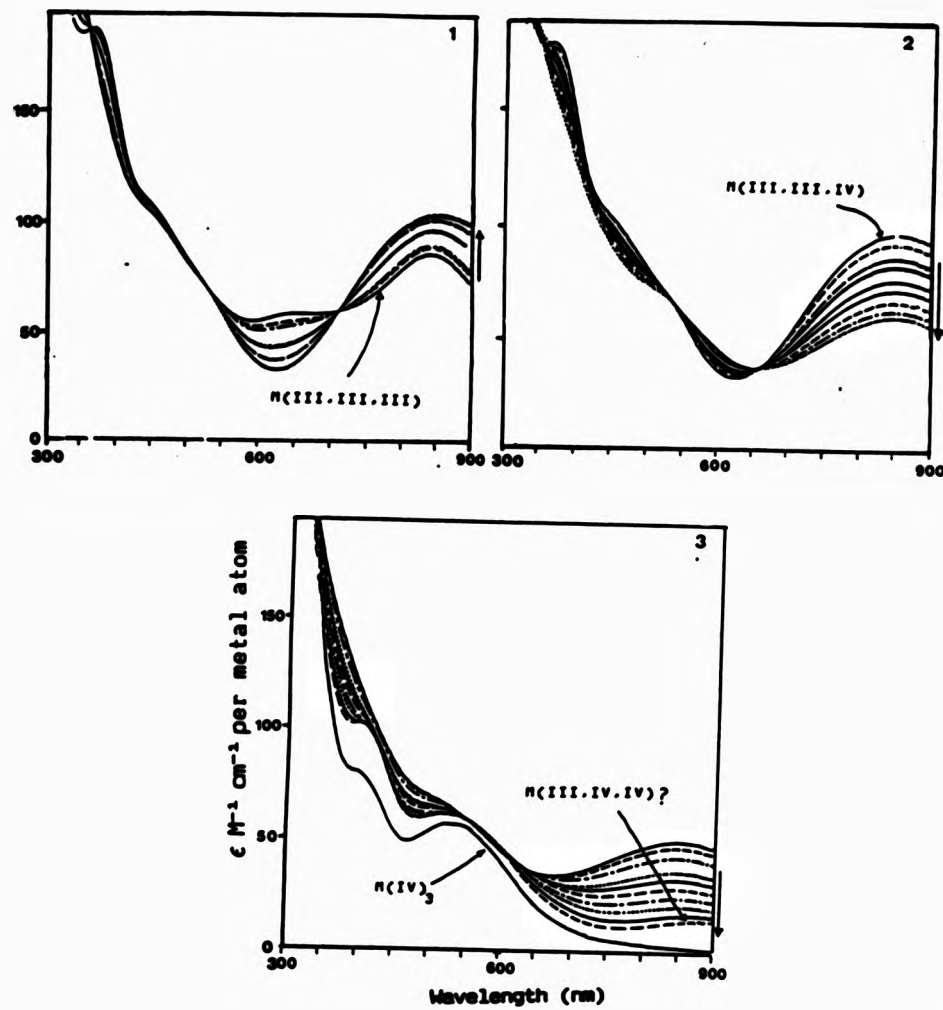


Figure 1.25 Electronic spectrum of the reduced $\text{Mo}_3\text{W}(\text{III})_3$ aqua ion in 3M HCl monitored over 60 min. in air.

$[\text{Mo}_3\text{WO}_4]^{4+}$ in the region 350 - 700 nm but in addition possessed a weak band having λ_{max} 900 nm ($\epsilon = 20 \text{ M}^{-1} \text{ cm}^{-1}$ per metal).

Attempts to accurately estimate the oxidation state of the expected other mixed-valence M(III.IV.IV) intermediate were thus impossible but the new band observed at 900 nm and loss of the isosbestic points provided indirect evidence of its existence.* Further air-oxidation eventually resulted in the regeneration of the spectrum of $[\text{Mo}_3\text{WO}_4]^{4+}$ (figure 1.25.3), demonstrating that the redox changes described were reversible and that trinuclear structure for $\text{Mo}_3\text{W}(\text{III})$ and the mixed-valence intermediates are probably relevant as observed with $[\text{Mo}_3\text{O}_4]^{4+}$ and $[\text{W}_3\text{O}_4]^{4+}$.

Thus there appears to be three distinct steps involved in the air oxidation of $\text{Mo}_3\text{W}(\text{III})_n$ to $\text{Mo}_3\text{W}(\text{IV})_n$.



A controlled potential reduction experiment was performed using a mercury pool working electrode in order to estimate the number of electrons involved in the two reduction waves observed in the Cyclic voltammogram of the $[\text{Mo}_3\text{WO}_4]^{4+}$ aqua ion. This was done by setting the potential firstly between the two waves (-0.15 V) and secondly after the second wave (-0.3 V).

* Similar incomplete retention of the isosbestic points during the air oxidation of the Mo(III.III.IV) aqua ion has been interpreted as indicating the formation of a small amount (few %) of the Mo(III.IV.IV) intermediate ion.**

The reduction was followed by measuring the current as a function of time. A current/time graph allows in theory the calculation of the number of electrons involved. Integration of the current-time decay was not as expected being much smaller and showing a large background catalytic current due to hydrogen evolution. A check of the rest potential showed that it was unaltered since the start of reduction indicating that no net reduction was taking place. This behaviour had been observed during attempts with the $[W_5O_4]^{4+}$ aqua ion where controlled reduction was also unsuccessful. It was concluded that the formed $Mo_5W(III.III.IV)$ was being spontaneously reoxidized by H_2O^+ with a rate comparable to that of the attempted electrochemical reduction. As with $[W_5O_4]^{4+}$ it appeared that reduction was only possible using chemical reductants such as Zn/Hg which reduce at a much greater rate.

1.6.6 Preparation of derivative complexes of the $[Mo_5WO_6]^{4+}$.

$[Mo_5O_6]^{4+}$ and $[W_5O_4]^{4+}$ aqua ions.

Thiocyanato complexes

Samples of the known thiocyanato complexes of $[Mo_5O_6]^{4+}$; $(Me_4N)_4[Mo_5O_6(NCS)_6(OH_2)]$ and $[W_5O_4]^{4+}$; $(Me_4N)_4[W_5O_4(NCS)_6]$ were prepared according to literature methods.⁴³⁻⁴⁶ Analytical data is given in table 1.9. The preparation of a similar thiocyanato derivative of $[Mo_5WO_6]^{4+}$ was thus attempted in the hope that the analytical data so obtained would further confirm the Mo_5W stoichiometry indicated above.

Ch. I: Experimental procedures & Results 80

A 4 M solution (5 cm³) of sodium thiocyanate (B.D.H., A.R.) was prepared and to it a small amount of (0.1 g) tetramethylammonium chloride was added. The initial precipitate (probably NaCl) redissolved on stirring. The solution was deoxygenated with a stream of N₂ and a sample of the purple [Mo₂WO₆]⁴⁻ aqua ion (10 cm³ of a 0.05 M solution in 2 M HCl) was carefully placed on top to form a floating layer. After several hours at room temperature, shiny brown flakes were observed to form between the diffusing layers. These were filtered and washed with ethanol and diethyl ether and dried over silica gel. The C.H.N. content was analyzed. For comparison the tetraethylammonium derivative was also isolated and similarly analyzed. The results are given in table 1.9. Crystalline samples of the NC₄⁻ derivative, suitable for X-ray analysis were however not obtained following recrystallization as hoped.

A methyliminodiacetato (MIDA) complex of the [Mo₂Mo₆]⁴⁻ aqua ion.

An attempt was made to prepare a crystalline MIDA derivative of the [Mo₂WO₆]⁴⁻ aqua ion using the method of Gheller et al.⁴⁴ A sample of [Mo₂WO₆]⁴⁻ was loaded onto a Dowex cation-exchange (50W-X2) column and following washing with water, soaked for 36 hours in acetate buffer (acetic acid (1M), sodium acetate (1M)). After this time a sharp red band was obtained which was slowly eluted with acetate buffer into an air-free solution (5 cm³) of NaMIDA (2.94 g, 20 mmol) and NaOH (1.6 g, 40 mmol). The resulting intense red solution was left to evaporate in a

Ch. 1: Experimental procedures & Results 81

desiccator for several weeks. Following this time, no crystals had come out of solution, therefore a solution of CsCl (1 cm³ of 1M) was added and the solution again left to evaporate. After a further 2 weeks tiny reddish-brown crystals were obtained which were separated and the CHN content analyzed (table 1.8). Crystals suitable for X-ray analysis are currently under investigation. A solution of the red crystals in water possessed two absorption maxima at 538 nm and 420 nm. These may be compared with those for the corresponding HIDA⁻ complex of [Mo₂O₆]⁴⁻ occurring at 529 nm and 421 nm. The shift of ~ 10 nm in the lowest energy band is similar to that observed for the respective aqua ions of [Mo₂WO₆]⁴⁻ (515 nm) and [Mo₂O₆]⁴⁻ (505 nm) in Hpts solution. It may be concluded that a HIDA⁻ complex of the [Mo₂WO₆]⁴⁻ aqua ion has been successfully prepared.

Table 1.8 Elemental analyses on derivative complexes.

Complex	Calculated			Found		
	C%	H%	N%	C%	H%	N%
(Hida) ₂ Mo ₂ O ₆ (SCN) ₂ ·(CH ₃) ₂ O	20.57	3.62	12.69	20.46	3.56	12.16
(Hida) ₂ Mo ₂ O ₆ (SCN) ₂ ·(CH ₃) ₂ O	29.20	5.04	11.02	29.83	4.77	11.53
Cs ₂ ·(Hida) ₂ Mo ₂ O ₆ (HIDA) ₂ ·H ₂ O	17.53	2.45	4.12	17.66	2.44	3.92
(Hida) ₂ Mo ₂ O ₆ (SCN) ₂ (H ₂ O)·3H ₂ O	24.32	4.73	14.19	24.39	4.73	12.23
(Hida) ₂ Mo ₂ O ₆ (SCN) ₂	22.33	3.99	13.02	22.40	4.30	11.54

From the analytical and spectroscopic data, it may be concluded that both MCS⁻ and MIDA⁻ complexes of $[\text{Mo}_2\text{O}_6]^{4-}$ have been successfully prepared. The MIDA⁻ complex appears to be a mixture of Na and Cs salts.

1.8.7 Attempts to prepare the mixed $[\text{W}_2\text{MoO}_6]^{4-}$ aqua ion.

Method I

Samples of $\text{K}_2[\text{WCl}_6]$ (2.35 g. 1.65 mmol) and $\text{K}_2[\text{MoCl}_6]$ (1.5 g. 0.8 mmol)* representing a W:Mo ratio of 2:1 were added to 2M HCl (20 cm³) in separate Schlenk vessels. The solutions were filtered using a pressure of N₂ and mixed. The resulting brown solution was kept at 80°C for 2 hours after which it was diluted to 0.5 M [H⁺] and purified using ion exchange techniques discussed earlier. The column behaviour was similar to that observed in the preparation of the $[\text{W}_2\text{O}_6]^{4-}$ aqua ion. As usual the column was washed with 0.5 M Hpts to remove the yellow $[\text{Mo}_2\text{O}_6]^{4-}$ ion. Upon elution with 2M Hpts an orange-brown solution was obtained which showed two shoulders in the electronic spectrum at 500 and 450 nm. Cyclic voltammetry measurements (Hg cup electrode) showed no evidence of reduction waves up to the hydrogen over potential (-0.4 V vs N.H.E.). Amalgamated Zinc reduction of the same solution gave rise to an emerald green colour resulting from the mixed-valence W(III.-III.IV) ion (λ_{max} 578 nm) described earlier. It was thus concluded that the main species present was the $[\text{W}_2\text{O}_6]^{4-}$ ion.

* double quantities of K_2MoCl_6 were used since it was 60% pure.

Method II

Samples of $K_2[WClo_4]$ (2.35 g), $K_2[MoCl_6]$ (2 g), and Na_2MoO_4 (3 g) were added to 2M HCl (40 cm³) in a Schlenk vessel and kept at 80°C for 2 hours. Upon column treatment a yellow solution was obtained. Its electronic spectrum confirmed the presence of only the $[Mo_2O_4]^{4+}$ aqua ion.

Method III

Freshly prepared $MoCl_6$ (1.2 g) and $K_2[WClo_4]$ (4.7 g) giving the ratio Mo:2W were added to 2M HCl (20 cm³) in a Schlenk vessel and the mixture kept at 80°C for 30 minutes. The immediate yellow brown colour changed to orange-brown within 5 minutes of the heating period. The mixture was then filtered and the solution was diluted 10 times with 0.5 M HCl (200 cm³). After allowing the orange brown solution to stand for 4 hours it was loaded onto a column of Dowex 50W-X2 cation-exchange resin. The column behaviour was again similar to the preparation of $[W_2O_4]^{4+}$. Lower charged species ($[Mo_2O_4]^{4+}$ aqua ion etc.) were removed by passing 0.5M and 1M HCl (500 cm³) down the column. The remaining orange brown species was eluted with 2M HCl. Its electronic spectrum showed two shoulders at 500 and 450 nm similar to those obtained from method I. Reduction using Zn/Hg produced a greenish-brown solution showing peaks at 680 and 820 nm. The peak at 680 was similar to the W(III,III,IV) reduction product from the $[W_2O_4]^{4+}$ aqua ion. The peak at 820 nm was similar to those observed from both the Mo₂W(III,III,IV) and Mo₂W(III) reduction products obtained from the $[Mo_2WO_4]^{4+}$ aqua

Ch. 1: Experimental procedures & Results 84

ion. Cyclic voltammetry indeed showed two waves at -0.08 and -0.25 V (vs N.H.E.) similar to those observed for the $[\text{Mo}_2\text{WO}_4]^{4+}$ aqua ion. It was concluded that the orange brown species was a mixture of the $[\text{W}_2\text{O}_4]^{4+}$ and the mixed $[\text{Mo}_2\text{WO}_4]^{4+}$ aqua ion.

1.6.6 Oxygen-17 NMR studies on the $[\text{Mo}_2\text{WO}_4]^{4+}$ aqua ion.

A sample (5 cm³) of ¹⁷O enriched (5.25%) 2M HCl was prepared by mixing 2.5 cm³ of 4 M HCl with 2.5 cm³ of 10.5 atom % H_2O^{17} (Yeda Co. Ltd.). Samples of $\text{K}_2[\text{WCl}_6]$ (1.0 g) and MoCl_4 (1.0 g) were weighed out to provide the 2Mo:1W ratio and added to the HCl solution. The mixture was heated to 80°C for 30 minutes. After filtration, the sample of enriched $[\text{Mo}_2\text{WO}_4]^{4+}$ was purified by cation-exchange chromatography as described previously. The final elution was carried out using Hpts (4.5 M) and a narrow column (5 cm x 1 cm). The 2cm³ sample appeared red in colour as hoped but the electronic spectrum showed a peak maximum at 505 nm indicating the presence of $[\text{Mo}_2\text{O}_4]^{4+}$. A sample of $\text{Mn}(\text{CF}_3\text{SO}_3)_2$ (0.034 g) was added in order to relax out the bulk water resonance line prior to the addition of a further 0.5 cm³ of 10.5 atom % H_2O^{17} . After allowing to equilibrate over 6 hour period a ¹⁷O NMR spectrum was run on the Brüker AM-300 instrument at St. Andrews over the range -400 to 1200 ppm. The ¹⁷O NMR features for the aqua ions of $[\text{Mo}_2\text{O}_4]^{4+}$; 794 ppm ($\mu_{\text{a}}-\text{O}^{17}$), 516 ppm ($\mu_{\text{s}}-\text{O}^{17}$), 28 ppm (H_2O^{17}) and -7 ppm (H_2O^{17}) and $[\text{Mo}_2\text{O}_4]^{4-}$; 964 ppm ($\text{yI}-\text{O}^{17}$) and 582 ppm ($\mu_{\text{a}}-\text{O}^{17}$) were indeed observed. In addition a peak at 440 ppm

Ch. 1: Experimental procedures & Results 85

($\text{Mo}_2\text{O}_4^{2+}$) for $[\text{W}_2\text{O}_4]^{2+}$) was also observed. Unfortunately there were no peaks that could be assigned to the presence of the mixed $[\text{Mo}_2\text{WO}_4]^{2+}$ aqua ion.

The failure in the preparation was thought due to a combination of both the small scale and high concentration of the reagents used owing to the limited quantities of H_2O^{2+} that were available and the fact that the MoCl_4 may have partially decomposed to oxo derivatives of Mo(V) and Mo(VI).

Another sample of the $[\text{Mo}_2\text{WO}_4]^{2+}$ aqua ion was prepared in 4 M Hpts using normal water samples and concentrated using a narrow Dowex 50W-X2 cation-exchange column. Its electronic spectrum was recorded and it showed the characteristic peak for a Hpts solution at 515 nm (ϵ 56 $\text{M}^{-1} \text{cm}^{-1}$) and a shoulder at 400 nm. The bound H_2O ligands of $[\text{Mo}_2\text{WO}_4]^{2+}$ were then enriched with ^{17}O by adding 0.5 cm³ of 10.5% H_2O^{2+} to 1.5 cm³ of the concentrated sample (final $[\text{Mo}_2\text{W}^{2+}] = 0.04\text{M}$). A sample of $\text{Mn}(\text{CF}_3\text{SO}_2)_2$ (0.03 g) was added and the solution equilibrated for 6 hours. During this time ^{17}O NMR spectra were recorded at 6 minute intervals and as observed with $[\text{Mo}_2\text{O}_4]^{2+}$ the water ligands observed at the most downfield shifts (+24 ppm) were enriched immediately upon mixing with H_2O^{2+} with a second bound water peak (-14 ppm) reaching a maximum intensity after 20 minutes at the temperature used (45°C).^{*} This exchange rate half life of ~ 6 min.

* A temperature of 45°C was required to dissolve $\text{Mn}(\text{pts})_2$ that was crystallising out at lower temperatures.

for the slower exchanging water ligands is roughly similar to that expected from the water ligands *trans* to the $\mu_2\text{-O}$ group on $[\text{Mo}_2\text{O}_6]^{4+}$. It was thus assumed that a similar process involving water exchange on the Mo sites *trans* to the $\mu_2\text{-O}$ group of $[\text{Mo}_2\text{WO}_6]^{4+}$ was being followed (see section on kinetics of NCS-anation on $[\text{Mo}_2\text{WO}_6]^{4+}$). The two bound water peaks are in 2:1 ratio as expected for an assignment from $[\text{Mo}_2\text{WO}_6(\text{OH}_2)_2]^{4+}$. The temperature of the solution was subsequently raised to 90°C in the hope of causing ^{17}O enrichment of the core oxygen groups via water exchange with the bulk H_2O^{17} present. After 8 hours at 90°C a new ^{17}O spectrum at 45°C over the range -400 to +1200 ppm was recorded. This spectrum is shown in figure 1.26. Weak resonances assigned to $[\text{Mo}_2\text{O}_6]^{4+}$ (964 and 562 ppm) were observed. However two resonances at 800 ppm and 640 ppm were also seen and are assigned to the following resonances of the $[\text{Mo}_2\text{WO}_6]^{4+}$ ion. The resonance at 800 ppm is assigned to the $\mu_2\text{-O}^{17}$ group linking the two Mo atoms (close to the resonance observed (797 ppm) in $[\text{Mo}_2\text{O}_6]^{4+}$). The resonance at 640 ppm is assigned to the two $\mu_2\text{-O}^{17}$ groups linking Mo and W atoms in $[\text{Mo}_2\text{WO}_6]^{4+}$ on the basis that it lies exactly between the resonances for $\mu_2\text{-O}^{17}$ groups on $[\text{Mo}_2\text{O}_6]^{4+}$ (797 ppm) and $[\text{W}_2\text{O}_6]^{4+}$ (560 ppm). There was no evidence of a resonance assignable to a $\mu_2\text{-O}^{17}$ group from either $[\text{Mo}_2\text{O}_6]^{4+}$, $[\text{W}_2\text{O}_6]^{4+}$ or $[\text{Mo}_2\text{WO}_6]^{4+}$. The absence of a peak at 516 ppm ($\mu_2\text{-O}^{17}$ for $[\text{Mo}_2\text{O}_6]^{4+}$) adds further support to the conclusion that the resonance at 800 ppm is due to the mixed $[\text{Mo}_2\text{WO}_6]^{4+}$ ion rather

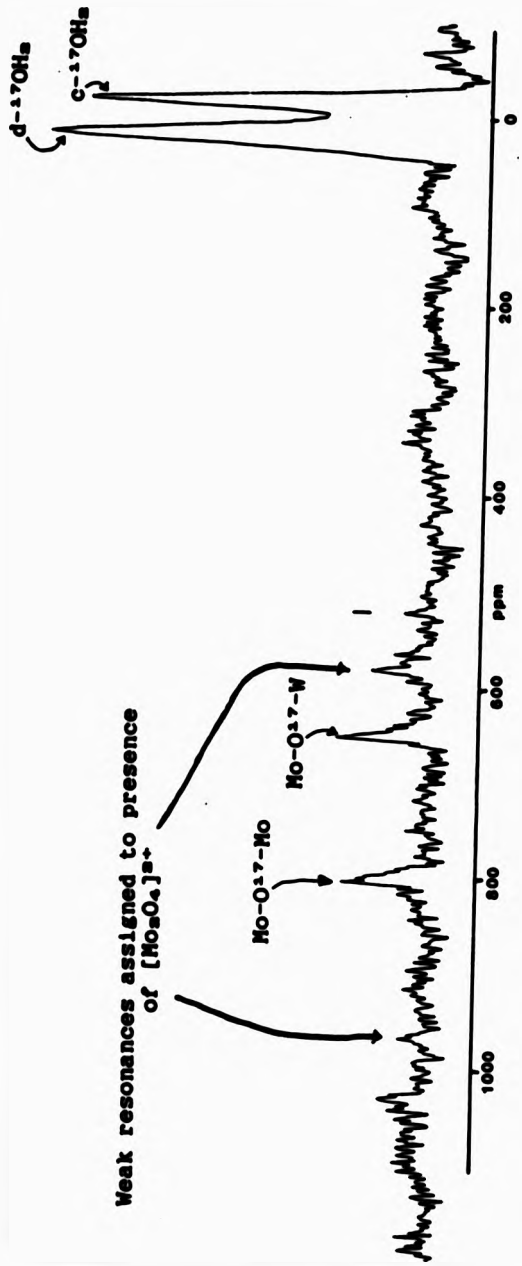


Figure 1.26 Oxygen-17 NMR spectrum of $[\text{Ho}_2\text{MoO}_4]^{4-}$ in 4.5 M Hpts recorded after 8 hours at 90°C.

than $[\text{Mo}_2\text{O}_6]^{4+}$. The expected 2:1 integration for the Mo-O¹⁷-W to Mo-O¹⁷-Mo resonances is not apparent from figure 1.26 but this may be merely due to a faster ¹⁷O exchange rate* at the Mo-O¹⁷-Mo site. Similarly, a slower exchange rate may account for the lack of appearance (as yet) of the μ -O¹⁷ resonance of $[\text{Mo}_2\text{WO}_6]^{4+}$ from these solutions.

These results if incomplete provide further evidence of the formation of a new mixed $[\text{Mo}_2\text{WO}_6]^{4+}$ aqua ion from these solutions.

1.9 Anation kinetics of Thiocyanate on $[\text{Mo}_2\text{WO}_6]^{4+}$.

Na(tfms) was prepared by neutralization of 4M Htfms with NaOH, followed by recrystallization from water. Solutions of Htfms were standardised by titration against NaOH using phenolphthalein as indicator. The $[\text{H}^+]$ of stock $[\text{Mo}_2\text{WO}_6]^{4+}$ solutions, and solutions of Na(tfms), were standardized by ion-exchange onto a Dowex 50W-X8 cation-exchange resin (H^+ form) and titration of the liberated $[\text{H}^+]$ with NaOH. Concentrations of $[\text{Mo}_2\text{WO}_6]^{4+}$ solutions were determined spectrophotometrically (peak at 515 nm $\epsilon = 168 \text{ M}^{-1} \text{ cm}^{-1}$ per mole aqua ion at 25°C).

$[\text{Mo}_2\text{WO}_6]^{4+}$ was prepared in Htfms medium by following the synthetic method already described. Final elution was carried out with 2M Htfms. Kinetic runs were on a time scale $t_n > 2 \text{ min}$

*¹⁷O exchange rates on oxygens coordinated to W would be expected to be slower than those coordinated to Mo if likely dissociative mechanism operates.

and were monitored at 325 nm by conventional spectrophotometry (fixed wavelength using an auto cell changer.* The [NCS⁻] was maintained at 10 fold excess. Four runs were done with the aqua ion itself in excess to establish the presence or absence of the statistical factor previously reported from studies on the [Mo₂O₆]⁴⁻ and [W₂O₆]⁴⁻ aqua ions.^{11a-11c} All sample measurements were carried out by using a Hamilton syringe capable of delivering 0.5 cm³ (\pm 0.01 cm³). For each run, the required amounts of Htfms, KSCN, Na(tfms), and distilled water (all rigorously deoxygenated) were added to a 1 cm quartz cell (final volume 3 cm³). The cell was then allowed to reach the required temperature in the cell manifold on the spectrophotometer (~ 30 minutes). The required amount of the aqua ion (also thermostatted at the appropriate temperature) was then added to the cell and following mixing the absorbance monitoring was commenced. The values of [NCS⁻] were in a range appropriate for 1:1 complex formation as the dominant process at any one metal atom. Even so there were small subsequent absorbance changes (most likely due to bis complex formation at a single metal atom), leading to uncertainty in absorbance A_{in} values and therefore the Swinbourne method (see appendix 3) was used to evaluate A_{in} for the initial stage. Using these values the first-order equilibration constants were evaluated from plots of ln(A_{in} - A_o) vs t (see figure 1.27 for typical plot).

*The Perkin Elmer Lambda 5 UV-visible spectrophotometer offers the facility whereby 5 samples can be studied simultaneously.

Ch. 1: Experimental procedures & Results 90

The temperature of all runs was 25.0 ± 0.1 °C except for the temperature dependence study and was controlled by means of electronic thermostatting. Ionic strengths were adjusted to 2.00 ± 0.05 using Htfms and Na(tfms).

Data was treated using unweighted linear least-squares fits.

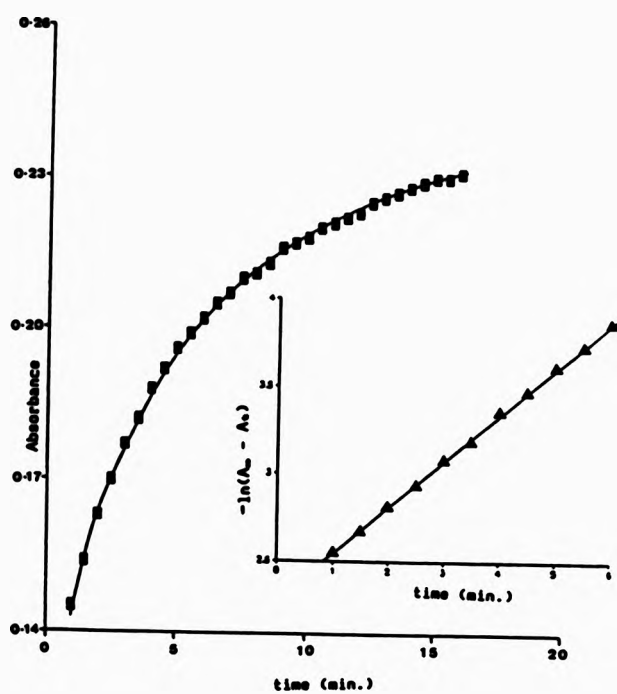


Figure 1.27 Plot of absorbance vs time and $\ln(A_0 - A_t)$ vs time (inset) for the reaction of $[\text{Mo}_2\text{WO}_4]^{4+}$ with NCS^- . $T=25^\circ\text{C}$, $[\text{NCS}^-]=3.5 \times 10^{-2}$ M, $[\text{Mo}_2\text{WO}_4]^{4+}=4.0 \times 10^{-2}$ M, wavelength= 325 nm and I=2.0M NaCF_3SO_3 .

DISCUSSION

At the commencement of this work, the only report of the $[W_5O_4]^{4+}$ aqua ion was from the previous studies of McMahon⁴⁸, who prepared the ion via amalgamated zinc reduction of W(V) ($Na_2[WO_3(C_2O_4)_2] \cdot 3H_2O$) in HCl followed by aquation and cation-exchange purification. Based on Ce(IV) titrations of the W(IV) ion to W(VI), an ϵ value of $89 M^{-1} cm^{-1}$ per W atom was reported⁴⁸ for the observed electronic peak maximum at 455 nm. While this work was in progress, Sasaki et al.⁴⁹ published an alternative method of preparation for $[W_5O_4]^{4+}$ via acid hydrolysis of $K_2[WClo_4]$. The reported value⁴⁹ for ϵ_{455} via this latter route was verified by the present work as $125 M^{-1} cm^{-1}$ per W atom. Unfortunately AAS analysis of the W content using well defined W(VI) standards were not reliable. A more suitable W(IV) standard was not found. Therefore verification of the ϵ value at 455 nm required the assumption that W(IV) was present.

Subsequent investigations employing ^{17}O and ^{183}W NMR spectroscopy, electrochemical and redox studies and UV-visible spectrophotometry have verified the presence of the oxidation state in the incomplete cuboidal structure, $[W_5O_4(OH_2)_6]^{4+}$ analogous to that formed by Mo(IV). Most alarming however is that the present NMR studies (^{17}O and ^{183}W) have shown that the main species produced via the published Sasaki route⁴⁹ is not the aqua ion ($[W_5O_4(OH_2)_6]^{4+}$) but almost certainly monochlorooctaqua species $[W_5O_4(OH_2)_6Cl]^{2+}$ with the chloride presumably

coordinated in the extremely inert positions *trans* to the capping μ_3 -oxo group. This coordinated Cl^- group had apparently survived the initial aquation and final cation-exchange treatment. Amounts of the true aqua ion were detected in later fractions. These findings explain the earlier lower ϵ_{450} value obtained via the method of McMahon.⁴² It is likely that incomplete aquation of oxalate also occurs here and that oxalato coordinated W(IV) species also survive the cation-exchange treatment. The lower ϵ value ($89 \text{ M}^{-1} \text{ cm}^{-1}$) is thus a reflection of the oxidation of both W(IV) and coordinated oxalate by Ce(IV). The assumption of W(IV) here as the only reductant for Ce(IV) is thus not valid. Subsequent Ce(IV) titration in the presence or absence of Cl^- show that the medium has little influence (oxidation of Cl^- by Ce(IV) occurring at a much slower rate and not interfering with the titration). The presence of the oxalato complexes in the previous W(IV) solutions⁴² may also have accounted for the apparent presence of a W(III,IV,IV) mixed-valence ion during the reduction studies not seen on using the present Cl^- route.

In conclusion, the present work has indicated that pure solutions of the $[\text{W}_3\text{O}_8(\text{OH}_2)_6]^{4+}$ are not produced via the two published methods and further work is needed perhaps employing acid aquation of W(IV) complexes with more favorable leaving groups such as tfms^- or pts^- etc. These findings also bring into questions the validity of the 1:1 MCS⁻ complexation

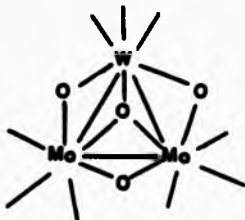
studies on $[W_2O_8]^{4-}$ carried out recently by Sykes and co-workers who used the published method via $K_2[WClo_4]$.²⁴

The present results have also verified that reduction leads only to the mixed-valence W(III.III.IV) ion with no evidence of a W(III) aqua ion. There appears no evidence from the present studies that an aqua ion of W(III) can be prepared in contrast to Mo(III) where there are at least three representative species known. Oxygen-17 NMR studies confirmed that protonation of the μ -O groups occurs on formation of W(III.III.IV), the apparent single $\mu(O^{17}H)$ resonance suggesting a structure: $[W_2(OH)_4]^{4-}$ containing only μ_2 -(OH) groups. A similar structure also exists for the Mo(III.III.IV) analogue however cyclic voltammetric experiments indicate that the W ion is more reducing by 0.7 V. The generally more reducing properties of the W ions vs Mo, the higher energy electronic spectral bands and more substitution inert (= 10 times) behaviour towards ligand replacement on W are all thought to reflect greater 5d orbital participation through the so-called relativistic expansion effect.* Most notable is the shift of the inter-valence band for the W(III.III.IV) aqua ions from 1050-680 nm (Mo \rightarrow W) reflecting much greater 5d orbital overlap in the W ion and hence greater delocalization.

Initial attempts to prepare the analogous mixed metal $[Mo_2WO_8]^{4-}$ and $[MoW_2O_8]^{4-}$ aqua ions by a comproportionation reaction involving Mo(VI), Mo(III) and W(IV) in the required

ratio were unsuccessful appearing to be due to oxidation of W(IV) by Mo(VI) to give tungsten blue precipitates. A successful new route to the preparation of $[W_3O_4]^{4+}$ via acid hydrolysis of the labile Mo(IV) monomeric complex $MoCl_4(MeCN)_2$ was thus developed in the expectation that acid hydrolysis of mixtures of both monomeric Mo(IV) and W(IV) complexes in the correct ratio might ultimately lead to assembly of the mixed Mo-W aqua ions. The failure in synthesising a mixed aqua ion via hydrolysis of a mixture of $K_2[WClo_4]$ and $MoCl_4(MeCN)_2$ lead to attempts to prepare the now well characterized $[W_3O_4]^{4+}$ via complexes such as $WCl_4(RCN)_2$ and $WCl_4(py)_2$. In each case acid hydrolysis lead to blue precipitates of poly-oxo tungsten (V)/(VI) and no evidence of $[W_3O_4]^{4+}$ production. Such behaviour can only be a result of reaction of RCM or py with respect to oxidation of reactive W(IV) intermediate species (possibly mononuclear) occurring with a rate presumed faster than that involved with the assembly of the trinuclear cluster unit. This led ultimately to the use of $MoCl_4$ as an alternative Mo(IV) reagent and the successful synthesis of the mixed aqua ion $[Mo_2WO_4(OH_2)_2]^{4+}$ (figure 1.28) via acid hydrolysis of a mixture of $K_2[WClo_4]$ and $MoCl_4$ in a 1:2 ratio.

Figure 1.28



MoCl₄ itself proved to be extremely air sensitive and quite difficult to handle. The success of the preparation was initially surprising given the knowledge that routes to [Mo₂O₄]⁴⁺ itself using MoCl₄ gave poor yields (30%) compared to those using MoCl₄(MeCN)₂ (70%). The [Mo₂O₄]⁴⁺ preparation involving MoCl₄ gave rise to large amounts of the yellow [Mo₂O₄]²⁺ following cation-exchange purification. This is believed to be due to the well known disproportionation of MoCl₄ in aqueous acid. This reaction has been reported in detail by Haight and co-workers¹⁰⁰ and is summarized below.



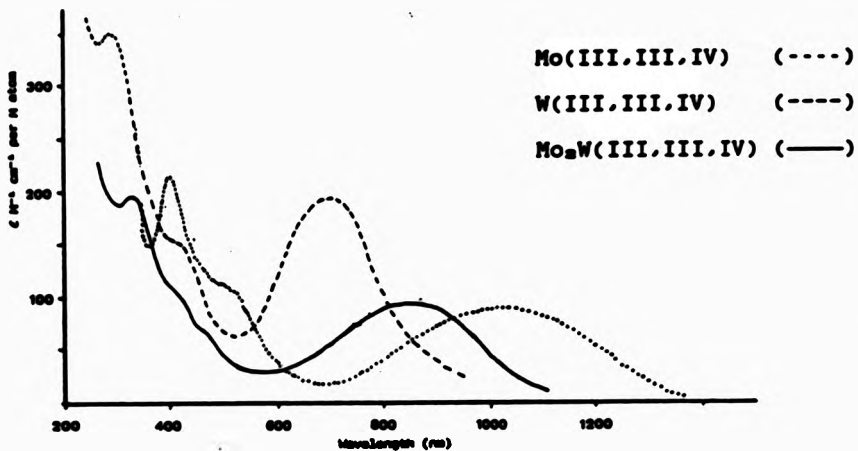
The success of the mixed Mo-W reaction is believed to be due to a faster reaction of the presumed intermediate chloroqua Mo(IV) species generated with W(IV) rather than with themselves thus preventing loss of the reducing equivalents by formation of the stable cluster ions, [Mo₂Cl₁₂]²⁻. On the basis of the electronic absorption maxima for [W₂O₄]⁴⁺ (455 nm) and [Mo₂O₄]⁴⁺ (505 nm), a maximum occurring at ~490 nm might have been expected for the mixed Mo₂W ion if a similar electronic structure applies. The observation of two bands at 515 and 400 nm implies that a truly delocalized d⁶ cluster unit is not relevant and electronically distinct Mo and W clusters are present as would be expected. The M.O. energy levels involved with overlap between 5d and 4d orbitals in the presumed Mo-W bonds present is likely to be different from that involved with

4d-4d and 5d-5d overlap and will lead to a more complicated electronic structure for the mixed cluster ion. The simplest interpretation of the low energy maximum at 515 nm is that it arises from a transition involving a bonding MO located within the Mo-W bonds being thus less stabilized than an equivalent bonding level arising from within the Mo-Mo or W-W bonds. As observed with both $[Mo_2O_4]^{4+}$ and $[W_2O_4]^{4+}$, a change in the medium from Hpts to HCl (3M) causes a shift in the absorption maximum, 515 to 530 nm. This is indicative of Cl^- equilibration with the water ligands which in the case of $[W_2O_4]^{4+}$, may involve an appreciable K_{eq} .

Amalgamated Zinc reduction of the reddish-purple $[Mo_2WO_4]^{4+}$ aqua ion (oxidation state 3.97 ± 0.01) produces an orange-brown solution which titrated for M(III)_a (oxidation state 3.03 ± 0.02). Re-oxidation of this d⁰ M(III)_a occurs rapidly, and careful spectroscopic monitoring shows two sets of isosbestic points suggesting that all species are of the same structural type. Similar studies by Richens and Sykes²⁷ on the $[Mo_2O_4]^{4+}$ aqua ion revealed that the ion can be completely reduced to the green Mo(III)_a (λ_{max} nm, ϵ M⁻¹ cm⁻¹ per Mo) 420(sh) (ca. 100), 635 (80), 625 (45). Partial re-oxidation of this as well as the $[W_2O_4]^{4+}$ aqua ion produces a mixed valence d⁰ M(III, III, IV) species (M = Mo or W). The similarity of the absorption spectra of these two species with the spectrum of the partially re-oxidized Mo₂W aqua ion, is strongly in support of a similar mixed-valence d⁰ species (figure 1.29).

Furthermore, the position and the intensity of the inter-valence band for the Mo₂W aqua ion (850 nm) strongly supports for it to be a genuine mixed Mo-W aqua ion rather than a 2:1 Mo:W mixture of the two homo aqua ions.

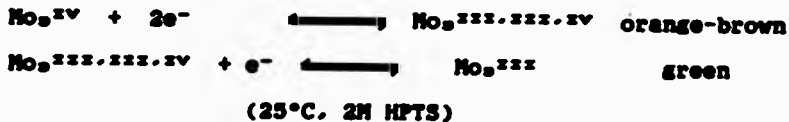
Figure 1.29 Electronic spectrum of mixed-valence aqua ions.



When the re-oxidation of the mixed aqua ion M(III)_x is continued beyond the M(III,III,IV) stage, new sets of isosbestic points are observed, which are then lost as the M(IV)_x reddish-purple aqua ion is regenerated suggesting a second stage with an absorption maximum at 900 nm being detected. This could be assigned to the inter-valence band of the mixed-valence species (d⁷ M(III,IV,IV)).

For the [Mo₂O₆]⁴⁻ ion, studies by Anson et al.¹⁴ and Richens and Sykes¹⁵ confirmed that the observed redox processes involved

two sequential electron transfer steps with formal potentials that are pH dependent.



Cyclic voltammetric studies on solutions of the $[\text{Mo}_2\text{WO}_6]^{4+}$ ion in 2M Hpts show two reversible reduction waves centred at -0.08 V and -0.25 V (vs N.H.E.). Unfortunately it has not been possible to assign formal oxidation states to the reduction products of these two waves due to the presence of large background currents. However, it has been observed that the relative height of these two waves does alter from preparation to preparation and it was noted that the first wave is extremely close to the wave at -0.09 V observed from solutions of $[\text{Mo}_2\text{O}_6]^{4+}$. It was thus concluded that this wave is due to amounts (up to 10%) of $[\text{Mo}_2\text{O}_6]^{4+}$ presence in the solutions of the $[\text{Mo}_2\text{WO}_6]^{4+}$ aqua ion. The second wave at -0.25 V is thus assigned to the formation of the Mo-W(III,III,IV) ion with a structure shown in figure 1.30 analogous to the homo Mo and W analogues.

The further reduction to Mo-W(III) is not seen in the cyclic voltammograms and presumably occurs beyond the hydrogen overpotential on the mercury working electrode (-0.4 V) under the conditions used consistent with reduction now at the W(IV) centre.

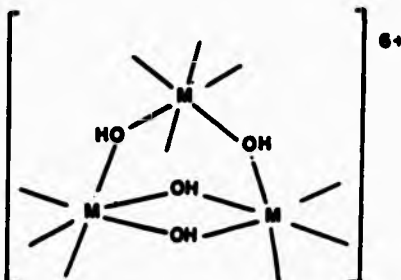


Figure 1.30 Proposed structure for the M(III,III,IV) mixed-valence aqua ion (M=Mo or W).

Given now the presence of the electronically inequivalent metal centres in the Mo-W aqua ion and the remarkably similar electronic structure of the $\text{Mo}_2\text{W}(\text{III},\text{III},\text{IV})$ ion with those of the homo Mo and W analogues, an assignment to an electronically delocalized structure (class III behaviour) for these mixed-valence ions would seem increasingly relevant. This would also be consistent with the single Mo^{+1}OH resonance observed in the ^{17}O NMR spectrum of the M(III,III,IV) ions (M=Mo or W). Further studies into the electronic structures of these interesting mixed-valence aqua ions are planned.

Finally, further support for the Mo-W ion has come from preliminary ^{17}O NMR studies on the reddish-purple solution. An attempt at the preparation of a fully enriched sample involving a small scale synthesis in $\text{H}_2\text{O}^{17}/\text{HCl}$ unfortunately failed to generate any $[\text{Mo}_2\text{WO}_4]^{6-}$ under the conditions used. However, a concentrated solution of the Mo_2W aqua ion was equilibrated

with MoO_4^{2-} and heated to 90°C for several hours. At 45°C, an ^{17}O NMR spectrum of the resulting solution showed evidence of a new Mo-O $^{2-}$ resonance at 640 ppm assignable to that linking Mo and W atoms in the mixed ion. Final conclusive evidence of the new mixed ion was obtained following kinetic studies of the 1:1 anation reaction with NCS^- and comparison with the similar studies reported on $[\text{Mo}_2\text{O}_4]^{4-}$ and $[\text{W}_2\text{O}_4]^{4-}$.^{54,55}

1.10 Kinetics of the substitution of EC5^- on the mixed [$\text{Mg}_2\text{WO}_4(\text{OH}_2)_8$] $^{4+}$ in trifluoromethanesulphonic acid medium.

RESULTS AND DISCUSSION

1.10.1 Dependence on $[\text{Mo}_5\text{WO}_4(\text{OH}_2)_8]^{4+}$ (abbreviated to $[\text{Mo}^{4+}]$).

With total NCS⁻ concentration in ≥ 10 fold excess, the kinetics of this reaction were found to be pseudo first order in $[Mn^{++}]$ with $\ln(A_m - A_t)$ plots linear to 3 half lives. A_m values estimated from Swinbourne analysis were not proportional to $[Mn^{++}]$.

1.10.2 Dependence on total NCS- concentration.

The dependence of the anation rate constant on the thiocyanate concentration was investigated in a series of runs with $[NCS^-]$ in large excess (≥ 10 fold). The $[NCS^-]$ was varied from 1.2×10^{-3} M to 3.5×10^{-3} M. At $[NCS^-]$ greater than 3.5×10^{-3} M extensive biphasing was observed in the absorbance vs time plots indicating that other competing reactions possibly involving rate-determining substitution of a second NCS^- ligand were involved. Values for k_{obs} were thus evaluated from $\ln(A_0 - A_t)$ vs t plots using A_0 estimated by the Swinbourne method. Such plots for the relevant first stage were linear to 2.5 to 3 half-lives.

Ch. I: Kinetic results and discussion 102

Under these conditions, a linear first-order dependence of k_{eq} on $[NCS^-]$ was found passing through an intercept. This meant that equilibrium kinetics were in operation ($k_{eq}=k_{me}$). Results for the four temperatures 20°, 25°, 30°, and 35°C are listed in table 1.10 and graphically illustrated in figure 1.31.

Table 1.10 First order equilibration rate constants k_{eq} (20°, 25°, 30°, and 35°C) for the reaction of $[Mo_2W_2]^{4+}$ ($\sim 4.0 \times 10^{-6}$ M) with NCS^- , $I=2.00$ M ($NaCF_3SO_3$)

$10^3[NCS^-]$ M	Temperature (°C)	$10^3 k_{eq}$ s ⁻¹
1.20	20	1.41
1.50		1.45
1.95		1.52
2.55		1.62
3.50		1.79
1.20	25	2.05
1.50		2.13
1.95		2.25
2.55		2.41
3.50		2.75
1.20	30	3.76
1.50		4.07
1.95		4.33
2.55		4.60
3.50		5.11
1.20	35	6.16
1.50		6.47
1.95		6.94
2.55		7.50
3.50		8.17

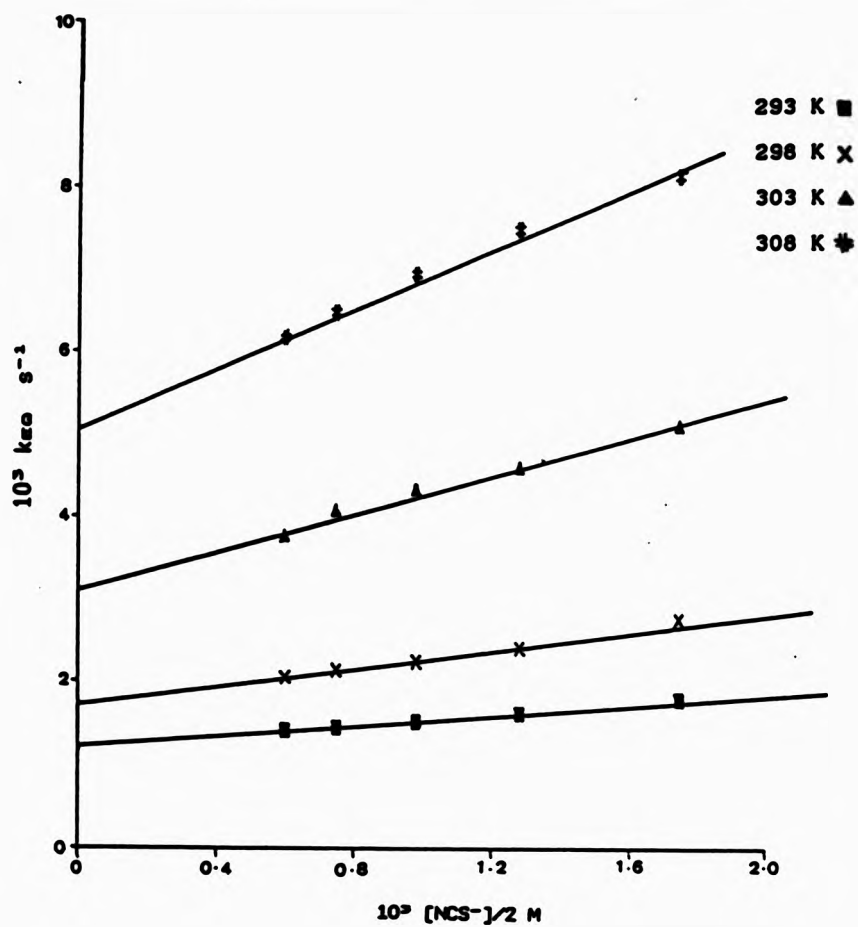


Figure 1.31 Equilibration rate constants vs $[NCS^-]$ as a function of temperature ($I=2.0M\ NaCF_3SO_3$) for the reaction of $[Mo_2W_4]^{4+}$ with thiocyanate.

1.10.3 Dependence on the hydrogen ion concentration

Previous studies^{24,25} on the $[Mo_3O_4]^{4+}$ and the $[W_3O_4]^{4+}$ with thiocyanate and oxalate has indicated that the substitution proceeds solely by the conjugate-base form $[Mo_3O_4(OH_2)_6(OH)]^{3+}$. In both studies, statistical kinetics applied (i.e. rate constants obtained with $[NCS^-]$ in large excess were three times those with $[Mo_3O_4]^{4+}$ in large excess, and to allow for this difference $[NCS^-]$ values were divided by 3). Since in the mixed aqua ion the metal atoms are not the same and the rate for substitution for the $[W_3O_4]^{4+}$ trimer are reported previously²⁴ to be slower by a factor of 10, the same 3-fold symmetry may now be absent and the same statistical factor may not now apply. In order to obtain the value for the relevant statistical factor, if present, four runs were performed with $[Mo^{4+}]$ present in ≥ 10 fold excess and the other runs were performed with $[NCS^-]$ in excess.

A statistical factor of 2 was obtained for the rate determining step in this study when values for the k_{eq} from $[Mo^{4+}]$ in excess were compared with those from $[NCS^-]$ in excess.²⁶ The first-order equilibration constants k_{eq} in the acid range 0.3–2.0 M are given in table 1.11 and graphically illustrated in figure 1.32.

²⁴In a recent study on $[Mo_3(Mo-S)(Mo-S)_2(\mu-O)(OH_2)_6]^{4+}$ with NCS^- , a statistical factor of 2 on the slow step was also seen. i.e. Substitution at the two identical Mo's with mixed μ -O and μ -S coordination spheres was slower than that at the single Mo with all μ -S.^{26a} The reverse case applies in this study. i.e. Substitution at the Mo's is faster than at W.

Table 1.11 k_{m} (25°C) for the reaction of $[\text{Mo}_5\text{WO}_4]^{4-}$ ($\sim 4 \times 10^{-3}$ M) with NCS^- , I = 2.0 M NaCF_3SO_3

$10^3 [\text{NCS}^-]$ M	$[\text{H}^+]$ M	$10^3 k_{\text{m}}$ s ⁻¹
1.50	0.3	10.15
1.95		10.38
2.55		10.95
3.50		11.51
1.20	0.6	6.33
1.50		6.54
1.95		6.64
2.55		7.01
3.50		7.60
1.20	1.0	4.17
1.50		4.40
1.95		4.65
2.55		4.86
3.50		5.30
1.20	1.5	2.78
1.50		2.91
1.95		3.04
2.55		3.28
3.50		3.63
1.20	2.0	2.05
1.50		2.13
1.95		2.25
2.00		2.37-
2.40		2.47-
2.55		2.41
2.60		2.57-
2.80		2.65-
3.50		2.75

*values obtained from studies where $[\text{Mo}_5\text{WO}_4]^{4-}$ was in excess.

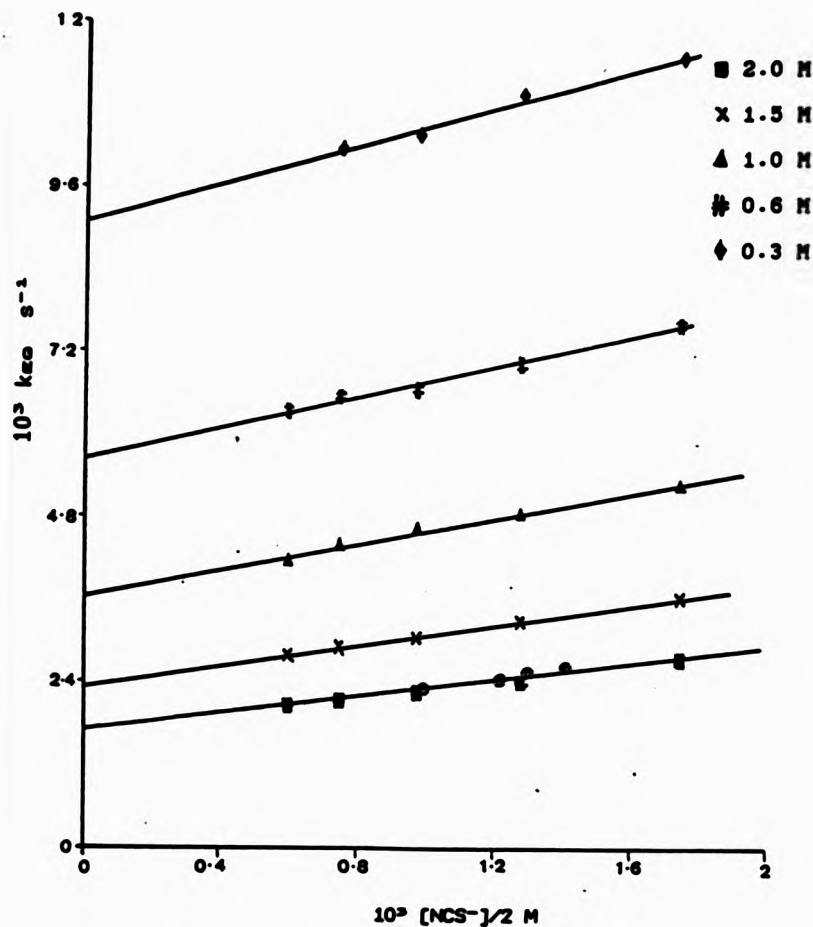


Figure 1.32 Equilibration rate constants vs $[NCS^-]$ as a function of $[H^+]$ ($T=25^\circ\text{C}$ and $I=2.0\text{M NaCF}_3\text{SO}_3$) for the reaction of $[\text{Mo}_6\text{WO}_4]^{4+}$ with thiocyanate. (●: values obtained from runs with $[\text{Mo}_6\text{WO}_4]^{4+}$ in excess)

From these results, the equilibration rate constant can be expressed as in (2).

$$k_{\text{ee}} = k_r [\text{NCS}^-]/2 + k_{\text{ee}} \dots \dots \dots \dots \dots \dots \dots \quad (2)$$

Values for k_r and k_{ee} , for formation and aquation steps involving $[\text{Mo}_2\text{O}_6]^{4+}$ and $[\text{Mo}_2\text{WO}_6\text{NCS}]^{2+}$ respectively, are listed in table 1.12.

Table 1.12 k_r and k_{ee} for $[\text{Mo}_2\text{O}_6]^{4+}$, $[\text{W}_2\text{O}_6]^{4+}$, and $[\text{Mo}_2\text{WO}_6]^{4+}$
at 25°C and I=2.0 M

$[\text{H}+] \text{ M}$	$[\text{Mo}_2\text{O}_6]^{4+}$		$[\text{Mo}_2\text{WO}_6]^{4+}$		$[\text{W}_2\text{O}_6]^{4+}$	
	k_r $\text{M}^{-1} \text{ s}^{-1}$	$10^3 k_{\text{ee}}$ s^{-1}	k_r $\text{M}^{-1} \text{ s}^{-1}$	$10^3 k_{\text{ee}}$ s^{-1}	k_r $\text{M}^{-1} \text{ s}^{-1}$	$10^3 k_{\text{ee}}$ s^{-1}
0.3	2.00	7.4	1.4	9.1	—	—
0.6	1.71	4.0	1.1	5.72	—	—
1.0	1.36	2.57	0.94	3.06	0.19	0.07
1.5	—	—	0.73	2.34	0.14	0.05
2.0	0.80	1.51	0.60	1.67	0.11	0.04
2.0	1.02 ^a	1.94 ^b	—	—	—	—
2.0	2.13 ^c	2.18 ^c	—	—	—	—

^a in H₂SO₄ (obtained from ref. 55)

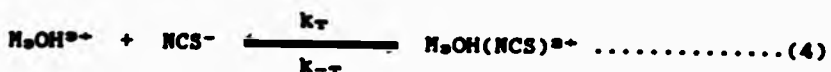
^b in H₂SO₄ (for $[\text{Mo}_2\text{O}_6]^{4+}$ ref. 105)

^c in perchloric acid (for $[\text{Mo}_2\text{O}_6]^{4+}$ ref. 105)
(for $[\text{W}_2\text{O}_6]^{4+}$ ref. 54)

A subsequent plot of k_r against $[\text{H}^+]^{-1}$ is curved, figure 1.33. Correspondingly a plot of $[k_r]^{-1}$ vs $[\text{H}^+]$ was found to be linear (inset figure 1.33) suggesting that the conjugate base form $[\text{Mo}_2\text{WO}_6\text{OH}]^{2+}$ was, not only the sole reactant for NCS⁻ anation

Ch. I: Kinetic results and discussion 108
 as observed with $[Mo_5O_4]^{4+}$, and $[W_5O_4]^{4+}$ separately, but also present in appreciable quantities in the $[H^+]$ range employed.

A subsequent plot of $[k_{Mo}]^{-1}$ vs $[H^+]$ was found to be linear (figure 1.34 inset) leading to the reaction scheme below :



A least squares fit to the plot of $[k_T]^{-1}$ vs $[H^+]$ (inset figure 1.33) gave k_T ($25^\circ C$) = $1.82 \pm 0.07 \text{ M}^{-1} \text{ s}^{-1}$ and K_{Mo} ($25^\circ C$) = $1.00 \pm 0.07 \text{ M}$. A graph of $k_T([H^+] + K_{Mo})$ against $[H^+]$ gives as best fit a horizontal line, and there is no evidence for a step involving reaction of Mo^{4+} with NCS^- . The reaction proceeds via the conjugate-base form only.

Similarly a plot of K_{Mo} against $[H^+]^{-1}$ is curved, figure 1.34. The expression (6)

$$K_{Mo} = \frac{k_T K_{MoT}}{[H^+] + K_{MoT}} \dots \dots \dots \quad (6)$$

can be derived from (2) - (5). A plot of $(K_{Mo})^{-1}$ against $[H^+]$ is linear, inset figure 1.34, with k_T ($25^\circ C$) = $0.19 \pm 0.1 \text{ s}^{-1}$ and K_{MoT} ($25^\circ C$) = 0.02 ± 0.05 .

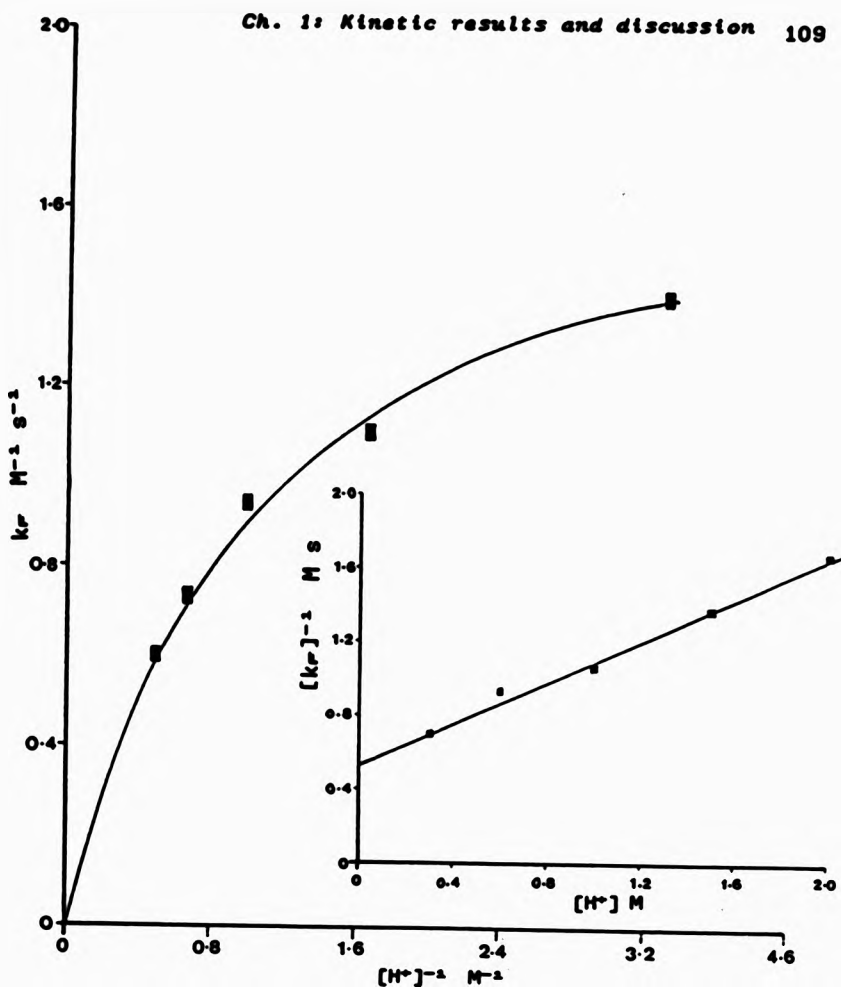


Figure 1.33 Plot of k_p vs $[H^+]^{-1}$ and $[k_p]^{-1}$ vs $[H^+]$ (inset) at $T=25^\circ\text{C}$ and $I=2.0\text{M NaCF}_3\text{SO}_3$ for the reaction of $[\text{Mo}_2\text{WO}_4]^{4+}$ with thiocyanate.

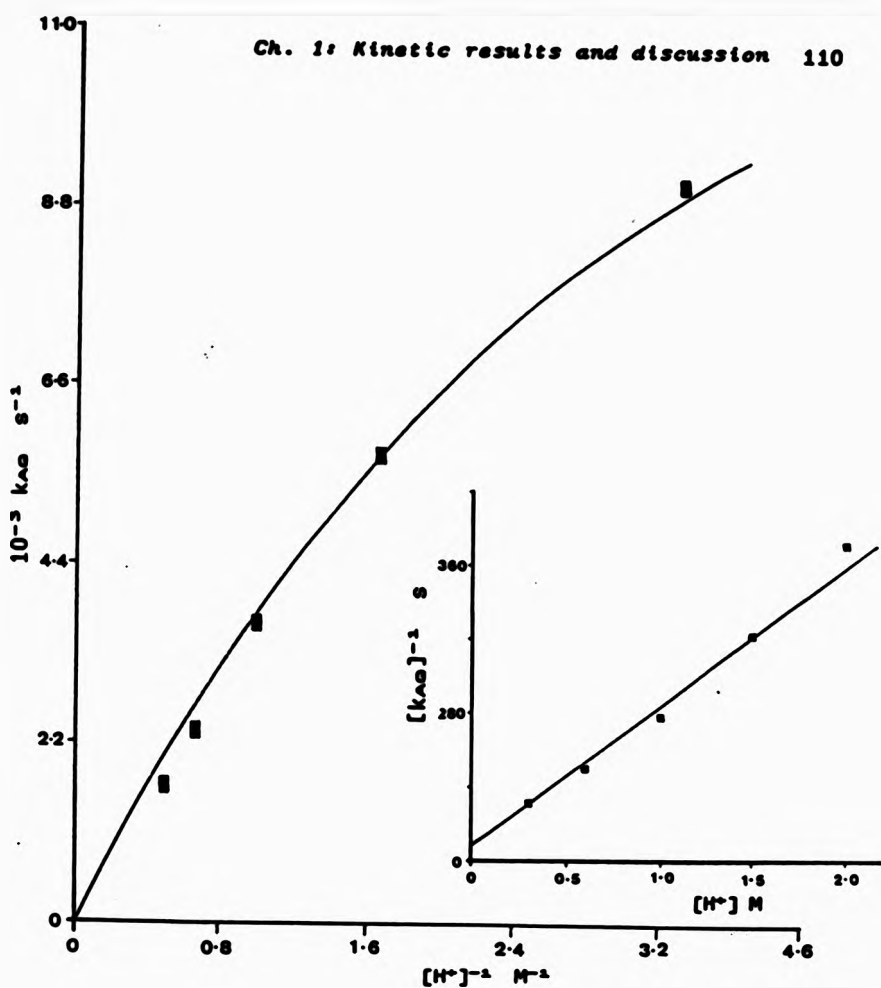


Figure 1.34 Plot of k_{app} vs $[H^+]^{-1}$ and $[k_{app}]^{-1}$ vs $[H^+]$ (inset) at $T=25^\circ\text{C}$ and $I=2.0\text{M NaCF}_3\text{SO}_3$ for the reaction of $[\text{Mo}_2\text{WO}_4]^{4+}$ with thiocyanate.

In order to determine the activation parameters for the substitution process (4), values for K_{app} and $K_{\text{app}'}^*$ at different temperatures are needed from an independent study. This was not possible in the time available. However activation parameters for the overall formation and aquation rate constants can be determined. For K_F $\Delta H^\ddagger = 81.95 \pm 3.32 \text{ kJ mol}^{-1}$ and $\Delta S^\ddagger = +25.7 \pm 11.0 \text{ J K}^{-1} \text{ mol}^{-1}$. For K_{app} $\Delta H^\ddagger = 73.02 \pm 6.12 \text{ kJ mol}^{-1}$ and $\Delta S^\ddagger = -52.2 \pm 20.4 \text{ J K}^{-1} \text{ mol}^{-1}$. The Eyring plot is shown in figure 1.35.

It is found from previous studies^{10a} that rate constants are lowest in Hpts and highest in perchloric acid (probably due to inner or outer-sphere association of pts⁻, tfms⁻, ClO₄⁻ anions to [Mo₂O₆]⁴⁻) and that values obtained in tfms⁻ are 15% greater than those obtained from Hpts (table 1.12). Rate constants therefore determined in the same medium are needed for comparison. It can be observed that the formation rate constants (at 25°C) obtained from this study on [Mo₂WO₆]⁴⁻ aqua ion are similar but somewhat smaller by almost a factor of 2 than the corresponding values for [Mo₂O₆]⁴⁻ ($I = 2M$ Htfms). This can be explained by the presence of the W exerting some electronic effect on the Mo centres. However, sole involvement of the conjugate base and the +ve ΔS^\ddagger value indicate the presence of the dissociative mechanism for 1:1 NCS⁻ substitution proposed to occur in the homo trinuclear [Mo₃O₆]⁴⁻ and [W₃O₆]⁴⁻ ions.

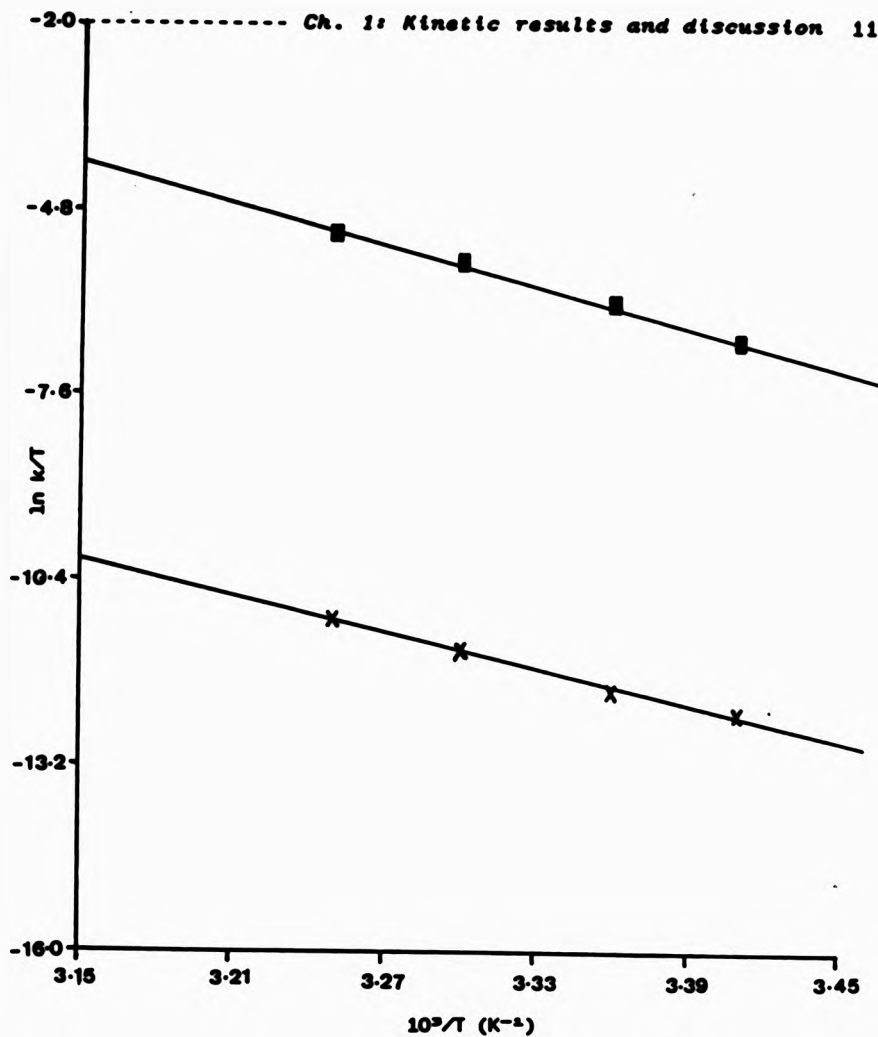


Figure 1-35 Eyring plots for thiocyanate anation on $[\text{Mo}_2\text{WO}_4]^{4-}$ at $T=25^\circ\text{C}$ and $I=2.0\text{M NaCF}_3\text{SO}_3$. k_f (—●—) and k_{Ae} (××).

Of interest however is the remarkably high kinetic value of K_{aw} for the Mo₂W ion (1.00 M) compared to those obtained from the corresponding studies on [Mo₂O₄]⁴⁻ (0.4 M)^{**} and [W₂O₄]⁴⁻ (0.22 M)^{**}. It will be important to test the validity of this value by an independent study as performed with [Mo₂O₄]⁴⁻.⁴⁷ This was not possible in the time available. One possible explanation for the high acidity could be a build up of positive charge on the Mo atoms of the mixed aqua ion perhaps by an electron withdrawing effect of the more electronegative W atom.* In turn the higher positive charge could be responsible for the slightly greater inertness shown by the coordinated water ligands of the mixed aqua ion towards NCS⁻ replacement. This may also reflect the slightly higher ΔH_f° value of 81.93 kJ mol⁻¹ when compared to that estimated for water exchange (71.0 ± 8.5 kJ mol⁻¹) if a dissociative mechanism at the d-sites, trans to the W-O group, is relevant. The intermediate position (325 nm) observed for the NCS⁻ → Mo₂⁴⁺ charge transfer band for the mixed aqua ion product (figure 1.36) compared with those observed on NCS⁻ anation with [Mo₂O₄]⁴⁻ (340 nm) and [W₂O₄]⁴⁻ (280 nm) further suggests an electronic involvement from the W atom on the Mo sites.

* W is more electronegative (1.40) on the Allred-Rochow scale than Mo (1.30).^{**} Calculated according to the following equation:

$$\chi_{AM} = [3590 \cdot Z_{eff.}/r^2] + 0.744 \quad \text{where } r \text{ is the covalent radius.}$$

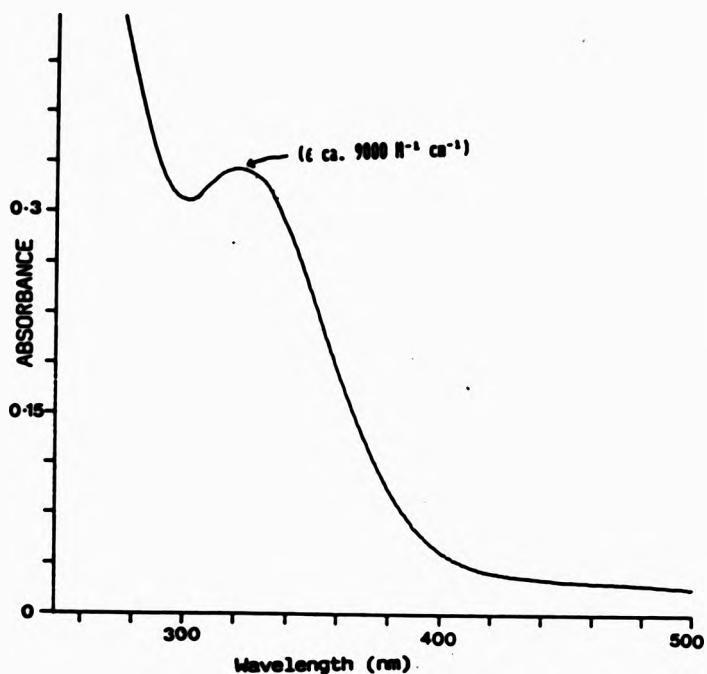


Figure 1.36 Electronic spectrum of final product of thiocyanate anation on $[Mo_2W_6]^{4+}$ ($I=2.0M$ $NaCF_3SO_3$).

On the other hand, the aquation rate constants for the mixed $[\text{Mo}_2\text{WO}_4(\text{OH})(\text{NCS})]^{2+}$ product seem to be in very close agreement with those obtained for the $[\text{Mo}_2\text{O}_4(\text{OH})(\text{NCS})]^{2+}$ showing little or no influence of the W atom. The 1:1 NCS⁻ complex is much less acidic ($K_{\text{a}_{\text{H}^+}} = 0.02 \text{ M}$), when compared to $[\text{Mo}_2\text{O}_4]^{2+}$, as observed with the corresponding values for the 1:1 NCS⁻ complexes with $[\text{Mo}_2\text{O}_4]^{2+}$ (0.19 M)²² and $[\text{W}_2\text{O}_4]^{2+}$ (0.07 M)²⁴ (all values at 25°C, I=2.0 M).

1.10.4 Product analysis.

No cation-exchange analysis of the final product of NCS⁻ anation with $[\text{Mo}_2\text{O}_4]^{2+}$ was carried out but the available kinetic evidence supports formation of a 1:1 complex $[\text{Mo}_2\text{WO}_4(\text{NCS})]^{2+}$ together with its conjugate base as the product of the rate determining steps described. The position of the L → M charge transfer band suggests that the coordination of the NCS⁻ ligand occurs through the nitrogen atom as confirmed crystallographically with $[\text{Mo}_2\text{O}_4]^{2+}$ ²¹ and $[\text{W}_2\text{O}_4]^{2+}$ ²⁰.

1.10.5 Site of 1:1 anation.

The ^{17}O NMR spectrum (figure 1.28) from a solution of $[\text{Mo}_2\text{WO}_4(\text{H}_2\text{O})_6]^{2+}$, revealed the presence of c and d-H₂O sites present in the cluster ion as observed with the Mo(IV) and W(IV) cluster ions. Brief studies on the water exchange at 40°C have shown that the c-H₂O ligands (trans to the μ₂-O) (more upfield shifted resonances) are much more inert than the d-H₂O ligands trans to the μ₂-O groups. Therefore it is likely that 1:1

anation has occurred preferentially at the Mo sites that are trans to the μ -O groups. Deprotonation is envisaged to occur at a further d-H₂O located on the same Mo atom being substituted (Figure 1.37).

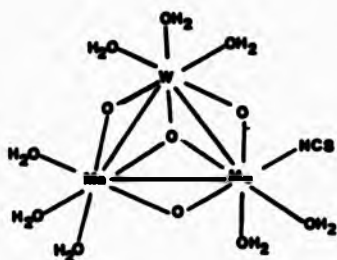


Figure 1.37 Probable structure of the 1:1 NCS⁻ complex with $[Mo_2WO_4(OH_2)_6(OH)]^{2+}$. (one diastereoisomer)

1.11 Conclusion

The evidence in support of the existence of the mixed Mo₂W aqua ion in acidic solution can now be summarised as follows :

- 1) AAS analysis confirmed the presence of Mo and W in a ratio 2:1 from chromatographically pure solutions of the reddish-purple aqua ion in 3M HCl.
- 2) Cyclic voltammetry experiments and chemical reduction with amalgamated zinc confirmed the presence of reduced mixed-valence M(III,III,IV) and M(III)₂ aqua ions showing electro-

Ch. 1: Kinetic results and discussion 117
chemical and spectroscopic properties consistent with new species and not with a 2:1 mixture of the corresponding homo Mo and W reduced ions (see figure 1.29).

- 3) Kinetic studies of the 1:1 complexation of the reddish-purple ion with NCS⁻ were consistent with N-bonded substitution occurring at the two statistically identical Mo(IV) sites in the mixed ion.
- 4) Finally, following heating of concentrated solutions of the reddish-purple ion in the presence of H₂O¹⁷, ¹⁷O NMR studies showed evidence of a new resonance (640 ppm) likely to be μ₂-O groups bridging between Mo and W atoms in the mixed [Mo_nWO₄]ⁿ⁺ aqua ion.

REFERENCES

1. Spence, J. T.; Lee, J. Y. Inorg. Chem., 1965, 4, 385.
2. Cotton, F. A.; Wilkinson, G. "Advance Inorganic Chemistry". fifth Ed., Wiley-interscience, 1988, 811.
3. Cruywagen, J. J.; Van der Merwe, I. P. I. J. Chem. Soc. Dalton Trans., 1987, 1701.
4. Klemperer, W. G.; Shum, W. J. Am. Chem. Soc., 1977, 99, 3544.
5. (a) Counterford, J. H.; Colton, R. "Halides of the second and third row transition metals". Wiley-interscience, 206.
(b) Parish, R. V. Adv. Inorg. Radiochem., 1966, 9, 324.
6. (a) Pykko, P.; Desclaux, J. P.; Acc. Chem. Res., 1979, 12, 276.
(b) McKelvey, D. R. J. Chem. Ed., 1983, 60, 112.
7. (a) Olsson, O. Chem. Ber., 1913, 46, 566.
(b) Collenberg, O.; Backer, J. Z. Elektrochem., 1924, 30, 230.
(c) Klemm, W.; Steinberg, H. Z. Anorg. Allgem. Chem., 1936, 227, 193.
(d) Lingane, J. J.; Small, L. A. J. Am. Chem. Soc., 1949, 71, 973.
(e) Kennedy, C. D.; Peacock, R. D. J. Chem. Soc., 1963, 3392.
(f) König, E. Inorg. Chem., 1963, 2, 1238.
8. König, E. Inorg. Chem., 1969, 8, 1278.
9. Filippo, J. S.; Pagan, P. J.; Di Salvo, P. J. Inorg. Chem., 1977, 16, 1016.
10. Watson, W. H.; Waser, J. Acta Cryst., 1958, 11, 689.
11. Laudise, R. A.; Young, R. C. Inorg. Syn., 1980, 6,
12. Lewis, J.; Nyholm, R. S.; Smith, P. J. Chem. Soc., A, 1969, 57.
13. Saillant, R.; Wentworth, R. A. D. Inorg. Chem., 1969, 8, 1226.

14. Coughlan, M. P. "Molybdenum and Molybdenum-containing Enzymes". Pergamon Press Ltd., NY, 1980.
15. Richens, D. T.; Sykes, A. G. Comm. Inorg. Chem. - 1981, 1, 141.
16. Paffett, M.T.; Anson, F. C. Inorg. Chem. - 1983, 22, 1347 and 1355.
17. Podall, H. E.; Prestridge, H. B.; Shapiro, H. J. Am. Chem. Soc., 1961, 83, 2057.
18. Lohmann, K. H.; Young, R. C. Inorg. Syn. - 1953, 4, 97.
19. Richens, D. T.; Sykes, A. G. Inorg. Syn. - 1985, 23, 130.
20. Brignole, A. B.; Cotton, F. A. Inorg. Syn. - 1972, 13, 88.
21. Brencic, J. V.; Cotton, F. A. Inorg. Chem. - 1970, 9, 351.
22. Cotton, F. A.; Bertram, F. A.; Pedersen, E.; Webb, T. R. Inorg. Chem. - 1975, 14, 391.
23. Bowen, A. R.; Taube, H. Inorg. Chem. - 1974, 13, 2245.
24. Brencic, J. V.; Cotton, F. A. Inorg. Chem. - 1969, 8, 7.
25. Bino, A. Inorg. Chem. - 1981, 20, 623.
26. Cotton, F. A.; Frenz, B. A.; Pedersen, E.; Webb, T. R. Inorg. Chem. - 1975, 14, 391.
27. Cotton, F. A.; Frenz, B. A.; Webb, T. R. J. Am. Chem. Soc., 1973, 95, 4431.
28. Chisholm, M. H. et al. Polyhedron, 1984, 3, 759.
29. Schrock, et al. Inorg. Chem. - 1983, 22, 2801.
30. Brencic, J. V.; Cotton, F. A. Inorg. Syn. - 1972, 13, 170.
31. Sasaki, Y.; Sykes, A. G. J. Chem. Soc. Chem. Commun. - 1973, 767.
32. Sasaki, Y.; Sykes, A. G. J. Chem. Soc. Dalton Trans. - 1975, 1048.
33. Richens, D. T.; Ducommun, Y.; Herbach, A. E. J. Am. Chem. Soc., 1987, 109, 603.
34. Ardon, M.; Pernick, A. Inorg. Chem. - 1974, 13, 2275.
35. Harmer, M. A.; Sykes, A. G. Inorg. Chem. - 1981, 20, 3963.
36. Kneale, C. G.; Geddes, A. J.; Sasaki, Y.; Shibahara, T.; Sykes, A. G. J. Chem. Soc. Chem. Commun. - 1975, 356.

37. Richens, D. T.; Helm, L.; Pittet, P. A.; Herbach, A. E. Inorg. Chim. Acta, 1987, 85, 132.
38. Souchay, P.; Cardiot, M.; Duhamaux, M. C. R. Acad. Sci., 1986, 262, 1524.
39. Ardon, M.; Pernick, A. J. Am. Chem. Soc., 1973, 95, 6871.
40. Bino, A.; Cotton, F. A.; Dori, Z. J. Am. Chem. Soc., 1978, 100, 5252.
41. Murmann, R. K.; Hussain, M. S.; Schlemper, E. O. Cryst. Struct. Commun., 1982, 11, 89.
42. Rodgers, K. R.; Murmann, R. K.; Schlemper, E. O.; Shelton, M. E. Inorg. Chem., 1985, 24, 1313.
43. Bino, A.; Cotton, F. A.; Dori, Z. J. Am. Chem. Soc., 1979, 101, 3842.
44. Wedd, A. G.; Snow, M. R.; O'Connor, M. G.; Brownlee, R. T. C.; Hambley, T. W.; Gheller, S. F. J. Am. Chem. Soc., 1983, 105, 1527.
45. Murmann, R. K.; Shelton, M. E. J. Am. Chem. Soc., 1980, 102, 3984.
46. Müller, A.; Jostes, R.; Cotton, F. A. Angew. Chem. Int. Ed. Engl., 1980, 19, 875.
47. Richens, D. T.; Helm, L.; Pittet, P. A.; Herbach, A. E.; Nicolo, F.; Chapius, G. Inorg. Chem., (in press).
48. Segawa, M.; Sasaki, Y. J. Am. Chem. Soc., 1985, 107, 5565.
49. McMahon, M. R. MSC Thesis, University of Stirling, 1986.
50. Cramer, S.P.; Gray, H. B.; Dori, Z.; Bino, A. J. Am. Chem. Soc., 1979, 101, 2770.
51. Ardon, M.; Bino, A.; Yahav, G. J. Am. Chem. Soc., 1976, 98, 2338.
52. Chalilpoyil, P.; Anson, F. C. Inorg. Chem., 1978, 17, 2418.
53. Ramasami, T.; Taylor, R. S.; Sykes, A. G. J. Am. Chem. Soc., 1975, 97, 5918.
54. Ooi, B. -L.; Petrou, A.; Sykes, A. G. Inorg. Chem., 1988, 27, 3626.
55. Ooi, B. -L.; Sykes, A. G. Inorg. Chem., 1988, 27, 310.

56. Van Felton, H.; Wernli, B.; Gamsjäger, H.; Baertschi, P. J. Chem. Soc. Dalton Trans.. 1978, 496.
57. (a) Richens, D. T.; Sykes, A. G. Inorg. Chem.. 1982, 21, 418.
(b) Richens, D. T.; Sykes, A. G. Inorg. Chim. Acta. 1981, 54, L3.
58. Richens, D. T. Unpublished work.
59. Kathirgamanathan, P.; Martinez, M.; Sykes, A. G. J. Chem. Soc. Chem. Commun.. 1985, 1437.
60. Martinez, M.; Ooi, B. -L.; Sykes, A. G. J. Am. Chem. Soc.. 1987, 109, 4615.
61. Shibahara, T.; Hattori, H.; Kuroya, H. J. Am. Chem. Soc.. 1984, 106, 2710.
62. Shibahara, T.; Kuroya, H. Fifth Int. Conf. on Chem. and Uses of Molybdenum. Abstracts, 1985, 59.
63. Kathirgamanathan, P.; Martinez, M.; Sykes, A. G. J. Chem. Soc. Chem. Commun.. 1985, 953.
64. Lovenberg, W. "Iron-Sulphur Proteins". 1973-1977, I-III. Acad. Press. (NY, London).
65. Cotton, F. A.; Diebold, M. P.; Dori, Z.; Llubar, R.; Schwatzer, W. J. Am. Chem. Soc.. 1985, 107, 6735.
66. Cotton, F. A.; Dori, Z.; Llubar, R.; Marler, D. O.; Schwatzer, W. Inorg. Chim. Acta. 1985, 102, L25.
67. Cotton, F. A.; Dori, Z.; Llubar, R.; Schwatzer, W. J. Am. Chem. Soc.. 1985, 107, 6734.
68. Dori, Z.; Cotton, F. A.; Llubar, R.; Schwatzer, W. Polyhedron. 1986, 5, 907.
69. Ooi, B. -L.; Martinez, M.; Shibahara, T.; Sykes, A. G. J. Chem. Soc. Chem. Commun.. 1988, 2239.
70. Shibahara, T.; Sheldrick, B.; Sykes, A. G. J. Chem. Soc. Chem. Commun.. 1976, 253.
71. Cayley, G. R.; Taylor, R. S.; Wharton, R. K.; Sykes, A. G. Inorg. Chem.. 1977, 16, 1377.
72. Sabat, H.; Rudolf, M. F.; Jezowska-Trezebiadowska, B. Inorg. Chim. Acta. 1973, 7, 365.

Ch. 3: References 122

73. Sharp, C.; Hills, E. F.; Sykes, A. G. J. Chem. Soc. Dalton Trans., 1987, 2293.
74. Sykes, A. G. Personal communication.
75. Cruywagen, J. J.; Heyns, J. B. B.; Rohwer, E. F. C. H. J. Inorg. Nucl. Chem., 1978, 40, 53.
76. Gansjäger, H.; Murmann, R. K. Adv. Inorg. Bioinorg. Mech., 1983, 2, 350.
77. Comba, P.; Herbach, A. E. Inorg. Chem., 1987, 27, 1415.
78. Klemperer, W. G. Angew. Chem. Int. Ed., 1978, 17, 246.
79. Filowits, M.; Klemperer, W. G.; Messerle, L.; Shum, W. J. Am. Chem. Soc., 1976, 98, 2345.
80. English, A. D.; Jesson, J. P.; Klemperer, W. G.; Mamounas, T.; Messerle, L.; Shum, W.; Tramontano, A. J. Am. Chem. Soc., 1975, 97, 4785.
81. Maksimovskaya, R. I.; Burtseva, K. G. Polyhedron, 1985, 4, 1559.
82. (a) Kazanskii, L. P.; Fedotov, M. A.; Spitsyn, V. I. Dokl. AN SSSR, 1977, 234, 1376.
(b) Fedotov, M. A.; Kazanskii, L. P.; Spitsyn, V. I. Dokl. AN SSSR, 1983, 272, 1179.
83. Pope, M. T.; Piepgrass, K. J. Am. Chem. Soc., 1987, 109, 1587.
84. Launay, J. P. J. Inorg. Nucl. Chem., 1976, 38, 107.
85. (a) Jackson, J. A.; Taube, H. J. Phys. Chem., 1965, 69, 1844.
(b) Piggis, B. N.; Kidd, R. G.; Nyholm, R. S. Can. J. Chem., 1965, 43, 145.
86. Filowits, M.; Klemperer, W. G. J. Chem. Soc. Chem. Commun., 1977, 201.
87. Filowits, M.; Klemperer, W. G. J. Chem. Soc. Chem. Commun., 1976, 233.
88. Day, V. W.; Fredrich, M. F.; Klemperer, W. G.; Shum, W. J. Am. Chem. Soc., 1977, 99, 952.

Ch. I: References 123

89. Day, V. W.; Fredrich, M. F.; Klemperer, W. G.; Shum, W. J. Am. Chem. Soc., 1977, 99, 6146.
90. Klemperer, W. G.; Shum, W. J. Am. Chem. Soc., 1978, 100, 4891.
91. Rhodes, L. F.; Huffman, J. C.; Coulton, K. G. J. Am. Chem. Soc., 1985, 107, 1759.
92. Bogan, L. E. Jr.; Rauchfuss, T. B.; Rheingold, A. L. J. Am. Chem. Soc., 1985, 107, 3843.
93. Arndt, L. W.; Darenbourg, H. Y.; Fackler, J. P. Jr.; Lusk, R. J.; Marler, D. O.; Youngdahl, K. A. J. Am. Chem. Soc., 1985, 107, 7218.
94. Doyle, G.; Eriksen, K. A.; Van Engen, D. J. Am. Chem. Soc., 1985, 107, 7914.
95. Kotavic, V.; Templeton, J. L.; Noymeier, R. J.; McCarley, R. E. J. Am. Chem. Soc., 1975, 97, 5300.
96. Kotavic, V.; McCarley, R. E. J. Am. Chem. Soc., 1978, 100, 5586.
97. Wang, B.; Sasaki, Y.; Nagasawa, A.; Ito, T. J. Am. Chem. Soc., 1986, 108, 6059.
98. Chisholm, M. H.; Folting, K.; Huffman, J. C.; Kober, E. M. Inorg. Chem., 1985, 24, 241.
99. Chisholm, M. H.; Folting, K.; Heppert, J. A.; Hoffman, D. M.; Huffman, J. C. J. Am. Chem. Soc., 1985, 107, 1234.
100. Sasaki, Y. Personal communication.
101. Allen, E. A.; Brindon, B. J.; Powles, G. W. A. J. Chem. Soc., 1964, 4531.
102. Larson, M. L.; Moore, F. W. Inorg. Chem., 1964, 3, 285.
103. Collenberg, O. Z. Anorg. Chem., 1918, 102, 247 detailed in: Powles, G. A. W. "Preparative Inorganic Reactions". Interscience, 1964, 1, 137.
104. Novak, J.; Podlaha, J. J. Inorg. Nucl. Chem., 1975, 36, 1061.

Ch. II: References 124

105. (a) McCarley, R. E.; Brown, T. M. Inorg. Chem.. 1964, 3, 1232.
(b) Carmichael, W. M.; Edwards, D. A.; Walton, R. A. Inorg. Chem.. 1966, 5, 97.
106. Naight, G. P.; Rahmoeller, K. M. Polyhedron. 1986, 5, 507.
107. Kathirgamanathan, P.; Soares, A. B.; Richens, D. T.; Sykes, A. G. Inorg. Chem.. 1985, 24, 2950.
108. Allred, A. L.; Rochow, E. G. J. Inorg. Nucl. Chem.. 1958, 2, 264.
109. Laudise, R. A.; Young, R. C. Inorg. Chem.. 1960, 6, 149.
110. Buckingham, D. A.; Frances, D. J.; Sargeson, A. M. Inorg. Chem.. 1974, 13, 2630.
111. (a) Pohl, M. C.; Espenson, J. H. Inorg. Chem.. 1980, 19, 235.
(b) Marty, W.; Espenson, J. H. Inorg. Chem.. 1979, 18, 1246.
112. Armstrong, F. A.; Henderson, R. A.; Sykes, A. G. J. Am. Chem. Soc.. 1980, 102, 6545.

CHAPTER TWO

2. Aqueous solution chemistry of ruthenium.

Much of the aqueous solution chemistry of ruthenium is dominated by the formation of complexes with halide and nitrogen donor ligands. Like the solution chemistry of molybdenum, it has many similarities with its third row counterpart osmium with a lesser resemblance to its lighter partner iron. Many similarities also exist with compounds of Rh and Ir leading to its inclusion as a member of the platinum metals. The greatest similarities between Ru and Os are found in the oxides (particularly the formation of a tetroxide), fluorides, and the chemistry of the lower oxidation state compounds with H-acid ligands (II to 0). Aqua ions of Ru^{xx} and Ru^{zzz} , are well established but the precise nature of the $\text{Ru}^{xx}_{(aq)}$ species is not known. In general, the aqueous solution chemistry of Ru is much less understood than both Mo and W. In the following pages the oxide and oxo compounds, the halide and halo- complexes, and the aqua ions of Ru are reviewed.

2.1 Oxide and oxo compounds of ruthenium.

The tetroxide (RuO_4) may be prepared by oxidation of the metal with hot solutions of powerful oxidizing agents such as periodate, and permanganate.¹⁻² A convenient method of preparing RuO_4 from acidic ruthenium solutions is by treatment of commercial RuCl_3 with MnO_4^- , BrO_3^- , OCl^- , etc. in the presence of carbon tetrachloride (CCl_4); the yellow RuO_4 then passing

into the organic layer.^{2,4,5} Along with OsO_4 , it is one of the two known volatile tetroxides, and has played a vital role synthetically in the aqueous solution chemistry of Ru. Furthermore, it has found wide applications as an oxidizing agent in organic chemistry, particularly when reduced to the ruthenate(VII, and VI) ions.^{6,7} The tetroxide is sparingly soluble in water, but highly soluble in CCl_4 giving yellow solutions. Raman spectroscopic studies confirm that the structure in both solvents is tetrahedral.⁸

Treatment of RuO_4 with aqueous alkali yields O_2 and the ruthenate(VII) (perruthenate, $[\text{RuO}_4]^{7-}$) species which is a milder oxidizing agent than RuO_4 . Prolonged treatment with aqueous alkali causes further reduction leading to the production of ruthenate(VI) ($[\text{RuO}_4]^{6-}$). Equations (1) and (2) summarise the reduction processes:⁹



The reduction of the green $[\text{RuO}_4]^{7-}$ in aqueous alkali to the orange $[\text{RuO}_4]^{6-}$ has been kinetically studied and a rate law of the form (3) was suggested.

$$\text{rate} = k_{\text{app}}([\text{RuO}_4]^{7-})^a([\text{OH}^-])^b \dots\dots\dots(3)$$

where k_{app} = apparent rate constant.

The proposed mechanism includes the formation of unstable intermediates with coordinated OH⁻ and expansion of the coordination sphere of the Ru such as [RuO₄(OH)_n]ⁿ⁻, and [RuO₄(OH)_n]ⁿ⁻, and the formation of H₂O_n. The addition of OH⁻ is in contrast to the reaction of 3d oxo anions, where there is no dominant OH⁻ involvement. In the case of O₂, the expansion of the coordination sphere is such that stable hydroxo species are formed.

Although treatment of the tetroxide with alkali gives the ruthenate(VII) and (-VI) species, more convenient methods for their preparation involve the oxidation of aqueous RuCl₃. The ruthenate(VII) ion is prepared by periodate oxidation¹⁰ while the ruthenate(VI) ion is prepared by peroxodisulphate oxidation of RuCl₃ in KOH.¹¹ The electronic spectra of RuO₄, [RuO₄]ⁿ⁻, and [RuO₄]ⁿ⁻ are shown in figure 2.1

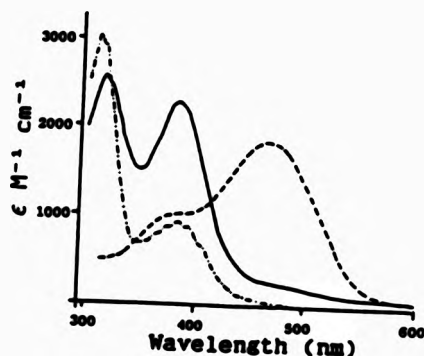


Figure 2.1 Electronic spectra of RuO₄ (----), [RuO₄]ⁿ⁻ (—), and [RuO₄]ⁿ⁻ (---) in aqueous solution.¹²

2.2 Halide and halo-complexes of Ruthenium.

The characteristic halide, halo and oxo-halo complexes are given in table 2.1. When RuO₄ is treated with gaseous HCl and Cl₂¹², the dioxo species [RuO₂Cl₄]²⁻ can be initially obtained but this undergoes rapid hydrolysis (4):

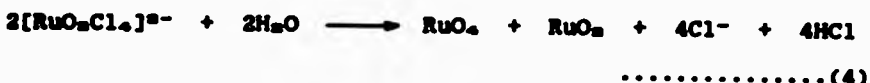


Table 2.1 Halide, halo- and oxo-halo compound of ruthenium.¹⁴

Compound	Oxidation state			
	III	IV	V	VI
Halides	$\alpha\text{-RuCl}_3$, $\beta\text{-RuCl}_3$, RuF_5 , RuI_5	RuF_4 , RuOCl_4	$(\text{RuF}_6)_4$	RuF_6
Halo- and Oxo-halo- complexes	$[\text{RuCl}_6]^{3-}$, $[\text{RuCl}_5]^2-$, $[\text{RuF}_5]^{2-}$, $[\text{RuI}_5]^{2-}$	$[\text{RuCl}_6]^{4-}$, $[\text{RuF}_5]^{3-}$, $[\text{RuOCl}_{4.5}]^{2-}$	$[\text{RuF}_6]^-$, $[\text{RuO}_2\text{Cl}_4]^{2-}$	

The deep red Cs^+ salt ($\text{Cs}_2[\text{RuO}_3\text{Cl}_4]$) has been isolated from the reaction of RuO_4 with HCl in the presence of CsCl .¹⁵ It is diamagnetic and the IR spectrum suggests that there is a linear $\text{O}=\text{Ru}=\text{O}$ grouping similar to the $\text{O}=\text{Os}=\text{O}$ moiety found in the "osmyl" complexes ($\text{K}_2[\text{OsO}_3\text{Cl}_4]^{1+}$ and $\text{K}_2[\text{OsO}_3(\text{OH})_4]^{1+}$) which have been structurally characterized by X-ray diffraction.

Further reduction of RuO_4 in HCl and in the presence of KCl gives the $[\text{Ru}_2\text{OCl}_{10}]^{4-}$ ion. This ion was initially formulated as $[\text{Ru}(\text{OH})\text{Cl}_9]^{4-}$, but the observed diamagnetism and a subsequent X-ray crystal study showed that the ion is indeed binuclear and that the Ru—O—Ru group is linear.¹⁰ The observed diamagnetism can be explained in terms of 2 three-centred two electron π -molecular orbitals that are perpendicular. The electron pairs in the $2p_x$ and $2p_m$ orbitals are assumed to interact with the singly occupied $4d_{mx}$ and $4d_{ms}$ orbitals on the Ru (taking Ru—O—Ru as the x axis) to form the 2 three-centred π -molecular orbitals (figure 2.2).

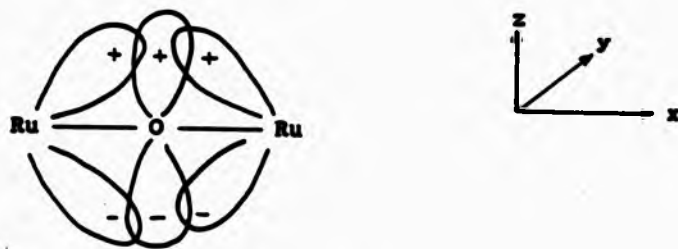


Figure 2.2 Bonding in $[\text{Ru}_2\text{OCl}_{10}]^{4-}$: $4d_{mx} - 2p_x - 4d_{ms}$ overlap. There will also be a similar $4d_{mx} - 2p_y - 4d_{ms}$ interaction.

Each of these MO's will have 2 electrons which are paired, and since the "non-bonding" $4d_{ms}$ orbitals on the Ru atoms will each contain an electron pair, overall diamagnetism will result.

Figure 2.3 shows the electronic spectrum of aqueous $[\text{Ru}_2\text{OCl}_{10}]^{4-}$.

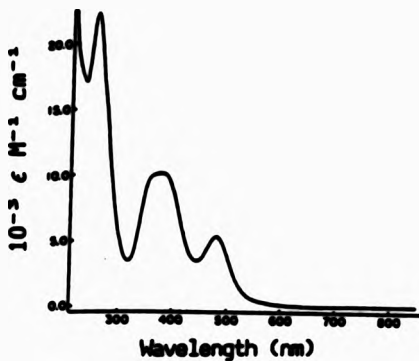


Figure 2.3 Electronic spectrum of aqueous $[\text{Ru}_2\text{OCl}_{10}]^{4-}$.

A similar bromo species was originally thought to exist²⁰ but more recently it has been confirmed as being $[\text{Ru}_2\text{Br}_6]^{4-}$.²¹ The species $[\text{RuCl}_6]^{4-}$ can be obtained in solution by treating $\text{K}_2[\text{Ru}_2\text{OCl}_{10}]$ in 1M HCl with H_2O_2 and then mixing the resulting solution with equal volume of concentrated HCl to achieve oxidation of the excess peroxide.²²

Ruthenium trichloride, RuCl_3 , is prepared in the pure form by direct combination of the metal with Cl_2 and exists in two allotrophic states; α - RuCl_3 (water and ethanol soluble) and β - RuCl_3 (water and ethanol insoluble). When RuO_4 solutions in concentrated HCl are left to evaporate, a dark red material $\text{RuCl}_3 \cdot n\text{H}_2\text{O}$ is obtained.²³ This is commonly known as "Commercial ruthenium trichloride" and it is by far the most common starting material for Ru chemistry. It is actually a mixture of mainly Ru(IV) species with some RuCl_3 .

Reduction of commercial RuCl_3 in 0.3M HCl with mercury gives solutions containing Ru^{III} complexes, which are re-oxidized by air to Ru^{IV} .²³ Ion exchange separation has allowed definite characterization of $[\text{Ru}(\text{OH}_2)_6]^{2+}$, $[\text{RuCl}(\text{OH}_2)_5]^{2+}$ and *cis* and *trans* $[\text{RuCl}_2(\text{OH}_2)_4]^{2+}$.²⁴ At high chloride concentrations $[\text{RuCl}_6]^{2-}$ has recently been identified.²⁴ The rate of aquation is found to increase with the number of Cl^- ions coordinated; thus the half life for aquation of $[\text{RuCl}_6]^{2-}$ to the aqua pentachloro species $[\text{RuCl}_4(\text{OH}_2)]^{2-}$ is of the order of seconds, whereas that for the conversion of the chloropentaqua species $[\text{RuCl}(\text{OH}_2)_5]^{2+}$ to $[\text{Ru}(\text{OH}_2)_6]^{2+}$ is about a year.²⁴ The vast difference in the rates of aquation may resemble a crystal field effect, Cl^- having a smaller crystal field splitting effect than water, or may arise from the greater polarisability of chloride.²⁴ Some evidence was found for a *trans* labilizing effect, the position *trans* to chloride in a complex appearing to have a greater reactivity than the position *trans* to water. For example, *mer*- $[\text{RuCl}_6(\text{OH}_2)_3]$ loses a Cl^- ion at least 10 x faster than does *fac*- $[\text{RuCl}_6(\text{OH}_2)_3]$. The X-ray crystal structure of $[\text{AsPh}_3][\text{trans-RuCl}_4(\text{OH}_2)_3]$ shows that the M-O distance is $2.12 \pm 0.01 \text{ \AA}$ and the M-Cl distance is $2.34 \pm 0.01 \text{ \AA}$.²⁵

The chloro complexes of ruthenium in the 3+ oxidation state have led to a great deal of interest in recent years because of their use in homogeneous catalysis.^{26a-d} Ruthenium(III)-chloride and its EDTA complex have recently been employed as

CH. 2: Aqueous solution chemistry of Ru 132
catalysts in the oxidation of allyl alcohol, ascorbic acid, and
cyclohexanol.²⁰

When Ru⁺⁺⁺ chloro complexes are reduced electrochemically or chemically using Zn, Zn/Mg, Ti⁺⁺⁺, Al, Cr⁺⁺, or H₂S in aqueous or ethanolic media, intensely blue solutions are produced.^{20,21} Treatment of Ru_n(O₂CMe)₄ with HCl also gives blue solutions. The exact constitution of these blue species is not settled. Several species may be present including polynuclear species containing both Ru⁺⁺ and Ru⁺⁺⁺. Cotton et al.²² have reported a green salt, isolated from the blue solution of Ru_n⁺⁺_{4-n}⁺⁺⁺(O₂CMe)₄Cl in 12M HCl, which has the structure:



From the same blue solutions, by varying the pH and chloride ion concentration, a number of workers have isolated different species. Thus, in 6M HCl, Godwood and Wardlaw²³ after adding [pyH]⁺ isolated a green compound [pyH]_n[RuCl₄]. Adamson²⁴, following addition of CsCl to the blue solution in 12M HCl, isolated a dark-blue solid which was highly air sensitive and had a Ru:Cl ratio of ~1:5.5. Rose and Wilkinson²⁵ repeated this work and found that the blue compound formed turned green during filtration (even under air-free conditions). They analyzed the green compound as impure Cs_n[RuCl₄]_nH₂O. The same workers have reported polymeric compounds which were isolated also from the blue solution in methanol. The three salts isolated all contained the [Ru_nCl₈]²⁻ core. Therefore it may

be concluded that the constitution of the blue species is by no means clear, and it is likely that an equilibrium mixture of both mono- and polynuclear species is present.

Rechnitz and Catherine²² have studied the oxidation of the ruthenium(II) blue species by H₂O and D₂O. The oxidation is quantitative according to the equation (5) giving a yellow solution of Ru(III).



The kinetics were followed by electronic spectrophotometry, the spectral change exhibiting an isosbestic point at 359 nm. The rate determining step does not involve H-O bond rupture (absence of the kinetic isotope effect) and the observed kinetics were consistent with the scheme:



The reaction follows pseudo first-order kinetics with $k = 4 \times 10^{-8} \text{ s}^{-1}$ (at pH 1.5, T= 30°C and [Cl⁻] = 2.5 M).

2.3 Ruthenium complexes with N donor ligands.

Both Ru²⁺ and Ru³⁺ form a wide range of complexes with nitrogen donor ligands of which the ammine complexes have been extensively studied.²³⁻²⁶ A notable characteristic of ruthenium ammine chemistry is the formation of intense red and brown

species usually referred to as ruthenium "red" and "brown". A diamagnetic red compound has been isolated from the red solution obtained by treating commercial RuCl₃ with aqueous NH₃ in the presence of Ti⁺⁺⁺.²⁰ The complex has been assigned the following structure :



Oxidation of the "red" species with Ce(IV) yields a paramagnetic brown complex which was assigned a similar structure with the Ru in (IV, III, IV) configuration.²⁰ The proposed similarity was supported by X-ray crystallographic studies²⁰ of the complexes based on the [Ru₃(O)₂]²⁺ cores. Recently Griffith et al.²¹ have reinvestigated earlier proposals using ¹⁹³Ru Mössbauer spectroscopy. The results for ruthenium brown and its derivatives revealed a delocalization of the odd electron amongst the three Ru centres. The diamagnetism of the "red" complexes can be ascribed to Ru—O—Ru II bonding as in the [Ru₃OCl₆]²⁻ complex mentioned earlier.

2.4 Mononuclear Ru(II) and Ru(III) aqua ions.

The hexaquaruthenium(III) ion ([Ru(OH₂)₆]²⁺) was first isolated in 1958 by Connick et al.²² who used ion-exchange separation techniques to remove the mono- and dichloro Ru(III) species. The first evidence for its existence came from studies on the polarographic reduction studies of "Ru(IV) perchlorate" solutions^{23,24} and from the oxidation of hexaaqua Ruthenium(II) ([Ru(OH₂)₆]²⁺).²⁵ Since then a more convenient method has been

reported by Kallen and Karley⁴⁶ for the isolation of both Ru(III) and Ru(II) aqua ions. The method involves the reduction of RuO₄ in HMF₄ solutions by Sn metal followed by ion exchange separation. Ludi et al found that this method results in substantial amounts of tin in solution which were difficult to remove. Using metallic lead as the reductant they obtained similar results but were able to remove the lead(II) ions generated in solution by precipitation as PbSO₄. This modification led to the isolation of crystalline salts for the two aqua ions $[\text{Ru}(\text{OH}_2)_6](\text{C}_7\text{H}_7\text{SO}_4)_2 \cdot 3\text{H}_2\text{O}$ and $[\text{Ru}(\text{OH}_2)_6](\text{C}_7\text{H}_7\text{SO}_4)_3$.⁴⁷ The availability of these solid samples of the aqua ions has opened up new facile synthetic routes to a variety of ruthenium complexes.

Both $[\text{Ru}(\text{OH}_2)_6]^{2+}$ and $[\text{Ru}(\text{OH}_2)_6]^{3+}$ have been the subject of recent water exchange kinetic studies using ¹⁷O NMR and rate constants for the water exchange as well as activation volumes, following high pressure measurements, have been determined. These are discussed in chapter 3. Normally slow substitution reactions of Cr(III),⁴⁸ and Ru(III)⁴⁹ and of other cations have been found to be catalyzed by more labile lower oxidation states of the same metal. Such kinetics involving $[\text{Ru}(\text{OH}_2)_6]^{2+}$ catalysis have been investigated for the substitution of Cl⁻, Br⁻ and I⁻ on the $[\text{Ru}(\text{OH}_2)_6]^{2+}$ aqua ion.⁴⁸ These reactions will be discussed in the general report of substitution reactions on $[\text{Ru}(\text{OH}_2)_6]^{2+}$ and $[\text{Ru}(\text{OH}_2)_6]^{3+}$ in chapter 3.

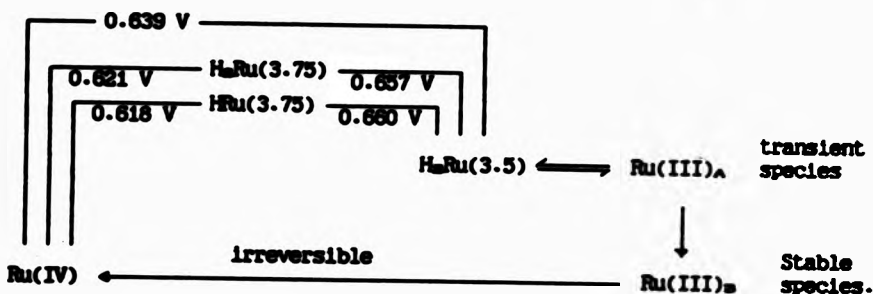
2.5 Studies on the nature of Ru(IV) in aqueous acidic solution.

The exact nature of the Ru(IV) species identified in acidic aqueous solutions is not established although a number of workers have proposed the involvement of various mono- and polynuclear structures.⁴⁸ The red-brown species containing Ru(IV) in perchloric acid solution may be conveniently prepared by reducing solutions of RuO₄, either electrochemically⁵⁰ or with reducing agents such as H₂O₂.⁴⁸⁻⁵¹ Gortsema and Cobble⁵¹ initially formulated the species as mononuclear ($[\text{RuO}(\text{OH}_2)_4]^{2+}$) whereas Wehner and Hindman from electrochemical studies suggested that the species was tetranuclear.⁵⁰ Ion exchange^{48,52} and paper electrophoretic⁵³ studies suggested that the principal species present carried 2 positive charges per Ru (0.05M [H⁺]). Polarographic studies of Atwood and De Vries⁵⁴ revealed that the species could be reduced to Ru(II) in 3 steps. They assigned the three waves to the following reductions: Ru(IV) → Ru(3.5) → Ru(III) → Ru(II).

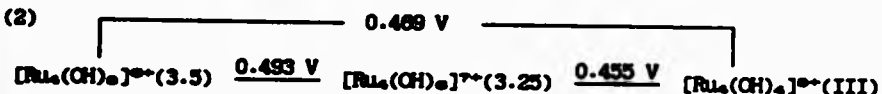
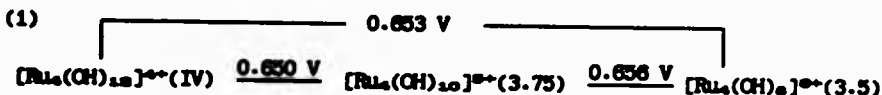
Further investigations by Wallace and Propst⁵⁵ using ion exchange and membrane techniques showed that in 0.5M HClO₄ the charge per Ru was 1+ and that the charge per species was 4+. Thus they proposed a tetranuclear structure under these conditions. Wallace and Propst also carried out coulometric, cyclic voltammetric and spectrophotometric studies in 0.1M HClO₄ and showed that the tetranuclear Ru(IV) species could be

⁴⁸Rard, J. A. Chem Rev., 1985, 85, 1.

reduced reversibly by two 1 electron processes to species with formal oxidation states 3.75 and 3.5. The Ru(3.5) could be further reduced reversibly to a transient species of Ru(III) which rapidly converted to a stable polynuclear species of Ru(III) that could be only re-oxidized to Ru(IV) irreversibly. The reversible redox potentials (vs N.H.E.) involved are illustrated in the following scheme:



Subsequent studies by Brémard et al suggested that the tetrานuclear Ru(IV) species was an oxo (hydroxo) species having one of two possible extreme formulae: $[\text{Ru}_4(\text{OH})_{12}]^{4+}$ or $[\text{Ru}_4\text{O}_6(\text{OH}_8)_{12}]^{4+}$. D'Olieslager et al⁵⁷ carried out further electrochemical studies and proposed possible formulae for the different reduction species reported by Wallace and Propst based on formula $[\text{Ru}_4(\text{OH})_{12}]^{4+}$.



(1) 1st wave. (2) 2nd wave. Potentials vs N.H.E in 1.0M HClO_4 .

Furthermore they were able to follow depolymerization kinetics of the proposed $[Ru_4(OH)_4]^{n+}$ species and characterize the reduction product.



A rate constant of $2.47 \times 10^{-3} \text{ s}^{-1}$ (at 25°C and pH 0-2) was determined and the stable Ru(III) species was formulated as dinuclear $[Ru_2(OH)_2]^{n+}$. Recently D'Olieslager et al have reported electrochemical oxidation studies on Ru(IV) and proposed the existence of a Ru(4.25) species (formulated as $[Ru_2(OH)_{1.25}]^{n+}$). Some indirect evidence for the existence of the dinuclear Ru(III) ion has been obtained by formation of a 2,2'-bipyridine derivative from solutions of stable Ru(III). The intensely green coloured complex showed electronic absorption maxima at 410 and 640 nm in acetonitrile solution. According to Weaver et al^{**}, a high intensity low energy band at around 650 nm is characteristic for oxo-bridged dimers such as $[(bipy)_2(H_2O)RuORu(H_2O)(bipy)_2]^{n+}$ (these authors preferred the diequa- μ -oxo formulation over the di- μ -hydroxy formulation proposed by Dwyer et al^{**} for similar 1,10 phenanthroline complexes). While dinuclear structures for stable Ru(III) may be relevant, it is clear from these results that $[Ru_2(OH)_2]^{n+}$ could not be assigned definitively as the correct solution species.

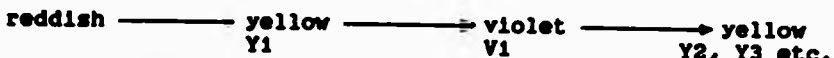
^{*}Heerman, L.; Van Nijen, H.; D'Olieslager, W. Inorg. Chem., 1988, 27, 4320.

2.6 The effect of chloride, bromide and thiocyanate on the nature of the Ru(IV) aqua species.

When chloride ions are added in increasing amounts to a solution of Ru(IV) in perchloric acid ($[Cl^-] < 0.1\text{ M}$; $[H^+] < 0.4\text{ M}$), the following colour changes are observed.²⁰



For $[Cl^-] > 0.1\text{ M}$; $[H^+] > 0.4\text{ M}$ ²¹



The electronic spectra associated with these colour changes are illustrated in figure 2.4. Wehner and Hindman²¹ have formulated Y₂ as $[\text{Ru}(\text{OH}_2)(\text{OH})_2\text{Cl}_2]^{2-}$, although other workers have identified it as $[\text{RuOCl}_2(\text{OH}_2)]^{2-}$ ²²⁻²⁴ or $[(\text{OH}_2)\text{Cl}_2\text{Ru}(\mu-\text{O})-\text{RuCl}_2(\text{OH}_2)]^{2-}$ ^{22, 24, 25}. The structure of Y₃ has been postulated by Wehner and Hindman as $[\text{Ru}(\text{OH})_2\text{Cl}_4]^{2-}$ whereas other Russian workers have tended to favour structures of the type $[\text{RuOCl}_4]^{2-}$ and $[(\text{OH}_2)\text{Cl}_4\text{Ru}-\text{O}-\text{RuCl}_4(\text{OH}_2)]^{2-}$. The Y₂ \longrightarrow Y₃ conversion was explained in terms of the dinuclear structures²² shown below:



At higher chloride concentrations, the electronic spectrum resembles that of $[\text{Ru}_2\text{OCl}_{10}]^{4-}$ in HCl leading to further support for the dinuclear structures.

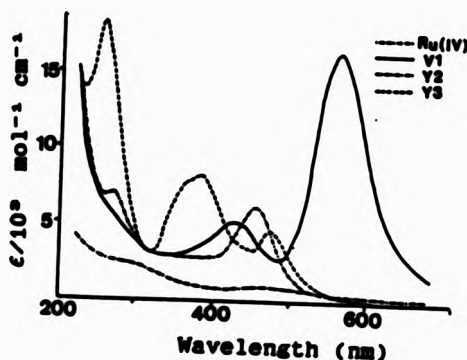
The nature of the transient violet species V₁ is far less certain. Wehner and Hindman have postulated it as $[\text{Ru}(\text{OH})_2\text{Cl}_2(\text{OH}_2)_2]$ although similar dinuclear structures as above can not be ruled out.

In the case of bromide ions the situation is very similar giving the following colour changes :—
reddish ————— blue ————— crimson ————— red-brown

B C R

The chloro- and bromo- species are assumed to be analogous and that B is similar to V₁, C to Y₂, and R to Y₃, etc.

Figure 2.4 Electronic spectra of the various chloro species of Ru(IV)_{ac} .



When Ru(IV) or Ru(III) solutions are treated with NCS- blue solutions are obtained which show an electronic absorption maximum due to a charge transfer transition at 590 nm.²⁸ The species responsible for this transition was originally thought

to be $[\text{Ru}(\text{OH}_2)_6(\text{NCS})_6]^{2-}$, but has been subsequently proved to be anionic in nature with $\lambda_{\text{max}} = 570 \text{ nm}$.⁷⁰ The fact that both Ru(IV) and Ru(III) gives the same blue species prompted some workers to follow the reaction using a known complex of Ru(IV). Finally the violet Ru(III) complex $[\text{NBu}_4]_2[\text{Ru}(\text{NCS})_6]$ was isolated⁷¹⁻⁷³ via the reaction of $\text{K}_2[\text{Ru}^{2+}\text{Cl}_6]$ with KSCN in water, followed by the addition of the tetrabutylammonium cation. The complex shows an electronic absorption maximum at 550 nm ($\epsilon 5800 \text{ M}^{-1} \text{ cm}^{-1}$) in ethanol. In dichloromethane two peaks are observed (550 nm ($\epsilon 7850$) and 408 nm ($\epsilon 1800$)). The complex also showed $\nu(\text{CN})$ at 2095 cm^{-1} , and $\nu(\text{CS})$ at 812 and 692 cm^{-1} and $\delta(\text{SCN})$ at 472, 453, and 428 cm^{-1} .⁷³ High voltage electrophoresis of aqueous solutions containing $[\text{Ru}(\text{NCS})_6]^{2-}$ showed that this species is an isomeric S and N-bonded mixture of the type $[\text{Ru}(\text{NCS})_n(\text{SCN})_{6-n}]^{2-}$ ($n = 1, 2, 3, \text{ or } 4$).⁷³ Each of these were isolated as their tetrabutylammonium salt. The exchange reactions of $[\text{S}^{2-}\text{CN}]^-$ with $[\text{Ru}(\text{NCS})_6]^{2-}$ have been studied: two of the ligands were found to be more labile than the other four.⁷⁴

2.7 Scope and objectives of present work.

It is clear that the representative Ru(IV) aqua ion species in acidic aqueous solution is poorly characterized and so far suggestions as to the exact structure have been speculative rather than conclusive. Surprisingly, ligand replacement techniques similar to those used for the identification of the trinuclear aqua ions of Mo(IV) and W(IV) have not been

attempted. The behaviour of Ru(IV) in chloride and thiocyanate solution suggests however that the aqua ion species is highly labile and hence prone to destruction. Chelating ligands such as EDTA, NIDA, hydridotris(i-pyrazolyl)borate, oxalate etc. may prove useful in obtaining a stable solid derivative to enable X-ray structural analysis of the core unit. Multinuclear NMR has also played a vital role in the characterization of the aqua ions $[\text{Mo}_2\text{O}_6]^{4+}$ and $[\text{W}_2\text{O}_6]^{4+}$ and hence an obvious extension would be to use ^{17}O NMR techniques to establish the nature of the Ru(IV) species if a fully enriched ^{17}O derivative could be prepared. The established method of preparation however involves the use of species (RuO_4 , NaOCl , and H_2O_2) $^{7+}$ that are known to undergo extremely slow exchange with ^{17}O . This may lead to partially exchanged intermediates which will be undesirable since accurately known enrichments will be needed if detailed structure determination is to be possible. Recently Deloume et al.^{7a} reported a new method for the preparation of Ru(IV) in non-complexing acid medium in which they also proposed a tetranuclear structure. The method avoided the generation of RuO_4 and was based on the stoichiometric oxidation of the Br^- ions of $\text{K}_3[\text{RuBr}_6]$ by BrO_3^- ion. Unfortunately the use of BrO_3^- also poses the problem of possible slow incomplete exchange and therefore it was decided that this method would also not be suitable for possible ^{17}O NMR studies. Finally the method of choice involved a route employing

Ch. 2: Aqueous solution chemistry of Ru 143
electrochemical generation of Ru(IV) from solutions of
 $[Ru(O^{2-}H_2)_6]^{2+}$ in H_2O^{2+}/HBF_4 solution.

The objectives of the present work can be divided into three sections:

1. A re-investigation of the various findings reported in the literature to set the platform for further studies (i.e. preparation, charge per metal and charge per species determination, effect of increasing acid, effect of Cl^- , effect of NCS^- , and studies to establish the solution stability of $Ru(IV)_{aq.}$)
2. The preparation of "stable" derivative complexes of Ru(IV) using chelating ligands such as EDTA, MIDA, and hydridotris-(1-pyrazolyl)borate for possible X-ray crystallographic studies.
3. Characterization of the Ru(IV) aqua ion in solution by ^{17}O NMR following successful synthesis of a fully enriched ^{17}O sample; variable temperature and water exchange studies. Comparison of the rate and mechanism with Ru(II) and Ru(III). Water ligand replacement studies on Ru(IV) monitored by ^{17}O NMR; investigations on the lability of the core unit.

EXPERIMENTAL PROCEDURES AND RESULTS

The preparation of Ru(IV) in perchloric acid medium has been reported by a number of workers^{49-51,55} all essentially involving the initial generation of RuO₄ which is then reduced by H₂O₂ to give the Ru(IV)_{aq}. In order to re-investigate some of the properties of Ru(IV) a modification of the method reported by Wallace and Propst⁵⁰ was used.

2.6 Preparation of Ru(IV) aqua ion from RuO₄.

The following procedure was carried out in a well ventilated fume cupboard due to the hazard associated with RuO₄. Commercial RuCl₃ (Johnson Matthey, 0.5 g) was added to industrial grade sodium hypochlorite, NaOCl (B.D.H., 200 cm³) in a 600 cm³ flask and the yellowish-brown solution was left to stir for 1 hour. Carbon tetrachloride, CCl₄ (200 cm³) was added to extract the yellow RuO₄ and stirring was continued for a further 30 minutes. The mixture was then transferred to a separating funnel and allowed to separate. The CCl₄ layer was drained into a flask containing 2M HClO₄ (B.D.H., 100 cm³) and H₂O₂ (B.D.H., 30% w/v, 3 cm³). The mixture was rigorously stirred for 1 hour during which time the yellow colour changed to red-brown. The red brown aqueous layer was then separated and heated to boiling to remove excess peroxide. Both extraction procedures were repeated at least three times to get complete phase transfer. After cooling, the red-brown solution was diluted 10 times with water and loaded on to a Dowex 50W-X2

cation-exchange column (10×0.5 cm). The behaviour of the aqua ion on the column was similar to the $[W_6O_4]^{4-}$ aqua ion in that the whole column became swamped with a dark brown band. After loading, 0.5M HClO₄ (500 cm³) was passed through the column to wash out any lower charged species. The Ru(IV) aqua ion was then eluted by displacement with Th⁴⁺ (0.25M in 0.1M HClO₄). Slow elution gave 3-5 cm³ of concentrated Th⁴⁺ free samples (The presence of the Th⁴⁺ detected by testing a small sample with oxalic acid). The electronic spectrum of the aqua ion showed a peak at 487 nm and a peak at 300 nm. The total yield of aqua ion was found to be 60% (based on $\epsilon_{487} = 710 \text{ M}^{-1} \text{ cm}^{-1}$ per Ru⁶⁺). Figure 2.5 shows the electronic spectrum of the Ru(IV) aqua ion.

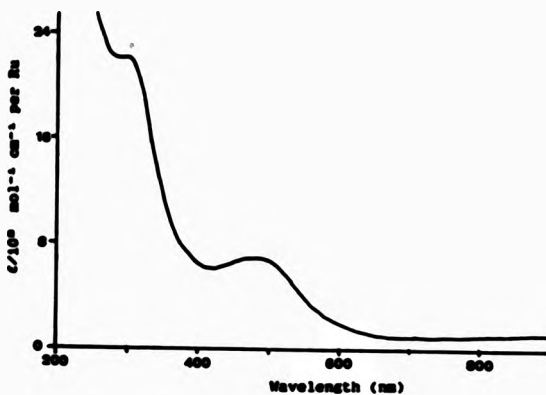


Figure 2.5 Electronic spectrum of Ru(IV) aqua ion.

The preparation was repeated and elution with 3M HClO₄ was attempted. After passing 30-50 cm³ of acid no aqua ion was eluted hence it was concluded that the aqua ion either carried

a charge greater than 4+ or that it became highly protonated upon passing acid through the column. Elution also failed even with concentrated HClO_4 and therefore the latter conclusion seemed to be more appropriate.

2.9 Preparation of the Ru(IV) aqua ion from the oxidation of bromide ions of RuBr_6^{2-} by bromate ion in acid medium.

Bispotassium hexabromoruthenate(IV). K_2RuBr_6 was prepared according to the method of Ferguson and Greenway.⁷⁷ Commercial RuCl_3 (0.4 g), and KBr (0.5 g) were added to a solution of HBr (B.D.H., 40%). Bromine vapour was bubbled through the solution using N_2 as carrier. The brown precipitate of K_2RuBr_6 which formed after 3 hours was filtered.

The oxidising solution was prepared from NaBrO_3 (Aldrich, AR) by weighing known amounts of the dry solid in water (1M solution was prepared). K_2RuBr_6 (0.67 g) was added to 2M HClO_4 (10 cm³) and while stirring, NaBrO_3 (1.22 cm³) was added. Br₂ was evolved and upon its completion, the electronic spectrum was recorded for the red-brown solution. This showed no apparent peak at 487 nm (expected for the aqua ion). Hence the solution was diluted 5 times and the aqua ion purified by ion exchange chromatography. Similar yields to the earlier preparations were again achieved (60% per Ru).

It was concluded that this latter method, although avoiding the handling of RuO_4 , did not have any significant advantages over the other methods.

2.10 Determination of the charge per Ru atom in the Ru(IV) aqua ion using an ion exchange technique.

A sample of the Ru(IV) aqua ion was prepared as described earlier. The pH of the solution was accurately measured using a pH meter and the Ru concentration was determined from the electronic spectrum ($\epsilon_{467} = 710 \text{ M}^{-1} \text{ cm}^{-1}$ per Ru). A known volume of the aqua ion was loaded onto a small column of Dowex 50W-X8 (3 x 1 cm) resin (H⁺ form, thoroughly washed with distilled water) and the liberated H⁺ titrated against standard NaOH (B.D.H. convol. 0.01M).

Volume of Ru(IV) aqua ion taken	= 5.00 cm ³
Concentration of Ru(IV)	= 0.016M
pH of Ru(IV) solution	= 1.74
Moles of H ⁺ (free)	= 9.10 x 10 ⁻⁴
Moles of Ru(IV)	= 9.00 x 10 ⁻⁴
"Calculated [H ⁺] if charge is 1+	= 1.81 x 10 ⁻⁴
Volume of NaOH (0.01M) required	a. 18.42 cm ³ (1.84 x 10 ⁻⁴) b. 18.46 ..(1.85 x ..) c. 18.45 ..(1.85 x ..)

The value for [H⁺] (1.85 x 10⁻⁴) is in good agreement with the calculated, hence from this experiment, it can be concluded that the charge per Ru atom in the Ru(IV) aqua ion is 1+ (± 0.03).

$$\text{Charge/Ru} = \frac{\text{No. of moles total charge} - \text{No. of moles free H}^+}{\text{No. of moles Ru}^{IV}}$$

2.11 The effect of perchloric acid concentration on the electronic spectrum of the Ru(IV) aqua ion.

A solution (0.25 cm^3) of the Ru(IV) aqua ion (0.001M per Ru in 0.1M HClO_4) was accurately diluted with 10M HClO_4 to give total acid concentration of 1.0, 2.0, 3.0, and 5.0, 6.0, and 9.8M and the electronic spectrum was monitored over a period of 3 days in a 1 cm quartz cell. The study showed that there were no significant changes to the spectrum in the 0.1 - 2 M acid range. Above 2 M however, the absorption maximum in the visible region showed shifts to higher energies (490 nm (upto 1M H^+), 475 nm(5M), 470 nm(10M), and the plateau in the ultra-violet region was profoundly affected. The 5.05M solution was then diluted accurately with water to 1M and 0.1M acid concentration. The electronic spectra of these (figure 2.6) showed that the original spectrum was again obtained. These findings were exactly in accord with those reported in the literature by Gortsema and Cobble²¹ and by Wehner and Hindman.²² The spectral changes are probably due to protonation of the Ru(IV) aqua ion and may be linked with the observed column behaviour (i.e. Elution only possible by displacement techniques).

An experiment to show that the aqua ion obeyed Beer's law was carried out by accurate dilutions with 0.2M HClO_4 ($[\text{H}^+]$ constant at 0.2 M) and superimposition of the electronic spectra. It was shown that under these conditions the aqua ion obeyed Beer's law.

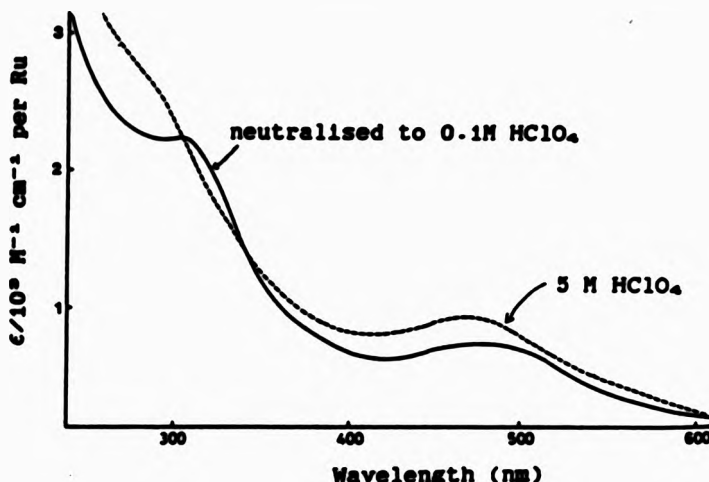


Figure 2.6 Effect of perchloric acid on the electronic spectrum of the Ru(IV) aqua ion.

In order to study the effect of decreasing the acid concentration, a sample of the aqua ion was neutralised with the addition of small quantities of solid NaHCO₃. A check of the electronic spectrum at every 0.5 unit of pH until pH 4 showed that there were no significant changes to the spectrum. Above pH 4, a brown precipitate was formed (probably ruthenium (IV) hydroxide).

These findings will be of use later where complexation with EDTA, MIDA and hydridotris(i-pyrazolyl)borate will be attempted. These ligands require high pH (= 4) for complexa-

Ch. 2: Experimental procedures & Results 150
tion and the fact that the electronic spectrum showed little change with increasing pH (upto pH 4) will enhance the chances for complexation of the core.

2.12 Effect of Cl⁻ and NCS⁻ ions on the Ru(IV) aqua ion.

Ions such as Cl⁻ and NCS⁻ have been useful in forming derivative complexes of the trinuclear Mo(IV) and W(IV) aqua ions to aid their characterization. In the case of the Ru(IV) aqua ion however, these ions are reported to have drastic effects. It was therefore decided to study further these effects in an attempt to characterize some of the species.

2.12.1 The effect of chloride ion on the Ru(IV) aqua ion.

When an excess of NaCl (>100 fold) was added to the Ru(IV) aqua ion ($[H^+] = 0.1\text{ M}$, $[Cl^-] = 4\text{ M}$), a range of colour changes were observed (yellow, blue, yellow brown). The reactions were monitored spectrophotometrically (figure 2.7). Initially a peak appeared at 570 nm as the blue species was formed. This peak then collapsed to give two other peaks at 470, 383 nm as the final yellow-brown species was formed. The initial blue colour was formed within the first 2 hours whereas the final yellow-brown colour took 2 days. A sample of the blue and the final yellow-brown species were loaded onto a Dowex 50W-X2 cation exchange column. Both were found to pass straight through the column indicating that they were anionic.

In an attempt to isolate the yellow-brown species, the final solution was left to evaporate in the presence of tetraethylam-

monium chloride. No characterizable compound was however isolated. The electronic spectrum of the final yellow-brown solution was very similar to that reported for the $[\text{Ru}_2\text{OCl}_{10}]^{4-}$ ion (figure 2.3). Thus it is probable that similar oligomeric species are responsible for the observed spectral changes. It is hoped that ^{17}O NMR studies would confirm the presence of μ -oxo/ μ -hydroxo groups.

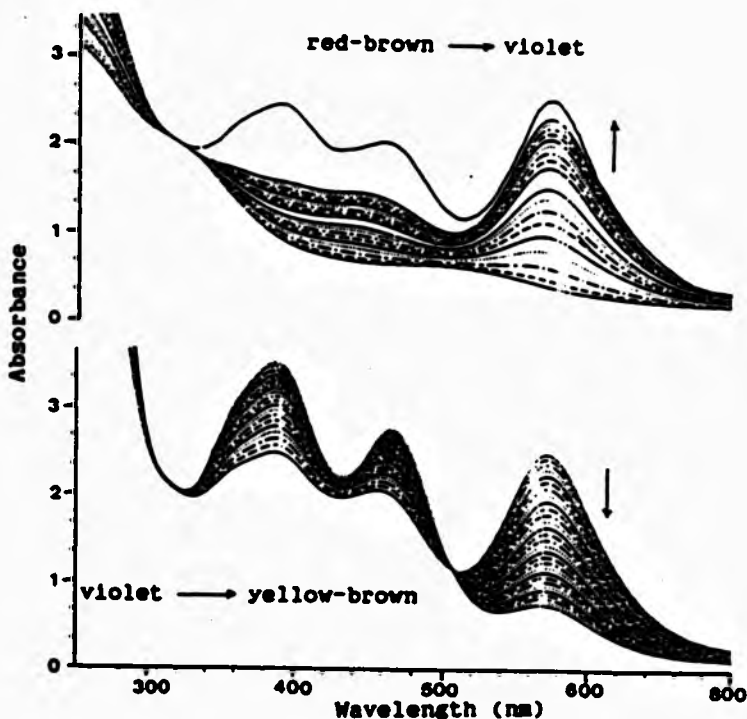


Figure 2.7 Electronic spectrum of Ru(IV) aqua ion in the presence of excess Cl^- (4M) monitored over two days.

2.12.2 Effect of thiocyanate on the Ru(IV) aqua ion.

When an excess of NaSCN (>100 fold) was added to the Ru(IV) aqua ion, the colour of the solution changed to purple within 30 minutes. Ion-exchange experiment showed that this blue species was anionic. When this solution was left to evaporate in the presence of tetraethylammonium and tetramethylammonium cations, a purple solid was obtained. The elemental analysis of this compound showed it to be hexathiocyanatoruthenate(III) complex. The elemental analysis of the products is shown in table 2.2.

In view of the report that both N and S-bonded ligands may be present²⁰ suitable crystals for X-ray analysis were sought and eventually obtained but the analysis has so far proved difficult. This may be related to the presence of the two isomeric ligands.

Table 2.2 CHN analysis of the thiocyanato complexes of Ru(III).

Compound	Calculated			Found ^a		
	C%	H%	N%	C%	H%	N%
(Me ₄ N) ₂ [Ru(SCN) ₆]	32.19	5.36	18.78	31.08	5.08	17.22
(Et ₄ N) ₂ [Ru(SCN) ₆]	42.90	7.15	15.02	41.25	6.87	14.29

The electronic spectrum of the complex in ethanol was found to be similar to that reported in the literature (peak at 550 nm

^aThe values are all low which suggests the likely presence of small amounts of co-crystallised NaCl.

with $\epsilon = \text{ca. } 6000 \text{ M}^{-1} \text{ cm}^{-1}$, figure 2.8.1).⁷⁴⁻⁷⁶ When dissolved in water, the electronic spectrum showed changes indicating replacement of NCS⁻ with water ligands (figure 2.8.2). The complex also showed $\nu(\text{CN})$ at 2110 cm^{-1} and $\nu(\text{CS})$ at 812 cm^{-1} in the infra-red spectrum. These vibration frequencies are indicative of the presence of both N-bonded ($\nu(\text{CS})$ in the range $860-780 \text{ cm}^{-1}$) and S-bonded ($\nu(\text{CN})$ 2110 cm^{-1}) complexes thus confirming previous findings that the compound is mixture of N- and S-bonded isomers.⁷² X-ray studies are continuing.

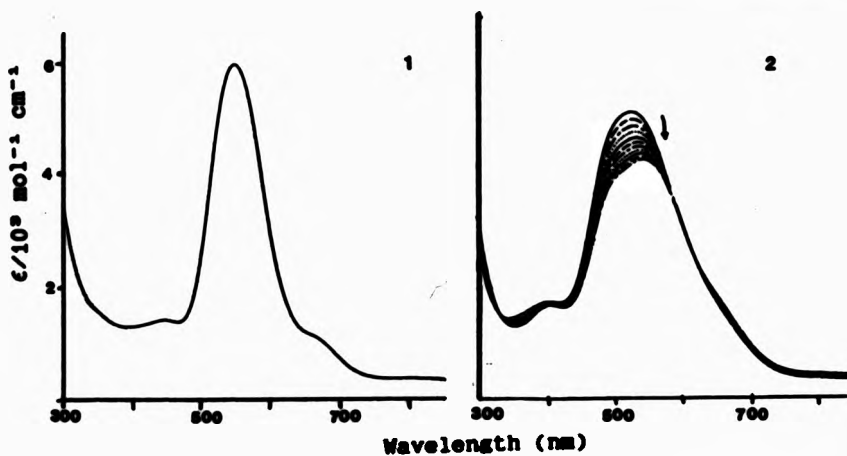


Figure 2.8 Electronic spectrum of $[\text{Ru}(\text{NCS})_6]^{3-}$ in ethanol (1) and in water (2, monitored over several hours).

2.12.3 Attempted Nitrogen-15 NMR study on the thiocyanato complexe.

In an attempt to further clarify the presence of N and S-bonded ligands a ^{15}N NMR study was attempted using the Brüker WP-80 spectrometer (working at 5.81 MHz) at Stirling with the help of Dr. F. Riddell and Dr. S. Arumugam. A sample of $[\text{Me}_4\text{N}]_2[\text{Ru}(\text{NCS})_6]$ was dissolved in DMSO (saturated sample). Samples of NH_4Cl , Me_4NClO_4 , NaSCN and Et_4NClO_4 (all -1M in DMSO) were also made up as possible reference solutions. Subsequent NMR spectrum of $[\text{Me}_4\text{N}]_2[\text{Ru}(\text{NCS})_6]$ only showed one peak corresponding to resonance of the symmetric Me_4N^+ cation. The NCS-resonances were not observed probably due to the influence of the paramagnetic Ru(III) and to the possible low symmetry of the complex.

2.13 Cyclic voltammetric studies on the Ru(IV) aqua ion.

Cyclic voltammetric studies were carried out on Ru(IV) aqua ion prepared in perchloric acid medium ($[\text{Ru}(\text{IV})] = 0.001 \text{ M}$, $[\text{H}^+] = 0.1 \text{ M}$, and I=1M NaClO_4) by following the method of Wallace and Propst.²² A Pt disc working electrode was used with a S.C.E. as the reference electrode and NaClO_4 as supporting electrolyte. The study showed the two reversible waves at +0.580 V and +0.410 V (vs N.H.E., figure 2.9) similar to those reported by Wallace and Propst²² (0.639 V and 0.4 V vs N.H.E., 0.1M $[\text{H}^+]$, I=1M). The two reduction waves correspond to the reduction of $\text{Ru}(\text{IV}) \rightarrow \text{Ru}(\text{3.5})$ and $\text{Ru}(\text{3.5}) \rightarrow \text{Ru}(\text{III})$ respectively.

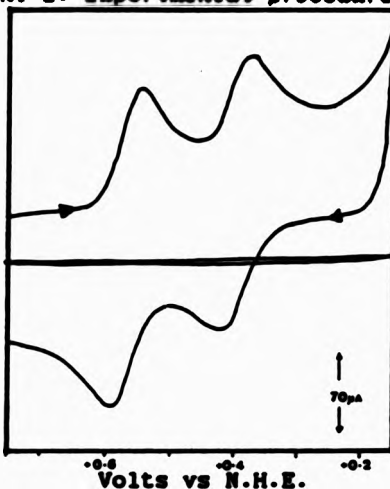


Figure 2.9 Cyclic voltammetric scan of Ru(IV) aqua ion in 0.1M HClO_4 and I=1.0M NaClO_4 .

In order to investigate the possibilities of applying ^{17}O NMR technique to probe the structure of the Ru(IV) aqua ion, it was necessary to find a synthetic method of introducing controlled ^{17}O enrichment into the aqua ion. It was clear that the two previously reported methods of preparation of $\text{Ru(IV)}_{\text{aq}}$ could not guarantee control and knowledge of the level of ^{17}O enrichment during the various stages involved. A method was required in which the level of ^{17}O enrichment of all of the oxygen present was known at all stages of the preparation. Recently it has been shown that the hexaquaruthenium(II) ion, $[\text{Ru}(\text{OH}_2)_6]^{2+}$, exchanges with H_2O^{17} in 1.0M Hfms with a half life of 38.5 s (25°C).⁷⁰ If solutions of this aqua ion can then be electrochemically oxidized to give the Ru(IV) aqua ion.

this would provide a convenient method of synthesizing known 170 O enriched samples for subsequent NMR studies.

2.14 Preparation of Ru(IV) aqua ion from electrochemical oxidation of $[Ru(OH_2)_6]^{2+}$ aqua ion.

The $[Ru(OH_2)_6]^{2+}$ was prepared in HBF₄ by following a slightly modified method to that described by Kallen and Earley.⁴⁶ A sample of commercial RuCl₃ (0.5 g) was treated as before with NaOCl (200 cm³) and the RuO₄ was extracted with CCl₄. The yellow CCl₄ extract was then added to a flask containing 2M HBF₄ (100 cm³) and Sn powder (Aldrich, 4 g). Upon stirring, the aqueous layer became pink and the CCl₄ completely colourless. The pink solution contained the Ru(II) aqua ion. Since it was oxygen sensitive, it was handled under air-free conditions. The pink solution was filtered and diluted 200 times with deoxygenated water before being loaded onto a column of Dowex 50W-X2 cation-exchange resin. After loading, 0.5 M HBF₄ (200 cm³) was passed through the column before the Ru(II) aqua ion was eluted with 2M HBF₄. The electronic spectrum showed a peak at 385 nm (assigned to the $^1A_{1g} \rightarrow ^3T_{2g}$ transition) and a peak at 530 nm (assigned to the $^1A_{1g} \rightarrow ^3T_{1g}$ transition). The ϵ values are reported to be 10.8, and 9.0 M⁻¹ cm⁻¹ per Ru respectively.⁴⁶ Using displacement elution with Th⁴⁺ or La³⁺, highly concentrated samples of $[Ru(OH_2)_6]^{2+}$ (0.5 M in 0.5M HBF₄) were achieved.

Ch. 2: Experimental procedures & Results 157

A sample (2 cm^3) of this concentrated solution of Ru(II) was oxidized electrochemically using a platinum gauze electrode in a two compartment cell at 0°C with a current of 0.3A . The oxidation was ceased after one minute intervals and the electronic spectrum was recorded. Under these conditions, complete oxidation occurred in 10-15 minutes. The colour changed during the oxidation to intense red-brown. After the oxidation, the red-brown solution was diluted 10 times and loaded onto a column of Dowex 50W-X2 resin. After the usual purification, the electronic spectrum was recorded and this confirmed the presence of the Ru(IV) aqua ion. It was clear that this method would enable synthesis of ^{17}O enriched samples of the Ru(IV) under conditions of complete control and thus allow the desired quantitative ^{17}O NMR studies to be performed.

2.15 Oxygen-17 NMR studies on the Ru(IV) aqua ion.

It was hoped that ^{17}O NMR studies would now provide conclusive information with regard to the structure of Ru(IV) aqua ion.

2.15.1 Oxygen-17 NMR spectrum of the Ru(IV) aqua ion.

A concentrated solution of the Ru(II) aqua ion in 2M HBF_4 was prepared as described above and a 2 cm^3 sample was then mixed with 2 cm^3 of H_2O^{17} (10 atom %, deoxygenated). The solution was left to exchange for 4 hours at 0°C . After this time the Ru(IV) aqua ion was prepared via the electrochemical method described above and purified by ion exchange chromatography. The concentration of Ru(IV) (0.122M per Ru) was determined from

its electronic spectrum ($\epsilon_{467} = 710 \text{ M}^{-1} \text{ cm}^{-1}$). The total perchlorate ion concentration was determined by loading a known volume of the aqua ion solution (0.5 cm³) onto a small column (1x3 cm) of Dowex 50W-X8 resin and titrating the liberated H⁺ with standard 0.1 M NaOH. After this a 1 cm³ sample of the aqua ion was added to a standard 10 mm NMR tube containing a further 1 cm³ of 8% H₂O¹⁷ and 0.0362 g (0.1 M) Mn(ClO₄)₂. The ¹⁷O NMR spectrum over the full range (2000 to -300 ppm) was then recorded on the Brüker AM-400 spectrometer at Lausanne with the help of Dr. Helm. Following 130,000 scans, the resulting spectrum showed 3 resonances at 1157, 288, and -24 ppm, figure 2.10). The single peak at 1157 ppm suggested an assignment to equivalent oxygen atoms of the core in the polynuclear ion. The peak at 288 ppm was due to ClO₄⁻ and proved useful as an internal standard. The remaining single resonance at -24 ppm was in the region assignable to the bound water ligands.

All ¹⁷O chemical shifts were measured with respect to the perchlorate line (+288 ppm) and reported relative to bulk water (=0 ppm). The crucial experiment involved integration of the two Ru(IV) ¹⁷O resonance lines with respect to the perchlorate line (4 oxygens being present, ClO₄⁻). As the resonances in question were far apart from the perchlorate line, it was possible to determine integrations by Lorentzian line simulation of the resonances following entry of an interactive

rolling baseline correction program (NINO)^a using the Brüker Aspect 2000 Data Station on the AM-400 spectrometer. Four independent electrolytic oxidations to Ru(IV) were carried out including one performed in a one compartment cell.^{**} The results are tabulated in table 2.3.

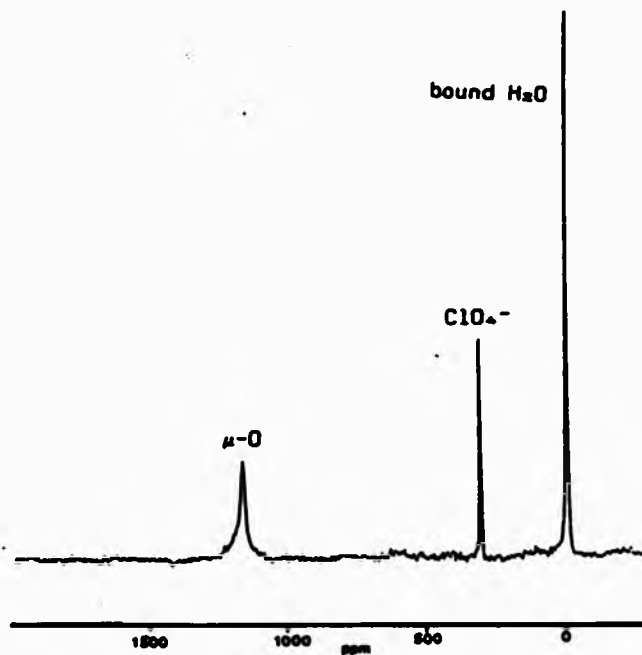


Figure 2.10 ¹⁷O NMR spectrum of the Ru(IV) aqua ion.

^aWenger, J. Program NINO. ICMA Program Library 1983.

^{**}When oxidation was carried out in a two compartment cell there was the possibility of the sample being diluted by the solution in the adjacent compartment and hence leading to an error in the enrichment. To eliminate this possibility the oxidation was performed in a one compartment cell.

Table 2.3 Determination of the Ru:core oxygen:bound H₂O ratio from the oxygen-17 NMR experiments.

[Ru ^{IV}] M	[ClO ₄ ⁻] M	Integrations (Arb. units)			Ratios	
		ClO ₄ ⁻ *	core-O(% en- richment)	b-H ₂ O(% en- richment)	core-O /Ru ^{IV}	b-H ₂ O /Ru ^{IV}
0.059	3.70	21.20	10.01(5.2)	-	0.84	-
0.043	2.82	16.29	10.00(5.2)	14.98(2.6)	1.14	3.21
0.031	1.34	28.35	40.04(5.2)	73.23(2.6)	0.88	3.23
0.186	2.90	78.97	113.47(3.5)	-	0.94	-
* Natural abundance (0.097%)					Av=0.93	3.22

It is clear from these results that, within experimental error, the respective stoichiometry (per Ru atom) of core oxygen (1157 ppm): bound water (-24 ppm) is 1:3 in support of an empirical formula under these conditions (0.07-1.2 M H⁺) of :



This structure is clearly coordinatively unsaturated and in support of a polynuclear structure for the Ru(IV) aqua ion as indicated earlier by the ion-exchange and electrochemical behaviour.²² If a tetranuclear structure is assumed at this stage, a formula [Ru₄O₆(OH)₈]²⁺ would be relevant under these conditions.

Having obtained a fully enriched representative ¹⁷O NMR spectrum of the Ru(IV) aqua ion in solution, it was decided to investigate the solution dynamics of the ion in terms of the

*Final set of values determined at St. Andrews. Ratios carry an error of ±0.1 for core oxygens and ±0.01 for bound-H₂O.

rate of H_2O^{17} exchange with both the core oxygen and bound water ligands. The effect of increasing the temperature was also studied.

2.15.2 Attempted study for the determination of the rate constant of water exchange on the Ru(IV) aqua ion.

Preliminary attempts had shown that H_2O^{17} exchange on the core oxygen atoms was immeasurably slow at 25°C but that exchange with the bound H_2O was immeasurably fast (complete within the time it took to record a spectrum) at 25°C. Hence it was decided to study the water exchange kinetics at 25°C using the "fast injection" kinetic apparatus designed in Lausanne for use with the Brüker AM-400 instrument (see appendix 2). A normal Ru(IV) aqua ion sample (1 cm³) was added to a 10 mm NMR tube which contained $\text{Mn}(\text{ClO}_4)_2$ (0.036g) and LiClO_4 (0.447 g) (LiClO_4 to adjust the ionic strength to 2M). The Hamilton syringe employed in the "fast injection" apparatus was filled with 1 cm³ of H_2O^{17} (~ 8%). The temperature of the apparatus was maintained at $25 \pm 0.5^\circ\text{C}$. By rapidly introducing the enriched water via the syringe into the NMR tube and monitoring the peak growth for the bound water, a measurement of the rate of water exchange was attempted. However, the exchange proved to be again faster than the time taken to obtain a spectrum (~1s) and it was concluded therefore that measurement of the rate of exchange was not possible at this temperature by this method. The experiment was repeated at 1°C and even here the exchange was too fast for measurement.

Finally a line broadening study was attempted in which the linewidth of the bound water resonance was measured as a function of temperature following simulation to a Lorentzian line shape. This method allows the transverse relaxation time ($1/T_2$ for bound water) to be determined. By plotting $\ln(1/T_2)$ vs $1/T$ the quadrupolar relaxation component ($1/T_{2q}$) can be separated from the kinetic exchange ($1/r$) and hence the rate of water exchange together with the activation parameters can be measured (see appendix 2 for more details on theory).

In a typical experiment a fully enriched sample (1 cm³ of 0.13M Ru(IV)) of the aqua ion + 1 cm³ of (~8%) H₂O¹⁷ + 0.036g Mn(ClO₄)₂ and 0.447g LiClO₄ to give I=2.00M, [H⁺]=0.5M) was used. A spectrum of the solution was obtained at 1.5°, 26.9°, 38.9°, 63.4° and 73.0°C and the linewidth of the bound-H₂O resonance at half height was measured by hand. $1/T_2$ was then calculated using equation (9).

The absorption mode signal, which is that normally observed, is given by the following equation for a Lorentzian lineshape⁷⁰:

$$g(v) = \frac{2 C T_2}{1 + 4 \pi^2 T_2^2 (v_1 - v)^2} \quad \dots \dots \dots \quad (8)$$

where T_2 is the transverse relaxation time, C is the surface of the Lorentzian line and is proportional to the intensity of the resonance, v is the frequency and v_1 is the Larmor precession frequency of the nucleus in Hz (27.115 MHz at 4.67 Tesla for

From this study the value for the rate constant (k_{obs}) of water exchange at 25°C was found to be $29.8 \pm 24.8 \text{ s}^{-1}$ with activation parameters $\Delta H^\ddagger = +85 \pm 16 \text{ kJ mol}^{-1}$ and $\Delta S^\ddagger = + 69 \pm 47 \text{ J K}^{-1} \text{ mol}^{-1}$.

During this variable temperature study it was noticed that profound changes were occurring to the spectrum apart from the broadening of the bound-H₂O resonance. This could explain the large errors associated with the measured parameters. Thus it was decided to further study the effect of temperature on the ¹⁷O spectrum of the Ru(IV) aqua ion.

2.15.3 The effect of temperature on the NMR spectrum of the Ru(IV) aqua ion.

A variable temperature study on a normal sample (core oxygens not enriched) of the aqua ion in which Mn²⁺ was added and the bound-H₂O ligands were enriched (~ 4%) was followed at 25°, 45°, 55°, 65° and 75°. At each temperature the ¹⁷O NMR spectrum was recorded. At the final temperature the sample was kept for 2 hours before cooling to 45°C and finally to 25°C. The spectra showed that as the temperature was increased the peak for the bound water became broad and merged with the base line. Other resonances appeared including a small peak at 1150 ppm (the position where the core-O resonance was observed, figure 2.12). Upon cooling the original spectrum was regained with the addition of the weak resonance at 1157 ppm.

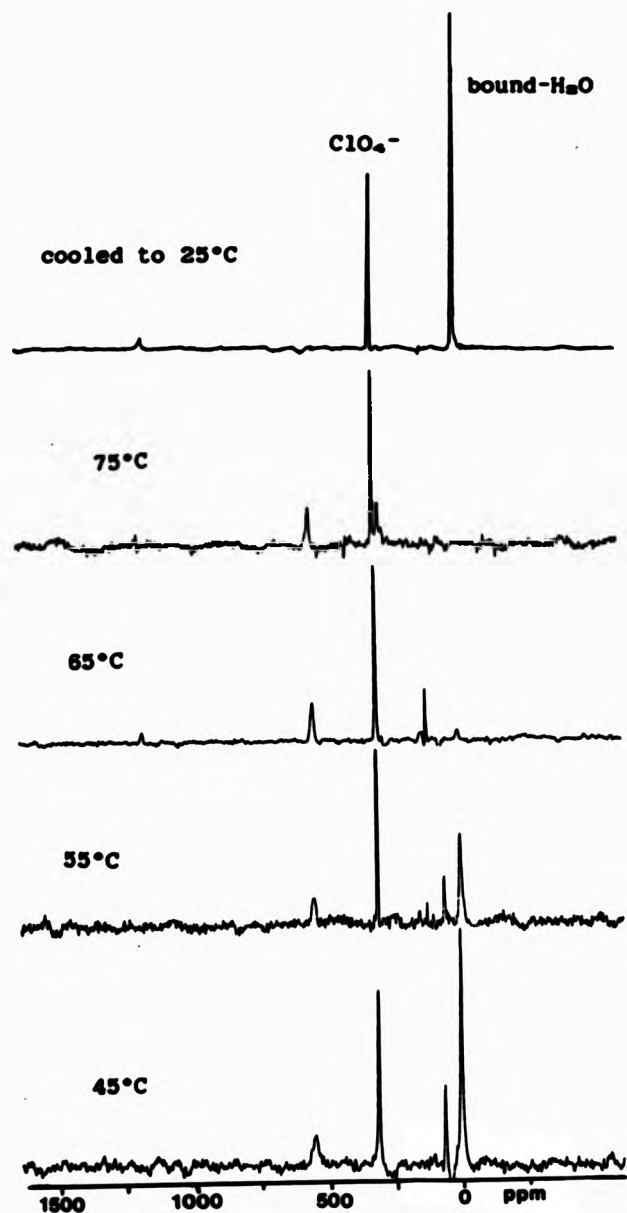


Figure 2.12 ^{17}O NMR spectrum of the Ru(IV) aqua ion as a function of temperature. [Ru(IV)] = 0.065M [H⁺] = 0.25M I = 2.00M

The additional resonance at 1157 ppm suggested that some enrichment had transferred to the core oxygen atoms while the structure was disturbed at the higher temperatures.

A similar study was done using electronic spectroscopy and it showed that the optical spectrum also displayed small reversible changes. The absorption spectra showing the effect of temperature are given in figures 2.13. Both these studies clearly indicated that reversible structural changes were occurring.

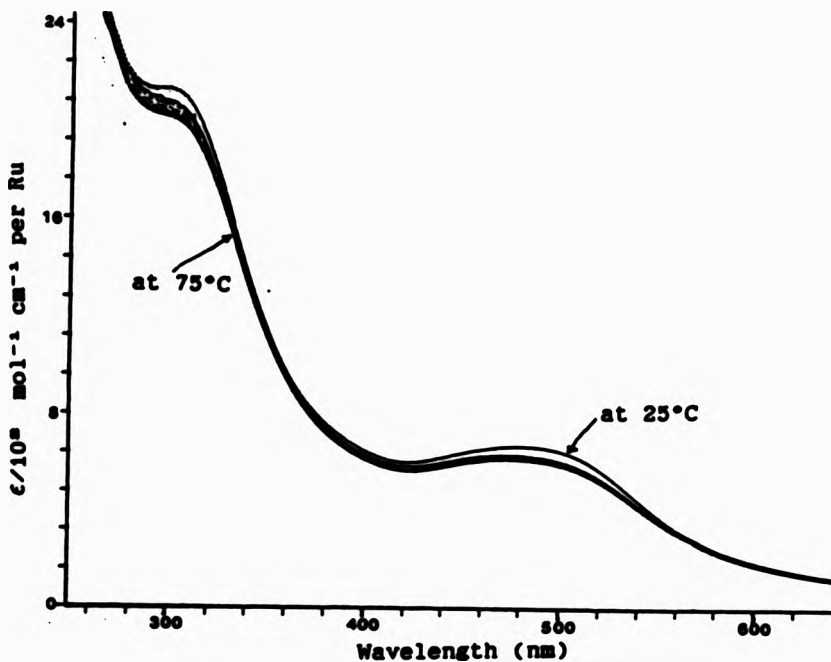


Figure 2.13 Electronic spectrum of the Ru(IV) monitored as a function of temperature.

2.15.4 Effect of thiocyanate and chloride on the NMR spectrum of the Ru(IV) aqua ion.

A sample of NaSCN (1 cm^3 , 4M) was added to a sample the fully enriched Ru(IV) aqua ion (1 cm^3 of 0.13 M Ru in 0.5M [H⁺]). The ^{17}O NMR spectrum of this mixture was then recorded over the range -300 to +1200 ppm and followed with time. Both the core oxygen (1157 ppm) and bound water (-24 ppm) resonances rapidly disappeared as the solution turned blue and no new resonances were observed. These results are entirely consistent with the destruction of the core structure under these conditions and formation of the mononuclear Ru(III) complex, $[\text{Ru}(\text{NCS})_6]^{3-}$.

A similar experiment was repeated in order to observe the effect of adding excess Cl⁻ (4M) on the Ru(IV) aqua ion. Successive ^{17}O NMR spectra were taken when the colour of the solution had turned blue and at the end of the reaction when the solution was yellow-brown. As with NCS⁻, both the peaks for the core oxygens and bound water ligands disappeared consistent with destruction of the core. The final yellow-brown solution showed three new resonances, two of approximately equal height in the range 600-700 ppm and one near 0 ppm. These findings suggested the presence of dinuclear μ -oxo aqua chloro ions of Ru(IV) or Ru(III) as proposed by both Woodhead and Fletcher²² and the extensive Russian studies²³⁻²⁴. No further characterization of these species was possible in the time available.

2.15.5 Oxygen-17 NMR studies of the Electrochemical reduction of Ru(IV) aqua ion to give the Ru(III)₄ ion and the Ru(III)₂ ion.

A ¹⁷O core enriched sample of the Ru(IV) aqua ion (0.13M Ru(IV) in 0.5M [H⁺] + Mn²⁺) was electrochemically reduced using Pt gauze electrode. Since the volume of liquid was small (2 cm³), the experiment was carried out in a one compartment cell (10 cm³ beaker). The reduction was stopped every 30 seconds and the electronic spectrum monitored. The reduction was ceased when the spectrum was similar to that reported by Wallace and Propst for 90% reduction to Ru(III).⁵⁶ At this stage a ¹⁷O NMR spectrum was recorded which showed the loss of both core oxygen and bound water resonances but no new resonances that could be assignable to the Ru(III) product. The solution was allowed to stand for 3 hours, the time that tetrameric Ru(III) is reported to convert to dimeric Ru(III).⁵⁷ A further ¹⁷O NMR spectrum of this solution again showed no evidence of any ¹⁷O resonances assignable to dimeric Ru(III).

2.16 Experiments aimed at obtaining crystalline derivatives of the Ru(IV) aqua ion core with various complexing ligands.

Derivative complexes involving replacement of bound water with other ligands proved useful in aiding characterization of the [Mo₂O₆]⁴⁻ and [W₂O₆]⁴⁻ aqua ions (Ch. 1). It was hoped that

^aformulated by D'Olieslager as Ru₄(OH)₄⁴⁺ and Ru₂(OH)₂⁴⁺.⁵⁷

similar crystalline derivatives of the Ru(IV) aqua ion obtained using EDTA, MIDA and hydridotris(1-pyrazolyl)borate ligands would provide similarly useful structural information hopefully leading to an X-ray study that would confirm the core structure at least in the solid state. These ligands were chosen as they are all potential tridentate ligands capable of substituting at the facial arrangement of three water ligands on each Ru(IV) apparently present on the basis of the empirical formula "RuO(OH₂)₃" deduced from the quantitative ¹⁷O NMR results.

2.16.1 Attempted preparation of an EDTA complex of the Ru(IV) aqua ion.

A sample of the Ru(IV) aqua ion (10 cm³ of 0.01M per Ru) was neutralised by the addition of solid NaHCO₃ until the solution was at pH 3.8-4.0. Solid Na₂EDTA (0.19 g of the Na salt) was added to the solution. The red-brown colour of the solution became much more intense and its electronic spectrum showed two absorption maxima at 360, 480 nm. The spectrum is shown in figure 2.14. Tetramethylammonium chloride was added and the solution left to evaporate. It was hoped that suitable crystals would form, but evaporation eventually to dryness left a glassy solid residue. Other cations (Cs⁺, tetraethylammonium, tetrabutylammonium), and modifications of the experiment (eg. eluting the aqua ion from the column with 0.2 M Na₂EDTA solution, precipitation of the excess EDTA by increasing the acid concentration after complexation had occurred)

were tried but none gave rise to any isolable crystals of the desired complex.

2.16.2 Preparation of a methyliminodiacetate (MIDA) complex of the Ru(IV) aqua ion.

A solution of Ru(IV) aqua ion was prepared as already described. Following loading of the aqua ion on to a Dowex 50W-X2 cation exchange column distilled water (100 cm^3) was passed through. The aqua ion was then eluted with a solution of 0.2M H_2MIDA (Aldrich) in water. A concentrated sample was obtained if the column was left soaking in MIDA for 2 hours before elution. A deep red solution was obtained. Further elutions with MIDA after leaving the column soaking in MIDA became progressively yellow indicating that further reactions were taking place accompanying substitution of the water ligands. The initial red solution itself became progressively yellow over several days during which it was left to evaporate in the presence of tetramethylammonium chloride. After this time dark-red crystals were observed to form in the solution. These crystals were removed by careful filtration and a sample analyzed for CHN content (found C=22.04%, H=4.29%, N=5.83%). The closest fit to these analytical figures was found for $(\text{Me}_4\text{N})_2\text{Ru}_2\text{O}_6(\text{MIDA})_2 \cdot (\text{OH}_2)_2$ (calculated C=24.27%, H=4.48%, N=6.15%). This formulation was consistent with a conductivity measurement of the complex in water (a value of $34 \text{ } \Omega^{-1} \text{ mol}^{-1}$

Ch. 2: Experimental procedures & Results 171
cm⁻¹ was obtained for a 10⁻⁴ M solution which compared well with known 2:1 electrolyte solutions.*

A few suitable crystals were removed with the help of a microscope and were sent to the crystallographic unit at Glasgow University for X-ray analysis. Upon investigation however, the crystals were found to be opaque and unsuitable for structure determination.

Several attempts were made to recrystallise the compound but each time the same intense red crystals were obtained from the solution. When the crystals were dissolved in water, however the resulting electronic spectrum was very similar to that of the aqua ion. The spectrum is shown in figure 2.14.

2.16.3 Preparation of a hydridotris(1-pyrazolyl)borate complex of the Ru(IV) aqua ion.

The ligand [HB(pz)₃]⁻ (pz=1-pyrazolyl) was prepared as its K⁺ salt according to the method described by Trofimenko.²⁰ Potassium tetrahydridoborate (Aldrich, 10 g) was added to an excess of molten pyrazole (Lancaster, 60 g) heated to 190°C. The heating was continued until the evolution of H₂ had subsided. Pouring the resulting melt into toluene gave K[HB(pz)₃] in 80% yield. The K⁺ salt was then recrystallized from anisole and dried in an oven at 100°C. Its melting point was determined and found to be 188-191°C (188-189°C reported by

*Cu(bipy)₂(ClO₄)₂ (10⁻⁴ M) and Cu(bipy)₂Cl₂ (10⁻⁴ M) which gave a value of 23 and 29 $\Omega^{-1} \text{ mol}^{-1} \text{ cm}^2$ respectively.

Trofimenko²¹). Elemental analysis were in good agreement (found C=42.01%, H=4.14%, N=33.81%, calculated C=42.87%, H=4.00%, N=33.33%). Both ¹¹B and ¹H NMR spectra of K[HB(pz)₂] were recorded. The ¹¹B spectrum showed the expected doublet confirming the presence of a single B-H bond. The ¹H NMR spectrum in D₂O showed three peaks due to CH hydrogens (at 6.15 s, 7.18 s and 7.57 s referenced to tms=0).²² The Infra-red spectrum (KBr disc) revealed the ν(B-H) vibration at 2550 cm⁻¹. These findings were in good agreement with literature values reported by Trofimenko.²¹

Ru(IV) aqua ion was prepared as before but this time it was eluted of the Dowex 50W-X2 column with a solution of Th(NO₃)₄ (0.2 M). This gave rise to solutions of the aqua ion at pH 1. The pH was then increased to 2 by neutralising the acid with solid NaHCO₃. A 1:1 Stoichiometric amount per Ru(IV) of the K[HB(pz)₂] solid was then added slowly. Upon addition of K[HB(pz)₂] the pH rises as it protonates. Hence the pH was adjusted to 2-2.5 upon each addition of the ligand. The colour of the solution became deep red and eventually deposited a dark purple precipitate. This was filtered, washed with water, and dried in a vacuum desiccator. An electronic spectrum was obtained by dissolving a small amount of the complex in water. The solution was red-purple and showed two absorption maxima at

²²These appeared as single resonances due to lack of resolution but are reported as being a pair of doublets and a triplet.²¹

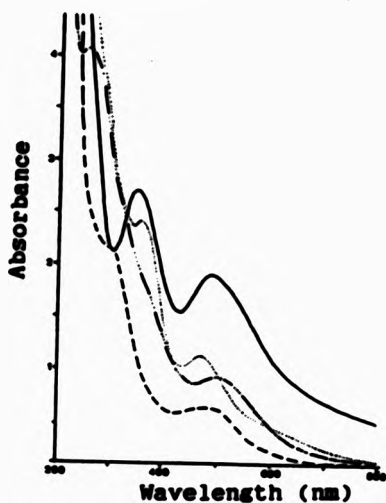


Figure 2.14 Electronic spectrum of Ru(IV) aqua ion (0.1M HClO_4) (---) and its derivative complexes: MIDA complex (—·—), EDTA complex (.....) and tris(pyrazolyl)borate complex (—) all dissolved in water.

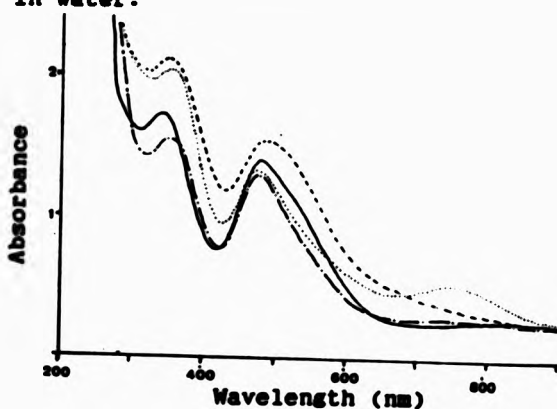


Figure 2.15 Electronic spectrum of the tris(pyrazolyl)borate complex dissolved in various solvents: DMSO (—), H_2O (---), EtOH (.....) and acetone (—·—).

492 and 358 nm (figure 2.14). The complex was found to be only partially soluble in water. Attempts were made to recrystallise it from different solvents where higher solubility was evident. These included acetone, ethanol, methanol, THF and DMSO). When the electronic spectrum was obtained in these solvents, it showed small changes to the spectrum compared with that in water (figure 2.15). The changes may be indicative of solvents becoming coordinated to the Ru(IV) with the loss of the $[\text{HB}(\text{pz})_3]^-$ ligand. Further evidence of solvent effects came from subsequent conductivity measurements in nitromethane and DMSO. In both solvents the value observed for a 10^{-3} M (130 and 160 $\Omega^{-1} \text{ mol}^{-1} \text{ cm}^2$ respectively) was consistent with a 2:1 electrolyte^{*} and inconsistent with a 4:1 electrolyte, the result expected from the elemental analysis which was in good agreement with that calculated for $[\text{H}_4\text{Ru}_4\text{O}_6(\text{HB}(\text{pz})_3)_4(\text{pzH})]^{4-}(\text{NO}_3)_4$ (1). By eluting the Ru(IV) aqua ion with $\text{La}(\text{tfms})_6$, $\text{La}(\text{pts})_6$ or $\text{La}(\text{ClO}_4)_6$ similar complexes with the respective anion were obtained. The elemental analyses on all of the isolated complexes obtained are given in table 2.4.

Following unsuccessful attempts to grow suitable crystals for X-ray analysis on these hydridotris(i-pyrazolyl)borate complexes and the worry with regard to the changes in the electronic spectrum on attempted recrystallization from several

*Ranges of conductance:	Solvent	1:1	2:1
	nitromethane	75-95	150-180
	DMF	65-90	130-170

organic solvents. It was decided to investigate the complex as isolated from the reaction mixture by +ve ion fast atom bombardment mass spectrometry given that the elemental analyses indicated the presence of cationic Ru-containing fragments. Use was made of the S.E.R.C MS centre at the University College of Wales at Swansea.

2.16.4 +ve ion FAB MS analysis of the hydridotris(i-pyrazolyl)-borate complexes of Ru(IV).

Complexes 1-3 and 6 (table 2.4) were analysed and good +ve ion MS were obtained consistent with the presence of the cationic Ru containing fragment (table 2.5). For the nitrate and tfms salts (complexes 1 and 2), an M⁺⁺ ion at m/e 1423 was obtained for the ¹⁰²Ru base peak which corresponded to the fragment [¹⁰²Ru₄O₆(HB(pz)₃)(pZH)]⁺⁺ as predicted from the elemental analysis. The first fragmentation corresponded to loss of the one free pyrazole molecule producing m/e 1356 (figure 2.16).

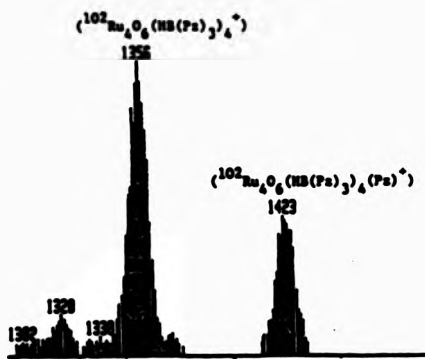


Figure 2.16 +ve ion FAB MS spectrum (molecular ion region) of $\text{H}_4[\text{Ru}_4\text{O}_6(\text{HB(pz)}_3)_4](\text{NO}_3)_4$.

The peak at 678 (table 2.5) is exactly half of the 1356 peak and shows half the isotopic distribution showing that it corresponds to an M^{2+} fragment arising from M^{3+} 1356. A further interesting stable fragment observed in all four complexes was the hitherto unknown monomeric Ru(III) ion $^{103}\text{Ru}(\text{B}(\text{pz})_5)_2^{2+}$ (528). The tosylate and ClO_4^- salts showed a similar fragmentation patterns but no evidence of the free pyrazole group also absent in the elemental analysis. A further salt with the large anion tetrphenylborate involved the addition of an ethanolic solution of $\text{Na[BPh}_4]$ (B.D.H.) to the reaction mixture. It was hoped but not substantiated that use of this large anion might yield suitable crystals for X-ray analysis. The resulting elemental analysis was in much poorer agreement with the stoichiometry obtained from use of the other anions. However +ve ion FAB MS analysis revealed the same apparent M^{2+} peak (- free pyrazole) as obtained with the others. It was concluded from these measurements that the main cationic fragment contained $[\text{H}_n\text{Ru}_4\text{O}_6(\text{HB}(\text{pz})_5)_4(\text{pzH})_m]^{(n=0-4, m=1 \text{ or } 0)}$. It is believed that these results provide the first definitive evidence that the Ru(IV) aqua ion exist in some kind of tetranuclear structure that has been proposed previously on the basis of charge/metal, charge/species and electrochemical measurements.²² On this basis it may be concluded that the relevant Ru(IV) aqua ion under these conditions ($\text{pH} \geq 2$) has the structure $[\text{Ru}_4\text{O}_6(\text{OH}_2)_{12}]^{4+}$.

Table 2.4 CHN analysis of derivative complexes of Ru(IV) ion.

Compound	Calculated			Found		
	C%	H%	N%	C%	H%	N%
1. $\text{H}_2\text{Ru}_2\text{O}_6(\text{HPz})_4(\text{pzH})(\text{NO}_3)_4$	28.00	2.67	23.13	28.47	3.18	23.64
2. As 1 with $(\text{CF}_3\text{SO}_3)_4 \cdot 2\text{H}_2\text{O}$	25.10	2.53	17.71	24.75	2.65	18.15
3. As 1 with $(\text{PTB})_4 \cdot 2\text{H}_2\text{O}$	37.49	3.73	16.87	33.28	3.85	17.52
4. As 1 with $(\text{ClO}_4)_4$	25.19	2.56	19.59	25.85	2.64	20.35
5. As 1 with $(\text{PF}_6)_4$	22.95	2.35	17.85	22.92	2.41	13.81
6. As 1 with $(\text{TPB})_4 \cdot 3\text{H}_2\text{O}$	49.33	4.44	17.20	47.08	4.40	14.83
7. 6 recrystallised from EtOH				45.94	4.04	15.23
8. 6 recrystallised from Aceton/ether				45.07	3.87	15.40

Complexes 3-6 do not contain Hpz molecule

Table 2.5 +ve ion FAB MS data for derivatives of Ru(IV) ion.

Compound	Mass of fragment	Probable species ^a
1. Nitrate salt	1423 1356 678 528	$[\text{^{102}\text{Ru}_2\text{O}_6}(\text{H}^{+1}\text{Hpz})_4(\text{pzH})]^{+-}$ (1424) (a) $[\text{Ru}_2\text{O}_6(\text{H}^{+1}\text{Hpz})_4]^{+-}$ (b) $[\text{Ru}_2\text{O}_6(\text{H}^{+1}\text{Hpz})_4]^{2+-}$ (c) $[\text{Ru}(\text{H}^{+1}\text{Hpz})_3]^{+-}$ (d)
2. Triflate salt	1424 1356 678 528	(a) (b) (c) (d)
3. Tosylate salt	1359 679 528	H_2 (b) H_2 (c) (d)
4. TPB salt	1358 680 528 464 423 417	H_2 (b) H_2 (c) (d) $\text{H}_2\text{Ru}_2\text{O}_6(\text{Hpz})$ $\text{H}_2\text{Ru}_2\text{O}_6(\text{pz})$ $\text{Ru}_2(\text{Hpz})$

^aThe fragments showed the characteristic isotope patterns for Ru in which the base peak given corresponds to the most abundant isotopes; ^{102}Ru and ^{104}Ru .

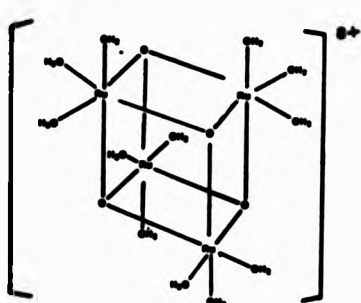
DISCUSSION

The present results have provided a more in depth discussion of the possible structure(s) for the red-brown aqua ion of Ru(IV) generated in non-complexing acidic media. Following, successful probing of the solution core structures of the Mo(IV) and W(IV) trinuclear aqua ions, hopes were high for a similar conclusive interpretation of the corresponding ^{17}O NMR spectrum of the Ru(IV) aqua ion following successful synthesis of a fully enriched ^{17}O derivative via electrochemical oxidation of $[\text{Ru}(\text{OH}_2)_6]^{2+}$.

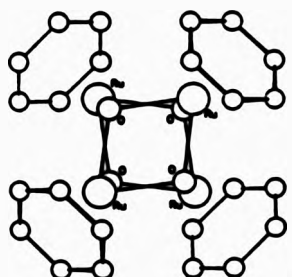
Consistent with the polynuclear formulation, resonances due both to bound water ligands (-24 ppm) and core oxygens (+1157 ppm) were observed. Analysis of peak integrations suggest an empirical formula/Ru of " $\text{RuO}(\text{H})(\text{OH}_2)_5^{2+}$ " clearly coordinatively unsaturated. The chemical shift of the core oxygen atom suggest an assignment to a μ -oxo group from comparisons with known species of Ru and Mo suggesting formula " $\text{RuO}(\text{OH}_2)_5^{2+}$ ". Figgis et al²¹ have reported ^{17}O chemical shifts for oxygen bound to transition metals. The compounds studied included $[\text{MoO}_4]^{2-}$, $[\text{WO}_4]^{2-}$ and RuO_4 (all d°). The chemical shifts reported for these three compounds are 540, 420 and 1119 ppm respectively (relative to bulk water). From our studies on the trinuclear W(IV) and Mo(IV) aqua ions the ^{17}O resonance for a μ -oxo group occurred at 519 ppm ($[\text{Mo}_2\text{O}_6]^{4+}$) and 319 ppm ($[\text{W}_2\text{O}_6]^{4+}$). From the work of Figgis it can be noticed that

there is a downfield shift of -700 ppm between $[\text{MoO}_4]^{2-}$ and $[\text{WO}_4]^{2-}$ and RuO_4 . Therefore a similar downfield shift for the $\mu_3\text{-O}$ in the Ru(IV) aqua ion would result in a resonance at around 1200 ppm. (± 150) This is consistent with the single resonance observed for the Ru(IV) aqua ion (1157 ppm).¹⁷ Thus it is concluded that the resonance at 1157 ppm is due to a μ_3 -oxo group.

The available evidence in the literature supports a tetrานuclear structure on the basis of ion-exchange and electrochemical measurements leading to a formula $[\text{Ru}_4\text{O}_4(\text{OH}_2)]^{4+}$. This would suggest the presence of the cube structure shown in (I).



(I)

Structure of $[(\text{n}^5\text{-C}_5\text{H}_5)\text{Ru}(\text{OH})_4]^{4+}$

(II)

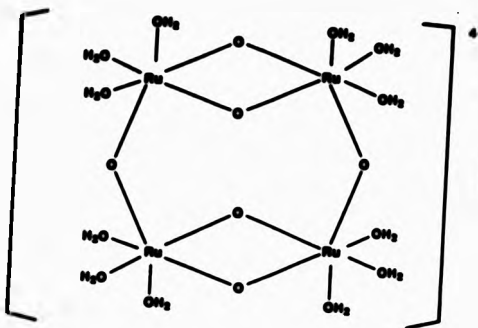
In this context, a tetrานuclear cube structure of Ru(II), shown in (II) has been prepared by Stephenson and co-workers¹⁸ albeit with N-acid ligands such as benzene. The high charge on the

¹⁷By similar arguments an $\eta_1\text{-O}$ group would be expected to show a resonance at around 1600 ppm and a $\mu_3\text{-O}$ group at around 1400 ppm for a Ru(IV) aqua ion having these types of oxo groups.

ion ($8+$) may explain why the ion is not elutable with $\geq 2M$ acid. However, the fact that the ion is elutable with 0.1M solutions of Th^{4+} or La^{3+} in 0.1M HClO_4 suggests that at $[\text{H}^+] < 2M$, the charge on the ion is lower. The charge/Ru on the ion was determined in the present work at pH 1.7 and found to have a value of 1.00 ± 0.03 which is in agreement with values determined in the literature at pH 1.0.²² In this same range, the charge/species was determined by membrane equilibrium measurements to be $4+$ suggestive of a tetrานuclear structure. It is thus concluded that the $[\text{Ru}_4\text{O}_4(\text{OH}_2)_{12}]^{4+}$ ion present at higher acidities, loses successive protons to give eventually $[\text{Ru}_4\text{O}_4(\text{OH})_4(\text{OH}_2)_8]^{4+}$ at pH 1. Since proton exchange is rapid on the NMR time scale, this formulation would still be consistent with the 3:1 bound water integration/Ru observed. A worry with this scheme however was the failure to detect the expected -ve shift in the bound water resonance as a result of protonation in the $[\text{H}^+] > 2M$ vs that at pH 1. Furthermore, there appears to be no evidence of any detectable change in the electronic spectrum of Ru(IV) in $[\text{H}^+] \text{ range } 0.01-3.0 \text{ M}$. It is conceivable that these properties are, for Ru(IV), insensitive to the exact charge on the ion in contrast to the behaviour of earlier transition metal aqua ions $[\text{Mo}_3\text{O}_6]^{4+}$ and $[\text{W}_3\text{O}_6]^{4+}$.

Following increase of the pH of the Ru(IV)_{ac} solution to between 2-3, successful preparation and isolation of a number of anionic and cationic derivative complexes of Ru(IV) was achieved in which the hydridotris(i-pyrazolyl)borate complexes

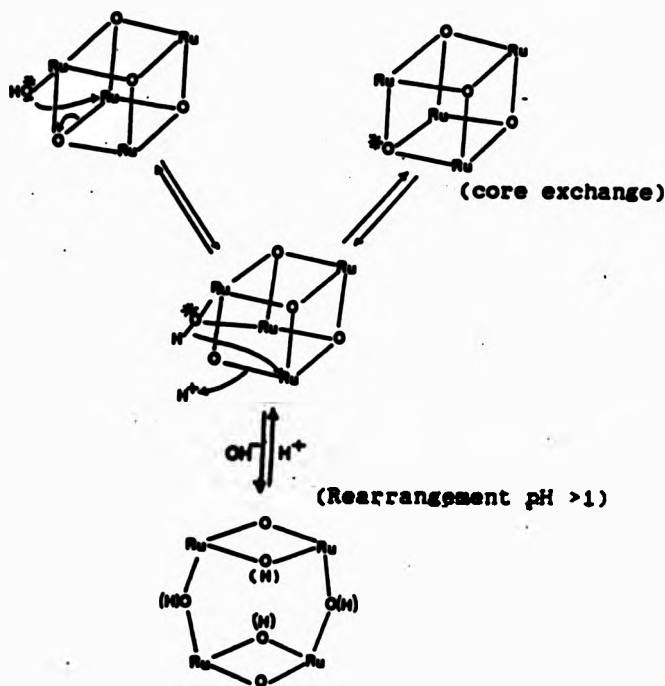
were the best characterized and most studied. The cationic nature of the Ru(IV) containing fragment was shown by conductivity and successful +ve ion FAB MS measurements at Swansea. The +ve ion FAB MS measurements revealed an apparent H^{+-} peak consistent with the fragment $[\text{H}_n^{\pm\pm\pm}\text{Ru}_4\text{O}_6(\text{H}^{1+}\text{B(pz)}_2)_4]^{+-/-/-}$ ($n=0-4$), some of which contain evidence of free pyrazole. Cotton et al.²⁸ reported an X-ray crystal structure of $\text{Mo}_4\text{S}_4[\text{H}^-\text{B(pz)}_2]_4(\text{pz})$ which showed the strange arrangement whereby two pyrazolylborate ligands function as typical tridentate chelating ligands whereas the other two function as bidentate ligands with one pyrazole ring dangling. A similar situation may be present in the case of the Ru(IV) derivative complexes. Elemental analysis on the cationic derivatives with NO_3^- and CFSO_3^- counter ions were also in support of the $[\text{H}_4\text{Ru}_4\text{O}_6-(\text{HB(pz)}_2)_4]^{4+}$ ion being present with four counter ions. Derivatives with other counter ions gave similar analytical and MS results. Such a finding seems not to be consistent with the $\text{Ru}_4\text{O}_6^{4+}$ core but suggests that some rearrangement may have occurred to the Ru(IV) core at these high pH's leading to derivatives based rather on a protonated $\text{Ru}_4\text{O}_6^{4+}$ core. Possibilities here would include a linear, adamantane-like or more likely the cyclic structure (III). Given that the isolation of all the derivative complexes prepared required a higher pH than that used for the ^{17}O NMR experiments, it remains conceivable that the $[\text{Ru}_4\text{O}_6(\text{OH})_4]^{4+}$ core (pH 1) rearranges at some point to give the $[\text{Ru}_4\text{O}_6]^{4+}$ core above pH 1.



(III)

Additional evidence for this presumed lability of the Ru(IV) core is indeed apparent from the variable temperature ^{17}O NMR studies of the bound water exchange. During broadening of the bound water resonance, additional resonances are observed to appear corresponding to new bound waters and/or core oxygen atoms leading to observed enrichment of the single core oxygen ($\mu_{\text{s}}\text{-O}$) resonance at +1157 ppm. Such behaviour can only have resulted it seems via some opening-up of the structure at the higher temperatures ($>40^\circ\text{C}$). Remarkably, cooling to room temperature restores the original Ru(IV) ^{17}O NMR spectrum showing the processes to be reversible at pH 1, the only difference being the trapped ^{17}O enrichment in the core oxygen resonance at 1157 ppm (see figure 2.12). During the variable temperature ^{17}O NMR study, simultaneous monitoring of the electronic spectrum of Ru(IV) as function of temperature showed evidence of small changes which were reversible on cooling, paralleling the ^{17}O NMR results. This observation provided

further confirmation that the electronic spectrum of Ru(IV) demonstrates relatively little sensitivity towards structural changes in the core and lends support to the possibility that the $[\text{Ru}_4\text{O}_6(\text{OH})_4]^{4-}$ can protonate undetected in the $[\text{H}^+]$ range 0.1-3.0M. Similar opening up of the structure at higher pH may occur irreversibly/reversibly leading to rearrangement to give the $[\text{Ru}_4\text{O}_6]^{4-}$ core (see scheme below).



In conclusion the present results support the tetrานuclear formulation for the Ru(IV) aqua ion though rule out structures based only on μ -hydroxo groups as suggested by some workers. A μ -oxo structure is the only one consistent with the ^{17}O NMR and analytical results.

The results appear to favour two interconverting structures depending upon the pH of the solution. High pH's > 1 appear to favour a structure based on a cyclic $\text{Ru}_4\text{O}_6^{4+}$ core whereas at pH's ≤ 1 , a cubic $\text{Ru}_4\text{O}_6^{4+}$ core structure appears relevant. Further experiments planned for the future will include an ^{17}O NMR study of the Ru(IV) aqua ion in the pH range 1-3. A shift in the μ -O resonance to lower field (1157 ppm (μ -O) to \sim 1400 ppm (μ -O)) and a Ru: μ -O:b-H₂O ratio of 1:1.5:3 will conclusively confirm the interconverting structures. Considerable lability in the $\text{Ru}_4\text{O}_6^{4+}$ core is evident from temperature dependent ^{17}O NMR studies at pH 1 adding further support for the structural interconversion proposed at higher pH.

From the variable temperature ^{17}O linebroadening study the rate constant for water exchange on Ru(IV) ($k_{\text{ex}}^{\text{app}}=29.8\pm24.8 \text{ s}^{-1}$) was found to be extremely large when compared with $k_{\text{ex}}^{\text{app}}$ values for $[\text{Ru}(\text{OH}_2)_6]^{2+}$ and $[\text{Ru}(\text{OH}_2)_6]^{4+}$ (1.8×10^{-8} and $3.5 \times 10^{-6} \text{ s}^{-1}$ respectively). Labilization due to the presence of trans μ -O groups and/or cis-conjugate base pathways are two possible explanations for this fast exchange.

REFERENCES

1. Ruff, O.; Vidic E. Z. Anorg. Allgem. Chem., 1924, 136, 49.
2. Brauer, G. "Handbook of Prep. Inorg. Chem.", Acad. Press. NY, 1965, 159.
3. Nakata, H. Tetrahedron, 1963, 19, 1959.
4. Berkowitz, L. M.; Rylander, P. N. J. Am. Chem. Soc., 1958, 80, 6682.
5. Wolfe, S.; Hasan, S. K.; Campbell, J. R. J. Chem. Soc. Dalton Trans., 1970, 1420.
6. Courtney, J. L.; Swanborough, K. F. Rev. Pure and Appl. Chem., 1972, 22, 47.
7. Torii, S. et al J. Org. Chem., 1985, 50, 4980.
8. Griffith, W. P. J. Chem. Soc., A, 1968, 1663.
9. Cotton, F. A.; Wilkinson, G. "Advance Inorg. Chem.", fifth ed., 1988, 881.
10. Griffith, W. P.; Ley, S. V.; Whitcombe, G. P.; White, A. D. J. Chem. Soc. Chem. Commun., 1987, 1625.
11. Green, G.; Griffith, W. P.; Hollinshead, D. M.; Ley, S. V.; Schröder, M. J. Chem. Soc. Perkin Trans. I, 1984, 681.
12. Connick, R. E.; Hurley, C. R. J. Am. Chem. Soc., 1952, 74, 5012.
13. Aoyama, S. Z. Anorg. Allgem. Chem., 1924, 138, 249.
14. Griffith, W. P. The chemistry of the rarer platinum metals, Interscience, London, 1967.
15. Howe, J. L. J. Am. Chem. Soc., 1901, 23, 779.
16. Kruse, F. H. Acta Crystallogr., 1961, 14, 1035.
17. Porai-Koshits, M. A.; Atovmyan, L. O.; Andrianov, V. G. J. Struct. Chem. (USSR), 1961, 2, 686.
18. Mathieson, A. McL.; Mellor, D. P.; Stephenson, N. C. Acta Crystallogr., 1952, 5, 185.
19. San Filippo, J. Jr; Fagan, P. J.; Di Salvo, F. Inorg. Chem., 1977, 16, 1016.

Ch. 2: References 186

20. Appleby, D.; Crisp, R. I.; Hitchcock, P. B.; Hussey, C. L.; Ryan, T. A.; Sanders, J. R.; Seddon, K. R.; Turp, J. E.; Zora, J. A. J. Chem. Soc. Chem. Commun.. 1986, 483.
21. Pshenitsyn, N. K.; Ezerskaya, N. A. Russ. J. Inorg. Chem., 1961, 6, 312.
22. Brauer, G. Handbook of Prep. Inorg. Chem.. Acad. Press, NY, 1965, 1597.
23. Connick, R. E.; Fine, D. A. J. Am. Chem. Soc., 1960, 82, 4187.
24. Campbell, W. J.; Davis, V. A.; Griffith, W. P.; Townend, T. J. J. Chem. Soc. Dalton Trans., 1985, 1673.
25. Ohyoshi, E.; Ohyoshi, A.; Shinagawa, M. Radiochim Acta, 1970, 13, 10.
26. Connick, R. E. Adv. in Chemistry of coordination compounds, ed. S. Kirschner, McMillan, NY, 1961.
27. Hopkins, T. E.; Zalkin, A.; Templeton, D. H.; Adamson, M. G. Inorg. Chem., 1966, 5, 1427.
28. (a) Taqui Khan, M. M. Pure Appl. Chem., 1983, 55(1), 159.
(b) Gore, E. S. Platinum Met. Rev., 1983, 27, 111.
(c) Harrod, J. E.; Coccone, S.; Halpern, J. Can. J. Chem., 1961, 39, 1372.
(d) Taqui Khan, M. M.; Ramachandraiah, G. Inorg. Chem., 1982, 21, 2109.
29. Taqui Khan, M. M.; Shukla, R. S. J. Mol. Catal., 1985, 34, 19.
30. Remy, H.; Wagner, T. Z. Anorg. Allg. Chem., 1928, 168, 1.
31. Zintl, E.; Zaimis, Ph. Chem. Ber., 1927, 60, 842.
32. Bino, A.; Cotton, F. A. J. Am. Chem. Soc., 1980, 102, 608.
33. Godwood, L. W. N.; Wardlaw, W. J. Chem. Soc., 1938, 1422.
34. Adamson, M. G. Aust. J. Chem., 1967, 20, 2517.
35. Rose, D.; Wilkinson, G. J. Chem. Soc., A, 1970, 1791.
36. Rechnitz, G. A.; Catherino, H. A. Inorg. Chem., 1965, 4, 112.

37. (a) Wishart, J. F.; Bino, A.; Taube, H. Inorg. Chem., 1986, 25, 3318.
(b) Shepherd, R. E. et al. J. Organomet. Chem., 1986, 3, 506.
(c) Ilan, Y.; Kapon, M. Inorg. Chem., 1986, 25, 2350.
(d) Winkler, J. R.; Netzel, T. L.; Creutz, C.; Sutin, N. J. Am. Chem. Soc., 1987, 109, 2381.
(e) Fürholz, U.; Haim, A. Inorg. Chem., 1987, 26, 3243.
(e) Taube, H. "Survey of Progress in chemistry". Acad. press, 1974, 6.
38. Fletcher, J. M.; Greenfield, B. F.; Hardy, C. J.; Scargill, D.; Woodhead, J. L. J. Chem. Soc., 1961, 2000.
39. Clausen, C.; Prados, R. A.; Good, M. L. Inorg. Nucl. Chem. Lett., 1971, 7, 485.
40. (a) Smith, P. M.; Pealey, T.; Earley, J.; Silverton, J. V. Inorg. Chem., 1971, 10, 1943.
(b) Carrondo, M. A. A. F. de C. T.; Griffith, W. P.; Hall, J. P.; Skapski, A. C. Biochim. Biophys. Acta, 1980, 627, 332.
41. Wagner, F. E.; Wordel, R.; Griffith, W. P.; McManus, N. T. J. Chem. Soc. Dalton Trans., 1988, 1679.
42. Cady, H. H.; Connick, R. E. J. Am. Chem. Soc., 1958, 80, 2646.
43. Niedrach, L. W.; Tevebaugh, A. D. J. Am. Chem. Soc., 1951, 73, 2851.
44. Atwood, D. K.; De Vries, T. J. Am. Chem. Soc., 1961, 83, 1509.
45. Mercer, E. E.; Buckley, R. R. Inorg. Chem., 1965, 4, 1692.
46. Kallen, T. W.; Earley, J. C. Inorg. Chem., 1971, 10, 1149.
47. Bernhard, P.; Bürgi, H. B.; Hauser, J.; Lehmann, H.; Ludi, A. Inorg. Chem., 1982, 21, 3936.
48. Hunt, J. B.; Earley, J. E. J. Am. Chem. Soc., 1960, 82, 5312.
49. Endicott, J. F.; Taube, H. J. Am. Chem. Soc., 1962, 84, 4984. Inorg. Chem., 1965, 4, 437.

Ch. 2: References 188

50. Wehner, P.; Hindman, J. C. J. Am. Chem. Soc., 1950, 72, 3911.
51. Gortsema, F. P.; Cobble, J. W. J. Am. Chem. Soc., 1961, 83, 4317.
52. Vdovenko, V. M.; Lazarev, L. N.; Khvorostin, Ya. S. Radikhimika, 1965, 7, 228.
53. Koch, H.; Bruchertseifer, H. Radiochim. Acta, 1965, 4, 82.
54. Atwood, D. K.; De Vries, T. J. Am. Chem. Soc., 1962, 84, 2659.
55. Wallace, R. M.; Propst, R. C. J. Am. Chem. Soc., 1969, 91, 3779.
56. Brémard, C.; Nowogrocki, G.; Tridot, G. Bull. Soc. Chim. Fr., 1974, 3-4, 392; 1974, 1-2, 110.
57. D'Olieslager, W.; Heerman, L.; Clarysse, M. Polyhedron, 1983, 2, 1107.
58. Weaver, T. R.; Meyer, T. J.; Adeyemi, S. A.; Brown, G. M.; Eckberg, R. T.; Hatfield, W. E.; Johnson, E. C.; Murray, R. W. J. Am. Chem. Soc., 1975, 97, 3039.
59. Dwyer, F. P.; Goodwin, H. A.; Gyarfas, E. C. Aust. J. Chem., 1963, 16, 544.
60. Shlenskaya, V. I.; Biryukov, A. A. Vestn. Mosk. Univ. Ser. II. Khim., 1963, 18, 75. [CA:59:13489h].
61. Wehner, P.; Hindman, J. C. J. Phys. Chem., 1952, 56, 10.
62. Alimarin, I. P.; Khvostova, V. P.; Pichugina, G. V.; Tikhonov, I. G.; Kuratashvili, Z. A. Izv. Sib. Otd. Akad. Nauk SSSR. Ser. Khim. Nauk, 1974, 31.
63. Shlenskaya, V. I.; Biryukov, A. A.; Kadomtseva, V. M. Russ. J. Inorg. Chem., 1972, 17, 572.
64. Tikhonov, I. G.; Bodnya, V. A.; Alimarin, I. P. Vestn. Mosk. Univ., Khim., 1975, 16, 714. [CA:84:144108].
65. Woodhead, J. L.; Fletcher, J. M. UKAEA A.G.R.E., R-4123.
66. Alimarin, I. P.; Shlenskaya, V. I.; Pichugina, G. V.; Khvostova, V. P. Bull. Acad. Sci. USSR, Div. Chem. Sci., 1974, 277.

67. Biryukov, A. A.; Shlenskaya, V. I.; Rabinovich, B. S. Russ. J. Inorg. Chem., 1969, 14, 413.
68. Shlenskaya, V. I.; Piskunov, E. N. Vestn. Mosk. Univ., Ser. II, Khim., 1963, 18, 35. [CA:59:2385h].
69. Yaffe, R. P.; Voigt, A. F. J. Am. Chem Soc., 1952, 74, 2500.
70. Forsythe, J. H. W.; Magee, R. J.; Wilson, C. L. Talanta, 1960, 3, 324.
71. Schmidtke, H. -H. J. Inorg. Nucl. Chem., 1966, 28, 1735.
72. Schmidtke, H. -H.; Garthoff, D. Helv. Chim. Acta, 1967, 50, 1631.
73. Schwerdtfeger, H. -J.; Preetz, W. Angew. Chem., Int. Ed. Engl., 1977, 16, 108.
74. Wajda, S.; Rachlewicz, K. Mukleoniaka, 1973, 18, 407. [CA:80:125346].
75. Gansjäger, H.; Murrmann, R. K. Adv. Inorg. Bioinorg. Mech., Acad. Press, 1983, 2, 317.
76. Deloume, J. P.; Duc, G.; Thomas-David, G. Polyhedron, 1985, 4, 877.
77. Ferguson, J. E.; Greenaway, A. M. Aust. J. Chem., 1978, 31, 497.
78. Rapaport, I.; Helm, L.; Merbach, A. E.; Bernhard, P.; Ludi, A. Inorg. Chem., 1988, 27, 873.
79. Harris, R. K. "NMR Spectroscopy", Pitman Publishing Co., London, 1983.
80. Trofimenko, S. J. Am. Chem. Soc., 1967, 89, 3170.
81. Figgis, B. N.; Kidd, R. G.; Nyholm, R. S. Proc. Royal Soc. Chem., 1962, A269, 469.
82. Gould, R. O.; Lynn Jones, C.; Robertson, D. R.; Stephen-son, T. A. J. Chem. Soc. Chem. Commun., 1977, 222.
83. Cotton, F. A.; Dori, Z.; Llusar, R.; Schwotzer, W. Inorg. Chem., 1986, 25, 3529.

CHAPTER THREE

3. Substitution reactions of octahedral complexes.

The most common geometry found in transition metal complexes is octahedral. It represents a very stable arrangement for a purely electrostatic interaction between a coordination acceptor centre and a donor ligand whose radius ratio sits within the right range (eg. $[Fe(OH_6)_6]^{2+}$). It is a stable arrangement for many partly electrovalent systems where an obvious explanation for the preferred geometry is not apparent on the basis of the number of d electrons (eg. $[Ni(OH_6)_6]^{2+}$ and $[Cr(OH_6)_6]^{2+}$ regular, $[Cr(OH_6)_6]^{3+}$, distorted); it is the strongly favoured geometry for the low-spin d⁶ configuration of the transition element ions (eg. Ru(II), Os(II), Rh(III), and Ir(III)). Kinetic studies on substitution reactions of octahedral complexes have been largely limited to two types of reactions:

- 1) Replacement of coordinated solvent (water).



When L is an anion, the reaction is often called *enation*.

- 2) Solvolysis.

Since the majority of studies are carried out in aqueous medium, a more appropriate term is *hydrolysis*. This reaction is essentially the opposite of reaction (1).

3.1 Classification of ligand substitution mechanisms

Ligand substitution reactions of octahedral complexes can be expressed by the generalized equation (2) where M is a metal

CH. 3: Subst'n reactions of octahedral complexes 191
ion, and X and Y are any two ligands, and L is the non exchanging ligand.



Different classification schemes have been used in an attempt to define these reactions in a systematic manner. One of the first was that of Ingold¹, based on the molecularity of organic substitution. He used the traditional S_N1 and S_N2 classification for uni- and bimolecular nucleophilic substitution respectively. Basolo and Pearson² expanded this classification to included limiting cases, denoted S_N1 lim and S_N2 lim. However, the classification that is used most often by Inorganic chemists is that of Langford and Gray.³ They divided the mechanistic analysis into two phases: the stoichiometric mechanism or the splitting of the reaction in terms of the succession of elementary steps and the intimate mechanism or the analysis of the rate constants of individual steps in terms of rearrangements of atoms and bonds.

Stoichiometrically three simple pathways are possible:

- 1) An Associative pathway (*A*), which results in the production of an intermediate of increased coordination number.
- 2) A Dissociative pathway (*D*), which results in the production of an intermediate of decreased coordination number.
- 3) An Interchange pathway (*I*), which involves the concerted exchange of X and Y between the inner and outer

coordination shells of the metal ion. The defining characteristic of this mechanism is the absence of a kinetically detectable intermediate in which the primary coordination number of the metal is modified.

The nature of the intermediate is the crucial factor in the stoichiometric scheme. Each of the three pathways are illustrated in equations (3), (4) and (5), where $\text{ML}_n\text{X}\dots\text{Y}$ is an outer sphere complex or ion-pair.



The necessary, but not sufficient condition for an *A* or *D* mechanism is that the lifetime of the intermediate is long enough for it to be able to kinetically distinguish between incoming nucleophiles and thus be kinetically detectable. This condition is rarely satisfied.² Interchange reactions may be subdivided into two further classes: those with *A*-like activation and those with *D*-like activation (classed as I_A and I_D). In an I_A process the entering group will play an important role in determining the activation energy for formation of the transition state while for an I_D process the entering group effect on the activation energy and rate of reaction will be small.

The application of the Langford and Gray classification to solvent exchange reactions poses some problems. Evidently, both the entering and leaving groups are identical. Thus the foregoing tests may not be directly applicable.⁴ In the case of solvent exchange (water in particular), the activation volume provides information about the mechanisms that would otherwise be unavailable (see later).

Even though the Langford-Gray approach to ligand substitution, has proven very useful in many cases, its rigorous operational approach causes some drawbacks. One case is that of Mn²⁺ where the negative volume of activation indicates an I_a mechanism, while the net substitution rates for Mn²⁺ complexes show no marked dependence on the nature of the incoming ligand.⁴ In fact Mn²⁺ reacts very rapidly, near to the diffusion controlled limit, and its high reactivity may lead to diminution of its selectivity.⁵

The operational definitions have also been criticised by Swaddle⁶ who regards them as being too rigid. He has proposed a slight adaptation of the strict Langford-Gray criterion for I_a activation, viz. that it is more useful to seek to distinguish between those interchange reactions in which there are clear indications of at least some associative contribution to the activation process (through incoming group influence within the encounter complex, steric effects, pressure phenomena etc.) and those in which there are not. Thus although the Langford

Ch. 3: Subst'n reactions of octahedral complexes 194
and Gray classification labels are used, their criteria are not
always strictly applied.

3.2 Diagnosis of the mechanism of substitution:

A variety of methods are used to establish the mechanism of a particular substitution reaction. These include the determination of the rate law, the activation parameters for the formation of the activated complex (ΔH^\ddagger , ΔS^\ddagger) from the temperature dependence of the rate constant, the activation volume parameter (ΔV^\ddagger) from variable-pressure studies, dependence of the rate on ionic strength and on solvent composition and careful measurement of rates and activation parameters during variance of the incoming ligand.

3.2.1 Rate law determination:

A first-order rate law often indicates a dissociative pathway whereas a second-order rate law is indicative of an associative pathway. However this rule does not always apply. In certain cases both *D* and *I_s* mechanisms may give second-order rate laws.

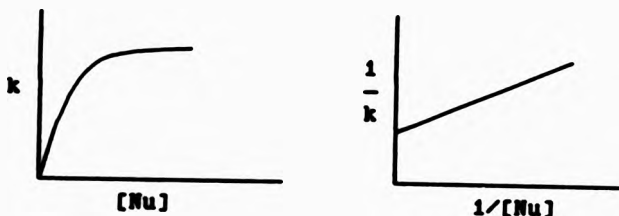


Figure 3.1 The dependence of rate constant on incoming nucleophile concentration for *D* substitution.

From figure 3.1 it can be seen that, at low nucleophile concentrations, the characteristic substitution behaviour for a D mechanism approximates to a straight line. In the case of a weak nucleophile, this straight line may extend to the highest accessible concentration, giving the misleading impression that the reaction is first-order in incoming ligand and second-order overall. Likewise, if the association between the complex and the incoming ligand is weak, then an I_s process also appears to follow a second-order rate law. Thus information based only on the rate law has to be viewed with some caution.

3.2.2 Rate comparisons.

The dependence of the rate with the nature of incoming ligand can often be indicative of a likely mechanism. For example, if the rate of reaction varies with the nature of the nucleophile, an associative mechanism is indicated. However, if the complex reacts with various nucleophiles at the same rate then a dissociative mechanism is more probable.

3.2.3 Activation parameters.

As in the case of rate comparison, if for a series of related reactions, the activation enthalpies and entropies ($\Delta H^\ddagger, \Delta S^\ddagger$) are similar then this would be a good indication of a common mechanism. Where comparisons are not possible, the activation entropy may give a diagnosis of the mechanism. This is based on the assumption that a dissociative process will tend to have positive entropy and that an associative process will tend to

have a negative activation entropy. Many other factors including solvation effects, chelation etc. can however affect the ΔS^\ddagger value so again caution against overinterpretation must be given.

The activation parameters ΔH^\ddagger and ΔS^\ddagger are readily obtainable from the temperature variation of reaction rates. The application of high pressure techniques^{9,10} has also allowed pressure variation of rates and hence the determination of ΔV^\ddagger is possible (equations 6 and 7).

$$\left. \frac{d \ln k}{dt} \right|_T = \frac{E_a}{RT^2} \quad \dots \dots (6)$$

$$\left. \frac{d \ln k}{dt} \right|_P = \frac{\Delta V^\ddagger}{RT} \quad \dots \dots (7)$$

For reactions in solution, these Arrhenius equations are considered in the light of the transition state theory. For the temperature dependence equation (8)^{*} is most widely used to calculate H^\ddagger and S^\ddagger .

$$\ln k = \ln \left[\frac{k_B T}{h} \right] + \left[\frac{\Delta S^\ddagger}{R} \right] - \left[\frac{\Delta H^\ddagger}{RT} \right] \quad \dots \dots (8)$$

Thus a plot of $\ln k$ vs T^{-1} (Arrhenius relationship, first differential of equation (8) giving $\ln k = \ln A + (-E_a/RT)$) or

* k_B , h and R are the Boltzmann, Planck and Gas constants respectively.

$\ln(k/T)$ vs T^{-1} (Eyring relationship, eqn (8)) is linear and the activation parameters may be calculated from the slope and intercept. Both Eyring and Arrhenius plots give very similar results.²²

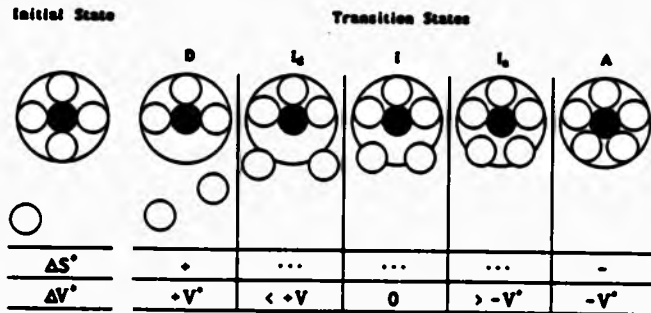
Various mathematical descriptions have been proposed²³ to account for the pressure dependence of ΔV^\ddagger . The most popular is the quadratic relationship (9), where ΔV^\ddagger is the volume of activation at zero pressure and β is the compressibility coefficient of activation, a measure of the pressure dependence of ΔV^\ddagger .

$$\ln k = \ln k_e - \left[\frac{\Delta V^\ddagger P}{RT} \right] + \left[\frac{\beta P^2}{2RT} \right] \dots \dots \dots \quad (9)$$

Bond stretching in a simple dissociative step gives rise to an increase in volume, which is manifested in a decrease in the rate of reaction with increasing pressure, i.e. a positive ΔV^\ddagger . Conversely, bond formation occurring in a simple associative process will lead to an increase in the rate constant with increasing pressure, i.e. a negative ΔV^\ddagger (figure 3.2).

The major drawback frequently with ΔS^\ddagger values is that they are estimated from data determined over a small temperature range via a large extrapolation to infinite temperature and hence are prone to large errors. The advantage of ΔV^\ddagger measurements is that they are determined directly from the slopes, and thus

carry small errors allowing definitive mechanistic information to be deduced with reasonable certainty.



where V^\ddagger is the partial molar volume

Figure 3.2 Schematic representation of solvent exchange reactions proceeding by different mechanisms.*

For substitution reactions, the measured volume of activation is usually considered to be the combination of an intrinsic contribution $\Delta V_{\text{ine}}^\ddagger$, resulting from changes in internuclear distances within the reactants during the formation of the transition state, and an electrostrictive contribution $\Delta V_{\text{elec}}^\ddagger$, resulting from the formation or neutralisation of ions or dipoles at the transition state. Where charge species are involved, the observed ΔV^\ddagger may be dominated by $\Delta V_{\text{elec}}^\ddagger$ even to

*The small black circle in the middle of the idealized "flat" complex represents the central atom. The small open circles represent the bound and free ligands (solvent molecules). The large circles represent the boundaries of the first coordination sphere.

the extent that the sign of ΔV^* may differ from that of ΔV_{int}^* . However, for solvent exchange reactions, the interpretation of the observed ΔV^* is rendered much easier due to the absence of electrostrictive changes ie $\Delta V^* = \Delta V_{\text{int}}^*$.¹³ The activation volume is a powerful diagnostic parameter and has permitted unambiguous assignment of mechanisms.¹⁴

3.2.4 Other methods for diagnosis of mechanism.

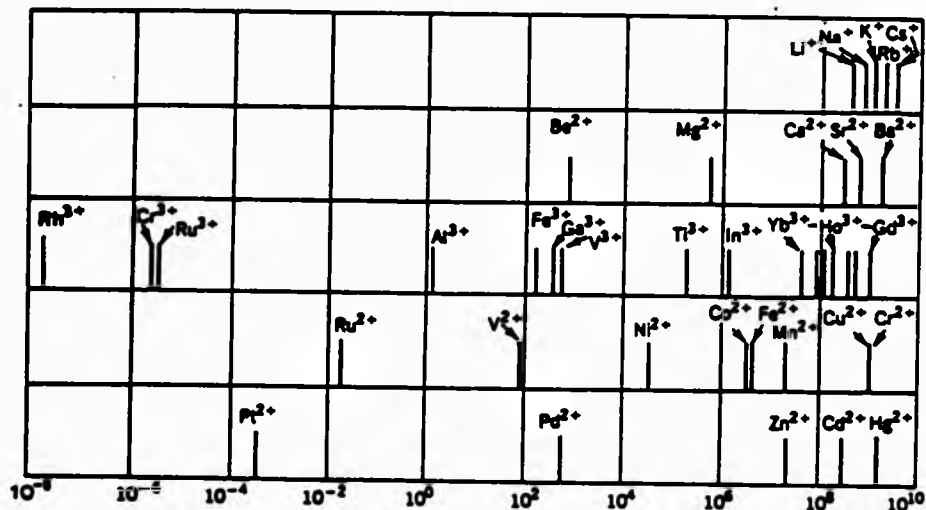
Other less common methods for establishing the mechanism of a substitution reaction include: dependence of the rate constant on ionic strength which indicate changes of charge involved in transition state formation, the variation of rate with ligand substituent which can prove informative when a series of compounds differing only in this respect can be synthesized and studied. The variation of rate with solvent composition (common in organic chemistry) has also been applied. All these methods give less precise and often controversial characterization.

3.3 Water exchange rates.

A great deal of information regarding substitution mechanisms on octahedral metal complexes has been obtained via examination of the simple process of exchange of coordinated water for bulk water. With the availability of powerful techniques (eg. multinuclear NMR line-broadening) to measure very fast reaction rates, it has now been possible to study almost all known aqua ions and derivatives. A number of studies have also been

carried out with cations contained in other coordinating solvents such as DMSO and DMF.¹⁶ The results for the various water exchange studies are summarized in figure 3.3.

Figure 3.3 Rate constant for water exchange on metal cations.^{16,17,18}



The water exchange rate constants cover about 18 orders of magnitude. In order to explain the mechanism of exchange, the activation volume parameter has been extensively employed.

3.3.1 Trivalent cations.

A general view of the volume of activation for the first row high spin transition metal trivalent ions is given in table 3.1.

Table 3.1 Volumes of activation ($\text{cm}^3 \text{ mol}^{-1}$) for solvent S exchange on $[\text{MS}_6]^{3+}$ of the first row T. M. series (ref. 10).^a

M^{3+} $\sim r_A(\text{pm})$ O_h^-	Sc 75 r_{eff}°	Tl 67 r_{eff}°	V 64 r_{eff}°	Cr 61 r_{eff}°	Fe 64 $r_{\text{eff}}^{\circ} r_{\text{ex}}^{\circ}$	Ga 62 $r_{\text{eff}}^{\circ} r_{\text{ex}}^{\circ}$
S = H ₂ O			-12.1	-6.9	-9.6	+5.0
DMSO				-11.3	-3.1	+13.1 ^b
DMP				-6.3	-0.9	+7.9 ^b
TBP	-21.3					+20.7 ^b

^aIn CD_3NO_2 as diluent.

A definite trend is observable across the series. The V values become increasingly negative on going along to Fe^{3+} , with a positive value for Ga^{3+} . This change over in mechanism from associative to dissociative activation mode is confirmed by a few results in non-aqueous solvents. The value for Tl^{3+} is markedly more negative than those for the following three members of the series. It is also rather close to the limiting value of $-13.5 \text{ cm}^3 \text{ mol}^{-1}$ proposed by Swaddle^c which corresponds

^bBy NMR except for Cr^{3+} which was obtained by ^{18}O isotope labelling

^c"Effective ionic radius.

Ch. 3: Subst'n reactions of octahedral complexes 202
 effectively to the partial molar volume change associated with take up or loss of a water molecule. Although a limiting associative mechanism cannot be attributed on the sole basis of this value, the mode of water exchange on Ti^{3+} can be asserted to be strongly associative. The smaller values for V^{2+} , Cr^{3+} , and Fe^{3+} on the other hand, tend to favour the conclusion that an A_n mode of activation is in operation.

Table 3.2 Rate constants and activation parameters for water exchange on some hexaaqua and monohydroxypentaqua metal ions.

	$K_{H_2O}^*$	K_{OH}^*/K_{H_2O}	ΔH^\ddagger kJ mol^{-1}	ΔS^\ddagger $J K^{-1}$ mol^{-1}	ΔV^\ddagger cm^3 mol^{-1}	pKa	Ref.
Ga^{3+} $Ga(OH)^{2+}$	4.0×10^8 1.4×10^8 1.1×10^8	275	67.1 110.9 58.9	+30.1 +149.2 -	+5.0 +7.7 +6.2	-3.9	19
Fe^{3+} $Fe(OH)^{2+}$	1.0×10^8 1.5×10^8 1.2×10^8	750	64.0 - 42.4	+12.1 - +5.3	-5.4 +7.8 +7.0	2.9	20
Cr^{3+} $Cr(OH)^{2+}$	2.4×10^{-6} 1.4×10^{-6} 1.8×10^{-6}	75	108.6 145.9 110.0	+11.6 +10.7 +33.6	-9.6 -1.1 +2.7	4.1	21
Ru^{3+} $Ru(OH)^{2+}$	3.5×10^{-6} 1.1×10^{-6} 5.9×10^{-6}	170	89.8 135.9 95.8	-48.2 +100.5 +14.9	-6.3 -2.1 +0.9	2.7	22

*In order $K_{H_2O}(s^{-1})$, $K_{OH} \times K_a (m s^{-1})$, $K_{OH} (s^{-1})$.

For Ga³⁺, Fe³⁺, Cr³⁺ and the low spin Ru³⁺ in water, hydrolysis is kinetically important. The conjugate base is in equilibrium with the hexaaquion (equation 10), offering an alternative pathway for water exchange, which must be accounted for.



The overall observed rate constant will therefore be the sum of contributions from the two reaction paths, the water exchange on the hexaaqua species with rate constant k_{ex} and on its hydrolysed form with rate constant k_{ow} (equation 11).

$$k = k_{ex} + k_{ow} \cdot K_a / [\text{H}^+] \dots \dots \dots \quad (11)$$

Two main features are apparent from the rate constants and activation parameters reported in table 3.2: a high reactivity (by a factor 75 to 750) and a larger dissociative character (more positive activation volume) for the water exchange on the monohydroxypentaqua metal ions. This drastic mechanistic difference between both exchange pathways may be due to the strong electron donating capability of HO⁻. The strong bonding between the metal centre and this group probably containing both σ and π contributions will weaken the remaining M-OH₂ bonds, most probably the trans one. The complex thus becomes more labile and a dissociative activation mode is favoured.

3.3.2 Divalent cations.

The volumes of activation for divalent members of the first row transition metal series are illustrated in table 3.3.

Table 3.3 Volumes of activation ($\text{cm}^3 \text{ mol}^{-1}$) for solvent S exchange on MS_6^{2+} of the first row transition metal series by HMR.¹⁰

M^{2+}	V	Mn	Fe	Co	Ni	Cu
$r_A (\text{pm})$ O_6^-	79 t_{ox}^*	63 $\text{t}_{\text{ox}}^*\text{t}_{\text{ox}}^*$	78 $\text{t}_{\text{ox}}^*\text{O}_6^-$	74 $\text{t}_{\text{ox}}^*\text{O}_6^-$	69 $\text{t}_{\text{ox}}^*\text{O}_6^-$	73 $\text{t}_{\text{ox}}^*\text{O}_6^-$
S =						
H_2O	-4.1	-5.4	+3.8	+6.1	+7.2	
MeOH		-5.0	+0.4	+6.9	+11.4	
MeCN		-7.0	+3.0	+6.1	+8.5	
DMF			+6.5	+6.7	+9.1	
NH_3^*					+5.9	+8.3

*In 15M aqueous NH_3 .

It is apparent from the above table that the same gradual changeover occurs across the series, from the associatively activated V^{2+} to the dissociatively activated Ni^{2+} , at least in water, MeOH and MeCN. The small ΔV^* values for Fe^{2+} are indicative of an interchange mechanism with almost equal contribution from bond breaking and bond forming. Very recently Ru^{2+} has been studied with regard to water and acetonitrile exchange giving ΔV^* of $-0.4 \pm 0.7 \text{ cm}^3 \text{ mol}^{-1}$ (H₂O) and $+0.4 \pm 0.6 \text{ cm}^3 \text{ mol}^{-1}$ (MeCN) respectively.²² These values are indicative of an I mechanism on the basis that these values of ΔV^* are all well below the limiting value of $\pm 13.5 \text{ cm}^3 \text{ mol}^{-1}$ proposed by Swaddle for limiting A or D mechanisms. Herbach favoured an interchange mechanism (I_a, I or I_d) for each of the cations reported in table 3.3.

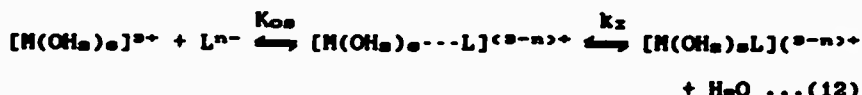
The use of the activation volume as the sole diagnosis for mechanisms has received some criticism²² particularly with regard to the neglect of bond length changes of the nonexchanging ligands although such criticisms have been strongly refuted by both Newman and Herbach²³ and Swaddle²⁴. Newman et al²⁵ have put forward theoretical models for the structure of the transition state for water exchange on hexaaqua divalent metal ions and has shown that the results are in accord with the volumes of activation obtained from the high-pressure NMR studies.

3.4 Formation of complexes from aqua ions.

The basic mechanism used to describe complex formation is that developed by Eigen and Wilkins.²⁷ They formulated this mechanism based on observations that the rates and activation parameters are generally similar for a given metal ion and that they are also similar to the kinetic parameters for water exchange at the same metal ion (especially for 2+ cations reacting with unidentate, uncharged ligands). These observation suggested a common dissociative mechanism. However much of the early work was based on observations with regard to reactions at octahedral Co(III) and Ni(II) which are now known to be primarily dissociative in nature. A mechanism involving only rate determining water loss would seem to be an over-

²²They restricted the application of bond energy calculation of Ca²⁺, Mn²⁺ and Zn²⁺ and showed that bond length changes in the nonreacting ligands going from octahedral to the transition-state were very small (maximum 2%).

simplification as the formation rates depend somewhat on both the nature and the concentration of the incoming ligand. They thus proposed the following sequence of reaction: a rapid equilibrium formation of an ion pair or outer sphere complex followed by the rate determining interchange step which can be associative or dissociative. For a hexaaqua trivalent metal ion we can write equation (12).



K_{as} is defined as the outer sphere association constant and k_2 is the rate constant for the outer sphere-inner sphere interchange reaction. The rate law for such a mechanism is :

$$\frac{d[\text{M}(\text{OH}_2)_6\text{L}]^{(2-n)+}}{dt} = \frac{K_{\text{as}} k_2 [\text{M}^{3+}][\text{L}^{n-}]}{(1 + K_{\text{as}} [\text{L}^{n-}])} \dots \dots \dots (13)$$

Under normal conditions K_{as} and the concentration of incoming ligand are small so equation (13) reduces to (14)

$$\frac{d[\text{M}(\text{OH}_2)_6\text{L}]^{(2-n)+}}{dt} = K_{\text{as}} k_2 [\text{M}^{3+}][\text{L}^{n-}] \dots \dots \dots (14)$$

The observed rate constant for complex formation, k_r , is given by $k_r = K_{\text{as}} \cdot k_2$. When the reaction rate and experimental conditions are favorable K_{as} can be measured and k_r separated into its components.⁴ However, for the vast majority of reactions K_{as} can only be estimated theoretically, usually using the electrostatic equation (15) derived by Fuoss.^{5a}

$$K_{os} = \left[\frac{4 \pi N a^3}{3000} \right] \cdot \exp \left[\frac{-z_m z_L e^2}{4 \pi a \epsilon_0 \epsilon k_B T} \right] \dots (15)$$

where N = Avogadro's number
 a = distance of closest approach between metal ion and the ligand (usually 4 - 5 Å)
 z_m and z_L = formal charges on the reacting species
 e = electronic charge
 ϵ_0 = vacuum permittivity
 ϵ = dielectric constant
 k_B = Boltzmann constant
 T = Temperature (K)

Values of K_{os} are often corrected for ionic strength I , using the Davis equation (16)** where $A = 0.5115$ for an aqueous solution at 298 K.**

$$\log f = - \left[\frac{A |z_m z_L| \sqrt{I}}{1 + \sqrt{I}} \right] + 0.1 |z_m z_L| I \dots (16)$$

Thus $K_{os} = K_{os} (\text{Fuoss}) \cdot f$. The agreement between theoretical and experimental values of K_{os} is however only fair, within two orders of magnitude*, since the estimation of K_{os} often involves uncertain and dubious assumptions, particularly for incoming groups of irregular geometry.*

The objective of the present work is to attempt to study the kinetics of oxalate anation on hexaaquaquaruthenium(II) and hexaaquaquaruthenium(III) ions. The results from these studies can then be compared with the recent water exchange studies carried out by Herbach et al.** These workers have reported variable-

Ch. 3: Subst'n reactions of octahedral complexes 208
pressure studies on both ions and found that solvent exchange on Ru²⁺ occurs via an interchange I mechanism ($\Delta V^\ddagger = -0.4$), on Ru³⁺ via an I_A mechanism ($\Delta V^\ddagger = -8.3$) and on the deprotonated species RuOH²⁺ via an I mechanism ($\Delta V^\ddagger = +0.9$).

In contrast to the wealth of information on low-spin ruthenium ammine complexes³¹⁻⁴, surprisingly few studies have dealt with the hexaaqua ions of ruthenium.³⁵⁻⁶ Most of the ammine studies have dealt with Ru(III) complexes in which only one ligand was replaced, the inert $[(\text{NH}_3)_5\text{RuX}]^{2+}$ ions (X=Cl, Br) being much studied. Information concerning the rates of slow substitution processes has often been obtained from combined electron-transfer and substitution studies. Studies by Kallen and Earley³⁵ showed that substitution by Cl⁻, Br⁻ and I⁻ on Ru(III) was catalyzed by the presence of Ru(II) due to rapid electron-transfer between the two ions. This type of catalysis was analogous to a similar observation on Cr(II)-Cr(III) systems.³⁶ They found that the reaction followed zero-order kinetics in Ru³⁺ for up to 60% of the absorbance changes and pseudo zero-order rate constants obeyed the rate law :

$$\frac{-d[\text{Ru}^{3+}]}{dt} = k_\infty [\text{Ru}^{3+}][\text{X}^-][\text{Ru}^{2+}]^0 \dots \dots \dots \dots \quad (17)$$

where $k_\infty = (6.5 \pm 0.2) \times 10^{-3} \text{ M}^{-1} \text{ s}^{-1}$, $(10.2 \pm 0.2) \times 10^{-3} \text{ M}^{-1} \text{ s}^{-1}$, and $(9.8 \pm 0.4) \times 10^{-3} \text{ M}^{-1} \text{ s}^{-1}$ for X⁻ = Cl⁻, Br⁻ and I⁻ respectively at 25°C and I=0.30M HBF₄. The rate of reaction was independent of [H⁺] in the range 0.112 to 0.292 M.

Activation enthalpies for all three reactions were within the narrow range $82.84 \pm 1.67 \text{ kJ mol}^{-1}$. The lack of significant variation of the ΔH^\ddagger with X^- implied that a common rate determining process was present which was predominantly dissociative. It was found that substitution on $[\text{Ru}(\text{OH}_2)_6]^{2+}$ was rate determining.

It has been generally concluded that Ru(III) complexes tended to react via an associative pathway and Ru(II) predominantly via a dissociative pathway.

The principle evidence in support of an associative mechanism on Ru(III) is:

- 1) A strong dependence of the rate constant upon the nature of the incoming group during the substitution on $[\text{Ru}(\text{EDTA})(\text{OH}_2)]^{2-}$.
- 2) Complete stereoretention in the substitution and base hydrolysis of chiral complexes.²⁴
- 3) Large negative volumes of activations in the aquation of $[\text{Ru}(\text{NH}_3)\text{Cl}]^{2+}$ and the anation of $[\text{Ru}(\text{NH}_3)(\text{OH}_2)]^{2+}$ (-30 and -20 $\text{cm}^3 \text{ mol}^{-1}$ respectively).²⁵

Recently Lay and Sasse²⁶ proposed that the initial step in the oxidation of water by the complexes $[\text{M}(\text{bpy})_3]^{2+}$ ($\text{M} = \text{Ru}, \text{Os}, \text{Fe}$) is the attack of H_2O on the M(III) centre to form a seven-coordinate intermediate.

In the case of Ru(II), evidence for the basis for a dissociative mechanism is based on:

- 1) For the complex $cis-[Ru(phen)_2(PY)_2]^{2+}$ the rate of substitution of PY by X^- (Cl^- , Br^- , I^- , NCS^- , Na^- , NO_2^-) was independent of the nature of X^- .²⁰
- 2) Rates and enthalpies of activation for the substitution of H_2O by Cl^- , Br^- and I^- in the $[Ru(OH_2)_6]^{2+}$ aqua ion were very similar²¹, indicating that the activation steps are identical for the different halides (i.e. dissociation of water).

The implication of the study by Kallen and Earley²² was that the water exchange rate constants for $[Ru(OH_2)_6]^{2+}$ should be $\sim 10^{-1} \text{ s}^{-1}$ and for $[Ru(OH_2)_5OH]^{2+}$ should be $\sim 10^{-6} \text{ s}^{-1}$. This was in fact confirmed by Herbach et al in their preliminary studies.²³ Their recently completed variable-pressure and variable-temperature studies²⁴ have given values for rate constants for water exchange on Ru^{2+} ($k_{w222}^{222} = (1.8 \pm 0.2) \times 10^{-1} \text{ s}^{-1}$) and on Ru^{3+} ($k_{w222}^{222} = (3.5 \pm 0.3) \times 10^{-6} \text{ s}^{-1}$) and on $RuOH^{2+}$ ($k_{w222}^{222} = (5.9 \pm 0.2) \times 10^{-4} \text{ s}^{-1}$).

It was hoped that detailed mechanistic information with regard to oxalate anation on these aqua ions would now be possible in the light of the water exchange data now available. Furthermore, studies with oxalate as incoming ligand were of interest in connection with studies already performed in this laboratory on $[Ir(OH_2)_6]^{2+}$ ²⁰ and $[Rh(OH_2)_6]^{2+}$ ²¹ which have similarly benefitted from knowledge of the water exchange rate. Here a common mechanism has been found having surprisingly little

Ch. 3: Subst'n reactions of octahedral complexes 211
dependence upon the metal ion. Extension of these studies to include Ru³⁺ and Ru²⁺ would seem highly appropriate at this time. The oxalate ligand has been widely employed as an incoming nucleophile with regard to elucidation of the mechanism of replacement of water on Ni²⁺, Co²⁺, Mo³⁺, Ti³⁺, and [M(NH₃)₆(OH₂)]²⁺ (M=Cr, Co, Ru)⁴⁺ as well as many other octahedrally coordinated metal ions.

Experimental proceduresGeneral details

Solutions of Htfms (Fluka Chemicals) and $K_2(C_2O_4)$ (Aldrich) were prepared from AnalR reagents. A sample of Na(tfms) was prepared by neutralizing NaOH with Htfms followed by evaporation and recrystallisation from a water-ethanol mixture.

Kinetic runs :

1) $[Ru(OH_2)_6]^{2+}$ study : Required amounts of Htfms, Na(tfms), $K_2(C_2O_4)$ and water were added to 1 cm quartz cells (final volume of solution = 3 cm³). The solution in each cell was deoxygenated by passing a slow stream of N_2/Ar through it (use being made of rubber seals, teflon tubing and stainless steel needles). After degassing for 30 minutes, each cell was sealed and thermostatted in the cell housing of the Perkin-Elmer lambda 5 UV-visible spectrophotometer. The required amounts of $[Ru(OH_2)_6]^{2+}$ were then added to the cells by means of a 0.5 cm³ Hamilton syringe. After addition of Ru²⁺, a small amount of "Evo-stick" glue was placed on the serum cap to seal the hole made by the syringe needle. Reactions were monitored at 445 nm for at least 5 hours and final absorbances (A_∞) were estimated using the Swinbourne method (see appendix 3). First-order equilibration constants were evaluated from plots of $\ln(A_\infty - A_t)$ vs t. A typical Absorbance vs time plot is shown in figure 3.4(a). The temperature of all runs was 25.0 ± 0.1 °C except for the temperature dependence study.

2) [Ru(OH₂)₆]³⁺ study : A similar procedure to the above was followed. In this study deoxygenation of solution was not required as solutions of [Ru(OH₂)₆]³⁺ were stable in air. Reactions were monitored at 325 nm and followed for at least 30 hours. A₀ again had to be estimated from Swinbourne analysis because further small absorbance changes were observed probably due to oxidation of Ru³⁺ to Ru⁴⁺ (see figure 3.4(b)). The temperature of all runs was 60.0 ± 0.1 °C except for the temperature dependence study.

In both studies the ionic strength was maintained at 1.00 ± 0.05 M using Htfms and Na(tfms). All data were treated using unweighted linear least-squares programs.

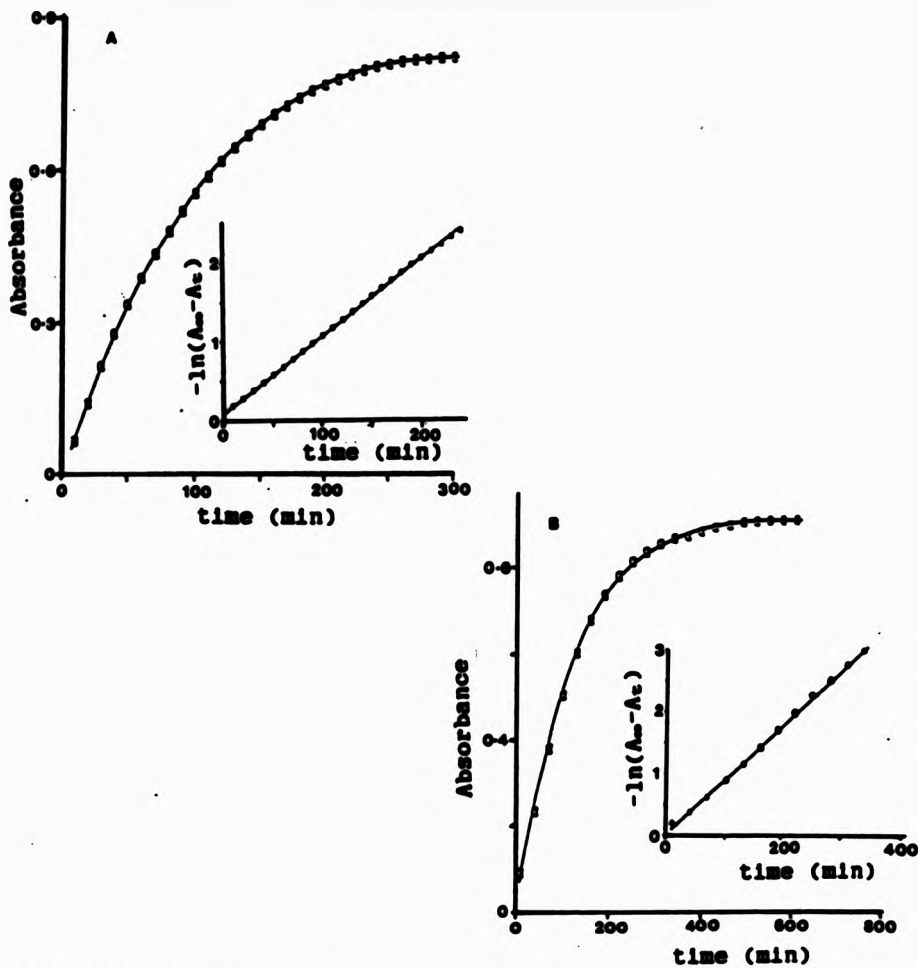


Figure 3.4 Plot of absorbance vs. time and $-\ln(A_\infty - A_t)$ vs. time (inset) for the reaction of: (a) $[\text{Ru}(\text{OH}_2)_6]^{3+}$ with oxalate ($\lambda = 445 \text{ nm}$, $T = 25^\circ\text{C}$, $[\text{H}^+] = 0.05\text{M}$); (b) $[\text{Ru}(\text{OH}_2)_6]^{3+}$ with oxalate ($\lambda = 325 \text{ nm}$, $T = 60^\circ\text{C}$, $[\text{H}^+] = 0.01\text{M}$). In both (a) and (b) $[\text{Ox}] = 0.01\text{M}$, $[\text{Ru}^{2+}] = [\text{Ru}^{3+}] = 0.001\text{M}$ and $I = 1.0\text{M NaCF}_3\text{SO}_3$.

3.5. Preparation of $[\text{Ru}(\text{OH}_2)_6]^{2+}$ and $[\text{Ru}(\text{OH}_2)_6]^{3+}$ in Htfms.

Hexaaquaruthenium(II) in Htfms was prepared by using a modification of the method described by Kallen and Earley²². The procedure has been described in detail in chapter 2 (section 2.14). The only change made here was that the aqua ion was eluted with 2 M Htfms instead of HBF₄. To obtain the hexaaquaruthenium(III) ion, the pink Ru(II) aqua ion was initially generated in 2 M HBF₄ by treating RuO₄ (in CCl₄) with Sn powder. Oxygen was then passed through the filtered pink solution for 2 hours whereupon the solution turned yellow. Dilution to 0.5 M H⁺ with distilled water and the usual ion-exchange purification yielded the $[\text{Ru}(\text{OH}_2)_6]^{3+}$ aqua ion. The final elution being done with Htfms (2 M). The concentration of both aqua ions was determined from their electronic spectra ($[\text{Ru}(\text{OH}_2)_6]^{2+}$: $\epsilon_{550} = 9 \text{ M}^{-1} \text{ cm}^{-1}$, $\epsilon_{360} = 10.8 \text{ M}^{-1} \text{ cm}^{-1}$; $[\text{Ru}(\text{OH}_2)_6]^{3+}$: $\epsilon_{550} = 30.4 \text{ M}^{-1} \text{ cm}^{-1}$).²² The background H⁺ concentration for both aqua ions was determined by loading a small sample of the aqua ion onto a Dowex 50W-X8 cation-exchange column and titrating the liberated H⁺ with 0.1 M NaOH.

3.6 Oxalate anation of the hexaaquaruthenium(II) ion.

This study was conducted with oxalate in 10 fold excess over the $[\text{Ru}(\text{OH}_2)_6]^{2+}$ concentration. The variations of anation rate with oxalate and hydrogen ion concentration and also with temperature were studied.

3.6.1 Dependence on oxalate concentration.

Initially this study was attempted with $[\text{Ru}(\text{OH}_2)_6]^{2+}$ ion in 10 fold excess over oxalate concentration but absorbance changes were very small and it was not possible to get meaningful data. The dependence was then investigated with a fixed ratio of 10:1 (i.e. $10[\text{Ox}]:[\text{Ru}^{2+}]$). The oxalate concentration was varied from 5×10^{-3} M to 2×10^{-2} M. The H^+ concentration was kept at 0.1 M.

3.6.2 Dependence on hydrogen ion concentration.

The H^+ dependence was investigated by repeating the oxalate dependence study at 0.04, 0.07, 0.1, 0.13, 0.15, and 0.20 M H^+ . The temperature was maintained at 25°C for all runs.

3.6.3 Temperature dependence.

At a constant $[\text{Ox}]:[\text{Ru}^{2+}]$ ratio of 10:1, the oxalate dependence study was repeated at 20°, 30°, 35°, 40° and 45°C in order to estimate the activation parameters for the substitution process.

3.7 Oxalate anation on the hexaaquaaruthenium(III) ion.

A similar procedure was used as in the case of the Ru^{2+} study with oxalate investigated at a fixed ratio 10:1 over Ru^{2+} . The main difference being the much higher temperature ($\geq 60^\circ\text{C}$) required. For the oxalate dependence the total oxalate concentration was varied between 4×10^{-3} and 1.2×10^{-2} M. For the acid dependence the H^+ concentration was varied between 0.04 and 0.3 M. Both of these studies were performed at 60°C.

The temperature dependence was investigated, as a function of the H⁺ concentration at 75°, 80° and 90°C and as a function of total oxalate concentration at 70°, 75° and 85°C.

3.8 Attempted study of the thiocyanate anation of hexaaqua-
ruthenium(II).

In an attempt to study the kinetics of NCS⁻ anation on [Ru(OH₂)₆]²⁺ the following solution mixture was prepared in a 1 cm quartz cell and deoxygenated prior to the addition of Ru²⁺.

$$\begin{aligned} [\text{Ru}^{2+}] &= 1.0 \times 10^{-3} \\ [\text{NCS}^-] &= 1.0 \times 10^{-2} \\ [\text{H}^+] &= 0.1 \text{ M} \\ I &= 1.0 \text{ M Na(tfms)} \end{aligned}$$

The cell was sealed with a serum cap and the electronic spectrum was monitored at 25°C over the range 200-900 nm. Although large absorbance changes were observed in the region 350-600 nm, the absorbance continued to increase over a period of 8-10 hours in what appeared to be a multistep process. Eventually a brown precipitate was produced from an orange-brown solution. Therefore it was not possible to obtain meaningful kinetic data from these results.

3.9 Attempted study of the thiourea anation of hexaaqua-
ruthenium(II).

Initially, the same conditions of concentration as in the above NCS⁻ study were used but this gave rise to very slow continuous absorbance changes so the concentration of SC(NH₂)₂ (abbreviated to tu) was increased to give a 50 fold excess.

Again there was a slow continuous absorbance change which eventually deposited orange crystals in the cell. A survey of the literature showed that a thiourea compound of Ru(II) had not been reported. Therefore our efforts focused on obtaining suitable crystals of this compound for X-ray analysis. The preparation was repeated on a larger scale. The analysis on the compound is given in the results and discussion section.

RESULTS AND DISCUSSION

3.10 Oxalate anation of hexaqua Ruthenium(II) trifluoromethane-sulphonate.

3.10.1 Dependence on Ru(II)

With total oxalate concentration in \approx 10 fold excess, the kinetics of this reaction were found to be pseudo first order in Ru(II) (1).

3.10.2 Dependence on total oxalate concentration

The dependence of the anation rate constant on free oxalate concentration was investigated in a series of runs at a fixed ratio of $[Ox]_T : [Ru^{2+}]$ of 10:1. The total oxalate concentration was varied from 5×10^{-3} M to 2×10^{-2} M in each case. At higher oxalate concentrations, extensive biphasing was observed in the absorbance vs time plots, indicating that other competing reactions possibly involving rate determining substitution of a second oxalate ligand were involved. For this reason all runs were done in the above specified range.

Under these conditions a first-order dependence of k_{obs} on the total oxalate concentration was found passing through an intercept. The intercept suggested that equilibrium kinetics were in operation. Results for the six temperatures 20°, 25°, 30°,

35°, 40°, and 45°C are shown in table 3.4 and illustrated graphically in figure 3.5.

Table 3.4 Pseudo first-order rate constants for reaction of the $[\text{Ru}(\text{Ox})_6]^{2+}$ ion with oxalate at 20°, 25°, 30°, 35°, 40° and 45°C. $[\text{H}^+] = 0.1\text{M}$, I = 1M (NaCF_3SO_3).

$[\text{Ox}]_0$ M	Temperature °C	$10^4 k_{\text{obs}}$ s^{-1}	$[\text{Ox}]_0$ M	Temperature °C	$10^4 k_{\text{obs}}$ s^{-1}
0.005 0.006 0.007 0.008 0.010 0.012 0.015 0.020	20	0.63	0.004	35	3.33
		0.67	0.005		3.45
		0.70	0.006		4.13
		0.87	0.007		4.42
		1.13	0.010		5.55
		1.33	0.012		6.50
		1.40	0.016		8.58
		2.00	0.020		10.67
0.005 0.006 0.010 0.012 0.014 0.016 0.018 0.020	25°	1.42	0.003	40	5.00
		1.63	0.005		6.04
		2.00	0.006		7.00
		2.17	0.007		7.42
		2.25	0.010		9.81
		2.50	0.012		11.60
		2.83	0.015		14.72
		3.17	0.020		17.54
0.003 0.004 0.005 0.006 0.007 0.008 0.010 0.012 0.015 0.020	30	1.67	0.003	45	10.13
		1.88	0.004		12.00
		2.08	0.005		13.72
		2.42	0.006		15.73
		2.68	0.007		17.70
		2.80			
		3.42			
		3.52			

*Values at 25°C were determined in duplicate. The estimated error on all values is ±5%.

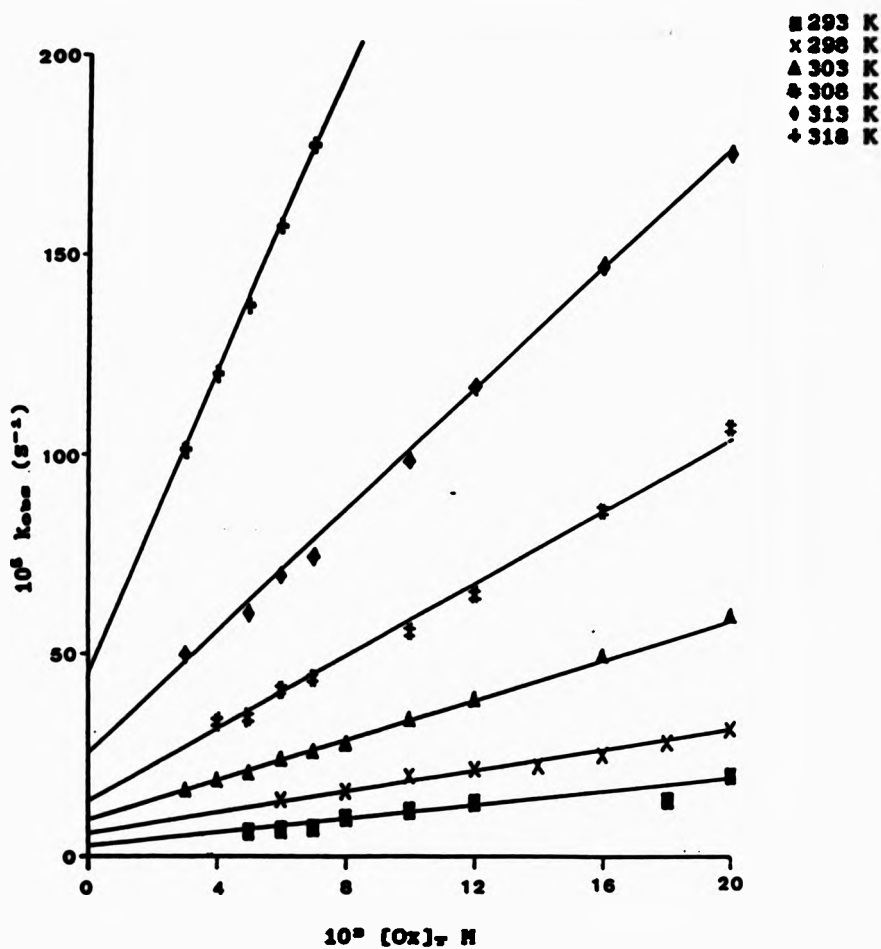


Figure 3.5 Observed rate constants vs $[Ox]_T$ as a function of temperature at $I=1.0\text{M NaClO}_4$, $[\text{H}^+]=0.1\text{M}$ for the reaction of $[\text{Ru}(\text{OH}_2)_6]^{2+}$ with oxalate.

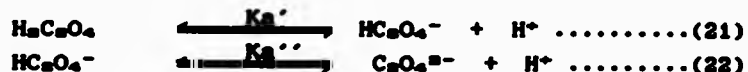
A second order rate expression (19) can be applied for the overall anation reaction:

$$\frac{-d[Ru^{2+}]}{dt} = k_p[Ru^{2+}][Ox]_T + k_a[Ru^{2+}] \quad \dots \dots \dots (19)$$

where k_{obs} (eq 18) = $k_p[\text{Ox}]_v + k_{\text{de}}$ (20)

3.10.3 Dependence on hydrogen ion concentration

Oxalic acid undergoes two successive proton dissociations (21) and (22) with respective acid dissociation constants K_a' and K_a'' .



(for K_a' $\Delta H^\circ = -15.76 \pm 0.47$ kJ mol $^{-1}$ and $\Delta S^\circ = -318.30 \pm 1.40$ J K $^{-1}$ mol $^{-1}$ and for K_a'' $\Delta H^\circ = -6.03 \pm 0.04$ kJ mol $^{-1}$ and $\Delta S^\circ = -333.20 \pm 0.10$ J K $^{-1}$ mol $^{-1}$ calculated from previously reported data at ionic strength 1.0M).***

Under the conditions used in this study (0.04M to 0.20M H⁺), amounts of the dianion, C₂O₄²⁻, may be neglected and the total oxalate concentration may be represented as comprising of oxalic acid and its monodeprotonated form (23) :

The H⁺ concentration was thus varied in order to establish whether MnC₂O₄ or HC₂O₄⁻ or indeed both species were involved as reactants with Ru²⁺. The K_{obs} values obtained as a function

of $[H^+]$ are listed in table 3.5 and graphically illustrated in figure 3.6.

Table 3.5 Observed rate constants for the reaction of
 $[Ru(OH_6)_6]^{2+}$ ion with oxalate at 25°C I=1.0M Na(CF₃SO₃)

$[Ox]_r$ M	$[H^+]$ M	$10^4 k_{obs}$ s^{-1}	$[Ox]_r$ M	$[H^+]$ M	$10^4 k_{obs}$ s^{-1}
0.004	0.04	0.83	0.006	0.13	1.25
0.006		1.13	0.008		1.58
0.008		1.58	0.010		1.82
0.010		1.90	0.012		2.00
0.012		2.17	0.013		2.12
0.014		2.67	0.014		2.22
0.016		2.82	0.016		2.50
0.018		3.30	0.020		3.00
0.020		3.73			
0.004	0.07	1.00	0.006	0.15	1.30
0.006		1.17	0.010		1.75
0.008		1.50	0.013		2.03
0.010		1.63	0.016		2.30
0.012		2.17	0.020		2.78
0.015		2.88			
0.020		3.50			
0.025		4.17			
0.030		5.08			
0.004	0.10 ^a	1.07	0.004	0.20	1.17
0.006		1.25	0.010		1.63
0.008		1.58	0.015		1.97
0.010		1.78	0.020		2.45
0.013		2.22	0.030		3.33
0.016		2.62			

^aValues determined in duplicate. Estimated error in k_{obs} is $\pm 5\%$.

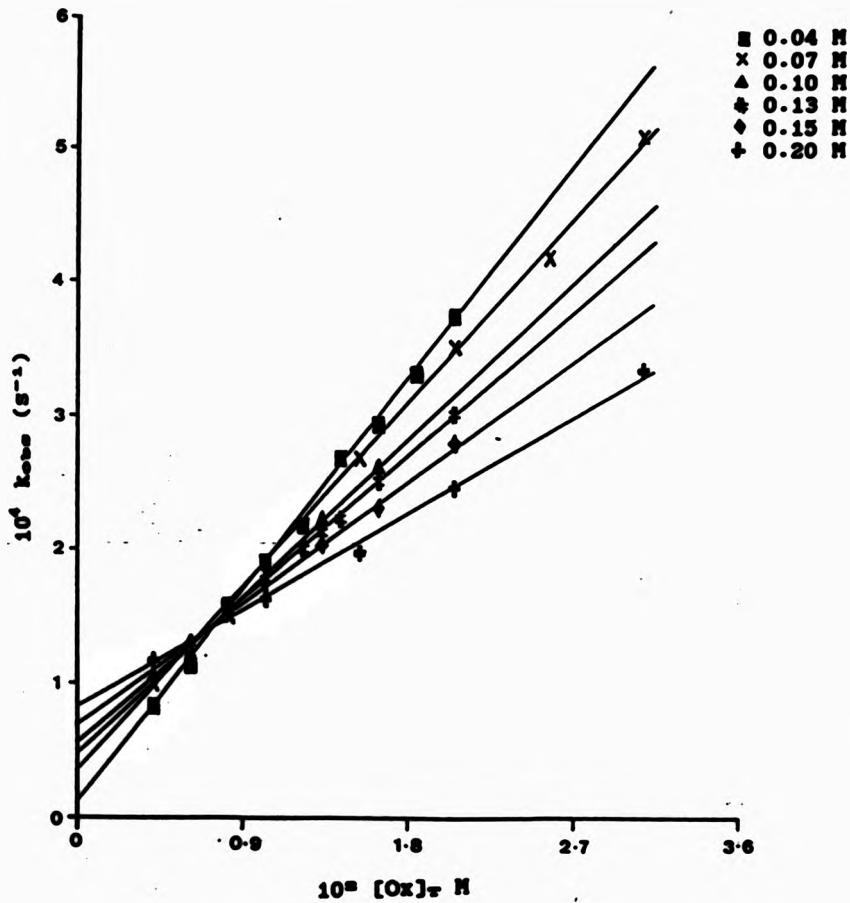


Figure 3.6 Observed rate constants vs $[Ox]_T$ as a function of $[H^+]$ at $I=1.0\text{M}$ NaCF_3SO_3 and $T=25^\circ\text{C}$ for the reaction of $[\text{Ru(OH}_2)_6]^{n+}$ with oxalate.

The observed full rate law was thus found to be of the form :

$$\frac{-d[Ru^{**}]}{dt} = \frac{k_r K_a' [Ox]_r [Ru^{**}]}{[H^+] + K_a'} + k_b [Ru^{**}] [H^+] \dots \dots \dots (24)$$

$$= k_{obs} [Ru(OH_2)_6]^{**} \dots \dots \dots \dots \dots \dots \dots \dots (25)$$

$$\text{where } k_{obs} = \frac{k_r K_a' [Ox]_r}{[H^+] + K_a'} + k_b [H^+] \dots \dots \dots \dots \dots \dots \dots \dots (26)$$

consistent with $HC_6O_4^-$ as the dominant anating reactant. The full derivation of this rate law is given in appendix 3. An involvement primarily from $HC_6O_4^-$ would seem likely on the basis of electrostatics and nucleophilicity. Similar involvement of the monodeprotonated form has been previously observed with the oxalate anation of $[Mo_2(OH_2)_6]^{4+}$, $[Mo(OH_2)_6]^{3+}$ and $[Fe(OH_2)_6]^{3+}$.

According to equation (26) a plot of (1/slope from fig. 3.6) vs $[H^+]$ should give a straight line with slope = $1/k_r K_a'$ and intercept $1/k_p$; the ratio of the slope to intercept being a kinetic estimate of K_a' . A plot of intercept from fig. 3.6 vs $[H^+]$ should be a straight line passing through the origin. Such plots are shown in figure 3.7 and 3.7(inset) and the value for K_a' so determined (0.08 M) is in good agreement with the value of 0.084 M (25°C I = 1.0 M) reported by Moorhead and Sutin. From this treatment k_p and k_b at 298 K were found to be $2.60 \times 10^{-8} M^{-1} s^{-1}$ and $7.12 \times 10^{-4} M^{-1} s^{-1}$ respectively.

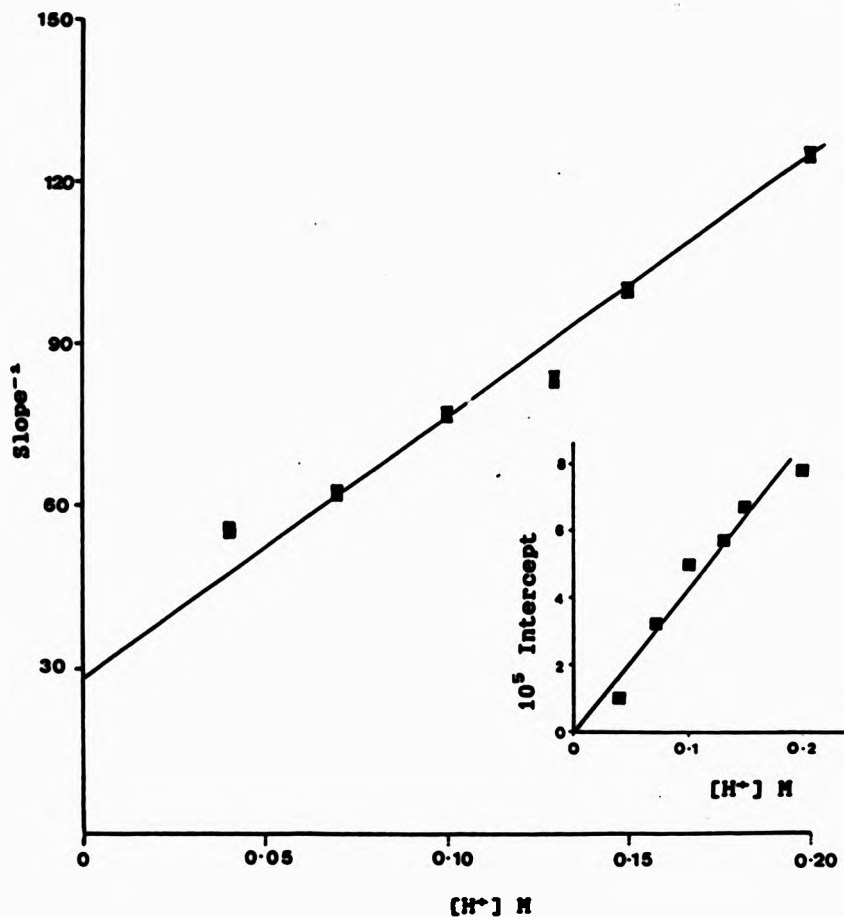


Figure 3.7 Plot of $1/\text{slope}$ from fig. 3.6 vs $[H^+]$ at $I=1.0\text{M}$ NaCF_3SO_3 and $T=25^\circ\text{C}$ for the reaction of $[\text{Ru}(\text{OH}_2)_6]^{2+}$ with oxalate. Inset: Intercept from fig. 3.6 vs $[H^+]$

From the temperature dependence study on k_{obs} at $H^+ = 0.1\text{ M}$ and $I = 1.0\text{M}$ NaCF_3SO_3 (figure 3.5) it is possible to obtain the values of k_f and k_b by substituting known values for K_a' at the various temperatures from equation (28). These values were then computed into the Eyring equation (8) to yield the activation parameters ΔH^\ddagger and ΔS^\ddagger for the forward and back reactions.

Table 3.6 gives the values for k_f and k_b at the different temperatures and figure 3.6 shows the resulting Eyring plot, the least squares analysis of which gave values of $\Delta H^\ddagger = 101.07 \pm 6.37\text{ kJ mol}^{-1}$ and $\Delta S^\ddagger = 65.1 \pm 20.9\text{ J K}^{-1}\text{ mol}^{-1}$ for the forward reaction and $\Delta H^\ddagger = 77.29 \pm 7.45\text{ kJ mol}^{-1}$ and $\Delta S^\ddagger = -48.5 \pm 24.4$ for the backward reaction.

Table 3.6 k_f and k_b as a function of temperature for the oxalate anation of $[\text{Ru}(\text{OH}_2)_6]^{2+}$ at $H^+ = 0.1\text{M}$ and $I = 1\text{M}$

NaCF_3SO_3

Temperature K	$10^6 k_f \text{ M}^{-1} \text{ s}^{-1}$	$10^6 k_b \text{ M}^{-1} \text{ s}^{-1}$
293	1.80	2.66
296	2.60	7.12
303	6.00	8.41
308	11.30	12.23
313	19.60	24.07
318	51.00	43.90

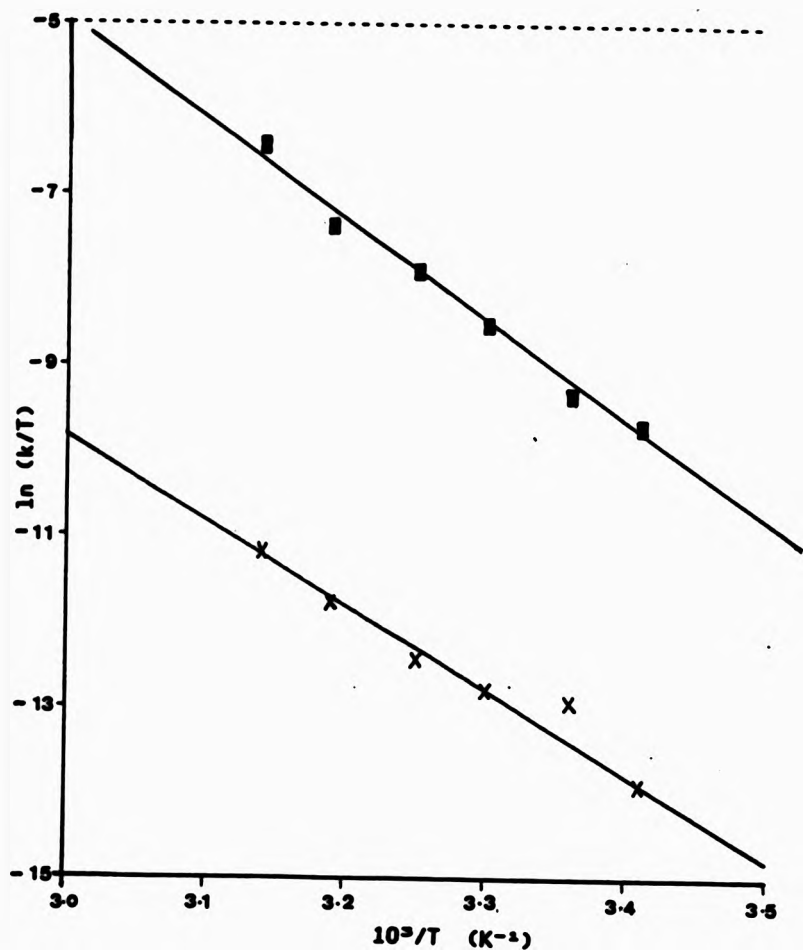


Figure 3.6 Eyring plot of oxalate anion on $[Ru(OH_2)_6]^{2+}$ at $I=1.0\text{ M NaCF}_3SO_3$. k_T (—●—) and k_a (x x x).

3.11 Oxalate anation of hexaqua[ruthenium(III)] trifluoromethanesulphonate.

3.9.1 Dependence on Ru(III)

With total oxalate concentration in ≈ 10 fold excess, the kinetics of this reaction were found to be pseudo first-order in Ru(III) (27).

$$-\frac{d[Ru^{3+}]}{dt} = k_{obs} [Ru^{3+}] \dots \dots \dots (27)$$

Values of k_{obs} were again estimated from the slopes of $\ln(A_\infty - A_t)$ vs time plots which were found to be linear over 3 half-lives (figure 3.4(b)). A_∞ values were estimated from the Swinbourne method as evidence was found for a much slower absorbance rise following initial exponential rise at 325 nm probably corresponding to some oxidation of Ru^{3+} to Ru^{4+} .

3.11.2 Dependence on the total oxalate concentration

The dependence of the anation rate constant k_{obs} on free oxalate concentration was investigated in a series of runs at a fixed ratio of $[Ox]_T:[Ru^{3+}]$ of 10:1. The total oxalate concentration was varied from 4×10^{-4} M to 1.2×10^{-3} M. Under these conditions a simple linear first-order dependence of k_{obs} on $[Ox]_T$ was found passing through the origin. A_∞ changes were found to be proportional to $[Ru^{3+}]$ and essentially

independent of $[Ox]_r$ (figure 3.9). Results for the four temperature are given in table 3.7 and graphically illustrated in figure 3.10.

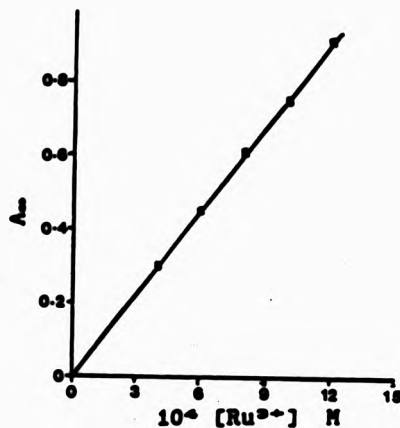


Figure 3.9 Plot of A_m vs $[Ru^{3+}]$ at $25^\circ C$ and $I=1.0M$ $NaCF_3SO_3$,

Table 3.7 Pseudo first-order rate constants for reaction of the $[Ru(OH_3)_6]^{3+}$ ion with oxalate at 60° , 70° , 75° , and $85^\circ C$. $I=1.0$ M $NaCF_3SO_3$ and $H^+=0.06$ M

$[Ox]_r$ M	Temperature $^\circ C$	$10^4 k_{obs}$ s^{-1}	$[Ox]_r$ M	Temperature $^\circ C$	$10^4 k_{obs}$ s^{-1}
0.004	60	0.15	0.004	75	0.80
		0.23	0.006		1.24
		0.32	0.008		1.65
		0.40	0.010		2.10
		0.48	0.012		2.55
0.004	70	0.40	0.004	85	1.49
		0.67	0.006		2.40
		0.83	0.008		3.10
		1.13	0.010		3.83
		1.33	0.012		4.65

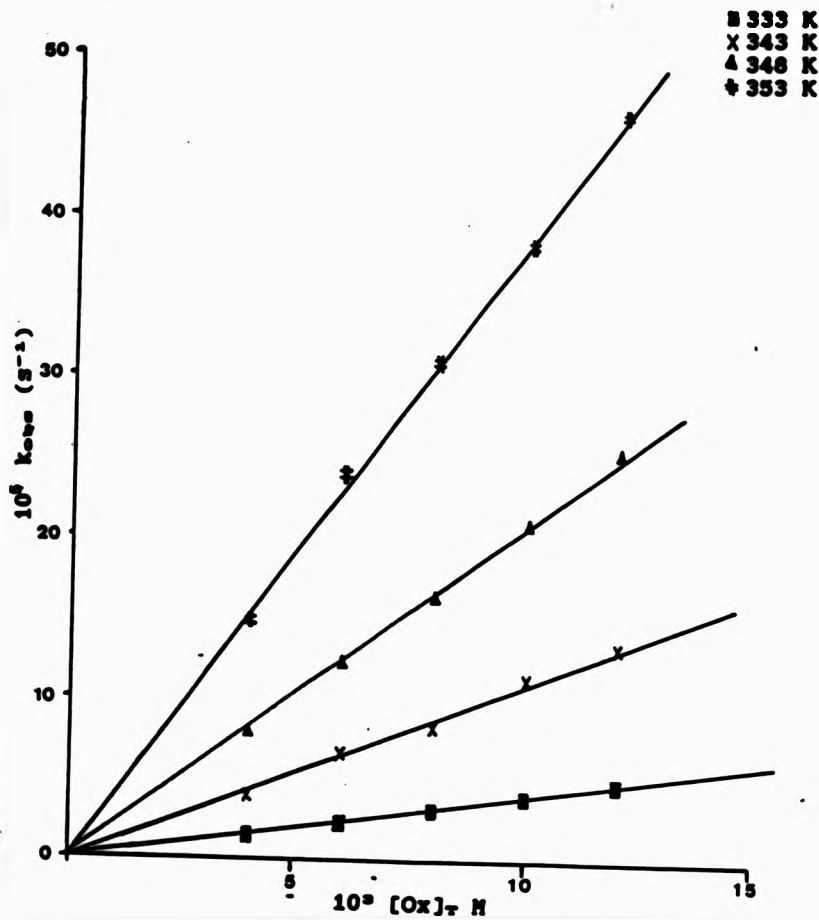


Figure 3.10 Observed rate constants vs $[Ox]_r$ as a function of temperature at $[H^+] = 0.05M$ and $I = 1.0M$ $NaCF_3SO_3$ for the reaction of $[Ru(OH_6)_6]^{2+}$ with oxalate.

A simple 2nd order rate expression (28) thus applies for the overall anation reaction :

$$\frac{-d[Ru^{3+}]}{dt} = k_{an} [Ru^{3+}][Ox]_r \dots\dots\dots\dots\dots (28)$$

$$\text{where } k_{an} = k_{an} [Ox]_r \dots\dots\dots\dots\dots (29)$$

3.11.3 Dependence on hydrogen ion concentration

As with the Ru(II) study, the acid concentration used (0.04 to 0.3 M) is such that the involvement of the dianion of oxalic acid ($C_2O_4^{2-}$) may be neglected and the total oxalate concentration may be represented as comprising only of oxalic acid and its monodeprotonated form. The H⁺ concentration was thus varied in order to establish whether $H_2C_2O_4$ or $HC_2O_4^-$ or indeed both species were involved as reactants with Ru³⁺. The results are obtained are listed in table 3.8 and graphically illustrated in figure 3.11.

These results shows that k_{an} decreases as the acidity is increased, implying that the monodeprotonated form ($HC_2O_4^-$) is either the dominant reactant or reacts at a much faster rate than the free acid. The involvement of the conjugate base $[Ru(OH_6)_5(OH)]^{2+}$ is also likely as it plays a dominant role in water exchange.²²

**Table 3.8 Observed rate constants for reaction of the
[Ru(OH₂)₅]²⁺ ion with oxalate at 60°C and I=1M NaCF₃SO₃.**

[Ox] _r M	[H ⁺] M	10 ⁶ k _{obs} s ⁻¹	[Ox] _r M	[H ⁺] M	10 ⁶ k _{obs} s ⁻¹
0.004	0.03	2.00	0.004	0.08	1.33
0.006		3.00	0.006		1.83
0.008		4.00	0.008		2.83
0.012		6.33	0.010		3.67
			0.012		4.17
0.004	0.04	1.83	0.004	0.13	0.83
0.006		2.67	0.006		1.33
0.008		3.83	0.008		1.77
0.010		4.67	0.010		2.33
0.012		5.67	0.012		2.80
0.004	0.06	1.50	0.004	0.15	0.73
0.006		2.33	0.006		1.12
0.008		3.17	0.008		1.50
0.010		4.00	0.010		2.00
0.012		4.83	0.012		2.33

The acid dependence was thus fitted to rate laws which accounted for the involvement or exclusion of the different species. The first of these was the one found for the Ru(II) oxalate anation reaction (ie consideration of the monodeprotonated form of oxalic acid as the sole reactant). However, the subsequent plot of (1/slope from fig. 3.11) vs [H⁺] (shown in figure 3.12) was found to be notably curved and it quickly became clear that the rate law was of a much more complicated form than in the Ru(II) oxalate anation study.

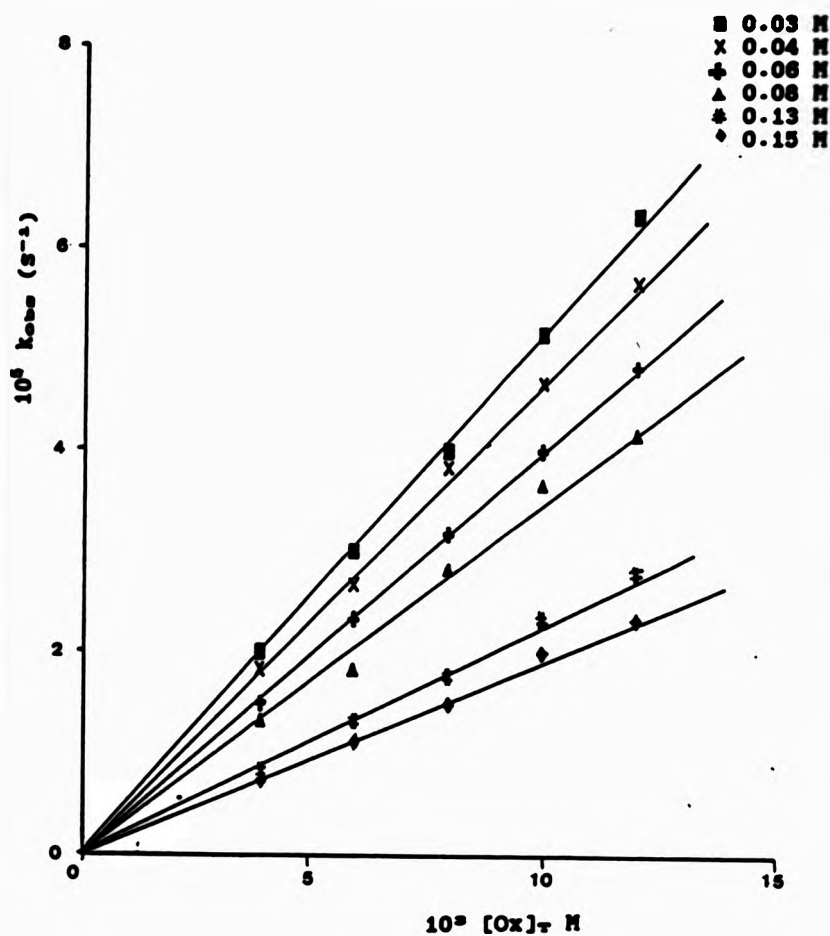


Figure 3.11 Observed rate constants vs $[Ox]_T$ as a function of $[H^+]$ at $T=60^\circ\text{C}$ and $I=1.0\text{M NaCF}_3\text{SO}_4$ for the reaction of $[\text{Ru(OH}_2]^{2+}$ with oxalate.

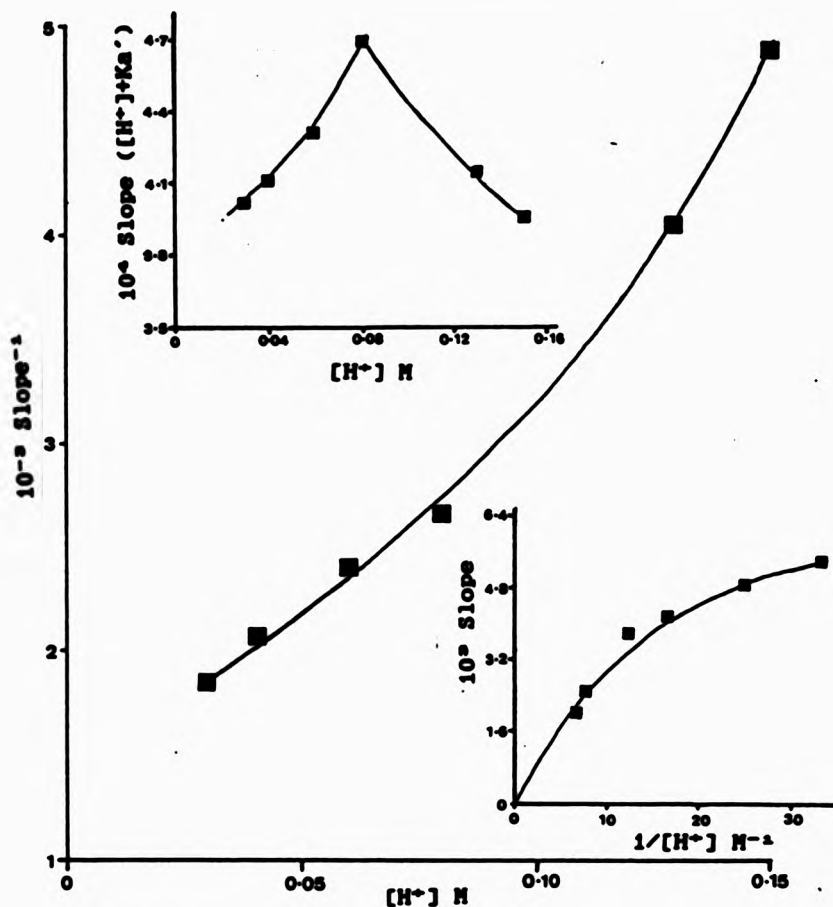


Figure 3.12 Plot of $1/\text{slope}$ from fig. 3.11 vs $[\text{H}^+]$ at $T=60^\circ\text{C}$ and $I=1.0\text{M}$ $\text{NaClF}_3\text{SO}_4$ for the reaction of $[\text{Ru}(\text{OH}_2)_6]^{2+}$ with oxalate. Insets: Slope from fig. 3.11 vs $1/[\text{H}^+]$ (bottom) and slope from fig. 3.11 x $([\text{H}^+]+\text{K}_a')$ vs $[\text{H}^+]$ (top).

The second fit involved the assumption that $K_a' \ll [H^+]$ such that $[H^+] + K_a' = [H^+]$, giving rise to the simple $1/[H^+]$ dependence (30)

$$\frac{-d[Ru^{3+}]}{dt} = \frac{k_2 K_a' [Ru^{3+}] [\text{Ox}]_\tau}{[H^+]} \dots \dots \dots (30)$$

A plot of slope from figure 3.11 vs $1/[H^+]$ is shown in figure 3.12(inset). The curved nature of this plot reveals that again this fit does not apply. This was not unexpected since the assumption used above in deriving equation (30) is probably not valid in the range of $[H^+]$ used.

Another fit tried involves the participation of oxalic acid $H_2C_2O_4$ thus adding another term to the overall rate law so far discussed (31).

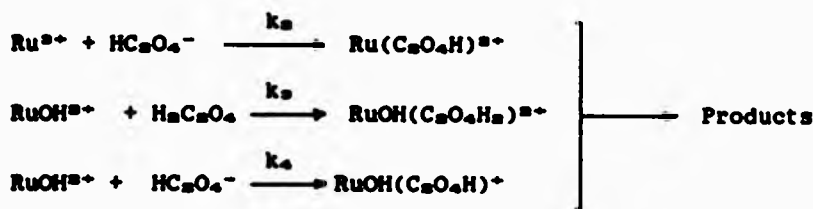
$$\frac{-d[Ru^{3+}]}{dt} = \frac{k_1 [H^+] [\text{Ox}]_\tau [Ru^{3+}]}{[H^+] + K_a'} + \frac{k_2 K_a' [\text{Ox}]_\tau [Ru^{3+}]}{[H^+] + K_a'} \dots \dots \dots (31)$$

This type of rate law has been observed in similar oxalate anation studies on $[\text{Ir}(\text{OH}_2)_6]^{3+}$ and $[\text{Rh}(\text{OH}_2)_6]^{3+}$ aqua ions.⁴⁰⁻⁴¹ A plot of $k_{obs} ([H^+] + K_a') / [\text{Ox}]_\tau$ vs should give a straight line with slope k_1 and intercept $k_2 K_a'$. This plot is shown in figure 3.12(top inset) and is notably curved thus ruling out a pathway involving $H_2C_2O_4$ and Ru^{3+} . This was a major finding in relation to the previous studies on Rh^{3+} and Ir^{3+} .

Finally a fit was attempted which involved the participation of the conjugate base $[\text{Ru}(\text{OH}_2)\text{OH}]^{2+}$ ($\text{pK}_a = 2.73^{**}$ at 298 K)*. The resulting rate law is then of the form :

$$\frac{-d[\text{Ru}^{3+}]}{dt} = \frac{k_a k_{a'} [\text{Ox}]_T [\text{Ru}^{3+}]}{([\text{H}^+] + K_{a'})} + \frac{k_a K_{au} [\text{H}^+] [\text{Ox}]_T [\text{Ru}^{3+}]}{([\text{H}^+] + K_{a'})([\text{H}^+] + K_{au})} \\ + \frac{k_a K_{au} k_a' [\text{Ox}]_T [\text{Ru}^{3+}]}{([\text{H}^+] + K_{a'})([\text{H}^+] + K_{au})} \dots \dots \dots \quad (32)$$

where k_a , $k_{a'}$, and k_a' are rate constants for the pathways involving $[\text{H}_2\text{C}_6\text{O}_4]$ and $[\text{HC}_6\text{O}_4^-]$ with Ru^{3+} and its conjugate base respectively. The rate law is derived from the following scheme :



$K_{a'}$ and K_{au} are defined as:

$$K_{a'} = \frac{[\text{HC}_6\text{O}_4^-][\text{H}^+]}{[\text{H}_2\text{C}_6\text{O}_4]} \quad K_{au} = \frac{[\text{RuOH}^{2+}][\text{H}^+]}{[\text{Ru}^{3+}]} \dots \dots \dots \quad (33)$$

Obtained from variable-temperature spectrophotometric studies which also gave the following values for the activation parameters: $\Delta H_{\text{Au}}^{} = 41.1 \pm 1.9 \text{ kJ mol}^{-1}$, $\Delta S_{\text{Au}}^{*} = 85.6 \pm 6.4 \text{ J K}^{-1} \text{ mol}^{-1}$. **

In the acid range used in this study



therefore

$$\begin{aligned} \frac{k_{\text{obs}}}{[\text{Ox}]_T} &= \frac{k_a k_a'}{([\text{H}^+] + k_a')} + \frac{k_a k_{\text{Ru}} [\text{H}^+]}{([\text{H}^+] + k_a') ([\text{H}^+] + k_{\text{Ru}})} \\ &+ \frac{k_a k_{\text{Ru}} k_a'}{([\text{H}^+] + k_a') ([\text{H}^+] + k_{\text{Ru}})} \end{aligned} \quad (35)$$

Rearranging equation (35) gives equation (36)

$$\begin{aligned} \frac{k_{\text{obs}}([\text{H}^+] + k_a') ([\text{H}^+] + k_{\text{Ru}})}{[\text{Ox}]_T} &= k_a k_a' ([\text{H}^+] + k_{\text{Ru}}) + k_a k_{\text{Ru}} [\text{H}^+] + k_a k_{\text{Ru}} k_a' \\ &= (k_a k_a' + k_a k_{\text{Ru}}) [\text{H}^+] + k_{\text{Ru}} k_a' (k_a + k_a') \end{aligned} \quad (36)$$

Therefore a plot of $k_{\text{obs}}([\text{H}^+] + k_a') ([\text{H}^+] + k_{\text{Ru}})/[\text{Ox}]_T$ vs $[\text{H}^+]$ should be a straight line with slope $(k_a k_a' + k_a k_{\text{Ru}})$ and intercept, $k_{\text{Ru}} k_a' (k_a + k_a')$. This is indeed observed (figure 3.13) and verifies the derived rate expression. The values are listed in table 3.9.

Involvement of the k_s term involving $\text{H}_2\text{C}_2\text{O}_4$ with Ru^{3+} would have given rise to a quadratic term in $[\text{H}^+]$ on the right hand side of equation (36) and this is not consistent with the linear plot of figure 3.13.

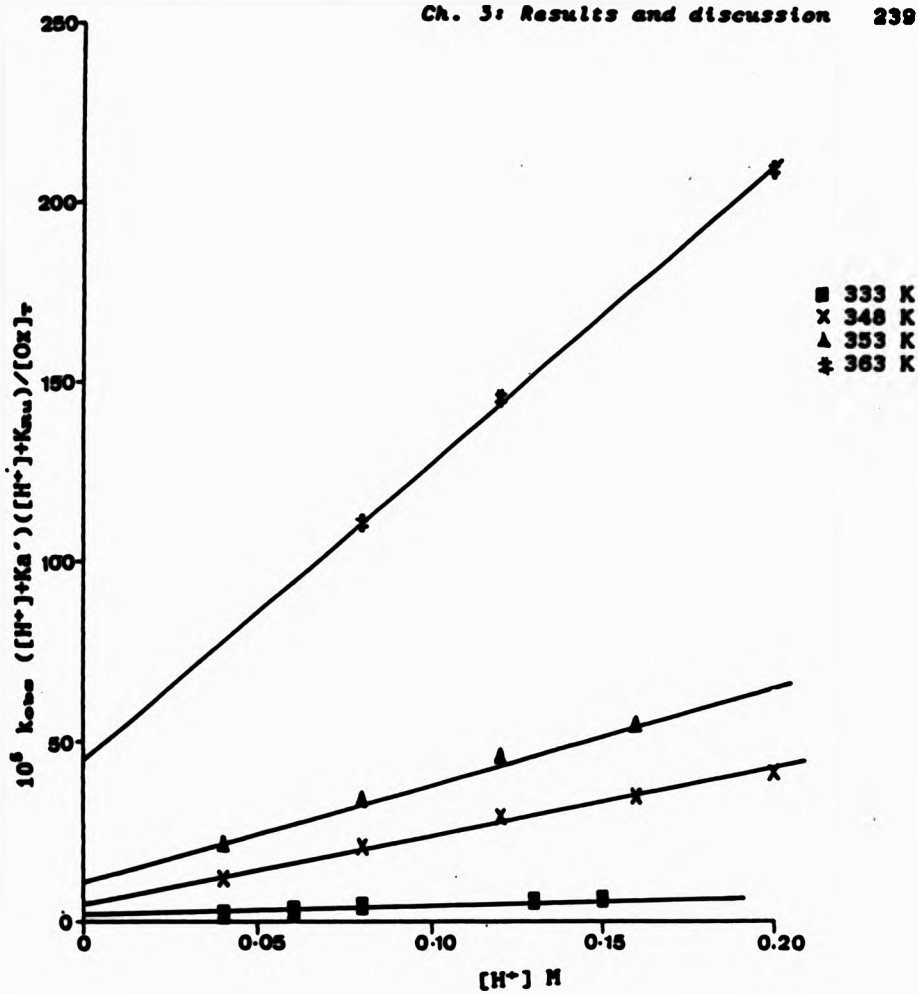


Figure 3.13 Plot of $k_{obs}([H^+] + K_{a'})([H^+] + K_{au})/[Ox]_T$ vs $[H^+]$ as a function of temperature I=1.0M NaCF₃SO₃ for the reaction of $[\text{Ru}(\text{OH}_2)_6]^{2+}$ with oxalate.

Table 3.9 Observed rate constants as a function of $[H^+]$ at 60°**75°, 80° and 90°C . $[Ox]_T = 0.01M$. I = 1 M NaCl₂SO₄.**

$10^6 k_{obs}$ s^{-1}	Temperature °C	$[H^+]$ M	$10^6 X^*$	K_a' M	K_{obs} M
4.67	60	0.04	2.10	0.048	0.011
4.00		0.06	3.07		
3.67		0.08	4.28		
2.33		0.13	5.85		
2.00		0.15	6.36		
25.33	75	0.04	12.01	0.039	0.020
17.33		0.06	20.62		
13.00		0.12	26.94		
9.67		0.16	34.64		
7.63		0.20	41.17		
43.67	80	0.04	21.86	0.037	0.025
27.67		0.06	33.99		
20.17		0.12	45.92		
15.00		0.16	54.67		
84.17	90	0.06	110.82	0.033	0.036
60.63		0.12	145.19		
38.00		0.20	206.95		

$$* X = K_{obs}([H^+] + K_a')([H^+] + K_{obs})/[Ox]_T$$

Unfortunately, as it stands equation (36) does not allow an to evaluation of the individual rate constants k_s , k_a , and k_e as a function of temperature and hence the activation parameters for each. One approach would be to consider extreme cases. In one case it can be assumed that the k_s pathway makes little or no contribution and that $H_2C_6O_4^-$ is the sole anating species. This is not an unreasonable assumption given that in the case of Rh^{3+} and Ir^{3+} where $H_2C_6O_4$ is involved, the conjugate base path makes no contribution.⁴⁰⁻⁴¹ In the second case the k_s pathway

may be assumed to be negligible and that only the conjugate base is involved in the anation reaction. Equation (36) then becomes (37) and (38) respectively.

$$\frac{k_{obs}([H^+]+K_a')([H^+]+K_{au})}{[Ox]_r} = k_a K_a' [H^+] + K_{au} K_a' (k_a + k_e) \quad [k_a=0] \dots (37)$$

$$= k_a K_a' [H^+] + K_{au} K_a' k_e \quad [k_a=0] \dots (38)$$

From (37), values of k_a and k_e can be evaluated as a function of temperature. Values of K_a' as a function of temperature were computed from the activation parameters used in the previous study on Ru^{2+} . Values of K_{au} as a function of temperature were similarly computed from the corresponding activation parameters.²² From equation (38) k_a and k_e can likewise be obtained. The values obtained are tabulated in table 3.10 and activation parameters are given in table 3.11.

Table 3.10 k_a , k_e and k_s values as a function of temperature.

$10^3 k_a \text{ M}^{-1} \text{ s}^{-1}$	$10^3 k_e \text{ M}^{-1} \text{ s}^{-1}$	Temperature °C
8.0	7.2	60
46.4	27.6	75
74.6	49.9	80
246.9	143.1	90
$10^3 k_s \text{ M}^{-1} \text{ s}^{-1}$	$10^3 k_e \text{ M}^{-1} \text{ s}^{-1}$	Temperature °C
3.6	1.1	60
9.0	7.4	75
11.0	12.4	80
22.6	39.0	90

*assuming $k_a=0$

**assuming $k_s=0$

Table 3.11 Rate constants at 298 K and activation parameters.

	Rate constant $M^{-1} s^{-1}$	ΔH^\ddagger kJ mol $^{-1}$	ΔS^\ddagger J K $^{-1}$ mol $^{-1}$
$k_{\text{a}}^{\text{oxane}}$	$6.17 \pm 1.07 \times 10^{-5}$	$+111.66 \pm 3.1$	$+45.81 \pm 8.9$
$k_{\text{a}}^{\text{acetone}}$	$9.58 \pm 3.88 \times 10^{-5}$	$+96.44 \pm 5.77$	$+1.8 \pm 16.5$
$k_{\text{a}}^{\text{DMSO}}$	$2.68 \pm 1.21 \times 10^{-5}$	$+57.96 \pm 3.73$	-99.60 ± 10.7
$k_{\text{a}}^{\text{CHCl}_3}$	$6.89 \pm 1.40 \times 10^{-5}$	$+116.88 \pm 1.62$	$+67.60 \pm 4.7$

*assuming $k_{\text{a}}=0$ *assuming $k_{\text{a}}=0$ 3.12 Analysis of the final anation products for the Ru(II) and Ru(III) oxalate system.

Following cation-exchange (Dowex 50W-X8) treatment of the final solution, the Ru(III) product was found to be anionic (no retention on the column) implying that it contained the either the bis or the tris-oxalato chelate complex. A comparison of the electronic spectrum with that reported for the tris-oxalato complex⁴⁴ led to the conclusion that the final product of anation on $[\text{Ru}(\text{OH}_2)_6]^{2+}$ was the tris-oxalato species. The actual spectrum of $[\text{Ru}(\text{C}_2\text{O}_4)_6]^{3-}$ contains four bands (nm) (ϵ_{max} , M $^{-1}$ cm $^{-1}$) (286 (320), 375 (350), 490 (28), 630 (11)) superimposed on a charge-transfer band at about 250 nm.

When the final product solution following oxalate anation on $[\text{Ru}(\text{OH}_2)_6]^{2+}$ was opened to air rapid changes to its electronic spectrum resulted. When the behaviour was followed spectrophotometrically, a systematic change was observed with an isosbestic point at 355 nm (figure 3.14). The final product

spectrum was found to be $[\text{Ru}(\text{C}_2\text{O}_4)_6]^{3-}$, the identical product to that obtained from oxalate anation on $[\text{Ru}(\text{OH}_6)_6]^{3+}$.

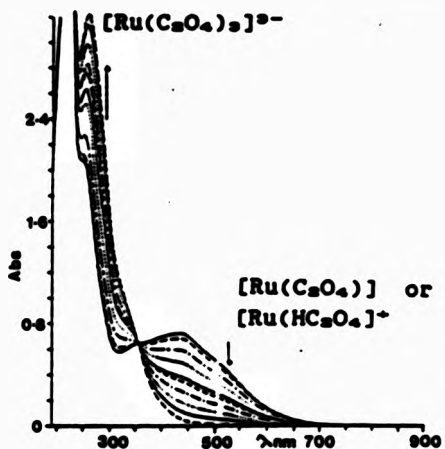
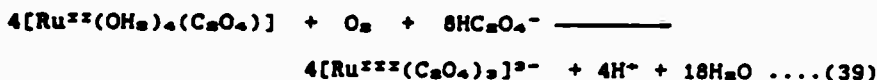


Figure 3.14 Electronic spectrum of final product of oxalate anation on Ru^{3+} monitored over 20 minutes in air.

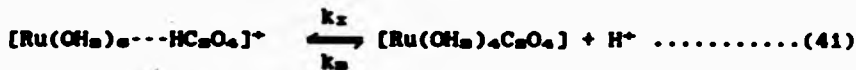
From the equilibrium kinetic behaviour shown by oxalate anation on $[\text{Ru}(\text{OH}_6)_6]^{3+}$, the final product is almost certainly the monooxalato Ru(II) product: $[\text{Ru}(\text{C}_2\text{O}_4)]$ or $[\text{Ru}(\text{HC}_2\text{O}_4)]^+$. Therefore the rapid changes observed on exposure of the final Ru(II) solution to air involve further rapid complexation/chelation of oxalate to give $[\text{Ru}(\text{C}_2\text{O}_4)_6]^{3-}$. A clean process, without any detectable intermediates, is indicated by the retention of the isosbestic point. The relevant equation is (39)



3.13 Possible mechanisms for the oxalate anation on hexaaqua-
ruthenium(II) and hexaaqua-
ruthenium(III).

3.13.1 The mechanism of anation by HC_2O_4^- on $[\text{Ru}(\text{OH}_2)_6]^{2+}$

The forward rate constant k_f at 25°C ($2.6 \times 10^{-8} \text{ M}^{-1} \text{ s}^{-1}$) can be assumed to consist of two terms according to $k_f = k_1 \cdot K_{\text{os}}$ discussed earlier (section 3.4). This is because all reactions between cationic metal ions and anionic reactants involve initial formation of an ion-pair complex prior to the actual substitution step (40) and (41).



If K_{os} is sufficiently large ($> 20 \text{ M}^{-1}$), it can be estimated from the observed curvature of k_{obs} vs $[\text{Ox}]_T$ plots. However, the plots in figure 3.5 are linear over the range of $[\text{Ox}]_T$ studied so that K_{os} is small perhaps close to unity. For 2+ cations with 1- anionic ligands such as HC_2O_4^- , values between 1 and 3 M^{-1} for K_{os} seem to be relevant* for solutions = 1M ionic strength.^{43a-43e} Assuming therefore, a value of 2 M^{-1} (298K) (independant of temperature), a value for k_1 can be estimated to be $1.3 \times 10^{-8} \text{ s}^{-1}$. This is extremely close to the value of k_{obs} for $[\text{Ru}(\text{OH}_2)_6]^{2+}$ of $1.8 \times 10^{-8} \text{ s}^{-1}$ determined at 298K in 1.0 M $\text{NaCF}_3\text{SO}_3^{2-}$, and lends support for a dissociative

*Calculated from Fuoss equation.

interchange mechanism (I_a) for HC_2O_4^- complexation. The value of ΔH^\ddagger for oxalate anation is higher (101 kJ mol $^{-1}$) than that for water exchange (87.6 kJ mol $^{-1}$) which may reflect the slightly more dissociative nature (i.e. dependence on bond breaking) of the HC_2O_4^- complexation reaction. The small volume of activation ($-0.4 \pm 0.7 \text{ cm}^3 \text{ mol}^{-1}$)⁴² has been cited as suggesting an interchange (I) mechanism. The positive ΔS^\ddagger (+85 J K $^{-1}$ mol $^{-1}$) for HC_2O_4^- complexation also would seem to support a more dissociative mode of activation but may also be a reflection of the loss of ion solvation following the complexation reaction.

For the aquation step, the dominating [H $^+$] dependant pathway has a lower ΔH^\ddagger and -ve ΔS^\ddagger from the expected increase in ion solvation. The lower rate constant observed may be a reflection of the need to break a possible chelate ring in the presumed 1:1 oxalato complex aided by protonation.

The involvement of HC_2O_4^- as sole reactant and of [H $^+$] dependent aquation paths for rate determining 1:1 complexation of oxalate has been previously observed with $[\text{Mo}(\text{OH}_2)_6]^{2+}$ and $[\text{Fe}(\text{OH}_2)_6]^{2+}$. ⁴³⁻⁴⁵ The present study appears to provide a further well defined example. However, whereas complexation on Mo $^{2+}$ appears consistent with an I_a mechanism⁴², the present study suggest an I_a mechanism for $[\text{Ru}(\text{OH}_2)_6]^{2+}$.

In conclusion, complexation of oxalate on $[\text{Ru}(\text{OH}_2)_6]^{2+}$ proceeds via HC_2O_4^- as the sole reactant under the conditions studied in

a dissociative interchange mechanism involving rate determining loss of a coordinated water ligand.

3.13.2 The mechanism of anation by oxalate on $[\text{Ru}(\text{OH}_2)_6]^{2+}$

The rate constant values (k_a , k_s and k_e at 298K) and the activation parameters given in table 3.11 may again be compared with the corresponding parameters for water exchange on Ru^{2+} and RuOH^{2+} (table 3.12)

Table 3.12 Activation parameters and rate constants for water exchange on Ru^{2+} and RuOH^{2+} (from ref. 22)

	$k_{\text{appo}}(298\text{K})$ s^{-1}	ΔH^\ddagger kJ mol^{-1}	ΔS^\ddagger $\text{J K}^{-1} \text{mol}^{-1}$	ΔV^\ddagger $\text{cm}^3 \text{mol}^{-1}$
Ru^{2+}	3.5×10^{-6}	89.8	-48.3	-8.3
RuOH^{2+}	5.9×10^{-4}	95.8	-14.9	+0.9

It may again be assumed that the anation rate constants involve a composite term containing the ion-pair association constant K_{appo} and the rate constant for k_x for the actual interchange step. Evaluation of K_{appo} allows k_x to be estimated and compared with k_{appo} .

It is clear from table 3.11 that the value for k_e (298 K) obtained from consideration of both extreme cases (i.e. $k_s=0$ or $k_s=\infty$) is very similar (9.58×10^{-6} and $6.89 \times 10^{-6} \text{ M}^{-1} \text{ s}^{-1}$) with similar ΔH^\ddagger and +ve ΔS^\ddagger . For the k_e step involving RuOH^{2+} , an ion-pair constant of 2 M^{-1} can be assumed^{***} as in the Ru^{2+}

study leading to an estimated value for k_2 of $4.2 \times 10^{-8} \text{ s}^{-1}$ which is only one tenth of the water exchange rate constant ($5.9 \times 10^{-4} \text{ s}^{-1}$) (keeping in mind the large error in k_2). Such values are largely in keeping with a dissociative interchange mode of activation for RuOH^{2+} similar to that found on Ru^{3+} . This mechanism gains further support from the value of ΔH^\ddagger (-107 kJ mol^{-1})^{*} being comparable to that found for water exchange (95.8 kJ mol^{-1}). As with Ru^{3+} , the more positive ΔS^\ddagger value ($-35 \text{ J K}^{-1} \text{ mol}^{-1}$)^{*} and lower rate constant implies a greater dependence on bond breaking (water dissociation) in the oxalate complexation reaction. Correspondingly for the k_2 path (assuming $k_3=0$), a slightly higher K_{eq} value of 2.6 M^{-1} may be estimated^{**} for a $3+/1-$ interaction. Assuming a value of 4M^{-1} , k_2 is estimated to be $1.54 \times 10^{-8} \text{ s}^{-1}$ which is approximately 10 times greater than the water exchange on Ru^{3+} . An I_∞ mechanism has been proposed for water exchange on $[\text{Ru}(\text{OH}_n)_3]^{2+}$ on the basis of the -ve ΔS^\ddagger and -ve ΔV^\ddagger values. Unfortunately few other complexation reactions have been reported on Ru^{3+} with which to further confirm this behaviour by observance of some dependence of rate on the incoming ligand. It is generally believed that substitution reactions of Ru(III) follow an associative activation mode. Studies on Ru(III)-EDTA complexes ($[(\text{Ru}(\text{EDTA})(\text{OH}_n)]^-$) with NCS^- , Na^+ , thiourea and substituted thiourea have shown low activation

^{*}estimated from an average of the k_2 values from table 3.11.

enthalpies ($22 \leq \Delta H^\ddagger \leq 37$ kJ mol $^{-1}$) negative activation entropies ($-105 \leq S \leq -99$ J K $^{-1}$ mol $^{-1}$) and negative activation volumes ($-12 \leq \Delta V^\ddagger \leq -7$ cm 3 mol $^{-1}$) thus supporting the operation of an associative ligand substitution mechanism.²⁴⁻²⁶ The present study provides some evidence of an associative mode of activation since for oxalate as incoming ligand, the rate constant (k_2) is in excess of the value for water exchange. However the large ΔH^\ddagger value (+111.66 kJ mol $^{-1}$) and the +ve ΔS^\ddagger value contradicts a proposal of an associative activation mode. Similar arguments may be made for the k_s path (assuming $k_s=0$) involving the conjugate base with oxalic acid. Here also a satisfactory explanation is not apparent. Involvement of RuOH $^{2+}$ would tend to imply a dissociative activation mode as seems present with H₂C₂O₄ $^-$. This would not be consistent with the observed low ΔH^\ddagger and -ve ΔS^\ddagger and rate constant (k_2) in excess of water exchange.²⁷ Such parameters rather suggest a mechanism analogous to that occurring with oxalic acid and Rh $^{3+}$ and Ir $^{3+}$ in which a concerted transition state is proposed allowing oxalate complexation without H-OH₂ bond breakage.²⁸⁻³¹ While such a process involving RuOH $^{2+}$ and H₂C₂O₄ cannot be discounted, it would then be surprising that Ru $^{3+}$ itself is not involved in such a mechanism.

Taking average values of k_s (at each temperature) determined from both extreme cases, an involvement of both k_s and k_a can

^a A K_{as} value <1.0 may be appropriate for the neutral ligand H₂C₂O₄.

be considered along with their corresponding activation parameters by substituting their values into equation (36). Such treatment however results in even more extreme values for the activation parameters: k_a ($\Delta H^\ddagger = 132 \text{ kJ mol}^{-1}$, $\Delta S^\ddagger = +102 \text{ J K}^{-1} \text{ mol}^{-1}$), k_s ($\Delta H^\ddagger = 35 \text{ kJ mol}^{-1}$, $\Delta S^\ddagger = -174 \text{ J K}^{-1} \text{ mol}^{-1}$). The values for k_s in particular are clearly erroneous and not consistent with some expected degree of associativeness on Ru³⁺ given the water exchange mechanism and general substitution behaviour on Ru(III). Therefore, in the absence of further comparative studies with respect to the ligand dependence on the rate of substitution on $[\text{Ru}(\text{OH}_2)_6]^{3+}$, a mechanism involving only RuOH²⁺ with both $\text{H}_2\text{C}_2\text{O}_4$ and HC_2O_4^- seems the only one reasonably compatible with the observed behaviour ($k_s=0$) suggesting RuOH²⁺ to be the dominant reactant with regard to substitution on Ru³⁺.

3.14 Characterization of hexathioureas Ruthenium(II) trifluoromethansulphonate.

The orange crystals obtained from the reaction of $[\text{Ru}(\text{OH}_2)_6]^{2+}$ with thiourea were analyzed using a number of techniques. Elemental analysis gave results consistent with an empirical formula $[\text{Ru}(\text{SC(NH}_2)_6)_6](\text{CF}_3\text{SO}_3)_6$; found: C, 11.70%, H, 2.78%, N, 19.03% calculated: C, 11.23%, H, 2.61%, N, 19.65%. +ve ion PAB MS showed a M/e peak of mass 856 consistent with $[\text{^{102}\text{Ru}}(\text{tu})_6(\text{tfms})_6]^{+}$. Conductivity measurement of a 10^{-3} M solution in water showed that the compound was a 2:1 electrolyte ($202 \Omega^{-1} \text{ mol}^{-1} \text{ cm}^2$). The IR characteristics (KBr disc) are given in table 3.13.

Table 3.13 Vibrational frequencies (cm^{-1}) of thiourea (tu) and $[\text{Ru(tu)}_6]^{2+}$

Thiourea	$[\text{Ru(tu)}_6](\text{CF}_3\text{SO}_3)_6$	Predominant mode
3300-3050	3300-3100	$\nu(\text{NH}_2)$
1540	1575	$\nu(\text{CN})$
680	655	$\nu(\text{CS})$

The infrared studies showed the expected increase in $\nu(\text{CN})$ and decrease in $\nu(\text{CS})$ consistent with S bonded thiourea.^a The electronic spectrum recorded in saturated thiourea solution (deoxygenated) showed a single absorption maximum at 490 nm (ϵ

^aNakamoto, K. "IR and Raman Spectra of Inorganic compounds", 3rd Edition, Wiley-Interscience, 1978.

$263 \text{ M}^{-1} \text{ cm}^{-4}$). When the solution was allowed to stand in air the orange colour eventually turned to blue-green. This corresponded to the findings of Yaffe and Voigt⁴⁸ who report the species responsible to be a Ru(tu)_6 chelate complex. Efforts to characterize this complex included the extraction of the blue species into organic solvents as it would be neutral and to monitor the pH of the solution as Ru(II) is oxidised by O_2 since chelation would result in the loss of protons thus decreasing the pH. Both attempts failed to give any meaningful results. Final confirmation of the S bonded $[\text{Ru(tu)}_6]^{2+}$ complex came from an X-ray structural analysis performed by Dr K Muir at Glasgow University. The structure is shown in figure 3.15. Cyclic voltammetric studies on the $[\text{Ru(tu)}_6]^{2+}$ ion as well as the $[\text{Ru(OH}_2)_6]^{2+}$ aqua ion and the $[\text{Ru(C}_6\text{O}_6)_6]^{4-}$ ion were performed. All showed a reversible wave. The potentials (vs N.H.E.) are given in table 3.14.

Table 3.14 E_h potentials (vs N.H.E., 0.1M NaCF_3SO_3) for $\text{Ru(II)}/\text{Ru(III)}$ couples.

Couple	ΔE_F (mV)	Scan rate (mV s ⁻¹)	E_h vs N.H.E	Ionic strength M NaCF_3SO_3
$[\text{Ru(tu)}_6]^{2+}/^{3+}$	60	200	+0.26	0.1
$^{+}[\text{Ru(OH}_2)_6]^{2+}/^{3+}$	62	200	+0.20	0.1 Hfms
$[\text{Ru(C}_6\text{O}_6)_6]^{4-}/^{3-}$	64	200	-0.26	0.2 Hfms

*Literature value +0.21 V vs N.H.E., 0.1 M Hpts $\Delta E_F = 64$ mV (ref. 32c)

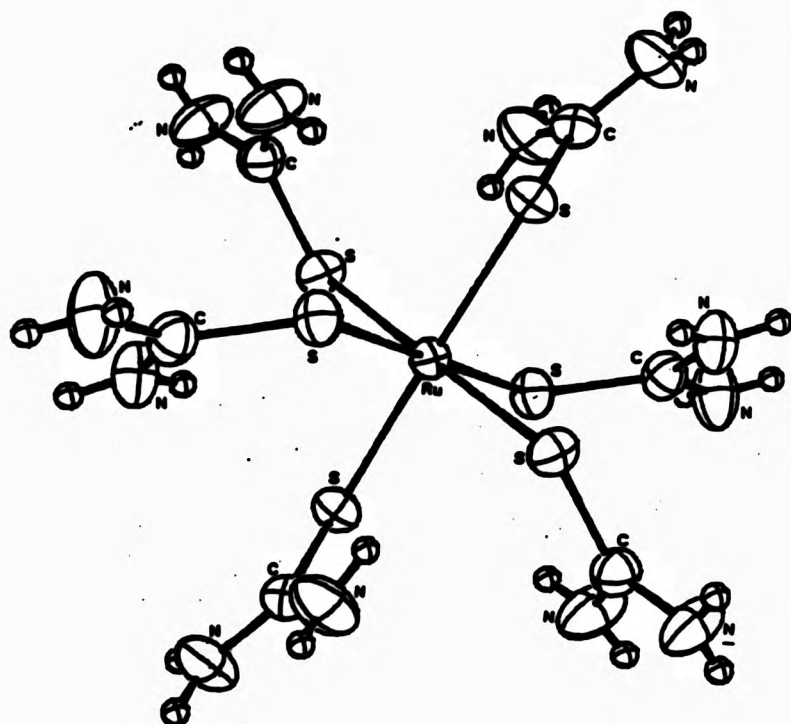


Figure 3.15 X-ray crystal structure of $[\text{Ru}(\text{tu})_6](\text{CF}_3\text{SO}_3)_2$

REFERENCES

1. Ingold, C. K. Structure and Mechanism in Organic Chemistry, Cornell Univ. Press, Ithaca, 1953.
2. Basolo, F.; Pearson, R. G. Mechanism of Inorganic Reactions, 2nd Ed., J. Wiley and sons, NY, 1967.
3. Langford, C. H.; Gray, H. B. Ligand Substitution Processes, W. A. Benjamin Inc., NY, 1966.
4. Burgess, J. Metal Ions in Solution, Ellis Horwood Ltd., Chichester, 1978.
5. Ducommun, Y.; Newman, K. E.; Herbach, A. E. Helv. Chim. Acta, 1979, 62, 2511.
6. Elding, L. I.; Helm, L.; Herbach, A. E. Inorg. Chem., 1983, 24, 1721.
7. Swaddle, T. W. Modern Aspects of Physical Chemistry at High Pressure, Ed. J. Osugi, Physico-Chemical Soc. of Japan, 1980.
8. Swaddle, T. W. Adv. Inorg. Bioinorg. Mechanisms, Ed. A. G. Sykes, 1983, 2, 95.
9. Kelm, M. High pressure Chemistry, Reidel, Dordrecht, 1978.
10. Van Eldik, R. High Pressure Inorganic Chemistry : Kinetics and Mechanisms, Elsevier, Amsterdam, 1986.
11. Harris, G. N. Chemical Kinetics, Heath, Boston, 1966.
12. Eckert, C. A. Ann. Rev. Phys. Chem., 1972, 23, 239.
13. Swaddle, T. W. Coord. Chem. Revs., 1974, 14, 217.
14. Herbach, A. E. Pure and Appl. Chem., 1982, 54, 1479.
15. Herbach, A. E. Inorg. Chem., 1984, 23, 4341.
16. Eigen, M. Pure and Appl. Chem., 1963, 6, 105
17. Herbach, A.; Comba, P. Pure and Appl. Chem., 1987, 59, 161.
18. Bennet, H. D.; Caldin, B. F. J. Chem. Soc. A, 1971, 2918.
19. Hugi-Cleary, D. PhD thesis, Univ. Lausanne, 1984.

20. Swaddle, T. W.; Herbach, A. E. Inorg. Chem., 1981, 20, 4212.
21. Xu, F. -C.; Swaddle, T. W. Inorg. Chem., 1985, 24, 267.
22. Rapaport, I.; Bernhard, P.; Helm, L.; Ludi, A.; Herbach, A. E. Inorg. Chem., 1988, 27, 873.
23. Langford, C. H. Inorg. Chem., 1979, 18, 3288.
24. Newman, K. E.; Herbach, A. E. Inorg. Chem., 1980, 19, 2481.
25. Swaddle, T. W. Inorg. Chem., 1980, 19, 3203.
26. Newman, K. E.; Adamson-Sharpe, K. M. Inorg. Chem., 1984, 3818.
27. Eigen, M.; Wilkins, R. G. Adv. Chem. Ser., 1965, 49, 55.
28. Fuoss, R. M. J. Am. Chem. Soc., 1958, 80, 5059.
29. Robinson, R. A.; Stokes, R. H. "Electrolyte Solutions", 2nd Ed., Butterworths, London, 1959.
30. Hammes, G. G.; Steinfeld, J. I. J. Am. Chem. Soc., 1962, 84, 4639.
31. (a) Endicott, J. F.; Taube, H. J. Am. Chem. Soc., 1962, 84, 4984.
(b) Stritar, J. A.; Taube, H. Inorg. Chem., 1969, 8, 2281.
(c) Allen, R. J.; Ford, P. C. Inorg. Chem., 1972, 11, 679.
(d) Shepherd, R. E.; Taube, H. Inorg. Chem., 1973, 12, 1392.
(e) Allen, R. J.; Ford, P. C. Inorg. Chem., 1974, 13, 237.
(f) Isied, S. S.; Taube, H. Inorg. Chem., 1976, 15, 3070.
(g) Taube, H. Comments Inorg. Chem., 1981, 1, 17 and references therein.
32. (a) Cady, H. H.; Connick, R. E. J. Am. Chem. Soc., 1958, 80, 2646.
(b) Mercer, E. E.; Buckley, R. R. Inorg. Chem., 1965, 4, 1692.
(c) Kallen, T. W.; Harley, J. E. Inorg. Chem., 1971, 10, 1149.
(d) Böttcher, W.; Brown, G. M.; Sutin, N. Inorg. Chem., 1979, 18, 1447.

- (e) Marzion, Z.; Navon, G. Inorg. Chem., 1980, 19, 2236.
(f) Bernhard, P.; Bürgi, H. B.; Hauser, J.; Lehmann, H.;
Ludi, A. Inorg. Chem., 1982, 21, 3936.
33. Hunt, J. B.; Harley, J. E. J. Am. Chem. Soc., 1960, 82,
5312.
34. (a) Matsubara, T.; Creutz, C. J. Am. Chem. Soc., 1978,
100, 6255; Inorg. Chem., 1979, 18, 1956.
(b) Bajaj, H. C.; Van Eldik, R. Inorg. Chem., 1988, 27,
4052.
35. Broomehead, J. A.; Kane-Maguire, L. A.; Wilson, D. Inorg. Chem., 1975, 14, 2575, 2579.
36. Fairhurst, M. T.; Swaddle, T. W. Inorg. Chem., 1979, 18,
3241.
37. Lay, P. A.; Sasse, W. H. F. Inorg. Chem., 1985, 24, 4707.
38. Bosnich, B.; Dwyer, F. P. Aust. J. Chem., 1966, 19, 2235.
39. Bernhard, P.; Helm, L.; Rapaport, I.; Ludi, A.; Herbach,
A. E. J. Chem. Soc. Chem. Commun., 1984, 302.
40. McMahon, M. R.; McKenzie, A.; Richens, D. T. J. Chem. Soc. Dalton Trans., 1988, 711
41. Richens, D. T.; Leitch, P. to be published.
42. (a) Nancollas, G. H.; Sutin, N. Inorg. Chem., 1964, 3,
360.
(b) Othman, Nor; Sykes, A. G. J. Chem. Soc. Dalton Trans.,
1973, 1232.
(c) Kelly, H. H.; Richens, D. T.; Sykes, A. G. J. Chem. Soc. Dalton Trans., 1984, 1229.
(d) Chaudhri, P.; Deibler, H. J. Chem. Soc. Dalton Trans.,
1977, 596.
(e) Moorhead, K.; Sutin, N. Inorg. Chem., 1966, 5, 1866.
(f) Davies, G.; Watkins, K. O. Inorg. Chem., 1970, 9,
2735.
(g) Ojo, J. F.; Olubuyide, O.; Oyetunji, O. J. Chem. Soc. Dalton Trans., 1987, 957.
43. Finholt, J. E.; Leupin, P.; Sykes, A. G. Inorg. Chem.,
1983, 22, 3315.

Ch. 3: References 256

44. (a) Wagnerova, D. M. Coll. Czech. Chem. Commun., 1962, 27,
1130.
(b) Olliff, R. W.; Odell, A. L. J. Chem. Soc., 1964, 2467.
(c) Bittel, R.; Bremard, C.; Nowogrocki, G.; Tridot, G.
Bull. Soc. Chim. France, 1969, 11, 3830.
45. Yaffe, R. P.; Voigt, A. F. J. Am. Chem. Soc., 1952, 74,
2503.

APPENDICES

Appendix ICyclic voltammetry

In cyclic voltammetry, the potential of an electrode in an unstirred solution is varied linearly from an initial value to a second value and back to the first to complete a cycle. If an electroactive species is present within this range of potential, current will flow as the potential for reduction (or oxidation) is approached and will increase until the concentration of electroactive species in the immediate vicinity of the electrode is depleted. At this point the current drops to a constant value that is maintained by diffusion of the electroactive species from the bulk solution. A plot of current vs potential shows a peak for this process. If the electron transfer process is reversible, the product from the initial electron transfer will also be electroactive and will undergo oxidation (or reduction) on the return sweep. For a diffusion controlled reversible process, the current flowing on oxidation is roughly equal to that flowing on reduction, and the average of the two peak potentials is close to the electrode potential for the process. Figure A1.1 illustrates the cyclic voltammogram of the $[\text{Ru}(\text{tu})_6]^{3+}$ complex dissolve in water ($I=0.1\text{M NaClO}_4$) and acetonitrile ($I=0.1\text{M }[(\text{C}_6\text{H}_5)_2\text{N}](\text{BF}_4)$, Pt disc working electrode and S.C.E electrode as reference). The various important values that are derivable from a such a plot are also shown. E_p (25°C) = 60 mV (RT/nF) for a one electron reversible process (30mV for $2e$, 20 mV for

Se etc). Processes that are not solely diffusion controlled give ΔE_p values that are in excess of this limit and vary with scan rate. This can make the determination of n difficult.

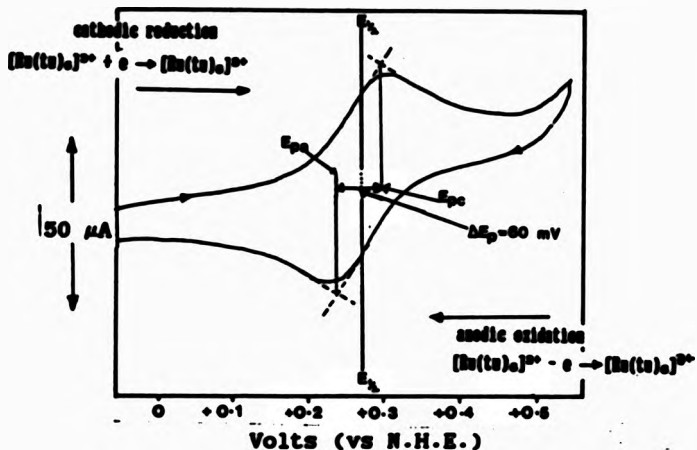


Figure A1.1 Cyclic voltammogram of $[\text{Ru}(\text{tu})_6]^{3+}$ at a Pt disc working electrode in water.

A more accurate method of determining the number of electrons involved in the redox process if the resulting electrode product is stable is that of controlled potential electrolysis. The current is measured at fixed potential (chosen in order to facilitate complete conversion to the desired product) as a function of time and the area plotted by a current vs time curve is calculated. The area is equal to the charge (Q) which is proportional to the chemical change (= n.F.no. of moles substance) Faraday equation where n is the number of electrons

and F is the Faraday constant (96487 C mol^{-1}). A typical cell used in cyclic voltammetry is shown in figure A1.2.

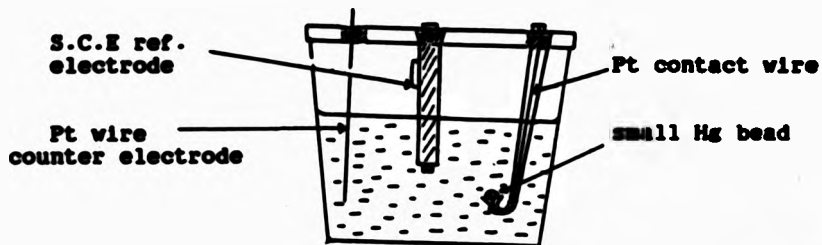


Figure A1.2 Diagram of cell used in cyclic voltammetry (employing the use of a mercury cup working electrode).

Appendix 2

A2.1 Brief theory of Nuclear Magnetic Resonance spectroscopy.

The NMR phenomenon is dependent upon the existence of a property which is conveniently referred to as the spin of a nucleus. Each isotope of an element can be assigned a ground state nuclear spin quantum number, I . When I is non-zero the nucleus has a magnetic moment² μ_z given by :

where γ_r is the magnetogyric ratio and is characteristic of the nucleus in question. The quantity \hbar is $\hbar/2\pi$ where \hbar is Planck's constant. When a nucleus with a non-zero I is placed in a strong magnetic field B_0 (usually between 1 and 10 T(Tesla)) the orientation of its spin axis becomes quantised, each possible orientation having a different energy. Suitable radiofrequency radiation will cause transition, which may be detected. These transitions form the basis of NMR spectroscopy.

Chemical shifts, coupling constants and relaxation times are the three types of measurable NMR parameters of value in chemistry. The relaxation time for a nucleus governs the rate at which it recovers its equilibrium properties after being disturbed. There are two distinct relaxation times: T_1 , the

^aHarris, R. K.; Mann, B. K. "NMR and the Periodic Table".
Acad. Press, London, 1976.

spin-lattice (longitudinal) relaxation time which relates to magnetisation parallel to B_0 , and T_2 , the spin-spin (transverse) relaxation time which refers to magnetisation perpendicular to B_0 . Relaxation times give important information about molecular dynamics.

In the present study the main concern was to obtain information regarding the resonance peak positions about the various types of core oxo groups present in oligomeric Mo, W and Ru aqua ions. For the Ru(IV) aqua ion, an attempt was however made to determine T_2 as a function of temperature and thereby obtain a value for the rate constant and activation parameters for water exchange on the aqua ion.

A2.2 Separation of the bulk and bound water peaks.

The ^{17}O NMR spectrum of an aqua ion in aqueous solutions contain, excluding any peaks for the core oxo/hydroxo groups, peaks both due to the bulk water and to the bound water ligands on the aqua ion. If the metal ion is diamagnetic, as in the case of Mo(IV), W(IV) and Ru(IV), the chemical shift between the bound and bulk water peaks can be very small. Since the ^{17}O lines are broad, this can make it difficult to distinguish between the large free and small bound water peaks. Observation of the bound water resonance is crucial for the initial estimate of the kinetic exchange rate. Diamagnetic ions have

very little influence on the bulk water resonance^a: chemical exchange generally neither broadens the line nor shifts it noticeably, thus this resonance is kinetically uninteresting. It is therefore necessary to separate the two resonances so that the bound water signal can be examined and the rate of water exchange between the first coordination sphere of a diamagnetic metal ion and the bulk water measured. Sometimes Δω, the chemical shift between the bound and free water peaks, is large as in the case of square planar tetraqua Pd and Pt ions.^b

There are two ways of separating the bound and bulk water peaks. The addition of paramagnetic shift reagent such as Co²⁺ causes a large average chemical shift of the bulk water resonance due to strong interaction of the rapidly exchanging bulk water with the labile paramagnetic Co²⁺ ion. This method was first proposed by Jackson, Lemons, and Taube^c who observed that the addition of Co²⁺ to an aqueous solution of $[(\text{NH}_3)_5\text{Co}(\text{OH}_2)]^{2+}$ caused an upfield shift of the bulk water peaks. The bound water peak was not significantly affected.

^aConnick, R. E.; Wüthrich, K. J. Chem. Phys.. 1969, **51**, 4506.

^bHelm, L.; Elding, L. I.; Herbach, A. E. Helv. Chim. Acta. 1984, **67**, 1453.

^cJackson, J.; Lemons, J. F.; Taube, H. J. Phys. Chem.. 1960, **62**, 553.

Another approach is to use a paramagnetic relaxation agent such as Mn⁺⁺.⁵ Due to a strong interaction with the electron spin of Mn⁺⁺, the bulk water relaxes so rapidly that its signal becomes extremely large. Its amplitude thus becomes negligible compared with that of the bound water resonance, and it disappears into the baseline.

A2.3 Temperature dependence of the transverse relaxation rate.

The transverse relaxation rate $1/T_B$, of an oxygen-17 nucleus in the first coordination sphere of a metal ion is given by the following expression where $1/T_{2D}$ is the dipolar relaxation term, $1/T_{2Q}$ is the quadrupolar relaxation rate and $1/\tau$ is the chemical exchange rate constant.

$$1/T_B = 1/T_{2D} + 1/T_{2Q} + 1/\tau \dots \dots \dots \quad (2)$$

For a quadrupolar nucleus such as ¹⁷O, with a quadrupolar moment of -2.6×10^{-30} m², dipole-dipole relaxation is completely overshadowed by the more efficient quadrupolar relaxation.⁶ Thus the dipolar relaxation term is considered to be insignificant and is omitted from all calculations.

A2.3.1 Quadrupolar relaxation.

Under extreme narrowing conditions $1/T_{2Q}$, the quadrupolar relaxation rate can be written as :⁷

⁵Neely, J. W. PhD thesis, Univ. of California (Berkeley). 1971. Report UCRL-20580.

⁶Martin, M., Martin, G., Delpuech, J. -J. "Practical NMR Spectroscopy". Heyden and sons Ltd.. London. 1980.

$$\frac{1}{T B_0} = \frac{3}{10} n^2 + \frac{2I+3}{I^*(2I+1)} \cdot X^2 + (1 + 1/3 n^2) \cdot r_0 \dots \dots (4)$$

where I is the nuclear spin ($5/2$ in the case of ^{17}O) and n is the asymmetry parameter of the electric field gradient ($nq_{\text{as}} = -q_x/q_{\text{as}}$ where q are the components of the electric field gradient). Normally n is defined as $0 < n < 1$. τ_c is the isotropic tumbling time or correlation time of a water molecule bound to a metal centre and is a function of viscosity. x is the nuclear quadrupole coupling constant ($x = e^2 q_{\text{as}} Q/h$), with e the electronic charge, q_{as} the biggest of the electric field gradient at the nucleus, Q the nuclear electric quadrupole moment and h Planck's constant.

T_c varies with temperature as follows :

where τ_0 is the correlation time at T_0 , E_a is an activation energy and R is the universal gas constant. The combination of equations (4) and (5) gives equation (6):

where $E_a = E_b$, the activation energy for the quadrupolar induced relaxation of the bound water resonance. A more convenient way to express equation (6) is :

"Campbell, J. A. "Chemical Systems", Freeman and Co., San Francisco, 1970.

$$\frac{1}{T_{Bn}} = \left[\frac{1}{T_{Bn}^{298}} \right]^{298} \cdot \exp \left[\frac{E_Q}{R} \left[\frac{1}{T} - \frac{1}{298.15} \right] \right] \dots \dots (7)$$

where $[1/T_{Bn}]^{298}$ is the quadrupolar relaxation rate at 298.15 K.

A2.3.2 Chemical exchange.

The temperature dependence of τ , the lifetime of the solvent molecule (in this case water) in the first coordination sphere of the metal ion is given by the Eyring equation.*

$$\frac{1}{\tau} = k_{ex} = \left[\frac{k_B T}{h} \right] \cdot \exp(\Delta S^\ddagger / R - \Delta H^\ddagger / RT) \dots \dots (8)$$

τ is the inverse of k_{ex} , the pseudo first-order rate constant for solvent exchange; ΔS^\ddagger and ΔH^\ddagger are respectively the entropy and enthalpy of activation for the water exchange reaction and k_B , h and R are the Boltzmann, Planck and gas constants respectively. k_{ex} can also be expressed in terms of k_{ex}^{298} , the rate constant at 298 K.

$$k_{ex} = k_{ex}^{298} \cdot T/298.15 \cdot \exp \left[- \frac{H}{R} \left[\frac{1}{T} - \frac{1}{298.15} \right] \right] \dots \dots (9)$$

*Eyring, H. Chem. Rev., 1935, 17, 65.

A.2.4 Fast injection measurements.

The fast injection measurements were performed using an apparatus built in Lausanne and illustrated in figure A2.1. The apparatus fits into the 50mm bore at the upper end of the wide bore cryomagnet and rest by means of a flange, on a heavy brass ring designed to absorb the shock of a pneumatically driven injection. The lower part of the device consists of a thermostating chamber which connects to the main thermostat of the spectrometer via the in- and outlets near the top of the apparatus. The glass syringe containing the liquid to be injected can be screwed into the thermostating chamber. The syringe can hold up to 1.0 cm³ of solution with a precision of 10ml and it is connected to a glass capillary (0.7 mm o.d., 0.4 mm i.d., and 115 mm long). The capillary fits into a shortened (150 mm) commercial 5 or 10 mm NMR tube which is rotated in the normal way. A Platinum resistor (100 Ω) inside the thermostating chamber allows the monitoring of the temperature ($\pm 0.05^{\circ}\text{C}$). The required volume is set using a micrometer screw located on top of the assembly. This screw forms part of the piston that propels the required volume into the spinning NMR tube located in the RF coils of the magnet. The piston can be activated by hand or by gas powered pneumatic drive. An optical trigger device starts the acquisition at the end of the injection. Depression of the piston causes rotation of a mirror into a vertical position (see the inset in figure A2.1). The subsequent reflection of infrared radiation from an IR emitter onto

a phototransistor triggers the spectrometer to start acquisition.

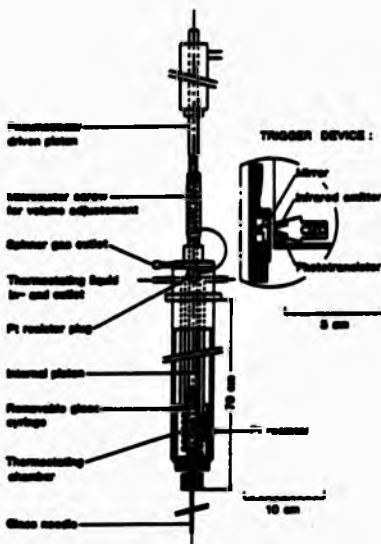


Figure A2.1 Schematic drawing of the fast injection assembly. The trigger device is magnified in the inset.

The temperature range accessible with this fast injection assembly is from 200 K to 370 K, depending upon the thermostat liquid used. The thermostating time of the solution in the syringe does not exceed 15 minutes, even for extreme temperatures. The mixing time of two 1 cm³ solutions in 10 mm spinning tubes is less than 50 ms. This apparatus is thus useful for studying solvent exchange reactions with half life periods ranging from seconds to several minutes.

Appendix 3A3.1 Estimation of final absorbance values (A_{∞}) using the Swinbourne method.

When kinetic reactions are monitored using conventional UV-visible spectrophotometry, the determination of final absorbance values can sometimes become difficult due to a drifting absorbance reading. This may be due to further rate-determining reactions becoming significant. Various methods have been used to estimate the rate constant as well as the final absorbance value for the initial rate determining process.¹⁻³ One of these is the method reported by Swinbourne.³

The course of a reaction may be followed by measuring the absorbance which varies with time according to equation (1).

$$(A_{\infty} - A) = (A_{\infty} - A_0) \exp(-kt) \dots \dots \dots \quad (1)$$

where A_0 and A_{∞} are the initial and final absorbance readings respectively and k is the rate constant for a simple first-order reaction. If readings A_1, A_2, \dots, A_n are made at times t_1, t_2, \dots, t_n , and a second series A'_1, A'_2, \dots, A'_n is made at the corresponding times $t_1 + dt, t_2 + dt, \dots, t_n + dt$ (where dt is constant) then,

¹Guggenheim, Phil. Mag., 1926, 2, 538.

²Hartley, Biometrika, 1948, 35, 32.

³Swinbourne, E. S. J. Chem. Soc., 1960, 2371.

$$(A_m - A_n) = (A_m - A_0) \exp(-kt_n) \dots \dots \dots (2)$$

and

$$(A_m - A'_n) = (A_m - A_0) \exp(-k(t_n + dt)) \dots \dots \dots (3)$$

Dividing (2) by (3) and rearranging gives,

$$A_n = A_m(1 - \exp(kdt)) + A_0 \exp(kdt) \dots \dots \dots (4)$$

A plot of A_n vs A'_n should be a straight line and the logarithm of the slope of this line is therefore an estimate of the rate constant k . Furthermore at $t=\infty$, $A_n=A'_n=A_m$; hence A_m is the point on the line when both A_n and A'_n are equal. The graph may also be used for easy extrapolation to A values outside the range of the recorded data. In order to obtain reliable estimates of k and A_m , the data should normally be recorded over a period of time greater than the half-life ($t_{1/2}$) and preferably greater than $2 t_{1/2}$ (this will depend on the accuracy of the recorded values. The dt value should be of the order of $0.5t_{1/2}$ to $t_{1/2}$.

A3.2 Derivation of rate law for the Ru(II) oxalate anation reaction.

The observed rate law was found to be of the form :

$$\frac{-d[Ru^{2+}]}{dt} = \frac{k_p K_a' [Ox]_r [Ru^{2+}]}{[H^+] + K_a'} + k_a [Ru^{2+}] [H^+] \dots \dots \dots (5)$$

and is derived as follows:



where

$$K_a' = \frac{[\text{HC}_6\text{O}_4^-][\text{H}^+]}{[\text{H}_2\text{C}_6\text{O}_4]} \dots \quad (7)$$

Rearranging equation 7 gives

$$[\text{H}_2\text{C}_6\text{O}_4] = \frac{[\text{HC}_6\text{O}_4^-][\text{H}^+]}{K_a'} \dots \quad (8)$$

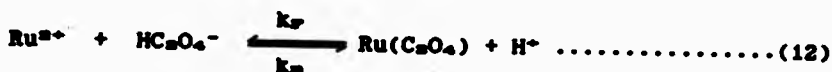
Thus expression $[\text{Ox}]_T = [\text{H}_2\text{C}_6\text{O}_4] + [\text{HC}_6\text{O}_4^-]$ can be written as

$$[\text{Ox}]_T = \frac{[\text{HC}_6\text{O}_4^-](K_a' + [\text{H}^+])}{K_a'} \dots \quad (9)$$

and therefore

$$[\text{HC}_6\text{O}_4^-] = \frac{K_a'[\text{Ox}]_T}{[\text{H}^+] + K_a'} \dots \quad (10)$$

Also



thus

$$\frac{-d[\text{Ru}^{2+}]}{dt} = k_p[\text{Ru}^{2+}][\text{HC}_6\text{O}_4^-] + k_s[\text{Ru}^{2+}][\text{H}^+] \dots \quad (13)$$

$$= \frac{k_p K_a' [\text{Ox}]_T [\text{Ru}^{2+}]}{[\text{H}^+] + K_a'} + k_s[\text{Ru}^{2+}][\text{H}^+] \dots \quad (14)$$

A3.3 Derivation of the Fyrine equation.

For reaction in solution, the temperature dependence of reaction rates can be based on the Absolute reaction-rate theory (Transition state theory). The theory postulates that in the rate-limiting step, the reacting species A and B, combine reversibly to form an "activated complex" AB, which then decomposes to form the products. Thus the following pseudo equilibrium constant is written :



where

The activated complex, AB^+ , is treated as a normal molecule except that one of its vibrations is considered to have little or no restoring force and to allow dissociation into products. The frequency, v , with which dissociation to products takes place is assumed to be given by equating the "vibrational" energy, $\hbar v$, to thermal energy, $k_B T$. Thus the following expression is written.

* k_B and \hbar are Boltzmann and Planck constants respectively.

The measurable rate constant is defined by

It can now be defined as

$$k = \left[\frac{k_B T}{h} \right] \frac{[AB^+]}{[A][B]} = \frac{k_B T}{h} K^+ \quad \dots \dots \dots (19)$$

The formation of this activated complex is governed by the thermodynamic considerations similar to those of ordinary chemical equilibria. Thus the free energy of activation can be defined as :

Thus the following expression (Kyring equation) may be written